

Aryl hydrocarbon Receptor activation in primary
human keratinocytes and epidermal equivalents:
The relevance to chloracne

Alison Ruth Forrester

B.Sc (Hons)

September 2011



Submitted in fulfilment of the requirements and the regulations for the
degree of Doctor of Philosophy
Newcastle University
Faculty of Medical Sciences
Institute of Cellular Medicine

Abstract

The Aryl hydrocarbon Receptor (AhR) mediates the toxic effects of 2,3,7,8-tetrachlorodibenzo-*p*-dioxin (TCDD) resulting in the human specific toxicity, chloracne. To test whether the chloracnegenic potential of AhR-agonists depends upon binding affinity for the AhR, residency and/or down-regulation of the AhR, we investigated the effects of different AhR agonists in primary human keratinocytes and epidermal equivalents. The AhR agonists used were high-affinity, high-residency and high-potency TCDD, and two agonists not known to induce chloracne; low-affinity, low-residency and low-potency β -naphthoflavone (β -NF) and the low-affinity, low-residency and high-potency physiological agonist 2-(1'H-indole-3'-carbonyl)-thiazole-4-carboxylic acid methyl ester (ITE). α -NF, a partial agonist was used to test AhR dependency. The effects of these agonists on AhR activation, terminal differentiation, autophagy and expression of cathepsin D (CTSD) in primary human keratinocytes and epidermal equivalents were determined.

All three agonists induced AhR activation by XRE-luciferase assay, which was inhibited by α -NF, demonstrating AhR dependence of the ligands. AhR degradation was induced by all ligands and CYP1A1 was induced strongly by TCDD but weakly by β -NF and ITE. CYP1A1 and XRE-luciferase induction correlated with ligand binding affinity; ranking levels of binding affinity as TCDD> β -NF>ITE.

TCDD treatment induced a chloracne-like phenotype in epidermal equivalents, with a decrease in viable cell layer thickness and compacted stratum corneum. This was not induced by β -NF or ITE. To investigate the differential effects of AhR-ligands on epidermal equivalent phenotype, we studied differentiation markers filaggrin, involucrin and TGM-1. TGM-1 expression was induced specifically by TCDD while aberrant expression of involucrin and filaggrin were induced by TCDD, β -NF and ITE. AhR activation was not associated with increased apoptosis. Caspase-3 independent cell death has been implicated as a mechanism of decreased thickness of the viable cell layer, so we studied the effects of AhR-agonists on autophagy.

Autophagy in keratinocytes and epidermal equivalents was characterised by induction of LC3 II, p62 degradation and transmission electron microscopy. TCDD robustly induced active autophagy, while ITE induced lower levels and β -NF blocked autophagy. TCDD- and ITE-induced autophagy in epidermal equivalents appeared to result in decreased numbers of lamellar bodies, which may account at least in part for the compacted stratum corneum phenotype shown by the TCDD-induced phenotype in epidermal equivalents and chloracne.

As CTSD has been implicated in keratinocyte differentiation and an XRE domain has been identified upstream of CTSD, we studied the effects of ligand-dependent AhR activation on lysosomal aspartic protease CTSD expression. CTSD was increased by AhR activity in epidermal equivalents.

Induction of CYP1A1 did not appear to be a specific biomarker of chloracnegenic potential of AhR agonists. The data presented have shown differential effects by TCDD, β -NF and ITE on autophagy that we hypothesise contributes to the chloracne phenotype. In this thesis, potential biomarkers specific to chloracne were identified in keratinocytes, TGM-1, CTSD, autophagy and decreased lamellar bodies, although further validation is required.

Contents

Abstract	i
List of Figures	vi
List of Tables	x
Abbreviations.....	xi
Acknowledgements	xii
Published Abstracts arising from this work	xiii
Declaration	xiv
1. Introduction	1
1.1 Aryl hydrocarbon Receptor.....	1
1.1.1 AhR pathway activation	1
1.1.2 AhR expression and activity	9
1.1.3 AhR-dependent toxicity.....	12
1.1.4 Ligands	14
1.2 Normal human skin	17
1.2.1 Keratinocyte differentiation	17
1.2.2 Metabolism	22
1.2.3 Epidermis and disease	23
1.2.4 Epidermal equivalents	24
1.3 Chloracne.....	26
1.4 Cathepsin D	29
1.4.1 CTSD: Regulation and processing.....	29
1.4.2 CTSD activity in cell death.....	30
1.4.3 CTSD in differentiation.....	32
1.5 Autophagy	33
1.5.1 Pathway.....	34
1.6 Aims	37

2	Materials and Methods	40
2.1	Cell culture	40
2.1.1	Monolayer culture	40
2.1.2	Epidermal Equivalents	40
2.2	Immunohistochemistry	41
2.2.1	Haematoxylin & eosin staining.....	41
2.2.2	Fluorescence	41
2.2.3	DAB	41
2.3	Sulforhodamine B Assays	43
2.3.1	Ligand preparation.....	44
2.4	Dual Luciferase assays	44
2.5	Western blotting	44
2.6	Confocal Microscopy	46
2.6.1	Fixed sample imaging.....	46
2.6.2	Live cell imaging using BODIPY FL-pepstatin A	46
2.7	AhR knock down assays	47
2.7.1	siRNA	47
2.7.2	Short hairpin RNA.....	48
2.8	Ingenuity pathway analysis	50
2.9	Statistical analysis.....	51
3	AhR activation in primary human keratinocytes	52
3.1	Introduction	52
3.1.1	Known effects of AhR activation	52
3.2	Preliminary studies	56
3.3	Main Studies	70
3.3.1	AhR activation by TCDD, β -NF and ITE	70
3.3.2	Inhibition of agonist induced AhR-activation by α -NF	81
3.3.3	The effects of α -NF on ligand induced AhR activation	86
3.4	Discussion.....	93
3.4.1	Summary of AhR activation and inhibition	93

3.4.2	AhR activation by TCDD, β -NF and ITE	94
4	AhR activation in epidermal equivalents	102
4.1.	Introduction	102
4.1.1	Models exerting chloracne-like effects.....	102
4.1.2	The epidermal equivalent model.....	103
4.3	Results	105
4.3.1	Effects of AhR ligands on epidermal equivalent phenotype	105
4.3.2	The effects of AhR ligands on differentiation	108
4.3.3	The effects of AhR ligands on apoptotic cell death.....	112
4.3.4	AhR induction in epidermal equivalents.....	117
4.4	Discussion.....	131
4.4.1	Summary	131
4.4.2	Is the TCDD/chloracne phenotype caused by AhR knock down?.....	134
5	Differential effects of AhR activation on autophagy	136
5.1	Introduction	136
5.2	Results	138
5.2.1	The effects of AhR activation on LC3 II induction	138
5.2.2	The effects of AhR activation on p62 degradation	139
5.2.3	The correlation of p62 and LC3 II	140
5.2.4	Effects of α -NF on AhR induced autophagy.....	146
5.2.5	The effects of autophagic block on LC3 II and p62.....	154
5.2.6	Active autophagy in epidermal equivalents.....	157
5.3	Discussion.....	168
5.3.1	Summary	168
5.3.2	TCDD and ITE induce active autophagy but β -NF blocks autophagy	169
5.3.3	Modulation of autophagy by α -NF.....	170
5.3.4	AhR activation effects lamellar bodies and desmosomes.....	172
6	AhR activation regulates Cathepsin D	174
6.1	Introduction	174

6.1.1	CTSD Regulation.....	174
6.2	Results	176
6.2.1	Regulation of Cathepsin D by AhR activation	176
6.2.2	Modulation of ligand induced AhR-dependent effects on Cathepsin D by α -NF	187
6.2.3	Effects of autophagic block on CTSD	195
6.2.4	Live cell localisation of CTSD	197
6.3	Discussion.....	201
6.3.1	Summary	201
6.3.2	CTSD expression is regulated by AhR	202
6.3.3	CTSD and autophagic block	205
7	General Discussion	207
7.1	Summary.....	207
7.2	Main hypotheses	209
7.3	Hypotheses arising from the project.....	212
7.3.1	Hypothesis 1. TCDD induced AhR degradation and the consequent effects	212
7.3.2	Hypothesis 2. Activated autophagy and Cathepsin D.....	218
7.3.3	Hypothesis 3. The effects of autophagy on the TCDD induced phenotype in epidermal equivalents	220
7.4	Future Work	222
7.4.1	Investigating ligand-induced AhR activation	222
7.4.2	Investigating the effects of AhR activation on keratinocyte differentiation	223
7.4.3	Investigating the effects of AhR activation on autophagy and CTSD.....	224
8	References	254

List of Figures

Figure 1.1 The functional domains of the Aryl hydrocarbon Receptor.....	2
Figure 1.2. The Aryl hydrocarbon Receptor pathway.	3
Figure 1.3. Regulatory sequences in the Cathepsin D promoter region.	8
Figure 1.4. The structures of AhR agonists.	16
Figure 1.5. Regulation of differentiation and the specific expression of proteins.	20
Figure 1.6. Schematic representation of the hair follicle.	21
Figure 1.7. The epidermal equivalent model and schematic representation of normal skin.....	26
Figure 1.8. Histology of chloracne.	27
Figure 1.9. Viktor Yushchenko pre-, during and post-chloracne.....	28
Figure 1.10. The processing steps of Cathepsin D Cathepsin D undergoes post translational modifications from inactive pre-pro CTSD to active CTSD.	30
Figure 1.11. Activation of the apoptotic pathway by cathepsin D.	31
Figure 1.12. Maturation of the autophagosome.....	35
Figure 2.1. Vector map of the pGIPZ lentiviral vector.....	49
Figure 2.2. Schematic representation of the transduction and treatment regime of primary keratinocytes with shRNA for AhR knock down epidermal equivalents and Western blot.	50
Figure 3.1. β -NF and ITE cause toxicity in a time and dose dependent manner.	58
Figure 3.2. AhR transcriptional activation was induced by TCDD, β -NF and ITE between 24h and 96h treatment.	62
Figure 3.3. β -Naphthoflavone quenched firefly luciferase activity.	64
Figure 3.4. Dioxane does not increase TCDD-induced XRE-luciferase activation in cell culture.	65
Figure 3.5. Proposed hypothesis for nuclear localization of AhR caused by loss of cell-cell contact.	67
Figure 3.6. Sparse cell confluency can induce AhR translocation to the nucleus.....	68

Figure 3.7. AhR transcriptional activity in keratinocytes is induced by treatment with TCDD, β -NF and ITE.....	72
Figure 3.8. Log dose response curve for AhR-agonists.	72
Figure 3.9. Dose dependent induction of AhR degradation and CYP1A1 by TCDD in primary keratinocytes.	74
Figure 3.10. Comparison of AhR activation by TCDD, β -NF and ITE at day 2.	77
Figure 3.11. Comparison of AhR activation by TCDD, β -NF and ITE at day 8.	78
Figure 3.12. β -NF (nM) induced AhR and CYP1A1 degradation in a time and dose dependent manner.	80
Figure 3.13. Partial agonist α -Naphthoflavone induces AhR transcriptional activity at high concentrations.	81
Figure 3.14. α -Naphthoflavone inhibits ligand induced AhR transcriptional activity.....	85
Figure 3.15. The effects of α -Naphthoflavone on ligand induced AhR activation.	91
Figure 3.16. The effects of α -Naphthoflavone on ligand induced AhR activation.	92
Figure 4.1. TCDD caused decreased thickness of the viable cell layer and compaction of the stratum corneum in the epidermal equivalent model.	107
Figure 4.2. TCDD caused a significant decrease in viable cell layer thickness.	108
Figure 4.3. AhR activation caused dysregulated expression of differentiation markers... ..	111
Figure 4.4. AhR activation does not induce Caspase-3 activation.....	114
Figure 4.5. AhR activation does not increase cleaved Lamin A staining in epidermal equivalents.	116
Figure 4.6. TCDD treatment causes a decrease in nuclear AhR expression in epidermal equivalents..	120
Figure 4.7. AhR knock down induces TCDD-like phenotype in epidermal equivalents... ..	123
Figure 4.8. GFP expression 48h after transduction of primary keratinocytes with lentiviral shRNA.....	125
Figure 4.9. AhR is knocked down by shRNA in monolayer primary keratinocytes.	127

Figure 4.10. AhR knock down by shRNA induces a TCDD-like phenotype.	128
Figure 4.11. GFP expression in epidermal equivalents cultured with shRNA transduced keratinocytes.....	130
Figure 5.1. Formation of the autolysosome and recruitment of LC3 II to the membrane of the autophagosome.	137
Figure 5.2. LC3 II is induced by TCDD treatment in primary human keratinocytes.	139
Figure 5.3. Comparison of the effects of TCDD, β -NF and ITE on p62 and LC3 II at day 2.....	144
Figure 5.4. Comparison of the effects of TCDD, β -NF and ITE on p62 and LC3 II at day 8.....	145
Figure 5.5. The effects of co-treatment with TCDD, β -NF or ITE plus α -NF on autophagy in primary keratinocytes.	152
Figure 5.6 The effects of co-treatment with TCDD, β -NF or ITE plus α -NF on autophagy in primary keratinocytes.	153
Figure 5.7. Bafilomycin A1 induced levels of LC3 II and p62 in primary keratinocytes....	156
Figure 5.8. Characteristic signs of autophagy in TCDD treated epidermal equivalents...	160
Figure 5.9. ITE induced low levels of active autophagy in epidermal equivalents.	161
Figure 5.10. Lamellar bodies fuse with membrane structures in the stratum corneum....	164
Figure 5.11. TCDD and ITE treatment leads to decreased numbers of lamellar bodies in epidermal equivalents.	165
Figure 5.12. Evidence of autophagy targeting lamellar bodies.....	166
Figure 5.13. AhR activation causes desmosomal re-arrangement.....	167
Figure 6.1. Cathepsin D staining increased and became dysregulated with AhR activation.....	179
Figure 6.2. Summary of the effects of AhR activation on CTSD at day 2.	184
Figure 6.3. Summary of the effects of AhR activation on CTSD at day 8.	185

Figure 6.4. Summary of the effects of AhR-agonists and α -NF on Cathepsin D.	193
Figure 6.5. Summary of the effects of AhR-agonists and α -NF on Cathepsin D.	194
Figure 6.6. Blocked autophagic by Bafilomycin A1 inhibits Cathepsin D processing.....	
.....	197
Figure 6.7. Autophagy causes Cathepsin D expression to increase and recruited to the membrane.....	200
Figure 7.1. Hypotheses for AhR-dependent decreased viable cell layer and compacted stratum corneum.. ..	212
Figure 7.2. Molecular characteristics of chloracne.	218

List of Tables

Table 1. Antibody details and fixation methods for IHC analysis.....	42
Table 2. Antibody specificity for IHC.....	43
Table 3. Primary antibodies used for Western blotting.....	46
Table 4. The characteristics of AhR-agonists TCDD, β -NF and ITE.....	52
Table 5. A summary of AhR activation by ligands and inhibition by co-treatment with agonist plus α -NF.....	94
Table 6. A summary of autophagic activation by AhR ligands and inhibition by co-treatment with agonist plus α -NF.....	168
Table 7. A summary of the effects of AhR activation on CTSD.....	201
Table 8. Summary of the effects of AhR activation by TCDD, β -NF and ITE, and inhibition by α -NF in epidermal equivalents.....	208

Abbreviations

AhR	Aryl hydrocarbon Receptor
AhRR	Aryl hydrocarbon Receptor repressor protein
AINT	ARNT interacting protein
α -NF	α -Naphthoflavone
AP-1	Activator protein 1
ARNT	AhR nuclear translocator
β -NF	β -naphthoflavone
BODIPY PA	BODIPY FI-pepstatin A
CTSD	Cathepsin D
CYP1A1	Cytochrome P450 1A1
CYP1B1	Cytochrome P450 1B1
EM	Transmission electron microscopy
ER	Oestrogen Receptor
EROD	7-Ethoxyresorufin O-deethylation
GST	Glutathione-s-transferase
HAH	Halogenated aromatic hydrocarbon
HI	Harlequins Ichthyosis
HIF1 α	Hypoxia-induced factor 1 α
Hsp90	Heat shock protein 90
IHC	Immunohistochemistry
ITE	2-(1'H-indolo-3'carbonyl) thiazole-4-carboxylic acid methyl ester
LC3	Microtubule-associated light chain 3B
MAPK	Mitogen-activated protein kinase
O/N	Over night
PAH	Polycyclic aromatic hydrocarbon
PF	Paraformaldehyde
RT	Room temperature
TBS-T20	TBS-Tween 20
TCDD	2,3,7,8-tetrachlorodibenzo- <i>p</i> -dioxin
TCDF	2,3,7,8-tetrachlorodibenzofuran
TGM-1	Transglutaminase-1
VCL	Viable cell layer
XRE	Xenobiotic response element

Acknowledgements

I would like to thank my supervisors Prof. Nick Reynolds and Prof. Faith Williams for their endless help, guidance and support throughout my PhD. You have made this experience a great one. Thanks to Dr. Mark Graham for his help and guidance both in Newcastle and at AstraZeneca and also the funding of this project. Thanks also to BBSRC for funding this CASE studentship with AstraZeneca.

I would like to thank Dr. Penny Lovat and Dr Jane Armstrong for their advice and collaboration on autophagy, and also for providing great support and good fun at all times. Thanks to Carole Todd for constant help and advice – without you this place would not work! Thanks to the Reynolds group and all in Dermatology for making this an enjoyable and memorable time.

Specific thanks to Kate Brown for help with immunostaining, Stephanie Roberts for bioinformatics and Simon Brocklehurst for EM, all at AstraZeneca. Thanks to Olaf Heidenrich for 293T cells and advice on lentiviral work and Alex Laude and Trevor Booth in the Bioimaging unit at Newcastle University for their help, advice and patience.

Many thanks to my friends and family who have supported me throughout my PhD. Thanks to my friends for their constant support and providing excellent diversions from my work in the lab through coffee breaks, dinners and tequila time.

Finally a very special thank you to my parents, Mike and Hannah and to my sisters, Liz and Hannah for their amazing support during my PhD. I could not have done this without you all.

Published Abstracts arising from this work

XII International Congress of Toxicology, July 2010, Barcelona, Spain

The Aryl hydrocarbon Receptor in Human Keratinocytes: Relevance to Chloracne
Forrester, A.R., Graham, M., Williams, F.M., Reynolds, N.J.

European Society of Dermatological Research, September 2010, Helsinki, Finland

Activation of the Aryl hydrocarbon Receptor and its relevance to chloracne.
Forrester, A.R., Graham, M., Williams, F.M., Reynolds, N.J. Journal of Investigative
Dermatology 2010 (130)

Autophagy Keystone Symposia, March 2011, Whistler, Canada

Dioxin (TCDD) induces autophagy in keratinocytes
Forrester, A.R., Graham, M., Williams, F.M., Reynolds, N.J.

Declaration

I declare that the composition and content of this thesis is my own work unless stated otherwise in the text. I certify that none of the material in this thesis has been submitted by me for any other qualification at this institute or any other.

1. Introduction

1.1 Aryl hydrocarbon Receptor

The aryl hydrocarbon receptor (AhR) is a member of the basic Helix-Loop-Helix PER-ARNT-SIM (bHLH PAS) family of ligand induced transcription factors (Burbach et al., 1992). The AhR plays an important role in the transduction of chemical signals (for example hormones and xenobiotics) to their cellular effects by induction of certain genes. These receptors have been well studied for their toxicity mediating roles, but also have important physiological roles that like the AhR, may not yet be fully elucidated. Many of their roles are converging, and cross talk between the receptors is a well known phenomenon which increases the potential number of genes regulated by their activation greatly.

AhR activation induces transcription of a large battery of genes including many involved in phase I and II metabolism (Akintobi et al., 2007; Harris et al., 2002a; Harris et al., 2002b; Kohle and Bock, 2007) reviewed in (Schrenk, 1998).

1.1.1 AhR pathway activation

1.1.1.1 *The structure of AhR*

The AhR structure consists of a basic helix-loop helix domain which is the site for hsp90 binding, dimerization and DNA binding, Per-Arnt-Sim A and B domains for ligand, hsp90 binding and dimerization and a Q rich domain for transcriptional activation (Figure 1.1) (Burbach et al., 1992; Dolwick et al., 1993; Ema et al., 1992; Fukunaga and Hankinson, 1996; Fukunaga et al., 1995). The ligand binding site of the human AhR has recently been shown to contain 4 available binding pockets (Salzano et al., 2011). Each ligand has a preferred binding pocket that is thought to be based on the volume of the binding pocket and size of the ligand, however most ligands are able to bind more than one pocket. Within each pocket is a number of possible binding sequences and these sequences correlate to the differences in mouse and human AhR sequences – the mouse AhR has additional binding sites to human AhR. It is suggested that the presence of different binding pockets and sequences within these pockets could provide differential ligand binding for both endogenous and exogenous ligands, leading to differential AhR activation and regulation of differential target genes. It also opens up the possibility of interactions between ligands (as opposed to the well documented

interactions between nuclear receptors (Kolodkin et al., 2010)), which could help to explain the wide ranging effects of AhR activation, especially in its lesser studied physiological role (Salzano et al., 2011).

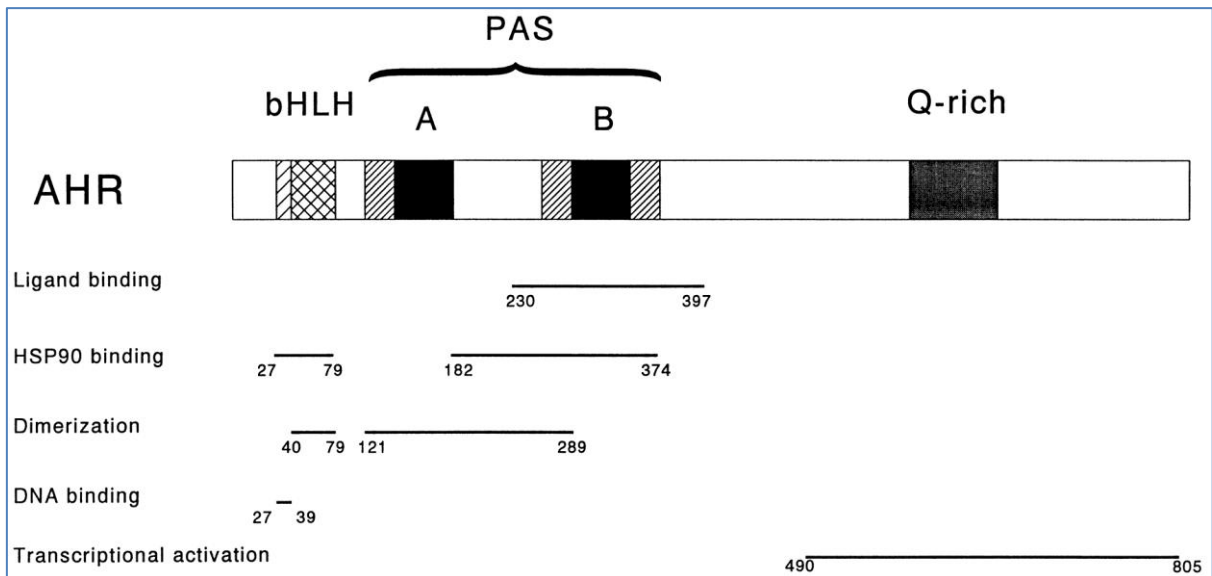


Figure 1.1 The functional domains of the Aryl hydrocarbon Receptor. The AhR is a member of the family of bHLH PAS transcription factors. The AhR is highly conserved across species. High levels of structural homology are present between mammalian forms of AhR for example human and mouse PAS domains show 87% homology (Hahn et al., 1997) and the differences in sequence are found in the different ligand binding pockets (Salzano et al., 2011). Figure modified from (Fukunaga et al., 1995)

1.1.1.2 Cytoplasmic AhR

The AhR activation pathway is summarised in Figure 1.2. In its inactivated state, the AhR resides in the cytoplasm in a complex with its chaperone proteins: the AhR interacting protein (AIP) (Ma and Whitlock, 1997), p23 (Nair et al., 1996) and heat shock protein 90 (hsp90)(Fukunaga et al., 1995; Perdew, 1988; Pongratz et al., 1992)(Figure 1.2). This complex has multiple functions involving keeping the AhR localised in the cytoplasm and repressing conformational changes that occur during activation (reviewed in (Carlson and Perdew, 2002; Petrusis and Perdew, 2002)). Chaperone complexes are thought to be common for nuclear receptors such as the AhR and the progesterone receptor and some chaperone molecules are common to more than one nuclear receptor (Nair et al., 1996). This project does not focus on these proteins, but an overview is included here as background on the regulation of the AhR.

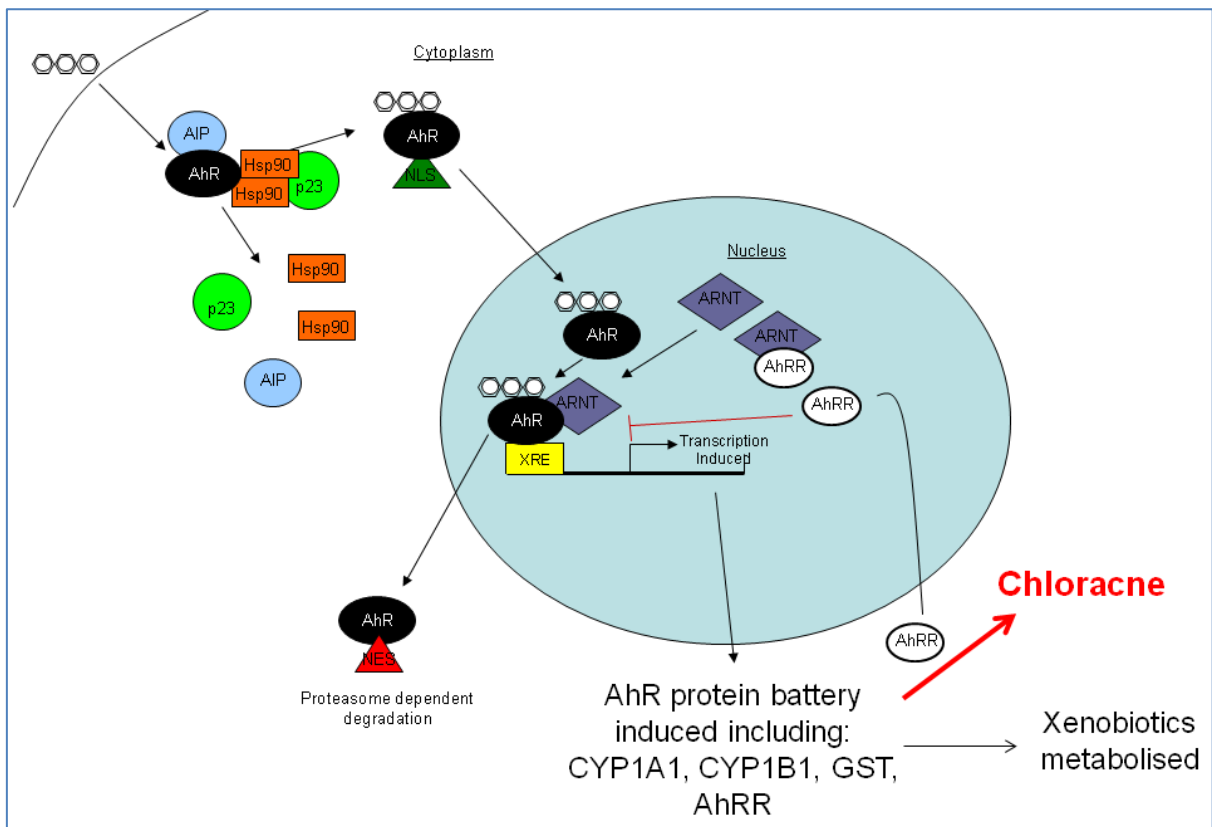


Figure 1.2. The Aryl hydrocarbon Receptor pathway. The inactive AhR resides in the cytoplasm with its chaperone proteins. Upon ligand binding, the chaperone proteins are released and the AhR translocates to the nucleus where it binds ARNT. The AhR-ARNT dimer binds the XRE, inducing transcription of a battery of genes involved mainly in phase I and phase II metabolism. Chloracne is a result of pathway activation specific to TCDD.

1.1.1.3 The chaperone molecules

AhR interacting protein (AIP or XAP2) is an immunophilin like protein that is part of the AhR-hsp90 complex (Ma and Whitlock, 1997), binding to both AhR and hsp90 in the absence of ligand (Bell and Poland, 2000). AIP binding to the AhR inhibits nuclear translocation by inhibiting importin β recognition of the NLS (Petruilis et al., 2003) and ligand binding therefore breaks the AIP-hsp90-AhR complex down which is thought to be required for AhR-hsp90 stability (Bell and Poland, 2000). Over expression of the AIP increases TCDD-induced CYP1A1 in a mouse hepatoma cell line (Ma and Whitlock, 1997) and AIP is required for AhR-dependent up-regulation of certain AhR-induced proteins; CYP1B1 and AhRR require AIP but CYP1A1 and CYP1A2 do not (Ma and Whitlock, 1997; Nukaya et al., 2010).

Heat shock protein 90 (hsp90) directly binds to cytoplasmic AhR. Binding is required for repression through holding the AhR in an inactive state in the cytoplasm, repressing

background/ligand-independent activation of the AhR (Henry et al., 1999; Whitelaw et al., 1995) and its dissociation from the AhR is required for AhR activation (Carver et al., 1994). One mechanism that contributes to this is the repression of the conformational change of the AhR to having a high DNA binding affinity (Pongratz et al., 1992). Removal of hsp90 from the AhR complex can promote ligand-independent translocation (Pollenz and Buggy, 2006) but the AhR can translocate without dissociation from hsp90 although the hsp90 inhibits AhR-ARNT dimer formation (Heid et al., 2000). p23 is a chaperone molecule for hsp90 and regulates the activation of hsp90 and its binding to the AhR. p23 does not directly bind the AhR (Cox and Miller, 2004; Hollingshead et al., 2004; Kekatpure et al., 2008).

1.1.1.4 Translocation and DNA binding

Upon activation, the ligand binds to the PAS domain of the AhR (Fukunaga et al., 1995) releasing the chaperone proteins (hsp90, AIP, p23) and inducing conformational changes of the AhR (Gasiewicz and Bauman, 1987; Henry et al., 1994). The changes that are induced are an increased AhR affinity for DNA, decreased AhR affinity for the ligand and an increased ability to bind ARNT (Carlson and Perdew, 2002; Petrulis and Perdew, 2002). These changes are induced to varying degrees by different ligands (under different conditions). For example TCDD binding induces a high DNA affinity form of the AhR (Gasiewicz and Bauman, 1987). But when α -NF binds AhR (in rat hepatic cytosol extracts), AhR activation is only induced to very low levels by high concentrations of α -NF. This is because the conformational changes induced by α -NF result in a low DNA affinity form of the AhR (Gasiewicz, 1991). The removal of the chaperone proteins also reveals the nuclear localisation signal (NLS) allowing the AhR to translocate to the nucleus (Ikuta et al., 2004; Ikuta et al., 2000; Song and Pollenz, 2002). Here it forms a dimer with ARNT (AhR nuclear translocator, described in more detail in the following paragraph)(Heid et al., 2000) and binds the xenobiotic response element (XRE) (Fukunaga et al., 1995; Whitelaw et al., 1993). The XRE is the AhR specific promoter region with a core sequence found upstream of genes directly regulated by AhR (Fujisawa-Sehara et al., 1988; Wang et al., 1998).

Included in this battery of genes is the AhR repressor protein (AhRR) which after translation, returns to the nucleus and competitively inhibits activation by forming a

dimer with ARNT and binding the XRE domain (Akintobi et al., 2007; Evans et al., 2008; Mimura et al., 1999).

1.1.1.5 ARNT

ARNT(also called hypoxia inducible factor 1 β (HIF1 β)) is a bHLH PAS protein similar to AhR and is required for AhR-XRE binding and activation, by inducing XRE binding ability in AhR (Hankinson, 1995; Reyes et al., 1992). As an integral member of the PAS proteins, it is involved in other pathways. This is the basis for a hypothesis on the mechanism of differential effects caused by TCDD; that the sequestering of ARNT in the TCDD-activated AhR pathway may cause inhibition of other ARNT mediated pathways. ARNT can dimerise with other molecules other than AhR and elicit its own ARNT specific effects: ARNT heterodimerises with HIF1 α , binding an hypoxic response element and up regulating its own battery of genes (Hogenesch et al., 1997). It can also form a homodimer and bind constitutively to the E box, shown to regulate development in drosophila (Antonsson et al., 1995). The importance of ARNT in development is demonstrated in knock out mice. Pups do not survive for more than 10.5 days due to developmental defects such as angiogenesis (Maltepe et al., 1997).

Pollenz et al. have shown that induction of the hypoxia pathway in human, mouse and rat hepatoma cells reduces TCDD-induced AhR-dependent CYP1A1 induction. Importantly, Pollenz et al showed that neither TCDD treatment nor hypoxia induced changes in levels of ARNT (Pollenz et al., 1999). Sadek et al. have identified AINT, the ARNT interacting protein, in many tissues of murine embryos that provides a link between ARNT and development. AINT is expressed in the cytoplasm of embryonic cells, and an overexpression (that can occur during embryogenesis (Aitola et al., 2003)) can cause ARNT to become cytoplasmic (Sadek et al., 2000). The effects of this may be an inhibition of the AhR pathway, but the authors claim that the AINT induced cytoplasmic localisation of ARNT can be overruled by AhR ligand-dependent activation, suggesting the AhR pathway may have priority over other ARNT pathways (Pollenz et al., 1999; Sadek et al., 2000)

In skin, ARNT plays a role in differentiation during development as demonstrated by keratinocyte targeting of ARNT knock out in mice. Geng et al showed that ARNT knock out mice exhibited compacted stratum corneum, and abnormal expression of involucrin, filaggrin and loricrin indicating abnormal terminal differentiation. Ceramide metabolism was also shown to be altered by ARNT knock out, resulting in corneosome retention

(Geng et al., 2006). A suggested link between ARNT and keratinocyte differentiation is the moderate hypoxic environment in the epidermis which increases with differentiation (Evans et al., 2006). Wier et al. show that acute hypoxia affects HIF1 α , but ARNT remains unaffected. Chronic hypoxia induced a post-translational decrease in ARNT (Weir et al., 2011), which would suggest that the AhR pathway would be compromised in this situation.

However, because of the complexities of this pathway and evidence of both AhR-dependent and independent pathways, ARNT was not considered an useful target to dissect out the mechanisms of AhR activation in skin or the pathophysiology of chloracne.

1.1.1.6 Molecular cross talk

There is known to be cross reactivity between the ligands and downstream effects of receptors such as the AhR, oestrogen, retinoic acid and progesterone receptors (Kolodkin et al., 2010; Nair et al., 1996; Wang et al., 1998). This can be the result of interactions at different levels of the receptor pathways, for example chaperone molecules (described in section 1.1.1.3) are common to a number of nuclear receptors (reviewed in (Nair et al., 1996), ligand promiscuity for receptors, or cross talk between response elements of receptors. This contributes to the large number of compounds that through activating receptors can exert very wide ranging and differential effects.

Many ligands may have the ability to activate more than one receptor. For example statins, which are well known for their wide ranging cellular effects, have been shown to differentially activate the constitutive androstane receptor (CAR), farnesoid X-receptor (FXR) and pregnane X-receptor (PXR), exerting the highest activity on PXR, revealing a mechanism for the wide ranging effects of statin treatment (Howe et al., 2011). Interactions between response elements can result in similar transcriptional regulation of proteins at low ligand concentrations, that at high concentrations become more receptor specific, demonstrated by Bailey et al. in the case of the PXR and vitamin D receptor (VDR) (Bailey et al., 2011).

There is also a promoter region that is common to a wide range of genes. The Sp1 binding site (TATA box) is often co-expressed with other response elements but is not robust enough to induce transcription without the presence of another transcription factor (Wang et al., 1998). It is involved in the regulation of maximal basal expression of

proteins (Fitzgerald et al., 1998; Wang et al., 1998; Wang et al., 1999) and the differential effects of interactions with inactive AhR compared to active AhR suggest a physiological role for the AhR (Wang et al., 1998). The joint regulation by receptors and Sp1 is complex, but a good example is the regulation of Cathepsin D (CTSD) by the oestrogen receptor (ER) and AhR (Figure 1.3). CTSD is a lysosomal aspartic protease which has important roles in the regulation of terminal differentiation in keratinocytes (section 1.4.3) and autophagy (section 1.4.2). The following studies were performed in the breast cancer cell line MCF-7, as the origin of this work is from the anti-oestrogenic capabilities of TCDD on oestrogen-dependent tumours, with an aim for use as a therapeutic target, however due to the importance of CTSD in epidermal differentiation, this data can be extrapolated; there are studies showing similar behaviour of CTSD in HaCaTs, which suggest conserved responses between human keratinocytes and MCF-7 cells (Vashishta et al., 2007). CTSD is regulated by both “housekeeping” (the Sp1 binding site, TATA box) and “inducible” response elements (AhR-ARNT response element, XRE) and both Sp1 and AhR-ARNT are required for maximal basal activity (Wang et al., 1999). Sp1 directly binds to the AhR as well as the TATA box, inducing maximal basal activity (Kobayashi et al., 1996; Wang et al., 1998; Wang et al., 1999). TCDD is known to have anti-oestrogenic effects when the XRE is present with ER and Sp1 binding sites, suggesting some XREs may be inhibitory (Gierthy et al., 1993). In the absence of the ER response element, the ER binds the Sp1 with no interaction with the DNA itself (Porter et al., 1997) and can also regulate transcription via the Sp1. The Sp1 protein is the intermediate factor between AhR and ER, without Sp1, the nuclear receptors do not interact (Wang et al., 1998), suggesting Sp1 may contribute to cross talk between receptors. It has been suggested that the basal expression of AhR itself is regulated by Sp1 (Fitzgerald et al., 1998). This is described in more detail in section 1.4.1.

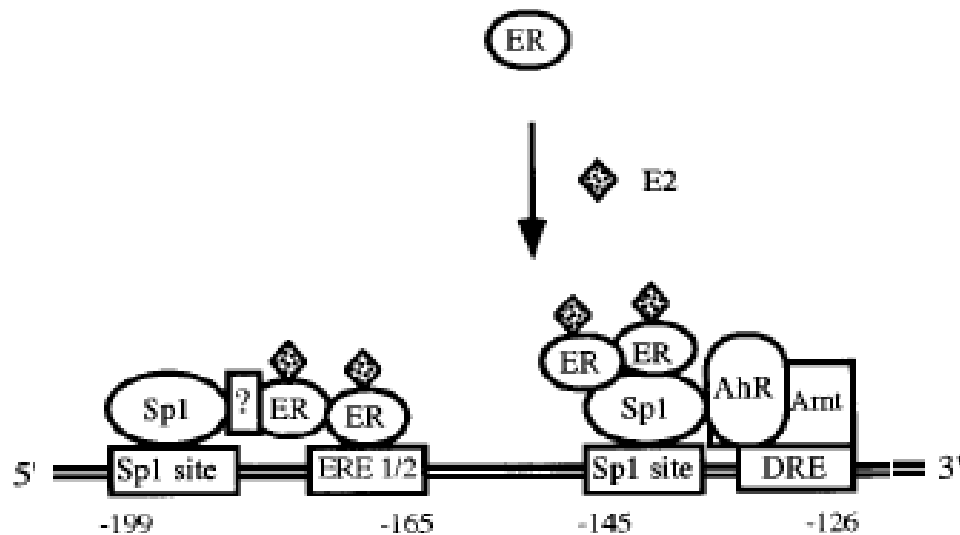


Figure 1.3. Regulatory sequences in the Cathepsin D promoter region. ER and AhR interact via SP1 in absence of the ER response element (ERE). ER, Oestrogen receptor; DRE, dioxin response element. Figure modified from (Wang et al., 1998).

1.1.1.7 Ligand-independent AhR activation

The AhR has been shown to become activated ligand-independently by loss of cell-cell contact. This has been demonstrated in the human keratinocyte cell line HaCaT, by showing sparse confluency inducing nuclear translocation of the AhR (Ikuta et al., 2004). Sparse confluency also induced transcriptional activation of the AhR (Ikuta et al., 2000; Sadek and Allen-Hoffmann, 1994a, b). This suggests a physiological role for AhR potentially in development and wound healing.

1.1.1.8 Degradation

Once activation has occurred, the AhR can be degraded within the nucleus by the 26S proteasome (Song and Pollenz, 2002). It can also be exported to the cytoplasm by revealing the nuclear export signal (Ikuta et al., 2004), where it is degraded by the cytoplasmic proteasome (Davarinos and Pollenz, 1999; Pollenz, 2007). The timescale for both pathways in the HepG2 cell line is ~3 hours (Song and Pollenz, 2002) but varies depending on cell type and the ligand that induced activation (Swanson and Perdew, 1993). Onset of TCDD induced AhR degradation in human cell lines ranges from 2-4 h and may last over 16h (Ikuta et al., 2000; Pollenz and Buggy, 2006; Sadek and Allen-Hoffmann, 1994a, b).

AhR degradation is used as a readout of AhR activation, but it isn't exclusively ligand-dependent. Geldanamycin is an hsp90 specific binding protein (Grenert et al., 1997), not a ligand for the AhR, that removes the hsp90 from the AhR allowing translocation and mimicking a step of ligand-induced activation. The AhR translocates to the nucleus and is degraded without binding the XRE (Pollenz and Buggy, 2006; Song and Pollenz, 2002).

The duration of ligand-dependent AhR degradation depends upon the residency of the ligand and forms the basis for a common hypothesis that differential effects of the AhR pathway depend in the residency of the ligand. TCDD induces sustained AhR degradation because of its low metabolic clearance, with ligands that are more quickly metabolised allowing recovery of AhR levels more quickly (Berghard et al., 1992; Henry et al., 2010). After ligand-dependent AhR degradation, the AhR can recover to higher levels than basal (Franc et al., 2001; Sloop and Lucier, 1987).

1.1.2 AhR expression and activity

1.1.2.1 AhR in Humans

AhR was first identified in skin as the mediator of benzo[a]pyrene toxicity (Levin et al., 1972) and even though AhR expression is ubiquitous, its levels of expression in tissues varies greatly. Dolwick et al show AhR mRNA expression in human tissues to be highest in placenta followed (in order of decreasing level) by lung, heart, pancreas, kidney, brain, muscle and liver (Dolwick et al., 1993). Expression in basal keratinocytes is low but is shown to increase with differentiation (Ray and Swanson, 2003).

Importantly, AhR activation in keratinocytes increases with differentiation (Coomes et al., 1983; Du et al., 2006a; Jones and Reiners, 1997; Pohl et al., 1984). AhR expression can also be increased in diseased states, for example levels of AhR protein in human lung carcinoma (Lin et al., 2003) and AhR mRNA in pancreatic cancer cells is increased strongly compared to normal pancreatic cells (Koliopoulos et al., 2002). This suggests that AhR has potential as a therapeutic target.

AhR expression and activity do not necessarily correlate – the presence of the AhR repressor (AhRR) protein is also variably expressed in tissues basally, as well as being directly upregulated by AhR activation. High levels of basal expression of the AhRR will result in low levels of AhR activity resulting in constitutively low AhR activity in certain

cells (Gradin et al., 1999). The induction of AhR expression also forms a negative feedback loop to tightly regulate ligand-induced AhR activation. Tight regulation of the AhR is crucial for maintaining homeostasis in the cell as over expression of the AhR results in severe toxicity in animals (Brunnberg et al., 2006; Tauchi et al., 2005) and the observation of increased AhR in tumours (Koliopanos et al., 2002; Lin et al., 2003) suggests overexpression may play a role in carcinogenesis.

1.1.2.2 AhR in Animals

There are high levels of interspecies variation in AhR expression and activity (Dere et al., 2011; FitzGerald et al., 1996). Levels of AhR response varies greatly between rat strains including some strains that are resistant to toxicity (Franc et al., 2001; Poland and Glover, 1990). This is not necessarily dependent on AhR expression regulation (degradation or recovery) (Franc et al., 2001), but is a result of variable AhR affinity for the ligand and DNA in different rat strains due to sequence differences in the AhR. Sequence differences between rat and human AhR also account for differences in affinity between humans and animals (Ema et al., 1994; Okey et al., 2005; Ramadoss and Perdew, 2004; Salzano et al., 2011).

AhR activation has been studied in variable strains to distinguish differential effects of AhR activation and the causes of toxicity. Although they have not revealed the differential causes of toxicity, they have provided a large amount of data on variable AhR activity inter- and intra-species. Alvares et al showed a 4 fold increase in basal AhR activity of primary keratinocytes from humans to rats and a 7 fold increase in basal AhR activity from humans to mice (Alvares et al., 1973). In AhR activity assays, there was a ~75 fold increase in basal AhR activity from skin to liver. This demonstrates the low basal activity of AhR in skin compared to liver (Raza and Mukhtar, 1993).

1.1.2.3 Wide ranging roles of AhR

The effects of AhR activation change depending on which cell type is being studied. As inducible AhR is present in a wide range of cell types, there is a wide range of cell-specific effects caused by AhR activation. AhR activation in primary keratinocytes causes early onset of terminal differentiation (Du et al., 2006a; Greenlee et al., 1985; Loertscher et al., 2001b; Osborne and Greenlee, 1985). There are also reports on TCDD-induced immortalisation of keratinocytes (Ray and Swanson, 2004). Fibroblasts were reported to be quite resistant to AhR-induced toxicity because of the high levels of

AhRR expressed (Gradin et al., 1999), however this seems to be specific to human skin fibroblasts and the AhR pathway in other fibroblasts remains active (Akintobi et al., 2007; Beedanagari et al., 2010; Cho et al., 2004; Henry et al., 2010). The AhR is also known to regulate the cell cycle, with AhR agonists suppressing the cell cycle (ligand dependently) in rat hepatoma cell lines (Reiners et al., 1999) and TCDD suppressing senescence in primary keratinocytes associated with differentiation, and increasing the amount of cells in the sub G1/G0 stage of the cell cycle (Ray and Swanson, 2003).

In more widely ranging cell and tissue types, AhR has been shown to directly induce expression of breast cancer resistance protein (Tan et al., 2010) and to have anti-oestrogenic effects (Wormke et al., 2003; Zhang et al., 2009), induce production of sperm (Ohbayashi et al., 2001) and regulate inflammatory (Tsuji et al., 2011; Vondracek et al., 2011) and immune responses (Simones and Shepherd, 2011; Stockinger et al., 2011). TCDD is also known (via AhR) to be carcinogenic in animals (although its status as a human carcinogen is under regular review) (Gelhaus et al., 2011; Shi et al., 2009). AhR has been shown to modulate susceptibility to apoptosis (Park et al., 2005; Reiners and Clift, 1999) and play a role in lysosomal fragility, the first step of CTSD induced apoptosis (Caruso et al., 2006). This is described in more detail in section 1.4.2 and Figure 1.11.

1.1.3 AhR-dependent toxicity

As described in the last paragraphs, the AhR pathway elicits wide ranging effects through both activation and absence of the AhR. A brief overview of the toxicities associated with the pathway follows.

Chloracne is a human and dioxin specific toxicity described in detail in section 1.3. There are animal models that exhibit chloracne-like disease (for example the rabbit ear model (Hambrick, 1957) and hairless mouse model (Panteleyev et al., 1997)), but because of differences in the hair follicle (the main site of TCDD induced changes causing chloracne) between human and animal, extrapolation from the animal models to human disease is difficult. The animal models are reviewed in (Panteleyev and Bickers, 2006). Chloracne-like epidermal lesions are known to occur in murine skin in response to both AhR knock out (Fernandez-Salguero et al., 1997) and constitutive AhR expression (Brunnberg et al., 2006; Tauchi et al., 2005).

An industrial accident in Seveso, Italy, which exposed residents to a cloud containing chlorophenols mainly identified as TCDD, resulted in chemical burns, diarrhoea and vomiting. Chloracne followed 30-60 days post exposure and had improved in most cases 2 years post exposure (Caputo et al., 1988). Many long term studies have been carried out on this cohort, identifying long term effects of TCDD toxicity in humans including the possible increased risk of breast cancer and decreased fertility (Mocarelli et al., 2008; Pesatori et al., 2009)

In animals, TCDD is highly toxic carcinogen (Huff et al., 1994) and a potent teratogen causing effects in rodents, most importantly cleft palate and hydronephrosis (Abbott et al., 1999; Mimura et al., 1997) reviewed in (Couture et al., 1990; Poland and Knutson, 1982; Schwetz et al., 1973)). The most effective method used to show the extent of the role of AhR is by using genetic AhR knock down. Fernandez-Salguero et al developed AhR knock out mice (-/-) and have shown AhR knock down to cause developmental defects in the heart, uterus, gastric tract, liver, spleen and skin and 23% of the mice died (Fernandez-Salguero et al., 1997). 100% developed hypertrophic but normally formed hearts, 100% showed T and B cell depletion, 81% exhibited hepatic vascular hypertrophy. 53% developed thickening and scaling of the skin. Interestingly, when the epidermal lesions began to form they caused alopecia and abnormal follicle formation. This caused epithelial hyperplasia, hyper granulosis and changes in the shape of the

hair (Fernandez-Salguero et al., 1997). Changes in follicles and hair development are characteristic of chloracne, see section 1.3 for details.

The effects of constitutive AhR expression bear similarities to AhR knock out. Brunnberg et al. showed that mice with constitutively active AhR exhibited hyperplasia of the liver, kidney and heart, with a decrease in thymus size (Brunnberg et al., 2006). This correlates well with the chronically TCDD treated model, suggesting perhaps paradoxically, that long term effects may be caused by increased AhR levels; chronic treatment has been shown to result in increased AhR levels at recovery (Franc et al., 2001; Sloop and Lucier, 1987), however the AhR knock out model, once again exhibits similar effects to the TCDD treated and constitutively active models. In summary, epidermal lesions are exhibited in AhR knock out, constitutively active and TCDD treated animal models (reviewed in (Poland and Knutson, 1982) which remains to be fully explained.

1.1.3.1 Physiological roles of AhR

The AhR is highly conserved and ubiquitously expressed (Hahn et al., 1997) suggesting it has an important physiological role, however this has not yet been elucidated. The AhR has been studied in detail as a mediator of toxicity, but few endogenous ligands and roles have been identified.

The endogenous ligands 2(1'H-indole-3'-carbonyl)-thiazole-4-carboxylic acid methyl ester (ITE) (Henry et al., 2006; Song et al., 2002) and 6-Formylindolo[3,2-*b*]carbazole (FICZ) (Wei et al., 2000) are the first endogenous AhR agonists to be discovered. ITE is a potent AhR ligand which was isolated from porcine lung and is described later in this chapter (section 1.1.4). FICZ was isolated as a tryptophan photoproduct (Wei et al., 1999) in skin/keratinocytes. Both induce CYP1A1 transiently, suggesting that binding to AhR is short lived possibly because they are metabolised rapidly and as physiological ligands this would be expected allowing efficient endogenous pathway signalling. FICZ is metabolised by CYP1A1 and CYP1A2 (Bergander et al., 2004). It has been suggested that FICZ mediates some of the UV effects in skin (Jux et al., 2011; Wincent et al., 2009).

TCDD activated AhR is known to induce anti-oestrogenic effects via the Sp1 protein and therefore antitumour effects by decreasing the overexpression of CTSD (Chen et al., 2001; Gierthy et al., 1993; Westley and May, 1987). However, non-ligand bound AhR is thought to be required for maximal basal expression of CTSD (Wang et al., 1998; Wang et al., 1999). This is described in more detail in section 1.4.1.

1.1.4 Ligands

1.1.4.1 General Ligands

The AhR is known to be activated by a wide range of compounds, the structure of which are normally planar aromatic molecules. Ligands are polycyclic aromatic hydrocarbons (PAH)(Ohura et al., 2007) or halogenated aromatic hydrocarbons (HAH)(Okey et al., 1994), which bind with a range of affinities for the AhR and induce changes in the AhR which result in varying degrees of AhR affinity for ligand, ARNT and DNA as described in section 1.1.1 (Gasiewicz and Bauman, 1987; Gasiewicz, 1991; Henry et al., 1994; Petrulis and Perdew, 2002). AhR agonists are known to be able to exert differential AhR-dependent effects to each other, for example TCDD induces TGM-1 mRNA and protein expression and cross linking activity, while β -NF does not (Du et al., 2006a) and there are differences in regulated genes, binding regions and binding sites between 3-methylcholanthrene (3-MC) and TCDD (reviewed in (Safe, 2010)).

1.1.4.2 AhR Agonists

TCDD

The most potent AhR ligand is 2,3,7,8-tetrachlorodibenzo-p-dioxin (TCDD). It is a planar halogenated aromatic hydrocarbon, the classic shape for an AhR agonist (Figure 1.4 A), with high-affinity for the AhR, is highly lipophilic and its metabolism is basally low (Henry et al., 2006; Henry et al., 2010; Kedderis et al., 1993) but can be induced to slightly higher levels by its own activation of the AhR (Neal et al., 1982; Sorg, 2009; Sutter et al., 2010). It is known to cause chloracne (Geusau et al., 2001; May, 1973; Schwetz et al., 1973) and the best example of this is the poisoning of Viktor Yushchenko (Sorg, 2009) which will be described in more detail in section 1.3. TCDD is a potential human carcinogen (Huff et al., 1994; Pesatori et al., 2009). The effects of TCDD have been well characterised *in vivo* (Couture et al., 1990; Pohjanvirta et al., 1999; Poland and Knutson, 1982; Schwetz et al., 1973) and *in vitro* (Loertscher et al., 2002; Loertscher et

al., 2001b; Okey et al., 1994; Osborne and Greenlee, 1985; Sloop and Lucier, 1987) as described in the previous sections.

TCDD induces early onset of terminal differentiation in keratinocytes *in vitro* (Geusau et al., 2005; Greenlee et al., 1985; Loertscher et al., 2001a; Loertscher et al., 2001b; Sutter et al., 2011) by direct AhR-dependent regulation of filaggrin (Sutter et al., 2011) and indirect increase of expression and activity of TGM-1 (Du et al., 2006a). It is known to induce a decrease in keratinocyte number independent of apoptosis (Loertscher et al., 2001a).

β-NF

β-Naphthoflavone (β-NF) is a polycyclic aromatic hydrocarbon (Figure 1.4 B) that has low-affinity for the AhR and low-residency with rapid clearance by CYP1A1 and CYP1A2 (Berghard et al., 1992; Maier et al., 1998; Song et al., 2002). It is known to induce the AhR battery of genes transiently because of its high metabolism (Berghard et al., 1992; Carver et al., 1994; Harris et al., 2002a), which is induced by AhR activation. β-NF is also known to induce AhR-dependent toxicities in rodents (Raza et al., 1992; Raza and Mukhtar, 1993; Tilton et al., 2008).

In keratinocytes, β-NF is known to induce aspects of terminal differentiation but not TGM-1 induction (Du et al., 2006a; Khan et al., 1992). Its activity is also known to induce AhR activation most highly in human sebaceous glands than differentiated human keratinocytes and basal keratinocytes at lowest levels (Harris et al., 2002a).

ITE

2(1'H-indole-3'-carbonyl)-thiazole-4-carboxylic acid methyl ester (ITE) is a more recently characterised AhR agonist (Figure 1.4 C). It is highly potent (~5 fold higher than β-NF, equal to potency of TCDD) but has a low-affinity for the AhR (roughly equal to that of β-NF) (Henry et al., 2006; Song et al., 2002). ITE is known to induce the AhR battery transiently (Henry et al., 2010) because of its presumed fast metabolism (and low-residency) based on the known metabolism of FICZ; as endogenous molecules, they must be cleared quickly to convey effective pathway regulation (Wincent et al., 2009).

ITE has not yet been tested in keratinocytes, but some effects of ITE have been reported to be similar to those of TCDD in vitro (Henry et al., 2010; Simones and Shepherd, 2011). Interestingly, ITE has been shown to inhibit TGF β 1-induced differentiation of primary corneal fibroblasts. Lehmann et al. use these cells as a model for myofibroblasts and scarring, and therefore conclude ITE could inhibit scar formation. This demonstrates cross talk of the AhR agonist on TGF β 1 signalling that had not been reported previously (Lehmann et al., 2011).

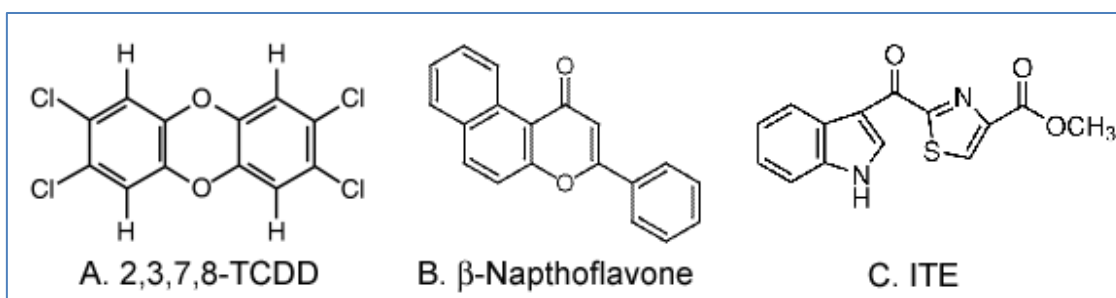


Figure 1.4. The structures of AhR agonists. AhR agonists are commonly planar aromatic molecules that are often halogenated or chlorinated, hence the term “chloracne”.

1.1.4.3 Pharmacological Inhibition of the AhR Pathway

Inhibitors of the AhR pathway include man made inhibitors such as α -NF (Merchant et al., 1990), 3-methoxy-4’nitroflavone (Henry et al., 2006) and naturally occurring compounds such as curcumin (Nishiumi et al., 2007). A relatively new AhR antagonist CH-223191 was defined that showed inhibition of TCDD-induced AhR activation in HepG2 and blocked TCDD induced toxicity in mice (Kim et al., 2006) however recently it was reported to be a specific inhibitor of halogenated aromatic hydrocarbons (Zhao et al., 2010). This is the first example of a ligand specific inhibitor for the AhR.

The mechanisms of inhibition vary between these antagonists. Firstly, α -NF is a partial agonist, inducing AhR-XRE binding in mouse hepatoma cells at concentrations equal to or higher than $\sim 1\mu\text{M}$ (Gasiewicz, 1991). Gasiewicz et al. suggest that α -NF inhibition of the AhR is a result of α -NF directly binding the AhR and inducing a low-DNA, high ligand affinity form of AhR. This causes an “inactive” form of AhR with either no binding or very transient binding to the XRE, competitively blocking higher affinity agonists from binding the AhR and forming high DNA affinity forms of AhR (Gasiewicz, 1991; Merchant et al., 1990; Santostefano et al., 1993). Nishiumi et al demonstrates that the

complete antagonist curcumin blocks the formation of the AhR-ARNT dimer by inhibiting protein kinase C phosphorylation of the AhR and ARNT (Nishiumi et al., 2007). These differential mechanisms of inhibition demonstrate the differences between ligands with partial agonist activity and full AhR inhibitors.

1.2 Normal human skin

The skin forms a protective barrier controlling water loss from the body, thermal regulation and it metabolises compounds entering the body. It consists of the dermis, a tough, elastic, thick layer mainly composed of collagen and connective tissue that provides protection from mechanical stress. It also contains fibroblasts and migratory cells involved in the inflammatory response. The epidermis is mainly composed of keratinocytes but also includes melanocytes and langerhans cells. This layer provides the functional barrier against chemical stress and maintenance of appendages such as the follicle, including the sebaceous gland and sweat glands pass through a number of layers including dermis and epidermis (Wolff et al., 2008).

1.2.1 Keratinocyte differentiation

The epidermis consists of several viable cell layers (VCL) that varies in thickness depending on the site of the body and a cornified layer (the stratum corneum) consisting mainly of keratinocytes. The VCL is a constantly renewing tissue where keratinocytes proliferate and then differentiate up into the stratum corneum, where cells become enucleated and are metabolically active. Lipids are an important component of the stratum corneum, providing a barrier against water loss and a waterproof barrier to external compounds.

The **basal layer** forms part of the dermal-epidermal junction. This includes hemidesmosomes and anchoring filaments to provide tensile strength. These keratinocytes are columnar, proliferating and nucleated cells. Keratin, the characteristic protein of the keratinocyte, forms small bundles around the nucleus which join into the desmosomes. This is also where some stem cells reside, providing a constant supply of proliferating basal cells (Kamstrup et al., 2008). Proteins expressed here are K5 and K14, and K6 in proliferating keratinocytes (Sandilands et al., 2009; Sun et al., 1983).

As keratinocytes begin to differentiate, they move upwards to the **spinous layer**. Here the cells begin to lose their columnar shape and the membranes take on a spinous phenotype which contain high numbers of desmosomes. Desmosomes act to anchor the cells together and maintain structural integrity of the epidermis (Thomason et al., 2010). The keratin fibres become larger and visible in the cells by transmission electron microscopy (EM) and the keratinocytes begin to flatten as they enter the upper spinous layers. K1 and K10 are expressed in the spinous layer (although K5 and K14 are stable and are therefore still expressed) (Sandilands et al., 2009; Sun et al., 1983). In the upper spinous layers keratinocytes start to express lamellar bodies (or lamellar granules) which are important in maintaining lipids within the stratum corneum. The role of lamellar bodies is described in more detail in the following sections.

Keratinocytes flatten more and express keratohyalin granules (Sandilands et al., 2009), the characteristic organelle of the **granular layer**. Here, formation of the cornified envelope occurs. This involves cross linking of proteins including involucrin (Steinert and Marekov, 1997; Yaffe et al., 1992; Yaffe et al., 1993), filaggrin (Sandilands et al., 2009) and loricrin (Yoneda et al., 1992a) making them insoluble and bound to the cell membrane, and takes place on the inner edge of the cell membrane by transglutaminase-1 (TGM-1) and TGM-3 (Eckert et al., 2005; Lambert et al., 2000; Steinert and Marekov, 1997; Yoneda et al., 1992b; Zeeuwen, 2004). Caspase 14 is expressed in differentiated and cornified cells, however this caspase is not part of the apoptotic pathway (Rendl et al., 2002). It regulates keratin filament processing during terminal differentiation and is essential for proper formation and function of the epidermal barrier and terminal differentiation (Demerjian et al., 2008; Denecker et al., 2007; Eckhart et al., 2000). Caspase 14 is only expressed in epithelia that undergoes cornification and is not activated by other caspases (Denecker et al., 2008). Regulation of caspase-14 activity can be strongly decreased by retinoic acid treatment, offering a therapeutic mechanism for retinoic acid treatment (Rendl et al., 2002). Terminal differentiation from the granular to the cornified cell involves the loss of most cellular contents. Apoptosis is thought to aid this conversion, but the complete process is unknown (Chaturvedi et al., 2006; Ishida-Yamamoto et al., 1999). Autophagy has recently been suggested to play a role in differentiation of keratinocytes, but the pathway has not been investigated fully (Aymard et al., 2011; Sato et al., 1997). CTSD is known to be expressed highly in granular and cornified cells (Horikoshi et al., 1998; Ohman and Vahlquist, 1994). The pH in the granular/cornified layers is ~5, providing an

environment in which CTSD can degrade cellular debris (Ohman and Vahlquist, 1994; Sato et al., 1997), including desmosomes (Igarashi et al., 2004).

The **stratum corneum** forms the main lipid barrier of the epidermis, maintaining metabolic activity that has increased as the keratinocytes differentiate (Du et al., 2006b; Harris et al., 2002a; Harris et al., 2002b). During the conversion from granular to cornified cells, the lamellar bodies fuse to the apical membrane of the granular cell and secrete their contents of lipids and hydrolytic enzymes into the extracellular space between cornified cells where a lipid raft is formed through remodelling of glycolipids and phospholipids (by hydrolytic enzymes)(Bouwstra et al., 2000; Menon et al., 1992b). Under normal conditions, cornified cells should contain nothing more than the cross linked proteins of the cornified envelope.

The regulatory pathways of differentiation are complex due to the huge number of processes involved in differentiation and terminal differentiation. Again, epidermal differentiation is a process which must be tightly regulated to avoid the formation of hyperproliferative diseases. Zeeuwen et al demonstrate the role of aspartic proteases and protease inhibitors in regulating terminal differentiation and TGM activity (Zeeuwen, 2004). This is summarized in Figure 1.5.

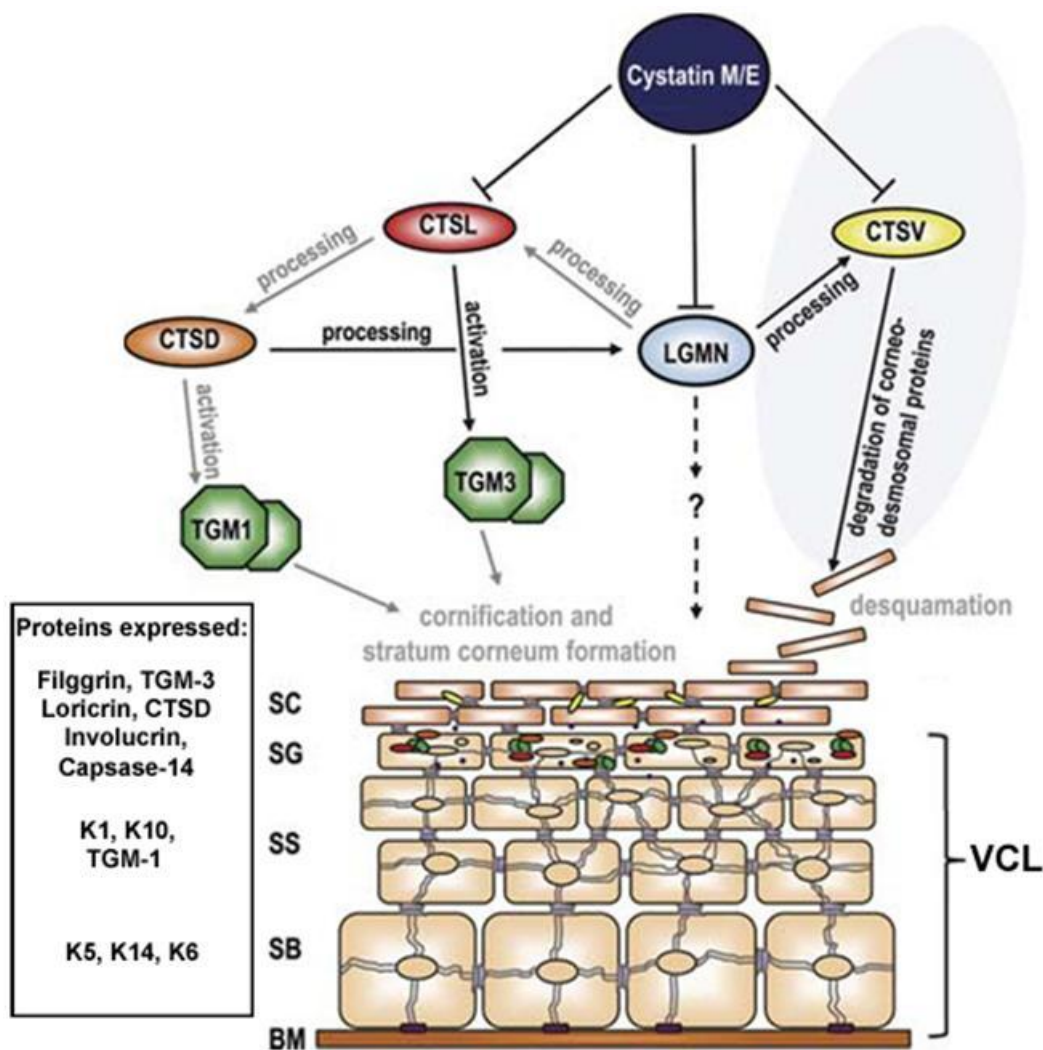


Figure 1.5. Regulation of differentiation and the specific expression of proteins. Cathepsins play an important role in differentiation – top. As cells differentiate they express specific markers to their location in the differentiation pathway which can be used as biomarkers. CTSL, Cathepsin L; CTSD, Cathepsin D; CTSV, Cathepsin V; LGMN, legumain; TGM-1 and -3, Transglutaminase-1 and -3. Figure modified from (Zeeuwen, 2004)

The epidermis and dermis house the hair follicle and sebaceous gland (Figure 1.6). The follicle is known to be the main region involved in chloracne, where the stratum corneum thickens and compacts, causing loss of the hair and a keratin plug in the follicle. This forms the comedone which is characteristic in chloracne. This process is described in more detail in section 1.3. The sebaceous gland has been shown to have high levels of AhR inducible metabolic activity (Harris et al., 2002a) and is involved during chloracne, however reports in the literature are mixed as to the details of sebaceous gland involvement (described in section 1.3).

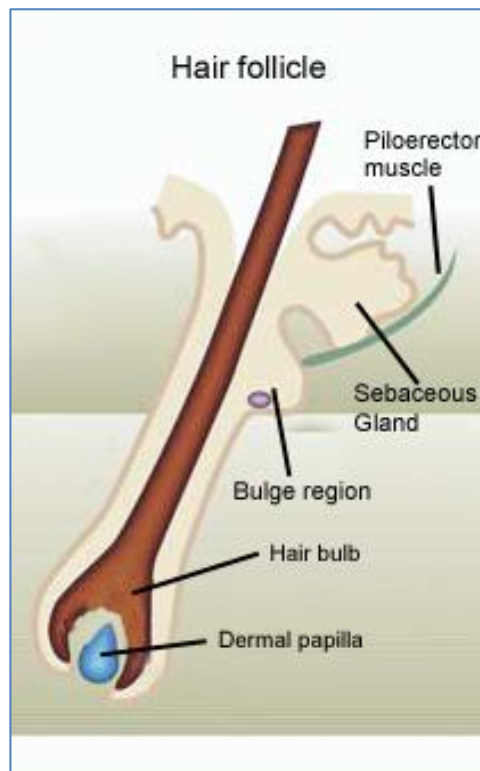


Figure 1.6. Schematic representation of the hair follicle. Modified from (Nishimura et al., 2002).

1.2.1.1 Lamellar Bodies

Lamellar bodies are membrane bound organelles expressed in the upper spinous and granular layers of the epidermis. They contain lipid lamellae which can be identified by EM (Bouwstra et al., 2003); the lipids contained include sphingolipids, phospholipids and cholesterol, and the lipid processing enzymes including acid sphingomyelinase and glucosylceramidase (Madison and Howard, 1996) to form the lipid rafts once the lamellar body contents have been extruded into the gap between the granular and cornified layers (Madison, 2003; Madison et al., 1998; Menon et al., 1992b). Lamellar bodies have characteristics of both secretory vesicles and lysosomes, exhibiting common features with lysosomes including their contents, for example hydrolases and Cathepsin D but their protein markers differ; lysosomes express LAMP1, but lamellar bodies express caveolin which is used as a structural scaffold for lipid raft formation (Madison and Howard, 1996; Sando et al., 2003).

The lamellar bodies are formed in the upper spinous layer and they are thought to originate from the golgi apparatus (like lysosomes) where main contents of the lamellar body, glucosylceramides are formed (Madison and Howard, 1996; Madison et al., 1998; Sando et al., 1996; Sando et al., 2003). At the granular layer they move to the apical

membrane where they fuse with the membrane to secrete their contents. The membrane here creates deep invaginations to accommodate the fusion of lamellar bodies and facilitate fast secretion of the lipid contents into the granular-cornified intracellular space (Bouwstra et al., 2003; Menon, 2003).

When the contents of the lamellar bodies have been secreted into the junction between the granular and cornified keratinocyte layers, lipid rafts are formed by the hydrolytic enzymes processing the lipids that were contained in the lamellar body (Madison, 2003). This forms a water tight barrier which controls transepidermal water loss and the inlet of external compounds (Bouwstra et al., 2000; Bouwstra et al., 2003).

The turnover of lamellar bodies is fast; Menon et al demonstrate that the decrease in lamellar body number (caused by mechanical barrier disruption) is reversed quickly with the formation of new lamellar bodies in the upper spinous/granular after 30 minutes. By 360 minutes, the number of lamellar bodies have returned to normal (Menon et al., 1992a; Menon et al., 1992b). This demonstrates the high levels of regulation and importance in maintaining the barrier function.

1.2.2 Metabolism

The skin forms an important barrier against both mechanical and chemical external insults. Because of its high exposure to exogenous chemicals and large surface area, the skin is an important site of xenobiotic metabolism in the body. The epidermal barrier is made from lipids so it is non-polar and this gives protection against any polar compounds, but non-polar compounds can freely cross the epidermal barrier. This has resulted in the need for increased basal expression and therefore increased metabolic induction potential of the differentiated layers of the epidermis.

The expression of phase I and phase II metabolising enzymes in human skin (including the follicle) and keratinocytes has been studied extensively and is reviewed in (Oesch et al., 2007). Generally, basal keratinocytes constitutively express low levels of metabolic enzymes including CYP1A1 (Harris et al., 2002a; Raza and Mukhtar, 1993), CYP2S1 and CYP26A1 (Pavez Lorie et al., 2009b). Glutathione-S-transferase (GST) alpha, mu and pi isoforms (Harris et al., 2002a; Raza and Mukhtar, 1993) and NADPH:quinone reductase (Harris et al., 2002b) are also thought to be expressed in low levels in basal

keratinocytes. But levels of xenobiotic metabolism increase as keratinocytes differentiate; this is often AhR dependent (Du et al., 2006a), but can also occur AhR-independently (Ledirac et al., 1997).

The basal expression of AhR increases as keratinocytes differentiate, resulting in higher inducibility of AhR-dependent phase I and II metabolising enzymes. The follicle, most importantly the sebaceous gland, also has basal levels of metabolic activity that include CYP1A1 and CYP1B1 (Harris et al., 2002a).

1.2.3 Epidermis and disease

Epidermal differentiation is a complex process that must be tightly regulated to avoid diseased states. A brief overview of the common areas of dysregulation and their consequent diseases is given in this section.

Malformation or low numbers of the anchoring organelles, hemidesmosomes and desmosomes between cells and at the dermal-epidermal junction, can cause blistering conditions (reviewed in (Burgeson and Christiano, 1997)).

The pairs of keratins can become expressed in the incorrect cells layer, or persist for too long, causing hyperproliferative diseases like psoriasis (Rao et al., 1996). CTSD is increased in psoriasis (and other hyperproliferative states such as tumours and wound healing)(Egberts et al., 2004) but opposite to this, a decrease in CTSD results in diseases such as lamellar ichthyosis, caused by down-regulation of TGM-1 (Matsuki et al., 1998). The causes of ichthyoses vary depending on the type of ichthyosis; lamellar ichthyosis is caused by TGM-1 down-regulation, ichthyosis vulgaris is caused by filaggrin mutation/down-regulation (Gunzel et al., 1991) and loricrin mutation/down-regulation can result in an ichthyosis variant of Vohwinkel's keratoderma (Egberts et al., 2004; Korge et al., 1997).

Ichthyoses can be a result of multiple problems; Sjorgen-Larsson syndrome is caused by a mutation in fatty aldehyde dehydrogenase (ALDH3A2), which regulated lipid metabolism, resulting in empty lamellar bodies. This causes the characterised compaction of the stratum corneum which is not sloughed off easily and forms thick, inflexible skin with increased transepidermal water loss. The epidermal barrier is also

compromised, caused by the malformation of the lipid raft because of the lack of lamellar contents (Rizzo et al., 2010).

The most severe form is harlequins ichthyosis which is caused by frameshift or nonsense substitution mutations in the gene encoding the ABCA12 transport protein a mutation in the ABCA12 transport protein which is involved in correct lipid transport and secretion by lamellar bodies (Harvey et al., 2010; Thomas et al., 2009).

Improper or incomplete terminal differentiation can result in parakeratosis, the persistence of nuclei that occurs in diseased states such as psoriasis and chloracne (Wolberink et al., 2011),

1.2.4 Epidermal equivalents

The epidermal equivalent model provides suitable cell-cell contact conditions, allowing primary keratinocytes to differentiate fully, forming discrete basal, granular and cornified layers (Figure 1.7). This model is robust and used widely for *in vitro* studies including metabolism (Harris et al., 2002a; Harris et al., 2002b; Jackh et al., 2011; Pavez Lorie et al., 2009a), cell death (Chaturvedi et al., 2006), differentiation (Geusau et al., 2005; Loertscher et al., 2001b), barrier function (Ponec et al., 2000), protein expression (Lee et al., 2010; Mazar et al., 2010), pigmentation (Nakajima et al., 2011) and irritation (Bernhofer et al., 1999).

Primary keratinocytes are seeded at high concentration on a polycarbonate membrane. 24h after seeding, the medium is removed from the top of the culture so the culture is fed from medium below, allowing cells to terminally differentiate. These models can be treated by compounds in the medium or directly applied to the surface. To harvest these cultures, the cells and membrane are cut from the plastic support, fixed and embedded as normal tissue (Poumay, 2004).

The 3D formation of the epidermal equivalent culture allows keratinocytes to be cultured in more physiologically relevant conditions than monolayer culture and therefore allows more physiologically relevant levels of cell-cell contact and the air-liquid interface allows cells to terminally differentiate fully (Figure 1.7)(Parenteau et al., 1992; Stark et al., 1999).

The epidermal equivalent model can already include collagen-fibroblast matrices that act as a feeder layer (Nolte et al., 1993; Parenteau et al., 1992) and melanocytes have also been successfully included in epidermal equivalents to study the co-culture of keratinocytes and melanocytes (Wang et al., 2008). Progress is being made at present to further improve the epidermal equivalent model to include co-culture of dermal papilla cells with a view to develop follicles within the epidermal equivalent.

The use of epidermal equivalents is becoming easier due to the quality of commercially available cultures. Poniec et al describe and compare the histology of commercially available cultures for barrier function and proper cellular differentiation. Overall, the quality is good but the cultures do vary in stratum corneum formation and VCL thickness from brand to brand (Poniec et al., 2000). Because of the ease of using a commercially available model that is increasingly reliable, epidermal equivalents will hopefully be used increasingly during future research, possibly replacing some animal models.

The main benefit of using epidermal equivalents in this project is to increase the physiological relevance for studying chloracnogenic biomarkers. As described in section 1.1.2, animal and human skin differs greatly in the follicle and response to AhR activation (especially chloracnogens) so that animal models are not entirely suitable (and the numbers of animals used in research should always be kept as low as possible if there are alternative models). However because of the importance of keratinocyte differentiation and cell-cell contact in projects on the AhR, keratinocyte monolayers are not entirely suitable either (Knutson and Poland, 1980). The epidermal equivalent provides a good model to investigate the hypotheses set out in the aims (section 1.6), and its development to include follicular cells will increase its effectiveness even more.

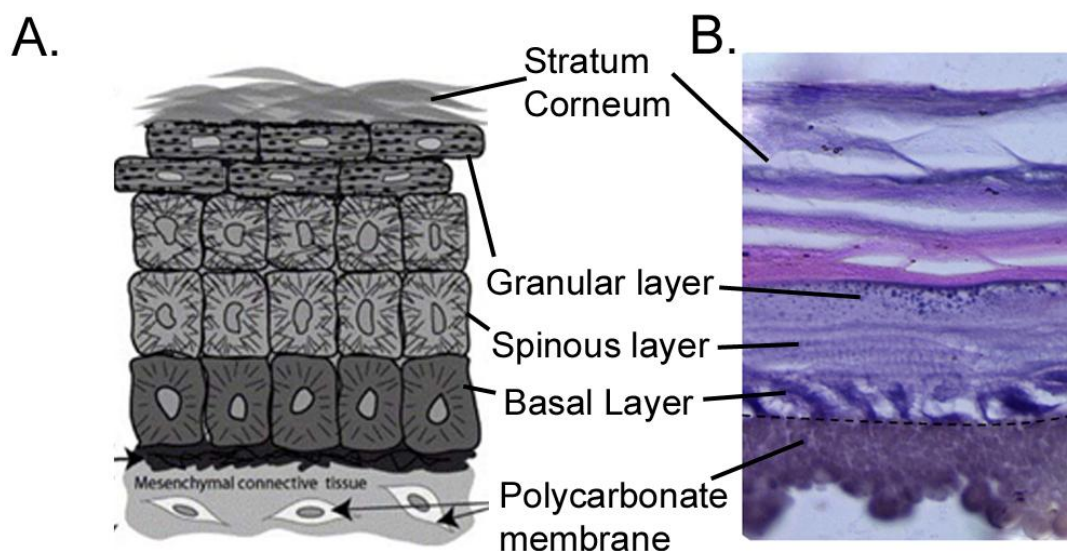


Figure 1.7. The epidermal equivalent model and schematic representation of normal skin. The epidermis is comprised of several VCL differentiating to form the stratum corneum. **A)** A schematic representation of normal skin. **B)** An H&E stained section from a vehicle treated epidermal equivalent. A is modified from (Swanson, 2004).

1.3 Chloracne

Chloracne is a skin disease specific to humans and TCDD. It consists of *acne vulgaris* like lesions including open and closed comedones and cysts, however unlike *acne vulgaris*, the lesions are sterile, non inflammatory (Scerri, 1995) and not characterised by increased sebum production (Gawkrodger et al., 2009). Localisation also differs from *acne vulgaris*, with limbs and trunk also sometimes involved in chloracne (Gawkrodger et al., 2009; Scerri, 1995). The follicles involved are always vellus follicles, there is no involvement with follicles on the scalp (Hambrick, 1957). Chloracne consists of abnormalities in keratinocyte differentiation in the follicle, causing thickened and compacted stratum corneum which leads to follicular plugging and characteristic comedones (Figure 1.8)(Scerri, 1995).

The involvement of sebum in chloracne is varied. Ju et al. describe decreased neutral lipid content of sebocytes in culture treated with TCDD for up to 7 days (Ju et al., 2011), but Pastor et al show histologically “well developed” sebaceous glands from a human chloracne biopsy. The reports on levels of sebum secreted also vary (within the same reports) for example Gawkrodger et al. report that out of 6 patients, 3 had increased levels of sebum, 2 had slightly reduced levels and 1 had no sebum excretion (Gawkrodger et al., 2009).

Some molecular investigations have been carried out on skin samples of chloracne. Tang et al show increased CYP1A1, GSTA1 and AhR mRNA in skin biopsies from industrial workers exposed to dioxins (Tang et al., 2008). CYP1A1 was significantly increased in chloracne sufferers compared to controls (age and sex matched). However AhR was also increased significantly in chloracne compared to control skin. This was not addressed in the paper, but could be a result of AhR recovery after ligand-dependent AhR activation (Franc et al., 2001; Sloop and Lucier, 1987), although if this was the case, levels of CYP1A1 would be expected to be decreased too.

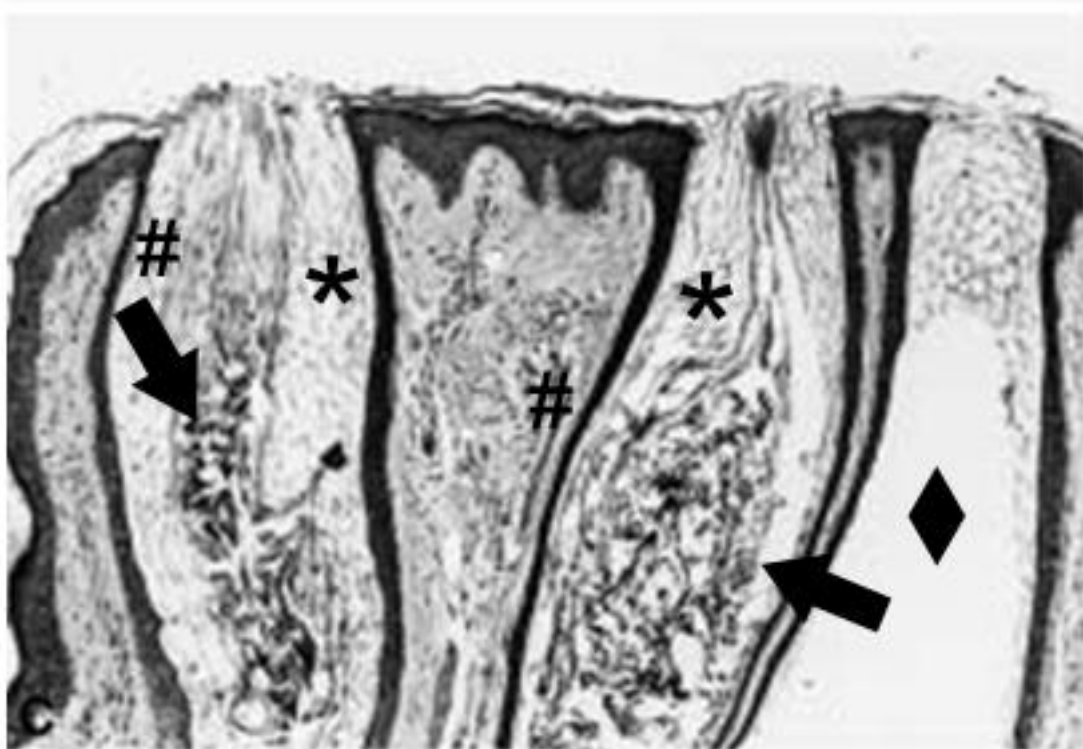


Figure 1.8. Histology of chloracne. Follicles involved in chloracne become plugged with keratotic material to form comedomes. # thickened and compacted stratum corneum and * thinner VCL suggest abnormal differentiation. Thickened stratum corneum contributes to formation of follicular plug (arrow). Diamond indicates a dilated follicle. Figure modified from (Pastor et al., 2002)

Most chloracne cases are from accidentally exposed individuals through chemical industry. As is the problem with many cases of accidental exposure, it often involves a cocktail of compounds, making it difficult to define the chloracnegenic compound responsible, or exposure is to novel uncharacterised compounds (Pastor et al., 2002). There is discussion whether other compounds too can be chloracnegenic (Gawkrödger et al., 2009; Scerri, 1995), and whether similarly structured compounds to TCDD can

also cause chloracne (Schwetz et al., 1973). The best case study there is to date is of Viktor Yushchenko (Figure 1.9)(Sorg, 2009), the Ukrainian president between 2005-2010. He was poisoned with high levels of pure TCDD in 2004. Unfortunately, no histological analysis has been carried out on his skin, however the metabolic data provides insight into the low but inducible metabolism of TCDD and the long term effects will continue to be followed throughout the course of Yushchenko's recovery.



Figure 1.9. Viktor Yushchenko pre-, during and post-chloracne. Yushchenko was poisoned with high concentrations of TCDD. Middle picture shows 3 months post exposure and chloracne involving every follicle on the face, creating a slate grey appearance. Right picture shows 3 years post poisoning and a remarkable recovery due to relatively fast clearance of TCDD induced by its own activation of AhR. Image modified from (Sorg, 2009)

TCDD is highly lipophilic and has a half life of ~10 years which is highly variable depending upon metabolic genotype, age and levels of exposure. Because of TCDDs high lipophilicity, it can become sequestered in the body fat (Kedderis et al., 1993) causing chloracne to persist for up to 15 years (May, 1973). Because of this TCDD can bioaccumulate and has the potential to cause high environmental impact.

1.4 Cathepsin D

Cathepsin D (CTSD) is an aspartic protease that has roles in differentiation and cell death. It can be localised to the lysosome or cytoplasm and undergoes a series of steps to form the active or mature form of CTSD. The processing pathway is reviewed in (Zaidi et al., 2008).

1.4.1 CTSD: Regulation and processing

1.4.1.1 Regulation by Sp1

Cathepsin D is regulated by three regulatory sequences in the CTSD promoter region; the “housekeeping” (SP1) and “inducible” sequences for the oestrogen receptor (ER, oestrogen responsive element, ERE) and the AhR promoter (XRE) (Krishnan et al., 1995; Wang et al., 1998; Wang et al., 1999). AhR is required for maximal expression of ER-dependent CTSD activation. Interestingly, ligand activation of AhR is not required for AhR-dependent enhancing of CTSD expression, but unbound nuclear AhR enhances CTSD expression. Ligand-induced activation of AhR in fact causes inhibition of the oestrogenic effects on CTSD described previously resulting in TCDD inhibited oestrogen dependent breast tissue tumours in mice (Krishnan et al., 1995). This is caused by active AhR-ARNT breaking the ER-Sp1 dimer by interaction of AhR with ER, decreasing CTSD induction (Khan et al., 2006). As described in section 1.1.2, Sp1 often requires another response element to induce transcription of a gene (Wang et al., 1998). Levels of transcriptional activation of CTSD depends upon the distance that the SP1 binding site and XRE are from each other and the presence of non-activated nuclear AhR (Krishnan et al., 1995; Wang et al., 1999).

1.4.1.2 Post translational maturation

Cathepsin D undergoes post translational modifications resulting in the presence of 3 main forms: pre-pro CTSD (52kDa), pro CTSD (48kDa) and active CTSD (34kDa). Formation of pre-pro CTSD occurs in the rough endoplasmic reticulum. As described in figure 1.10, pre-pro CTSD is cleaved forming pro CTSD which undergoes glycosylation in the endoplasmic reticulum. Pro CTSD then travels to the Golgi body where it undergoes phosphorylation which allows its targeted movement to the endosomal pathway. Here, low pH breaks down the molecule further generating intermediate forms of CTSD which result in a 48kDa molecule which is then cleaved by cathepsins B and L to the active 2 chain mature CTSD, as reviewed in (Zaidi et al., 2008). CTSD is only

active at certain pH, and degrades cellular proteins at acidic, lysosomal pH. The stratum corneum has a pH of ~5, inducing CTSD degradation of desmosomes (Horikoshi et al., 1999).

As the final stages of CTSD activation are by cleavage of CTSD by cathepsins B and L, CTSD also activates other proteases. Cathepsin B, L, and capsases 3 and 9 are all activated by CTSD. This demonstrates the role of CTSD in regulating proteolysis (Minarowska et al., 2008).

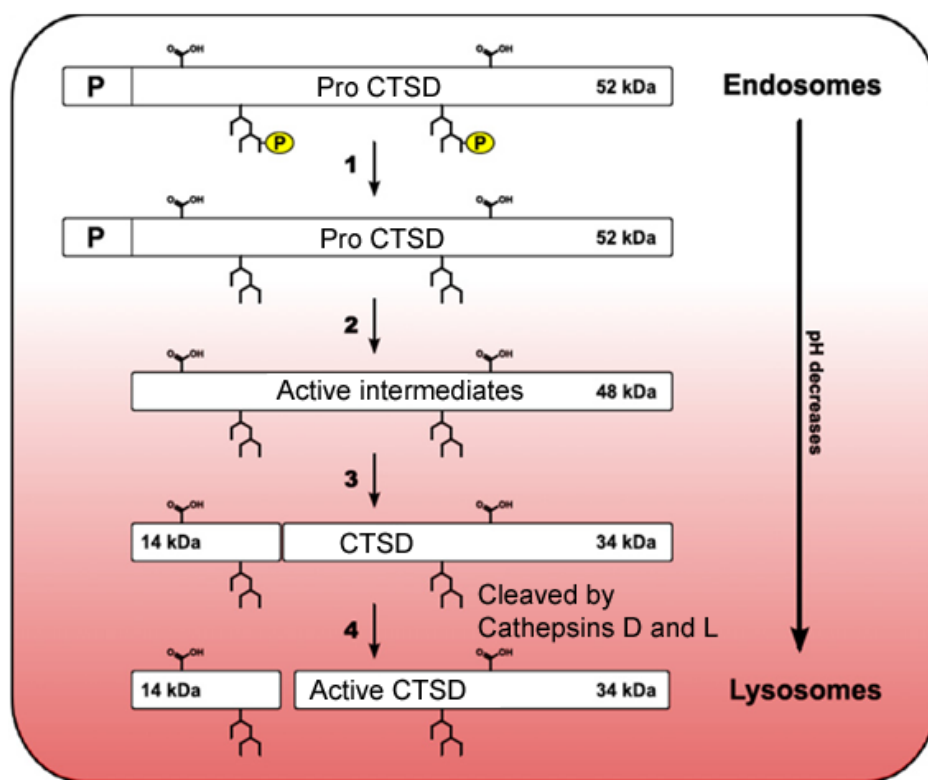


Figure 1.10. The processing steps of Cathepsin D Cathepsin D undergoes post translational modifications from inactive pre-pro CTSD to active CTSD. During these steps the molecule moves from the rough endoplasmic reticulum, through the endosomes to the lysosomes. Modified from (Zaidi et al., 2008)

1.4.2 CTSD activity in cell death

1.4.2.1 Apoptosis

Activation of apoptosis can be induced by the permeabilization of lysosomes, resulting in cytoplasmic CTSD (Figure 1.11) (Guicciardi et al., 2004). Baumgartner et al have shown that lysosomal permeabilisation by oxidative stress induced the release of

cathepsins D and E which in turn activate caspase 8 and caspase 3 (Baumgartner et al., 2007). Apoptosis induced by lysosomal disruption can also be caspase-8 independent via cleavage of Bid by cytoplasmic CTSD (Heinrich et al., 2004). AhR can modulate this pathway through TNF- α and AhR deficiency blocks the permeabilisation of the lysosome, blocking CTSD release to the cytoplasm and cleavage of Bid and procaspase-8 (Caruso et al., 2006). This shows that AhR effects the stability of lysosomes and can induce susceptibility to apoptosis (Caruso et al., 2004; Park et al., 2005; Reiners and Clift, 1999).

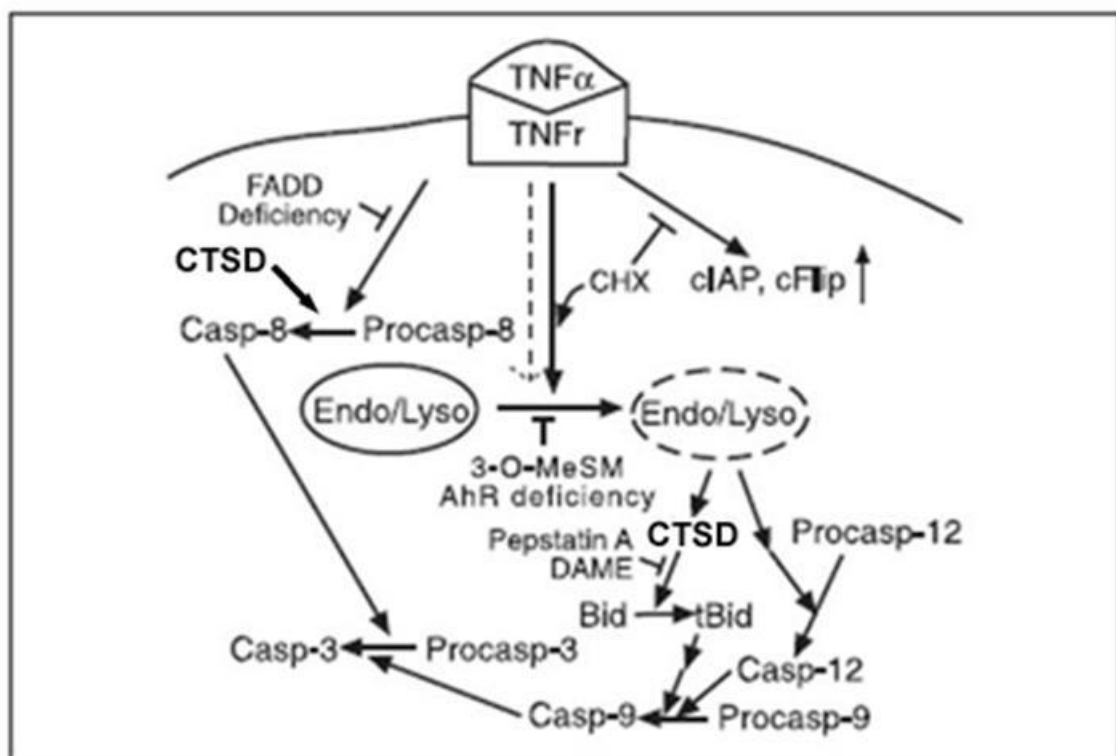


Figure 1.11. Activation of the apoptotic pathway by cathepsin D. Disruption of the lysosomal membrane releases CTSD into the cytoplasm where it activates caspase 8 or cleaves Bid, resulting in activated caspase-3. Inhibitory steps are included – AhR deficiency blocks permeabilisation of the lysosome. Image modified from (Caruso et al., 2006)

1.4.2.2 Autophagy

The role of lysosomes in autophagy is well understood and described in more detail in section 1.5. The lysosome is a degradative vesicle that contains CTSD and other proteases that degrade cellular debris (Raymond et al., 2008). During autophagy, the lysosome fuses with the autophagosome creating the autolysosome (Huynh et al.,

2007), which degrades the contents of the autophagosome. However, beyond this, the relationship between CTSD and autophagy is not understood. It has been suggested that an increase in lysosomes could induce autophagy, as the two processes are interdependent (Settembre et al., 2011).

Carew et al. have shown that blocked autophagy by novel agent lucanthrone increases levels of CTSD in breast cancer cell lines. They show that blocked autophagy causes increased CTSD, and that this accumulation induces apoptosis. The paper does not state which form of CTSD is increased though, and only shows one band by Western blot (Carew et al., 2011). So from this we cannot draw any conclusions on the effects that inhibited autophagy has on the CTSD pathway. Autophagy has been shown to cause a decrease in CTSD levels in MCF-7 cells, suggesting that CTSD may be degraded by autophagy, but there is not enough data to show that the CTSD decrease is autophagy-dependent. Byun et al have also shown an increase in CTSD expression in senescent MCF-7 cells (Byun et al., 2009).

1.4.3 CTSD in differentiation

Egberts et al. show that in basal keratinocytes, all 3 isoforms of CTSD are present, with the 48kDa form predominant. In differentiated keratinocytes, protein expression increases significantly, the main forms being expressed pre-pro CTSD and 48kDa form, the membrane bound active intermediate. CTSD protein expression in keratinocytes has been shown to correlate well with CTSD activity, showing an increase in activity as keratinocytes differentiate. This correlates with the increased role of CTSD in degradation of cellular organelles during terminal differentiation. In HaCaTs, TGM-1 cross linking increases with CTSD treatment, and the increased expression of CTSD, TGM-1, involucrin and loricrin all increase with keratinocyte differentiation. This increase is CTSD dependent; in CTSD knockout mouse skin there is a large decrease in TGM-1 activity and an absence of involucrin, loricrin and filaggrin staining (in CTSD^{+/-} mice the expression is lower and also disrupted) (Egberts et al., 2004). These effects result in the development of an ichthyosis-like phenotype in CTSD^{-/-} mouse skin, with a decreased VCL and thickened stratum corneum.

1.4.3.1 Overexpression

The role of CTSD in maintaining barrier function is further demonstrated by its increase in response to mechanical damage to the epidermal barrier such as tape stripping or in

in vivo situations when the barrier has been compromised such as wound healing (Egberts et al., 2004). The expression of CTSD has also been shown to be increased during embryogenesis. In areas where remodelling occurs through programmed cell death (apoptosis), levels of CTSD are also increased such as in the limb and heart (Zuzarte-Luis et al., 2007).

CTSD is also expressed at increased levels in some cancers. This can be due to disrupted sorting of CTSD into the late endosome/lysosome by mannose-6-phosphate (Kokkonen et al., 2004) or by increased transcription in oestrogen dependent cancers such as breast or endometrial cancer (Rocheffort et al., 1989; Zhang et al., 2009). Increased transcriptional activation of CTSD by oestrogen occurs via the oestrogen receptor response element (ERE) and Sp1 binding site as described in section 1.1.1, molecular cross talk (Cavaillès et al., 1993; Chen et al., 2001; Safe and Wormke, 2003). TCDD inhibits mammary tumours in mice, demonstrating the anti-oestrogenic effects of TCDD-activated AhR on CTSD induction (Gierthy et al., 1993; Holcomb and Safe, 1994). The role of CTSD in tumours has been shown to involve secretion of pro-CTSD to act in a paracrine or autocrine manner, increasing proliferation, invasion and metastatic potential of the cells in the tumour (Ohri et al., 2008; Vashishta et al., 2007; Zhang et al., 2009). This has been shown in MCF-7 cells, a human breast cancer cell line (Ohri et al., 2008; Zhang et al., 2009), and also HaCaTs, that showed pro-CTSD was secreted by HaCaTs under starvation conditions and that treatment of HaCaTs with exogenous pro CTSD increased proliferation (Vashishta et al., 2007). This suggests that CTSD is not only involved in cancer but physiological conditions such as wound healing.

1.5 Autophagy

Macro autophagy (which will be referred to in this thesis as autophagy) is a cell survival/cell death pathway which specifically degrades proteins and organelles, recycling the materials for further use in the cell and producing energy for cellular processes (Settembre and Ballabio, 2011). It is a ubiquitous process basally active in all cells and essential for normal tissue homeostasis; defective autophagy has been considered the mechanism of various diseases including certain liver diseases, cystic fibrosis and breast cancer (Kongara et al., 2010; Luciani et al., 2010; Rautou et al., 2010).

1.5.1 Pathway

Autophagy is a process that packages and degrades specific proteins and organelles by engulfing material in the autophagic vacuole and fusing to lysosomes to form degradative autolysosomes.

The formation of the autophagic vacuole begins with the induction phase, forming the isolation membrane from the golgi body. This structure undergoes expansion and closure, forming the characteristic double membraned autophagosome (Figure 1.12). The autophagosome can then fuse to lysosomes, forming the degradative autolysosome (Eskelinen, 2005; Longatti and Tooze, 2009; Lukacs et al., 1990). During this maturation, microtubule associated protein light chain 3 (LC3) is recruited to the autophagosome from the cytoplasm where it resides during low levels of autophagy, as LC3 I. Conversion of LC3 I to LC3 II occurs upon recruitment to the autophagosome membrane and is used as one of the main markers of autophagy (Mizushima and Yoshimori, 2007), but as discussed in chapter 5, it is not a good marker for autophagy if used alone. The formation and degradation of autophagosomes and their respective markers can be followed to show increases and decreases of autophagy speed, or flux, caused by the effects of chemicals inducing or blocking active autophagy (as opposed to basal autophagy). This flux varies over time both basally and in induced states and is one of the main characteristics of autophagic measurement (Huang et al., 2010; Shvets and Elazar, 2009).

Specific targeting of damaged or un-needed materials must occur to provide the autolysosome with material to degrade. This process is by ubiquitination and is a mechanism that is also used to target material for degradation by the 26s proteasome; it is thought that large proteins/organelles that are too big for 26s proteasome degradation are degraded by autophagy (Kraft et al., 2010). p62 is the “cargo receptor” and binds to the ubiquitinated material transporting it to the autophagosome membrane (dependent on self oligomerisation and localisation with autophagosome membrane proteins) for degradation (Itakura and Mizushima, 2011). p62 and LC3 are both degraded by autophagy (Jaakkola and Pursiheimo, 2009).

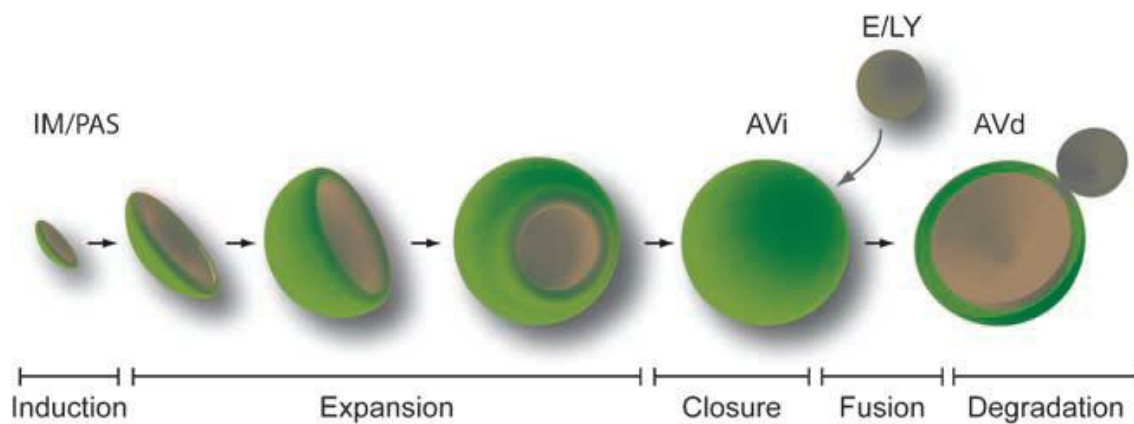


Figure 1.12. Maturation of the autophagosome. IM, isolation membrane; PAS, pre-autophagosomal structure; AVi, immature autophagosome; E, endosome; LY, lysosomes; AVd, degradative autophagosome. Modified from (Longatti and Tooze, 2009)

1.5.1.1 Regulation

Regulation of autophagy occurs through a host of mechanisms. It can be cellular or chemical and promises to be a powerful tool as a pharmacological target. One of the main regulatory and characteristic mechanisms for inducing autophagy is through serum starvation. When ATP is not widely available (for example, under starvation conditions or nutrient low conditions like tumours) then cells induce autophagy to create their own supply of ATP (Bennett et al., 2010; Rosenfeldt and Ryan, 2011; Williams et al., 2009). This is the major survival process that autophagy is responsible for. Hypoxic conditions also induce autophagy, for example, in tumours (using the HeLa cervical cancer cell line) hypoxia is thought to induce autophagy, increasing cell survival (Pursiheimo et al., 2009). This would suggest that in this case, blocking autophagy may slow tumour growth. This has recently been described as a mechanism for successful chemotherapy. Autophagy is induced by cells to survive chemotherapy, but if autophagy is inhibited, cells are no longer resistant to chemotherapy (Yang et al., 2011).

Autophagy is also a cell death pathway which is demonstrated by autophagic activation exhibiting signs of apoptosis cell death eg. vacuoles (Gonzalez-Polo et al., 2005). Induction of autophagy is thought to induce cell death by increasing cellular turnover to an extent that the cell can no longer survive (Kanzawa et al., 2005; Turcotte et al., 2008).

As well as general roles in cell survival and cell death, autophagy also induces tissue specific effects by targeted degradation of certain organelles. Autophagy is thought to

have a role in regulating lipid metabolism (a main store for ATP) and induction of autophagy has been shown to target the degradation of lipid droplets in the liver, being one of the most efficient organelles to target for releasing ATP (Singh et al., 2009b). Specific targeting of organelles in other tissues can be the cause for degenerative disease such as Alzheimer's and dementia (Funk et al., 2011; Lagalwar et al., 2007).

1.5.1.2 Autophagy in skin

Autophagy has been shown to occur in skin and be involved in skin cancer, an increase in autophagy is seen in melanoma caused by increased cellular stress (Lazova et al., 2010; Proikas-Cezanne et al., 2004). This can be used to a therapeutic advantage, targeting defective autophagy with chemotherapeutic drugs (Armstrong et al., 2011). Autophagy plays a role in other processes in the skin too, for example inflammation regulated by autophagy and p62 (Lee et al., 2011), UVA photodamage (Lamore and Wondrak, 2011) and as a target for reduction of scarring by induction of autophagy in human dermal fibroblasts (Oikarinen, 2009). Autophagy has been suggested to be involved in keratinocyte differentiation (Aymard et al., 2011), but little has been published on this.

1.5.1.3 Autophagy and apoptosis

Biomarkers characteristic of autophagy are an increase in autophagic vacuoles, and for apoptosis it is the formation of vacuoles, nuclear fragmentation and chromatin condensation but there is some crossover. Vacuoles are also observed in cells undergoing autophagy, suggesting that the two types of cell death are not as clear cut (Gonzalez-Polo et al., 2005).

There is also a link between the two methods of cell death by cathepsins. As described in section 1.4.2, lysosomal CTSD is involved in autophagic degradation, but lysosomal permeabilisation and release of CTSD into the cytoplasm is a very important mechanism of apoptotic activation. The pathways are closely related and have been suggested to be interdependent.

Inhibition of autophagy has been shown to result in induced apoptosis (Boya et al., 2005). This can be caused by an accumulation of CTSD leading to lysosomal permeability and induction of apoptosis (Carew et al., 2011). Induction of apoptosis through autophagic inhibition by different chemical agents (eg, lucanthrone, 3-methyladenine or chemotherapy) seems to occur through caspase-8 activation and

consequent Bid cleavage (Bohensky et al., 2007). This pathway is also shown to bypass autophagy when activated first. For example Li et al show that treatment with chemotherapeutic agent camptothecin blocks autophagy by caspase-8 induced cleavage of beclin-1, a member of the autophagic pathway (Li et al., 2011). The involvement of caspase 8 in all of these pathways suggests a connection between autophagy and apoptosis may be cathepsin dependent (CTSD cleaves caspase-8)(Baumgartner et al., 2007; Heinrich et al., 2004) or dependent on LC3, inhibition of proteasomal degradation induces LC3-dependent caspase-8 activation and apoptosis (Pan et al., 2011).

1.6 Aims

The main aims of this project were to increase understanding of the physiological role of AhR in skin and to develop a mechanistic understanding of the pathophysiology of chloracne induced by TCDD. Our aim was to assess potential biomarkers for predicting physiological effects of novel AhR agonists that could be used in cell culture models to predict the main human AhR-dependent toxicity, chloracne. We aimed to characterise the effects of AhR activation (proliferation, differentiation and cell death) in normal human epidermal keratinocytes and epidermal equivalent models and thereby gain an understanding of chloracne pathogenesis. We hypothesised that the affinity of ligands for the AhR and their binding dynamics would correlate with transactivation of specific genes and downstream effects on primary keratinocyte growth, differentiation and apoptosis. We planned to dissect the contribution of specific components of the pathway utilising pharmacological inhibitors and a genetic approach using siRNA knockdown.

It is unclear whether the downstream effects resulting from AhR activation stem from the lack of AhR caused by activation-dependent down-regulation, up-regulation of transcriptional activation pathways or sequestering of ARNT, a promiscuous PAS protein, into the AhR pathway leading to deficiency of ARNT for other ARNT-dependent pathways. We hypothesised that because of the high-residency of TCDD due to its lipophilicity and low rates of metabolism, TCDD-induced AhR activation and its downstream effects would be prolonged, exacerbating the effects of AhR activation.

Further work is required to determine whether CYP1A1 induction represents a biomarker of chloracne potential. During drug development in industry, all compounds are screened for AhR activation. CYP1A1 is commonly used as a readout for AhR activation; however it is not necessarily a specific marker of chloracne. At present most compounds that activate the AhR (as assessed by CYP1A1 induction in a liver cell line) will be discarded early on during the drug development pathway. Thus, potentially useful compounds are discarded because of potential cutaneous toxicity. A more specific biomarker for chloracne would potentially reduce the number of novel compounds discarded that would potentially be beneficial and not cause AhR induced toxicity.

One hypothesis to account for the phenotypic changes induced by TCDD in epidermis (including comedones) is non apoptotic cell death (Chapter 5). Therefore we aimed to characterise cell death induced by AhR agonists and investigate a potential role for autophagy induced by the AhR pathway and hypothesised that this process might contribute to the phenotype of chloracne. Using EM we observed the effects of AhR activation by TCDD, ITE or β -NF on cellular morphology and autophagic processes visible at this level.

Links between AhR and CTSD are described in the literature (Wang et al., 1999), although regulation is complex. As CTSD has been implicated in the regulation of terminal differentiation (Zeeuwen, 2004; Zuzarte-Luis et al., 2007), we then hypothesised that AhR activation may upregulate CTSD activation, linking AhR activation with early onset of terminal differentiation.

Hypotheses

- Affinity of ligands for AhR and their binding dynamics will correlate with transactivation of AhR degradation and CYP1A1 induction, and downstream effects on keratinocyte differentiation
- That residency is the main contributing factor for a compound to have chloracnegenic properties. Many compounds would exert chloracnegenic effects if their residencies were increased to equal TCDD. To test the hypothesis we utilised 3 compounds with different agonist characteristics of affinity, residency and origin (physiological or non-physiological) to increase the understanding of AhR activation in the skin
- AhR activation plays a role in keratinocyte differentiation and comedone formation and pathogenesis of chloracne
- AhR activation induces autophagy in keratinocytes which contributes to the phenotype of chloracne.

2 Materials and Methods

2.1 Cell culture

2.1.1 Monolayer culture

Primary human keratinocytes were isolated from redundant skin samples, following approval by the Newcastle and North Tyneside Research ethics committee and informed consent.

Skin samples were washed in PBS and subcutaneous tissue removed, then scored and incubated overnight in dispase at 4°C. The next day the dermis and epidermis were separated and epidermis incubated in trypsin for 5 mins at 37°C. Trypsin was neutralised with foetal calf serum and centrifuged for 3000g for 5 minutes. Cells were resuspended in Epilife medium and seeded into T175 flasks in Epilife (Lonza, Basel, Switzerland) supplemented with 60µM CaCl₂, penicillin/streptomycin and Human Keratinocyte Growth Supplements (Lonza) at 37°C with 5% CO₂ in a humidified atmosphere. Medium was changed after 24h to remove pieces of intact skin and residual trypsin and foetal calf serum.

Trypinization was carried out by washing the cells in PBS, then replacing medium with 5ml Trypsin + EDTA (Lonza) for 10±5 minutes at 37°C. Trypsin was neutralised with foetal calf serum and cells were centrifuged for 5 minutes at 3000g. The pellet was resuspended in complete Epilife and cells cultured in T175 flasks up to passage 5.

2.1.2 Epidermal Equivalents

Three dimensional epidermal equivalents were formed by seeding primary keratinocytes (maximum passage 4) on cell culture inserts (0.4µm pore, 12mm diameter, Millicell, Millipore), Bedford, MA in Epilife containing 1.5mM CaCl₂. The next day the culture was brought to the air liquid interface and the high CaCl₂ Epilife was supplemented with 5mg/ml Vitamin C. Supplemented medium was changed every 48h for a further 5 days. The epidermal equivalents were then treated every 48h for a further 7 days and harvested. Cells were either snap frozen in OCT or fixed in 4% paraformaldehyde overnight and embedded in paraffin for analysis.

2.2 Immunohistochemistry

2.2.1 Haematoxylin & eosin staining

The structure of epidermal equivalents was observed using H&E staining. Paraffin embedded sections were cut at 4µm and baked onto superfrost ultra plus slides (VWR) overnight at 56°C. The following day, paraffin was removed with histoclear (30 minutes) and sections were dehydrated in decreasing dilutions of ethanol. Sections were stained with haematoxylin and eosin for ~10s each. Images were taken by light microscopy with a Zeiss Axioimager microscope.

2.2.2 Fluorescence

To visualise the localisation and levels of expression of differentiation markers, AhR and caspase-3, immunohistochemical analysis was performed for the antibodies described in Table 1. Paraffin embedded sections were cut and baked onto slides as above and heat induced epitope retrieval was used (3 x 5 mins). For TGM-1 and caspase-3 antibodies, OCT embedded sections were cut using a cryostat at 4µm, dried onto superfrost ultra plus slides and stored at -80°C. Fixation methods are described in Table 1. Sections were permeabilised with 0.2% Triton X-100, blocked in normal goat serum in BSA/ PBS (S-1000, Vector labs) and incubated with primary antibody as described in Table 1 or isotype IgG control (at equal concentration to primary antibody), in phosphate buffered saline/BSA for 1h at RT (TGM-1 was incubated at 37°C). Oregon green or Alexa fluor (488) conjugated secondary antibodies (Invitrogen, anti-mouse no. 06380 or anti-rabbit no. 06381) diluted 1:300 in BSA/PBS were applied for 1h at RT. Nuclei were stained using RNase pretreatment and To-Pro 3 (Invitrogen, 642/661). Table 2 describes antibody specificity for each protein. Images were analysed using a Leica confocal inverted TC II SP2 system.

2.2.3 DAB

To visualise the localisation and expression of cleaved Lamin A and CTSD, immunochemical analysis was carried out at AstraZeneca with the DAKO envision system (DAKO) on paraffin embedded epidermal equivalents or skin sections obtained with permission from the catalogue at Astra Zeneca. Sections were cut at 4µm and baked onto superfrost plus ultra slides at 56°C overnight. Epitope retrieval was performed by heating sections to 98°C for 10 minutes in target retrieval solution, citrate pH6 (Dako) and sections were blocked with 3% peroxidase followed by 20% goat serum then primary antibody for 1h at RT as described in Table 1 or isotype control. Dako

envison FLEX HRP labelled secondary antibody was applied for 30 minutes then DAB stained using DAKO Envision buffer and chromogen (Vector Laboratories) for up to 5 minutes. Sections were counterstained with haematoxylin and images taken using the Zeiss Axioimager light microscope.

Primary Antibody	Cat. number	Company		Embedding and Fixation	Dilution
Fluorescence					
AhR	Sc-5579	SantaCruz	Rabbit polyclonal	Paraffin 4% PF	1:200
Active Caspase-3	AF835	R+D systems	Rabbit polyclonal	OCT Acetone: methanol 1:1	1:50
Filaggrin	MS-449-P1	Thermo Scientific	Mouse monoclonal	Paraffin 4% PF	1:500
Involucrin	NCL-INV	Novocastra	Mouse monoclonal	Paraffin 4% PF	1:50
TGM-1	BT-621	Biomedical technologies	Mouse monoclonal	OCT Acetone	1:100 1h at 37°C
DAB					
Cleaved Lamin A	2035	Cell signalling	Rabbit polyclonal	Paraffin 4% PF	1:50
CTSD	1910-8997	Abd serotec	Mouse monoclonal	Paraffin 4% PF	1:200

Table 1. Antibody details and fixation methods for IHC analysis. Conditions were at room temperature (RT) unless otherwise stated. PF = paraformaldehyde

Primary antibody	Catalogue no.	Specificity
AhR	Sc-5579	Corresponds to amino acids 637-848 of human AhR
Active caspase-3	AF 835	Detects p17 subunit of cleaved caspase-3
Filaggrin	MS-449-P1	Clone FLG01. Corresponds to epitope present in each filaggrin molecule, detects profilaggrin and filaggrin.
Involucrin	NCL-INV	Clone SY5
TGM-1	BT-621	Clone B.C1
Cleaved Lamin-A	2035	Detects small subunit of Lamin A and C after cleavage at aspartic acid 230 by caspase-6
CTSD	1910-8997	Clone C5

Table 2. Antibody specificity for IHC.

2.3 Sulforhodamine B Assays

Sulphorhodamine B (SRB) assays provide a sensitive measure of total cellular protein, are linear with cell number and cellular protein at densities from 1-200% and perform similarly compared with other proliferation assays such as MTT assay or clonogenic assays (Skehan et al., 1990). Keratinocytes were seeded into flat bottomed 48 well plates with 5×10^3 cells per well and SRB assay performed. Cells were treated with DMSO vehicle (0.2% maximum) or with AhR agonists TCDD, β -NF or ITE up to 8 days. Fresh medium and agonist was applied every 48h. To harvest the cells, medium was removed from wells and cells were fixed with 200 μ l 10% Trichloroacetic acid (TCA) for 1h at 4°C. Plates were washed 5 times in water and drained well. 200 μ l of SRB (0.4% in 1% acetic acid) was added to each well for 20 minutes at RT. Plates were washed 5 times in 5% glacial acetic acid and dried over night at RT or for 1h at 37°C. Protein was solubilised in 200 μ l of Tris-base pH10 (10mM) on a rocker for 20 mins. Absorbance was

read at 564nm using a plate reader (Spectra MAX 250, Molecular Devices, USA). Cell growth was expressed as optical density units.

2.3.1 Ligand preparation

2,3,7,8-Tetrachlorodibenzo-*p*-dioxin was purchased from Supelco, Sigma Aldrich. Stock solutions (10 μ M) were diluted in dimethylsulfoxide (DMSO) and kept at room temperature protected from light. β -Naphthoflavone (Sigma Aldrich) stock solutions (60mM or 15mM) were made in DMSO and kept at 4°C, protected from light. ITE (2-(1'H-Indole-3'-carbonyl)-thiazole-4-carboxylic acid) (Sigma Aldrich) stock solution (5mM) was made in DMSO and also kept at 4°C protected from light. Due to toxicity in primary keratinocytes, the DMSO concentration in primary keratinocyte medium was kept below 0.01%.

2.4 Dual Luciferase assays

AhR activity was measured using an XRE-dependent luciferase reporter (pXRE4-SV40-Luc) (Mimura et al., 1999) (a kind gift from Y. Fujii-Kuriyama, Tohoko University, Japan). Cells were co-transfected with a renilla luciferase construct internal control vector (pRLTK, Promega). Primary keratinocytes were seeded into 24-well culture plates and transfected at 70% confluency with 0.5 μ g Firefly reporter plus 0.0125 μ g renilla control using TransIT Keratinocyte transfection reagent (Geneflow) according to manufacturer's instructions. Cells were treated with vehicle or AhR agonist TCDD, β -NF or ITE as described and at 48h or up to 96h for the time course shown in section 3.2.1.2. For α -NF inhibition assays, cells were co treated with vehicle or AhR agonist plus α -NF concurrently. Keratinocytes were harvested and assayed using the Dual luciferase reported system (Promega), which allows measurement of the inducible firefly luciferase and housekeeping renilla construct almost simultaneously using a Perkin Elmer luminometer microplate reader. Values were presented as Firefly: renilla ratio, normalised to vehicle.

2.5 Western blotting

Primary keratinocytes were cultured in 6 well plates and treated at 80% confluency with vehicle (DMSO), TCDD, β -NF or ITE. For inhibition studies with α -NF, keratinocytes

were treated with medium containing AhR ligand and α -NF was added immediately, directly into the medium. Cells were lysed in ice cold buffer containing 50mM Tris-HCl (pH7.5), 1% NP40, 0.25% Sodium deoxycholate, 150mM sodium chloride, 1mM sodium fluoride, 1mM PMSF, 1mM sodium orthovanadate, plus a protease inhibitor cocktail (Roche). Samples were probe sonicated at an amplitude of 8 μ m for 3 x 5s pulses. Levels of protein were determined by BCA protein assay kit (Thermo Scientific, Rockford, IL, USA) Samples were combined with 4x sample buffer and NuPAGE antioxidant (Invitrogen) and heated for 3 minutes at 100°C. Samples were loaded (20 μ g/well) immediately into 4-12% NOVEX Bis-Tris precast gels (Invitrogen) with CYP1A1 positive control (human liver microsomes) and pre-stained ladder (NuPAGE, Invitrogen) on each gel. 200 V was applied for ~30 minutes in NuPAGE MES Running buffer (Invitrogen) containing 2.5% antioxidant. Protein was then transferred to a nitrocellulose membrane at 100 V for 1h in NuPAGE Transfer buffer.

Membranes were blocked in 5% non-fat milk in TBS/T for 1h at RT. Primary antibodies were used at concentrations described in Table 3. Equal protein loading was confirmed with monoclonal β -actin antibody (1:20,000) in TBS-T + 5% non-fat milk for 45 mins at RT (Sigma-Aldrich, St. Louis, MO, USA). Anti-mouse or anti-Rabbit IgG peroxidise conjugated secondary (Vector Labs) 1:1,000 in TBS-T + 5% non-fat milk for 1h at RT. Signals were detected using ECL Plus (Amersham GE healthcare) for 10 minutes (except β -actin, incubated for 5 minutes). Membranes were imaged using a Fujifilm FLA-3000 fluorescence image analyser.

Bands were analysed according to densitometry and presented as a ratio of CYP1A1, AhR, p62, LC3 II, CTSD : β -actin using Multigauge V2.2 software and statistical analysis carried out in Prism 5. Details are described in section 2.9.

Western blots presented in this thesis are not mixed between donors at any time point. Where indicated, figures showing increasing time points show data from 2 different donors, but this does not occur regularly. In all cases, stacked images of bands from different antibodies are from probing the same membrane with different antibodies. On occasion, lanes of illustrated blots were reorganised (within samples from the same donor) from the original blot, to show relevant samples. The lines at the side of the Western blots in Appendices X to AA represent molecular weight markers run on each Western blot gel.

Primary Antibody	Cat. no.			Conditions in TBS-Tween 20
AhR	MA1-514	Affinity Bioreagents	Mouse monoclonal	1:1000 + 5% milk O/N at 4°C
CYP1A1	sc-25304	Santacruz	Mouse monoclonal	1:1000 + 5% BSA O/N at 4°C
p62	sc-28359	Santacruz	Mouse monoclonal	1:1000 + 5% milk 1h at RT
LC3B	2775	Cell Signalling	Rabbit polyclonal	1:1000 + 5% BSA O/N at 4°C
CTSD	219361	Calbiochem	Rabbit polyclonal	1:1000 + 5% milk 1h at RT
β -actin	A5316	Sigma	Mouse monoclonal	1:20,000 + 5% milk 45 mins at RT

Table 3. Primary antibodies used for Western blotting

2.6 Confocal Microscopy

2.6.1 Fixed sample imaging

Immunohistochemical staining was imaged using a Leica TC2 SP II laser scanning confocal microscope.

2.6.2 Live cell imaging using BODIPY FL-pepstatin A

To observe the levels of expression and localisation of CTSD in live primary keratinocytes, the liquid dye BODIPY FL-Pepstatin A (Invitrogen) was added to cells treated with vehicle, 10nM TCDD or 5 μ M dithranol (autophagy positive control). BODIPY FL-pepstatin A was taken up by cells by endocytosis and binds selectively to

the active site of CTSD when exposed at an acidic lysosomal pH and has been shown to localise mainly to the lysosomes (Chen et al., 2000).

The protocol was modified from (Chen et al., 2000). Primary keratinocytes were seeded onto glass bottomed dishes and at 80% confluency keratinocytes were preincubated at 37°C for 1h with vehicle, 10nM TCDD or 5µM dithranol in fresh complete Epilife. 1µM BODIPY FL-pepstatin A was added to the medium for 30 minutes pre-incubation at 37°C. Live cell imaging was performed by confocal microscopy, using a heated stage and air flow through to maintain 37°C and 5% CO₂. Preliminary studies were carried out to test levels of evaporation from the medium in a non-humidified atmosphere. The levels of evaporation overnight were found to be very low in the system and the atmosphere was therefore not humidified.

BODIPY FI-pepstatin A is excited at a wavelength of 488nm, with an emission peak at ~500-520nm. Confocal images were taken within this window with transmitted light to allow definition of cell morphology. Pre-treated keratinocytes were imaged overnight (up to 11 h) with z-stacks taken every 5 minutes. Primary keratinocytes were treated with vehicle, TCDD and dithranol and were run over consecutive day and night sessions with keratinocytes seeded accordingly to reach the same confluency. This was repeated in 3 donors.

2.7 AhR knock down assays

2.7.1 siRNA

siRNA constructs were purchased from Dharmacon Thermo Scientific in a kit of 4 constructs against human AhR (ON-TARGET plus, Thermo Scientific). The constructs were targeted against the sequences GCAAGUAAUGGCAUGUUU (construct ID J-004990-**05**), GAACUCAAGCUGUAUGGUA (construct ID J-004990-**06**), GCACGAGAGGCUCAGGUUA (construct ID J-004990-**07**) or GCAACAAGAUGAGUCUAUU (construct ID J-004990-**08**) which were referred to as the numbers in bold (McManus and Sharp, 2002). After optimisation of transfection techniques between nucleofection and Lipofectamine plus, Lipofectamine and plus was chosen based on the viability and proliferation abilities of the cells after transfection. Optimisation of Lipofectamine plus transfection of siRNA constructs was based on

previous work carried out in our group (Baba Taal PhD thesis 2009), (Dalby et al., 2004) and the manufacturer's instructions.

Primary keratinocytes were seeded at 9×10^4 /well of a 6 well plate and grown to ~70% confluency. Transfection master mixes were made as follows: tube A, 100 μ l transfection medium, 2 μ l plus (Invitrogen) and 18nM (final concentration) siRNA. Tube B, 100 μ l transfection medium and 2 μ l Lipofectamine reagent (Invitrogen). Tubes were incubated separately for 15 minutes, together for 15 minutes then diluted further in transfection medium and incubated with keratinocytes for 5 h. After this incubation time cells were washed with PBS and lysed after 24 h or 48 h for Western blots or seeded after 24 h to form epidermal equivalents.

2.7.2 Short hairpin RNA

To create stable AhR knock down in primary keratinocytes for longer term experiments, lentiviral short hairpin RNA (shRNA) against AhR was transduced into primary keratinocytes. Using a hairpin shaped piece of RNA, shRNA constructs use RNA interference to silence the translation of a gene (Paddison et al., 2002).

Lentiviral shRNA pGIPZ vectors against AhR (known as 1380, 1382, 2320, 3803, corresponding to part of their identification numbers) and control sequences scrambled and empty GFP (EGFP) were purchased from Open Biosystems (AhR Target set number RHS4531, empty vector: RHS4349 or non silencing controls: RHS4346). The pGIPZ vectors contained an internal ribosome entry site (IRES) sequence allowing GFP to be transcribed in parallel with the shRNA, resulting in successfully transduced cells being GFP positive and a puromycin resistance gene to allow puromycin selection for transduced cells (Figure 2.1). The transfection protocol and the vector system used were based on the protocols from the Trono laboratory, Switzerland (Klages et al., 2000; Naldini et al., 1996).

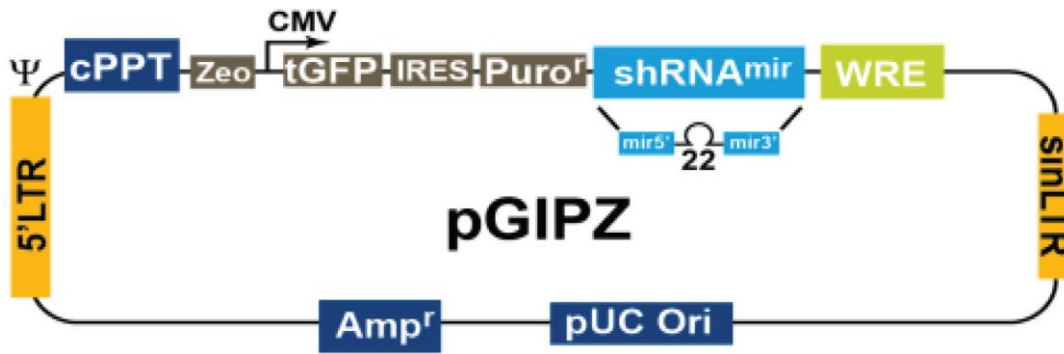


Figure 2.1. Vector map of the pGIPZ lentiviral vector. pGIPZ vectors included sequences for GFP and IRES controlled puromycin resistance, as well as shRNA mir targeting sequence. Image modified from Thermo scientific open biosystems shRNA technical manual.

2.7.2.1 Packaging and production of the shRNA vector in 293T cells

The packaging cell line 293T cells were seeded in 10cm culture dishes and cultured in complete DMEM containing 4mM L-Glutamine and FCS. When cells were ~30% confluent, cells were transfected by the calcium chloride precipitation method with 15µg envelope plasmid, 15µg packaging plasmid and 20µg shRNA construct against AhR (The CaCl₂ precipitation transfection solution contained 0.125M CaCl₂ buffered with NaCl and HEPES at pH 7, which was mixed by air bubbling with 20µg shRNA construct, 15µg envelope plasmid and 15µg packaging plasmid. After incubation for 30 mins at RT to allow precipitate formation, the mixture was added dropwise into 10ml complete growth medium on 293T cells. The next day 293T cells were washed in PBS and medium was replaced with fresh complete growth medium. 293T cells were incubated at 37°C in 5% CO₂ and a humidified atmosphere for 3 days. After this time, the viral particles secreted into the medium were harvested, centrifuged at 3000rpm for 15 mins to remove cellular debris and stored at - 80°C.

2.7.2.2 Transduction of primary keratinocytes with lentiviral shRNA

Primary keratinocytes were seeded at 10x10⁴ per well of a 6 well plate for transduction the next day at 70-80% confluence. Keratinocytes were washed with PBS and medium was replaced with 2ml virus per well with 0.1µg/ml polybrene. Keratinocytes were spin transduced for 90 mins at 1500rpm, washed in PBS and incubated in complete Epilife as normal. Maximal GFP expression was 48h post transduction and images were taken by fluorescent microscopy to record transduction efficiency (Figure 4.8). This varied greatly between experiment and construct. 48h post transduction keratinocytes were put

into selection medium consisting of complete Epilife containing 1µg/ml puromycin. Medium containing puromycin was changed every 48h. After ~5 days puromycin selection cells were checked by fluorescent microscopy and expressed ~90% GFP positivity. Keratinocytes were then seeded in 6 well plates for Western blotting lysates or at high confluency in millicell inserts to form epidermal equivalents. Once keratinocytes were stably transfected, puromycin selection was continued in order to maintain shRNA expression – if puromycin was removed from the medium then daughter cells would not be GFP positive, suggesting modification by the cell to bypass shRNA transcription. Constant use of selection media would keep the cells under selection pressure so puromycin resistance was required for survival and cells maintained shRNA transcription.

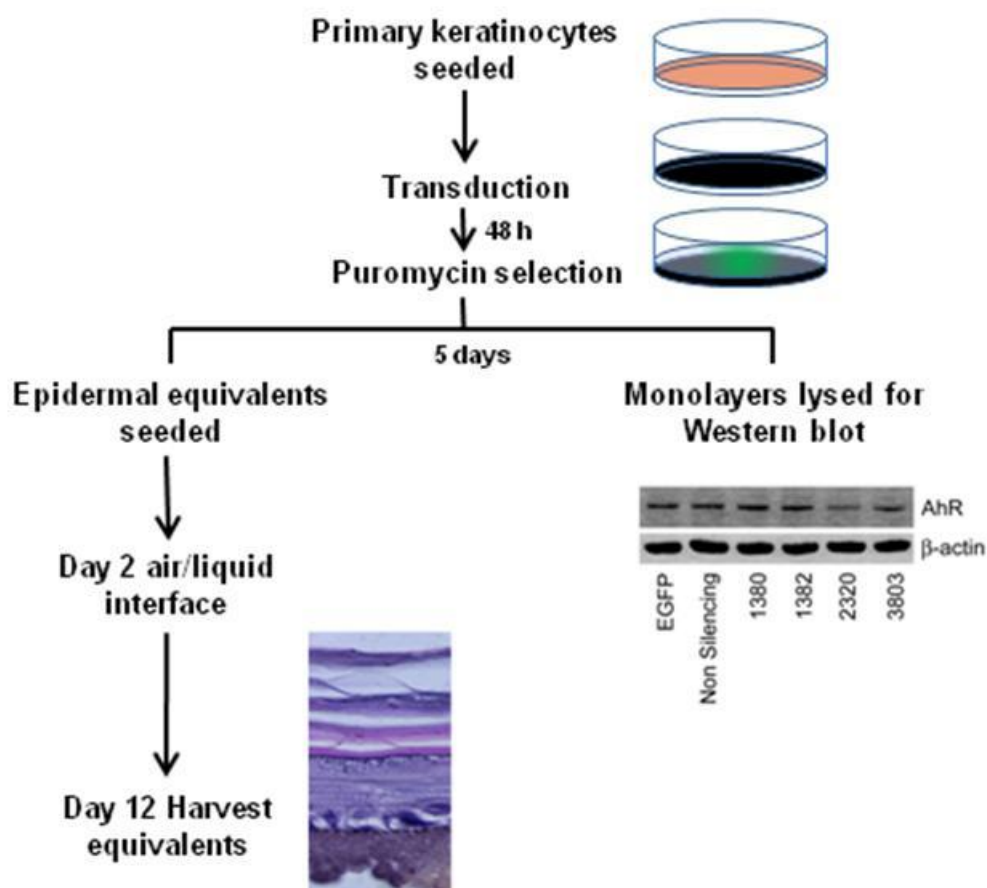


Figure 2.2. Schematic representation of the transduction and treatment regime of primary keratinocytes with shRNA for AhR knock down epidermal equivalents and Western blot.

2.8 Ingenuity pathway analysis

To identify known interactions in the literature between pathways or key phrases, ingenuity pathway analysis (IPA) can be used in 2 ways. 1) To identify direct and

indirect links between pathways and their associated proteins. 2) Text mining to identify the relationship between key phrases. IPA was performed on our behalf by Stephanie Roberts at AstraZeneca. IPA was used in this project to investigate the relationship between the observed phenotype of compacted stratum corneum in TCDD treated epidermal equivalents which is also common in the well researched group of ichthyosis skin disease and the AhR pathway. More details are given in section 6.1.1.2.

2.9 Statistical analysis

All statistical analysis was performed using Graphpad Prism 5. Different methods were used between luciferase assays and Western blots because Western blots showed that time became an important factor. Statistical analysis was not performed on preliminary data because sample size (number of donors that each assay was replicated in) was too low.

Luciferase assays

Mean values were taken from triplicate wells for each donor. Values were normalised by Log transformation for analysis. One-way ANOVAs were performed for each ligand, comparing vehicle to each dose, then for inhibition assays, ligand at each dose was compared to both concentrations of α -NF by one-way ANOVA. This answered two questions: the effect of ligand and the effect of α -NF on ligand responses. Post hoc tests used were Dunnetts or analysis of linear trend chosen depending on the linearity of the dose response. Dunnetts post test was used to compare vehicle to each separate dose when no linear dose response was observed. Analysis of linear trend was performed to measure dose responses when present.

Western blots

Densitometry was carried out on representative blots from 3 donors and normalised to β -actin. Values were normalised by Log transformation for analysis. Data sets showing the effects of AhR agonist on protein levels were analysed using two-way ANOVA, comparing ligand dose and time. Inhibition studies were also analysed by two-way ANOVA, comparing the effects of α -NF and time. Post hoc tests were not performed for two-way ANOVAs.

3 AhR activation in primary human keratinocytes

3.1 Introduction

3.1.1 Known effects of AhR activation

The AhR is the mediator of a wide range of toxicities from developmental defects to neurological disorders and cancers (Gasiewicz et al., 2008; Singh et al., 2009a; Williamson et al., 2005). AhR activation by TCDD mediates the well known human toxicity chloracne, an acne-like skin lesion resulting from exposure to TCDD (Panteleyev and Bickers, 2006; Sorg, 2009). Chloracne is defined and described in detail in the introduction (section 1.3). The defining characteristics of a chloracnegen are unknown but some hypotheses are that high-residency of the ligand or high-affinity for the AhR are required to cause chloracne. To study this further, we used three ligands with different characteristics: chloracnegenic TCDD which displays high-affinity and residency (Table 4)(Schwetz et al., 1973; Sorg, 2009), low-affinity exogenous agonist β -NF that is not chloracnegenic (see section 1.1.4.2)(Maier et al., 1998; Song et al., 2002) and highly potent physiological agonist ITE that is not known to be chloracnegenic but has not been fully characterised in skin or models of chloracne (section 1.1.4.2)(Henry et al., 2006; Henry et al., 2010; Song et al., 2002). The characteristics of these agonists are described in detail in the introduction (section 1.1.4.2).

	AhR affinity	Residency	Metabolism	Potency
TCDD (nM)	+++	+++	+	+++
β-NF (μM)	+	+	+++	+
ITE (μM)	++	+	+++	++

Table 4. The characteristics of AhR-agonists TCDD, β -NF and ITE.

Plus sign represents strength of characteristic for each ligand. Information is taken from the literature as described in Chapter 1.

AhR is known to induce wide ranging effects including immunosuppression (Lundberg et al., 1991; Matulka et al., 1997) and anti-inflammatory effects (Benson and Shepherd, 2011; Wu et al., 2011). There are tissue specific effects intraspecies variation in AhR responses that include variation of AhR degradation (eg. low AhR activation in mouse fibroblasts and high AhR activation in embryonic carcinoma)(FitzGerald et al., 1996)

and induced migration in MCF-7 cells, caused by autocrine activity of CTSD (Ohri et al., 2008; Seifert et al., 2009). Levels of AhR response are dependent in part on expression of the AhR (Dolwick et al., 1993; Mason and Okey, 1982) and also the AhR repressor protein (AhRR) (which is induced by AhR activation) as described in the introduction (section 1.1.2). For example, human fibroblasts are thought to show low AhR activity because of low expression of AhR and high expression of AhRR (Akintobi et al., 2007; Gradin et al., 1999). The effects of AhR activation also appear to be species specific; the differences are thought mainly to be caused by variation in affinity of the AhR to the ligand (Henry et al., 1989; Ramadoss and Perdew, 2004; Schwetz et al., 1973). For example, Perdew and Glover showed forms of AhR with different ligand affinity in mouse strains (Poland and Glover, 1990), while Ramadoss and Perdew showed that AhR affinity in humans was lower than mouse AhR in competition binding experiments (Ramadoss and Perdew, 2004).

As discussed in the introduction (section 1.1.1) CYP1A1 is a commonly used readout of AhR activation and potential for chloracnegenic toxicity. During drug development in industry all novel compounds are screened for causing CYP1A1 induction. However, CYP1A1 expression may not correlate directly to AhR induced toxicity. Thus compounds such as β -NF may induce CYP1A1 in specific cell types yet β -NF is known not to have chloracnegenic potential. One aim of the studies described was to test whether that the different characteristics of these ligands would correlate with different downstream effects in cultures keratinocytes and cutaneous models, suggesting toxicity specific markers.

The first step in the project was to characterise AhR activation in primary keratinocyte monolayers, justifying dose ranges and time points and forming treatment regimes to put into the epidermal equivalent model. This model is important in studying the AhR because a) TCDD induces changes in keratinocyte differentiation that appear relevant to chloracne in this model and b) the effects of confluency on AhR localisation (Ikuta et al., 2004; Sadek and Allen-Hoffmann, 1994a, b) and the effects of differentiation (Du et al., 2006a) on AhR activation in keratinocyte monolayer culture. Studies in monolayer culture therefore required carefully controlled and defined conditions.

3.1.1.1 Comparisons of AhR agonists in the literature

Comparisons of AhR activation by TCDD, ITE and β -NF have been previously reported in the literature. Du et al utilised keratinocyte cultures differentiated in high calcium medium to compare the AhR mediated effects of β -NF and TCDD treatment on proliferating or differentiating keratinocytes over 6 days (Du et al., 2006a). CYP1A1 protein was induced to similar levels at 6 to 8 days by 30 μ M β -NF and 10nM TCDD, with AhR degradation observed in parallel. TCDD induced more AhR degradation than β -NF. Du et al showed up-regulation of TGM-1 expression and TGM activity by TCDD and not β -NF, concluding that this could be a contributing factor of TCDD induced chloracne (Du et al., 2006a). Keratinocytes were cultured in high calcium medium for 16 days and were shown to developed a basic type of 3D culture (Du et al., 2006b). However this model did not include media supplements of vitamin C or an air liquid interface to allow cornification of keratinocytes (as in epidermal equivalents used in this project or by Loertscher or Geaseau, details shown in introduction and next chapter). Data complementary to these papers is presented in this thesis; I have shown studies in monolayer keratinocyte cultures treated with TCDD and β -NF, including novel data on ITE in keratinocytes and comparisons between TCDD/ β -NF and ITE. I also present novel data on the treatment of epidermal equivalents with ITE (and β -NF which has not been studied in epidermal equivalents in regards to its phenotypic effects) and again compare the effects to TCDD.

ITE has been recently studied and compared to TCDD and β -NF to define its properties but no previous studies have investigated ITE in keratinocytes or epidermal equivalents. Song et al compared levels of AhR activation induced by 100nM – 10 μ M ITE or 10nM – 100 μ M β -NF in a mouse hepatoma cell line and also used isolated murine and human AhR for in vitro binding studies (Song et al., 2002). Binding studies showed that 0.5 and 5 μ M ITE could compete against 2nM TCDD for AhR binding. The authors concluded that binding affinities of β -NF and ITE for the AhR were similar whereas binding affinity of TCDD for the AhR was slightly higher (k_i (nM) for murine AhR: ITE = 3, β -NF = 2, TCDD = 0.5). Based on luciferase assays in a mouse hepatoma cell line, potencies were different; μ M ITE was 5 times more potent than the same concentrations of β -NF. They hypothesise that this may have been due to greater stability of ITE (compared to β -NF), that ITE may have greater access to the nucleus or that it may induce conformational changes that causes AhR to be more efficient at binding DNA. Henry et al. studied levels of AhR activity induced in Hepa cells by a range of concentrations of

ITE and TCDD (1-5000nM ITE and 0.01 – 1nM TCDD) by luciferase assay and Western blot (Henry et al., 2006). The XRE-luciferase activity was induced to similar levels by both ligands (at doses of ITE 1000 fold higher than TCDD) and AhR activity was measured by Western blot (down-regulation of AhR and up-regulation of CYP1A1), showing similar levels of activation by 0.1 – 1 nM TCDD and 0.1 – 5µM ITE. Differences were seen in that TCDD induced sustained activation, where as ITE-treated samples showed partial AhR recovery by 24h. Conclusions drawn from this paper are that potency of ITE (at doses 1000 fold higher than TCDD) was equal to that of TCDD. Rapid AhR protein recovery over 24 h was thought to be caused by low stability of ITE. Very short time points were used in the study by Henry et al (Henry et al., 2006)(4 h and 24 h), so comments on sustained activation by TCDD compared to ITE were only over 24h. It would have been interesting if this time course had been expanded further to show effects over prolonged treatment. Further studies were carried out by Henry et al. (Henry et al., 2010) in primary mouse lung fibroblasts and produced similar results as in (Henry et al., 2006), showing equal activation induced by 0.25 – 2.5µM ITE and 0.2 – 1nM TCDD (Henry et al., 2010). The Henry and the Song papers report data on ITE compared to TCDD (Henry et al., 2006; Henry et al., 2010) and ITE compared to β-NF (Song et al., 2002) in mouse hepatoma cell lines. Comments are made on the comparable potencies of the agonists; TCDD and ITE have similar potencies but prolonged activation is only induced by TCDD due to the relatively fast metabolism of ITE (Henry et al., 2006); the Song paper compares ITE to β-NF and reports that ITE has a similar affinity for the AhR as β-NF (reporting murine K_i : ITE = 3, β-NF = 2, TCDD = 0.5nM) but that ITE has a higher potency due to its increased stability (compared to β-NF). Neither paper references any metabolic studies of ITE. It is presumed that as a physiological agonist, it must be relatively quickly cleared to act efficiently as part of a signalling pathway.

These doses were chosen based on the literature in keratinocytes, a relevant treatment model in a rat hepatoma cell line (Du et al., 2006a; Khan et al., 1992; Song et al., 2002) and epidermal equivalents (Geusau et al., 2005; Loertscher et al., 2001a; Loertscher et al., 2001b). ITE had not been tested in keratinocytes or epidermis, so the concentrations utilised in experiments were based on the comparisons by (Henry et al., 2006; Song et al., 2002). Different time courses were used in hepatic cell lines and epidermal cultures to show optimal AhR activation in literature; In hepatic cell lines Western blots were performed at 24h and luciferase assays at 1h -24h showing a peak

between 4 and 8 h (Henry et al., 2006; Song et al., 2002), whereas in differentiating keratinocyte cultures, Western blots were performed at time points up to 8 days. Du et al show low induction of CYP1A1 at day 6 (TCDD and β -NF treatment) and stronger induction at day 8, so this suggests that protein effects of AhR activation in the skin are not seen until then (Du et al., 2006a). To test this theory I included time points at days 2 and 4 in preliminary luciferase studies (Figure 3.2 A). Henry et al. show luciferase assay peaks between 4 and 8 h, so to test if there was early activation in keratinocytes, we included an 8 h time point in our luciferase studies (Figure 3.2). We show novel comparisons of AhR ligands TCDD, β -NF and ITE in their ability to activate AhR transcriptional activation and effects on AhR and CYP1A1 protein levels in primary keratinocytes.

3.2 Preliminary studies

3.2.1.1 Assessing potential of AhR agonist-induced toxicity in vitro

To define the optimal dose ranges and time points for the treatment of primary keratinocytes in cell culture models, preliminary studies were conducted to define treatment ranges that would exert AhR-dependent effects but not toxicity, allowing assessment of growth and differentiation in the cell culture models.

The Sulforhodamine B (SRB) assay is a cell viability assay where the protein binding dye SRB is applied to fixed cells cultured in monolayer and solubilised in a 10mM Tris. The absorbance of this solution is read at specified wavelengths, and optical density units (ODU) plotted; increased ODU correlated closely with increased levels of protein and is considered a robust and reliable readout of cell viability and proliferation (Houghton et al., 2007; Papazisis et al., 1997; Skehan et al., 1990).

Primary keratinocytes were seeded and treated for up to 6 days as described in materials and methods and cell viability/proliferation assessed by SRB assay. Over time, vehicle treated primary keratinocytes proliferated as indicated by increasing levels of protein and SRB staining. Figure 3.1 A shows results from SRB assays of primary keratinocytes treated with 1, 5 or 10nM TCDD for up to 6 days. Although this assay does not include TCDD treatment up to 8 days, no morphological evidence of TCDD-induced toxicity was observed up to 8 days in keratinocyte culture (or reduced renilla values, see Figure 3.2, Figure 3.14 and Appendix A).

Figure 3.1 B shows cells treated with 3, 15 or 30 μ M β -NF. After day 4 at the higher doses 15 and 30 μ M β -NF (note the higher concentrations than those used with TCDD) cells did not proliferate. Moreover, the reduced ODU value in the SRB assay was most likely indicative of cell death as a result of β -NF toxicity. We therefore did not use doses over 15 μ M β -NF in future studies apart from during protein induction assays which involved time points at 2 and 4 days. 30 μ M β -NF was included in those assays due to its strong agonist activity and low toxicity at the early time points. Figure 3.1 C shows primary keratinocytes treated with 1 or 5 μ M ITE. At later time points (day 6 and 8) proliferation of cells was inhibited in presence of 5 μ M ITE. Cells were less viable after 6 days treatment by μ M β -NF and ITE. This was not reflected by treatment of keratinocytes with nM TCDD, and differential effects are probably due to the 1000 fold increase in treatment between TCDD and β -NF/ITE causing toxicity. TCDD has been shown to induce differentiation in primary keratinocytes (Du et al., 2006a; Greenlee et al., 1985; Osborne and Greenlee, 1985), which can be seen as a decrease in keratinocyte growth or increased senescence (Ray and Swanson, 2003; Ray and Swanson, 2004), however the decrease in proliferation caused by TCDD are very small compared to the effects of β -NF and ITE. The concentrations of β -NF and ITE were also 1000 fold higher than TCDD, therefore toxicity exerted by β -NF and ITE was probably due to high concentrations of compound and not increased differentiation by AhR-activation. High concentrations of β -NF and ITE were used in Western blot assays because the levels of toxicity observed were acceptable for monolayer cultures, enough cells were viable with each dose at all time points to form lysates for Western blots, except 30 μ M β -NF at 8 days that sometimes caused too much toxicity to run well on Western blot. These assays also included early time points, days 2 and 4, at which neither β -NF nor ITE showed high levels of toxicity.

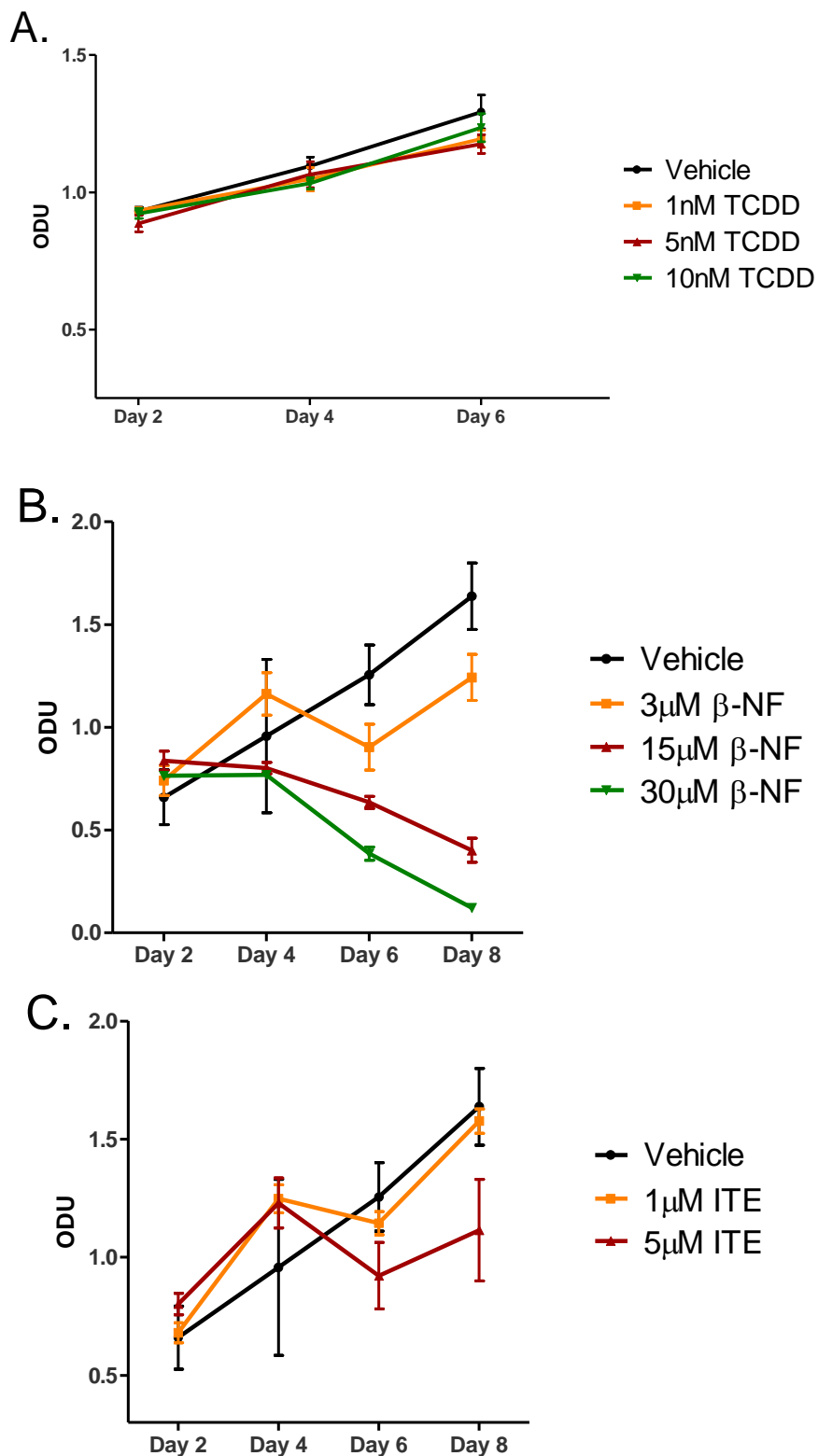


Figure 3.1. β-NF and ITE cause toxicity in a time and dose dependent manner. Primary keratinocytes were seeded and treated after 24h at ~70% confluency with concentrations of vehicle or **A)** TCDD **B)** β-NF or **C)** ITE as indicated for up to 6 or 8 days. Levels of protein were measured by the Sulforhodamine B (SRB) assay and expressed as optical densitometry units (ODU). All error bars show mean ± sem, n = 3, triplicate wells from 1 donor. Statistical analysis has not been performed due to low sample number.

3.2.1.2 Assessing pharmacologically active time and dose ranges

In order to measure levels of transcriptional activation by AhR over time and to define which time points should be used in the subsequent assays, keratinocytes were transfected with a pXRE4-SV40-luciferase construct as described in materials and methods. Constructs transfected into keratinocytes are usually transcribed within 24h (Mimura et al., 1999; Sekine et al., 2006), so keratinocytes were left for 24h before treatment. As cells were transiently transfected, the longest time point used was 4 days of treatment. An early time point (8h after treatment) was used in transfected keratinocytes treated with TCDD (Figure 3.2 A) to test for any early activation, as reported the literature (Henry et al., 2006). Henry et al. showed a peak in AhR transcriptional activation between 4 and 8h using mouse and human hepatoma cell lines transfected with AhR-dependent luciferase and treated with ranges of 1nM – 1 μ M ITE or 0.1nM – 1nM TCDD (Henry et al., 2006). AhR activation in keratinocytes did not occur at 8h (Figure 3.2 A), even at the higher concentrations of TCDD that we used. This difference is thought to be because the liver cell lines used in these early studies have higher levels of AhR protein and activity (Dolwick et al., 1993; Khan et al., 1992).

Maximal induction of AhR dependent activation in response to TCDD occurred after 24h treatment and persisted for at least 96h. However as the level of TCDD induced XRE-luciferase activation at 24h varied to a greater extent among different donors than at later time points, future studies focused on AhR activation at 48h. AhR activation decreased time dependently to 72 h, increasing slightly again at 96 h, but losing the dose dependent response pattern seen at earlier time points. At 24 and 48h time points, the dose response of AhR activation induced by TCDD was increased by 0.5, 5 and maximally (in this model) by 10nM TCDD.

The concentrations of β -NF shown in Figure 3.2 A were nM β -NF, which is low compared to the doses used in the literature (Du et al., 2006a; Gelardi et al., 2001). This was because when luciferase assays were performed using μ M β -NF, very low firefly:renilla ratios were induced. On closer inspection, firefly luciferase activity was decreased to values normally shown in empty control wells. This was addressed and is shown in Figure 3.3, suggesting the decreased firefly values were not a result of toxicity because renilla values (internal control for transfection efficiency and viability) were

unaffected and suggested that the presence of β -NF in cell lysates quenched firefly luciferase activity. Figure 3.2 B shows that nM concentrations of β -NF induced AhR transcriptional activation which was maximal at 20nM β -NF. Figure 3.2 B shows that β -NF induced transcriptional activation peaked at 20nM, but by 200nM, activity had started to decrease. As discussed in regards to TCDD, the 24h time point induced high transcriptional AhR activation but the results varied between donors. As with TCDD, 48h was chosen for future studies. Figure 3.2 C shows induction of AhR transcriptional activation by ITE. Induction by all concentrations of ITE was very high, maximum induction was roughly ~4 fold higher by 10 μ M ITE than 10nM TCDD. Considering the 1000 fold difference in concentration, this is not surprising. A 1000 fold difference in dose between ITE and TCDD has been used previously in the literature (Henry et al., 2010) to directly compare activation in mouse fibroblasts. Their results showed similar effects from both ligands on AhR degradation and CYP1B1 induction by Western blot. These data were not compared to AhR activation tested by luciferase assay (Henry et al., 2010) but we went on to compare AhR activation induced by TCDD, β -NF and ITE by Western blot and luciferase assay as described later in this chapter (section 3.3.1).

The lowest concentrations of both TCDD (0.5nM) and ITE (0.1 and 0.5 μ M) showed high levels of AhR transcriptional induction. This could be caused by the poor solubility of higher concentrations of lipophilic agonists in the media. At low concentrations, lipophilic compounds remain in solution, however at higher concentrations the ligands often come out of solution. At low concentrations luciferase activity was high possibly due to high solubility and availability of the ligand, however at medium concentrations (eg. 1nM TCDD), availability is low due to less solubility and lower ligand present. The stronger response caused by the higher doses (10nM TCDD) could be due to high levels of the compound providing a constant supply of ligand when solubilised ligand has been used or metabolized over the 48h treatment.

To test this theory, primary keratinocytes were treated with low concentrations of TCDD to test whether protein levels (AhR degradation and CYP1A1 induction) would show higher AhR activation with 0.5nM TCDD than 1nM TCDD as in the luciferase assays in Figure 3.2 A. These results are shown in Figure 3.9.

Therefore, concentrations of ligand for future assays were chosen based on levels of toxicity (Figure 3.1) and activity (Figure 3.2). 48h was chosen as the time point for future

luciferase assays to be undertaken because of less variability in values between donors at this time point. TCDD exhibited a good dose response by 1, 5 and 10nM TCDD in both luciferase assay (Figure 3.7) and Western blot (Figure 3.9) and literature conclusively showed use of 1 and 10nM TCDD in primary human keratinocytes (Du et al., 2006a; Geusau et al., 2005; Loertscher et al., 2001b). β -NF concentrations were based on data from Figure 3.1 and the literature (Du et al., 2006a; Gelardi et al., 2001; Khan et al., 1992), and concentrations of ITE were chosen based on levels of activation, toxicity and the literature (Henry et al., 2006; Henry et al., 2010; Song et al., 2002). Figure 3.2 C shows high activation by all concentrations of ITE, however based on the literature, 1000 fold higher concentrations of ITE were used compared to TCDD (Henry et al., 2010). 5 μ M ITE induced high levels of toxicity (Figure 3.1) so higher concentrations of ITE were not used despite high AhR transcriptional induction, resulting in 1 and 5 μ M ITE being carried through to main studies.

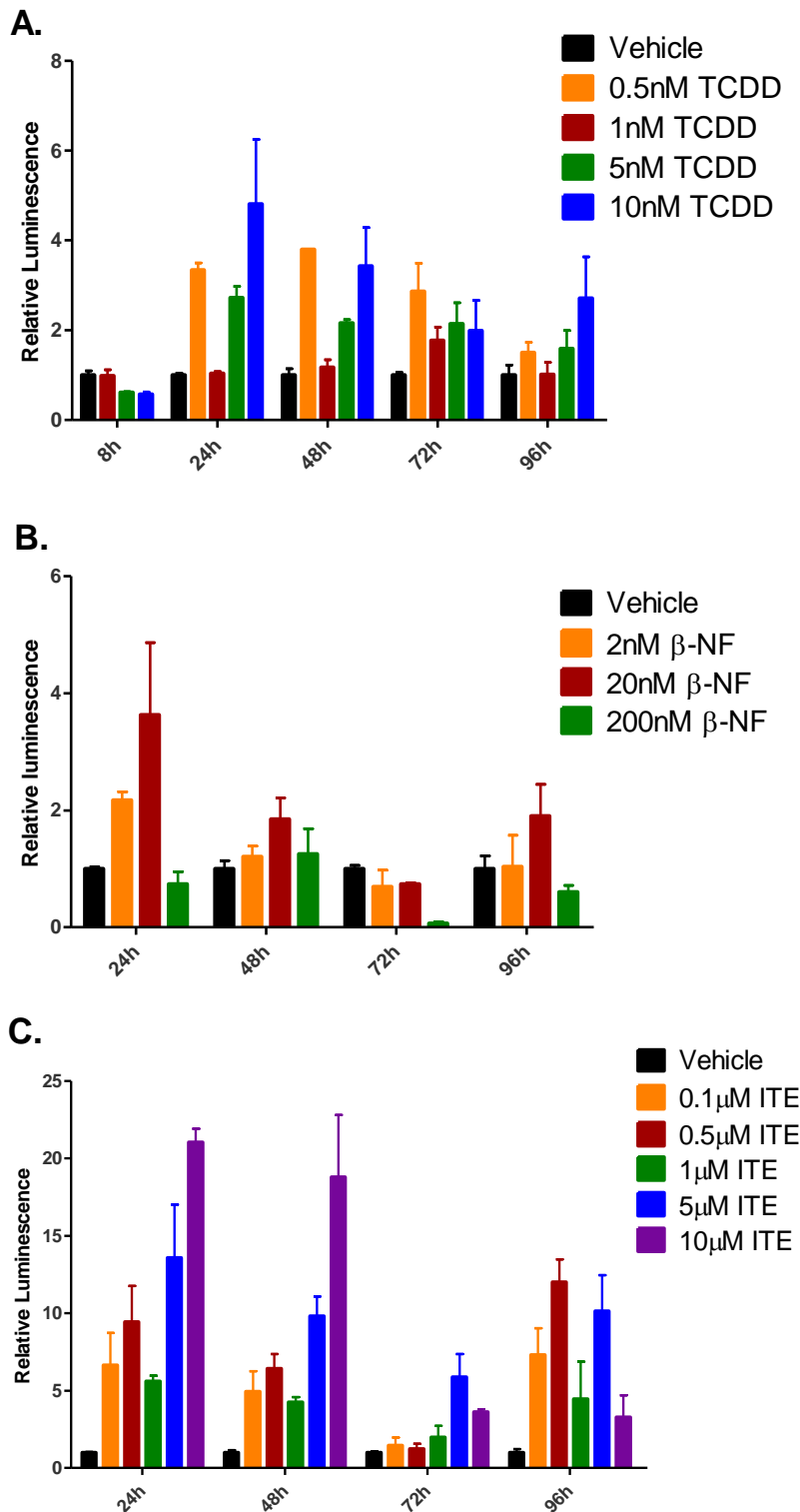


Figure 3.2. AhR transcriptional activation was induced by TCDD, β -NF and ITE between 24h and 96h treatment. Primary keratinocytes were transfected with XRE-luciferase and renilla constructs as described in materials and methods. 24 h later keratinocytes were treated with vehicle or concentrations of **A)** TCDD, **B)** β -NF or **C)** ITE as indicated for up to 96h and XRE luciferase activity measured using a dual luciferase kit and luminometer. Results are expressed as mean firefly luciferase/renilla ratios (\pm sem) normalized to vehicle. n = 3 triplicate wells from 1 donor. Statistical analysis has not been performed due to low sample number.

3.2.1.3 Problem solving 1:

Defining the reasons for inhibition of luciferase by β -NF

As discussed in the previous paragraph, μ M concentrations of β -NF resulted in low firefly:renilla ratios. To study this further, primary keratinocytes were transfected with XRE-luciferase as described in materials and methods then treated with concentrations of β -NF as indicated. Figure 3.3. A shows decreased firefly:renilla activity with higher β -NF concentration. At ≥ 1000 nM β -NF, relative luminescence had decreased to negligible values (ratio ~ 0.05). To test whether β -NF was having a quenching effect, we added vehicle (DMSO) or β -NF (final concentration 15 or 30 μ M β -NF) to TCDD treated primary keratinocyte lysates prior to measuring luciferase activity. As shown in Figure 3.3. B, firefly:renilla ratios decreased sharply with addition of β -NF to the lysate *in vitro*. Looking at the raw firefly and renilla luciferase values, it was apparent that firefly luciferase had been quenched (Figure 3.3. C), while renilla values remained unaffected (Figure 3.3. D). To test if this observation was specific to the construct, the assay was repeated with primary keratinocytes transfected with an alternative XRE-luciferase construct (details are described in materials and methods) with similar results. Ratios and raw values for the parallel experiment with the alternative construct are shown in Appendix A. Inhibition and quenching of firefly luciferase activity at higher doses of β -NF (from 0.1 μ M β -NF) has previously been reported (Wang, 2002), showing the phenomenon of firefly luciferase quenching was specific to β -NF. These effects were cell line and construct independent and specific to β -NF, α -NF was also tested for quenching effects on firefly luciferase. β -NF-dependent quenching was tested at a range of 0.1 – 2 μ M β -NF and EC50 was defined at of 0.1 μ M β -NF, leading to complete quenching of firefly luciferase by 2 μ M β -NF (Wang, 2002). Our results correspond well with this paper, clearly showing that β -NF ($\geq 1\mu$ β -NF) *in vitro* markedly inhibited firefly luciferase, specifically showing quenched firefly luminescence by adding β -NF (at a final concentration of 15 or 30 μ M β -NF) to the lysate before assaying.

Direct quenching effects of 15 and 30 μ M β -NF have been shown on firefly luciferase, however we have not investigated the quenching effects of low levels (2nM-3 μ M) of β -NF. Figure 3.3. A shows peak XRE luciferase activity at 20nM β -NF. At concentrations from 200nM β -NF, activity started to decrease, reaching complete inhibition at 1000nM β -NF. This decrease appears to be due to onset of β -NF-dependent firefly luciferase quenching. If we compare this to the effects of nM β -NF on AhR activation by Western blot (Figure 3.12), we see the onset of β -NF-dependent AhR activation by AhR

degradation from 20nM β -NF at days 2 and 6. Luciferase activation would be expected to increase more above concentrations of 20nM but as my data does not show this it would suggest that this concentration is where luciferase assays may start to be partially inhibited by β -NF. This is consistent with the observations from Wang 2002 (Wang, 2002), where they defined the EC50 of β -NF quenching at 0.1 μ M β -NF and the level for complete quenching at 2 μ M β -NF. To directly compare transcriptional activation with the effect of β -NF on protein levels, a different non-luciferase reporter assay would have to be used. In view of these results low levels of β -NF (<200nM β -NF) were used in further XRE-luciferase assays.

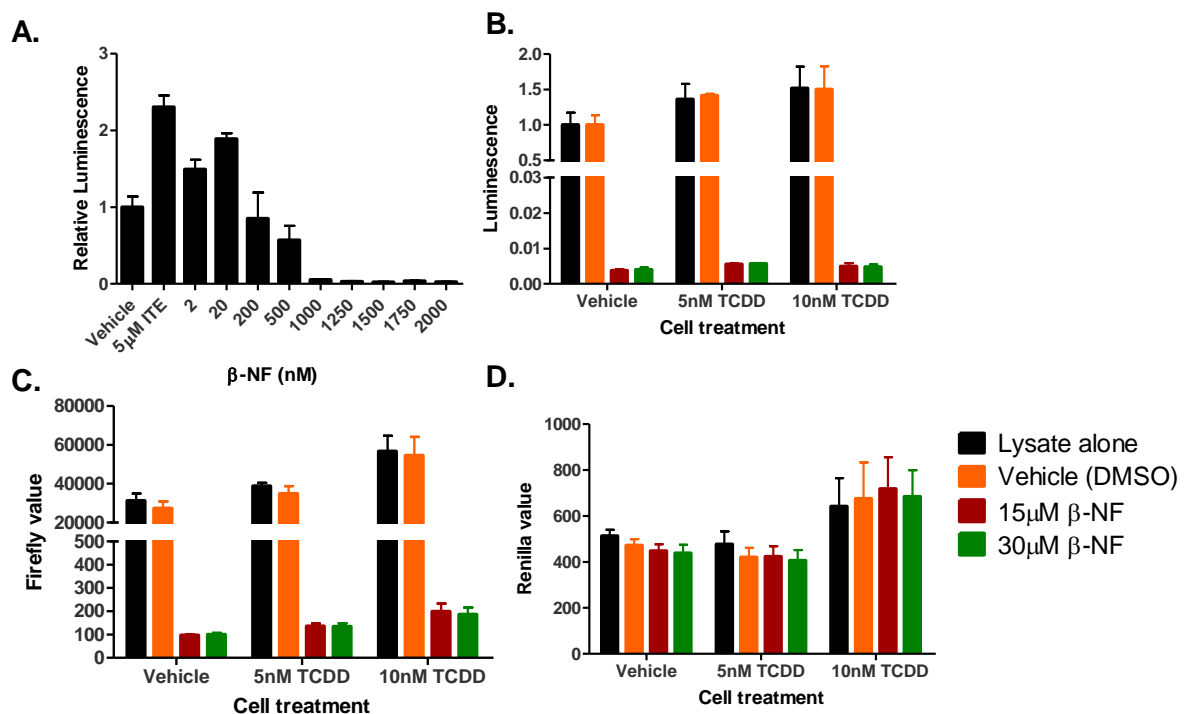


Figure 3.3. β -Naphthoflavone quenched firefly luciferase activity. Primary keratinocytes were co-transfected with XRE-luciferase and renilla housekeeping luciferase reporter. **A)** Cells were treated with vehicle, 5 μ M ITE or specified concentrations of β -NF for 48h. **B)** Cells were treated with vehicle, 5 or 10nM TCDD for 48h and lysed. Before luminescence was read, vehicle or β -NF (15 or 30 μ M β -NF final concentration) was added to the TCDD-treated cell lysate. Results are expressed as A) mean firefly luciferase/renilla ratios (\pm sem) normalized to vehicle, B) mean firefly:renilla luciferase ratios (\pm sem), C) mean firefly raw values (\pm sem), or D) mean renilla raw values (\pm sem). **A)** n = 3 (triplicate wells from one donor), data is representative of 3 individual donors. **B)** n=3, triplicate wells from 1 donor, representative of data from 2 donors. Statistical analysis has not been performed due to low sample number.

3.2.1.4 Problem solving 2: Addressing low solubility of TCDD

To address the possible issues caused by low solubility of TCDD accounting for data shown in luciferase assays (Figure 3.2 A), an alternative vehicle for TCDD was tested. Dioxane is less polar than DMSO (retaining enough polarity to remain miscible in water) and was tested to see if it would hold higher concentrations of TCDD in solution more effectively (Drake et al., 2006). Primary keratinocytes were transfected with XRE-luciferase and treated with vehicle, TCDD diluted in dioxane (at concentrations shown) or 10nM TCDD diluted in DMSO as previously used (Figure 3.2 and Figure 3.3.). Figure 3.4 shows a dose dependent increase of AhR transcriptional activation with TCDD diluted in dioxane, however 10nM TCDD diluted in DMSO induced slightly higher AhR transcriptional activation than 10nM TCDD in dioxane. This suggests that dioxane did not increase availability of TCDD in culture medium compared to DMSO. We therefore continued to use DMSO as the vehicle for all ligands tested.

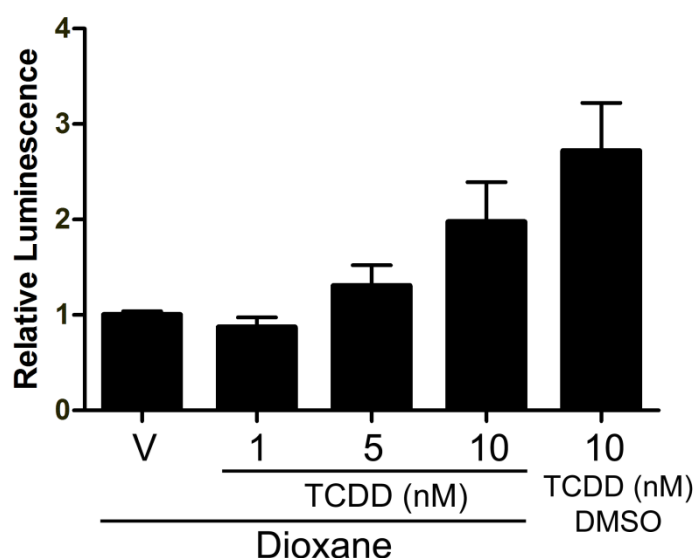


Figure 3.4. Dioxane does not increase TCDD-induced XRE-luciferase activation in cell culture. Primary keratinocytes were co-transfected with XRE-luciferase and renilla internal control constructs and treated with vehicle, 1, 5 or 10nM TCDD in dioxane or dioxane alone (vehicle) for 48h compared to 10nM TCDD in DMSO. XRE-luciferase activity was measured. Results are expressed as mean firefly luciferase/renilla ratios (\pm sem) normalized to vehicle. n=6, triplicate wells from 2 independent donors. Statistical analysis has not been performed due to low sample number.

3.2.1.5 Problem solving 3: Addressing the effect of confluency on AhR response

Ligand-dependent activation of the AhR results in translocation of the AhR to the nucleus where the AhR/ARNT dimer binds the XRE (see introduction for details and references). Translocation is an important part of the process and can also occur by

ligand-independent mechanisms such as cell density (Cho et al., 2004; Ikuta et al., 2004; Sadek and Allen-Hoffmann, 1994a, b) and the removal of AhR chaperone molecule hsp90 from the AhR-complex (Petrulis et al., 2003; Pollenz and Buggy, 2006; Pongratz et al., 1992). Ikuta et al. (Ikuta et al., 2004) previously showed that cell density affects localization of the AhR in the human keratinocyte line HaCaT. When cells were sparse the AhR was nuclear, when confluent the AhR was cytoplasmic. They correlated nuclear AhR in sub confluent cells with upregulated transcriptional activation by luciferase activity and CYP1A1 induction by Western blot. There are other reports of ligand-independent AhR translocation and activation in the literature (Sadek and Allen-Hoffmann, 1994a, b) but this demonstrates that AhR translocation does not necessarily result in AhR transcriptional activation.

As described in the introduction and the following literature, hsp90 is an AhR chaperone molecule which keeps the AhR in the cytoplasm when in its inactive state. If the AhR/hsp90 complex is broken, the AhR is no longer anchored in the cytoplasm by hsp90 and is able to translocate to the nucleus. Pollenz and Buggy previously showed the effects of treatment with specific Hsp90 dimerisation partner, geldanamycin (Grenert et al., 1999; Grenert et al., 1997) on a number of human cell lines. It has been hypothesized that geldanamycin has the ability to inhibit hsp90 binding to the AhR, as is has been shown to do with other hsp90 complexes (An et al., 2000; Schulte et al., 1995). Treatment with geldanamycin causing hypothesized breakdown of the AhR/hsp90 complex, resulted in AhR translocation and degradation but no AhR transcriptional activation (Pollenz and Buggy, 2006; Song and Pollenz, 2002).

The mechanism of AhR translocation by loss of cell-cell contact is not known but there are several hypotheses. Ikuta et al hypothesise that increased cell density accelerates nuclear export of the AhR via the p38 MAPK signaling pathway that is involved in nuclear accumulation of p53 and oestrogen receptor α . Increased cell confluency caused rapid phosphorylation of p38 MAPK in HaCaTs, increasing phosphorylation of the NES and therefore inhibiting nuclear export, via differential activation of phosphatase caused by cell confluency as shown in Figure 3.5 (Ikuta et al., 2004).

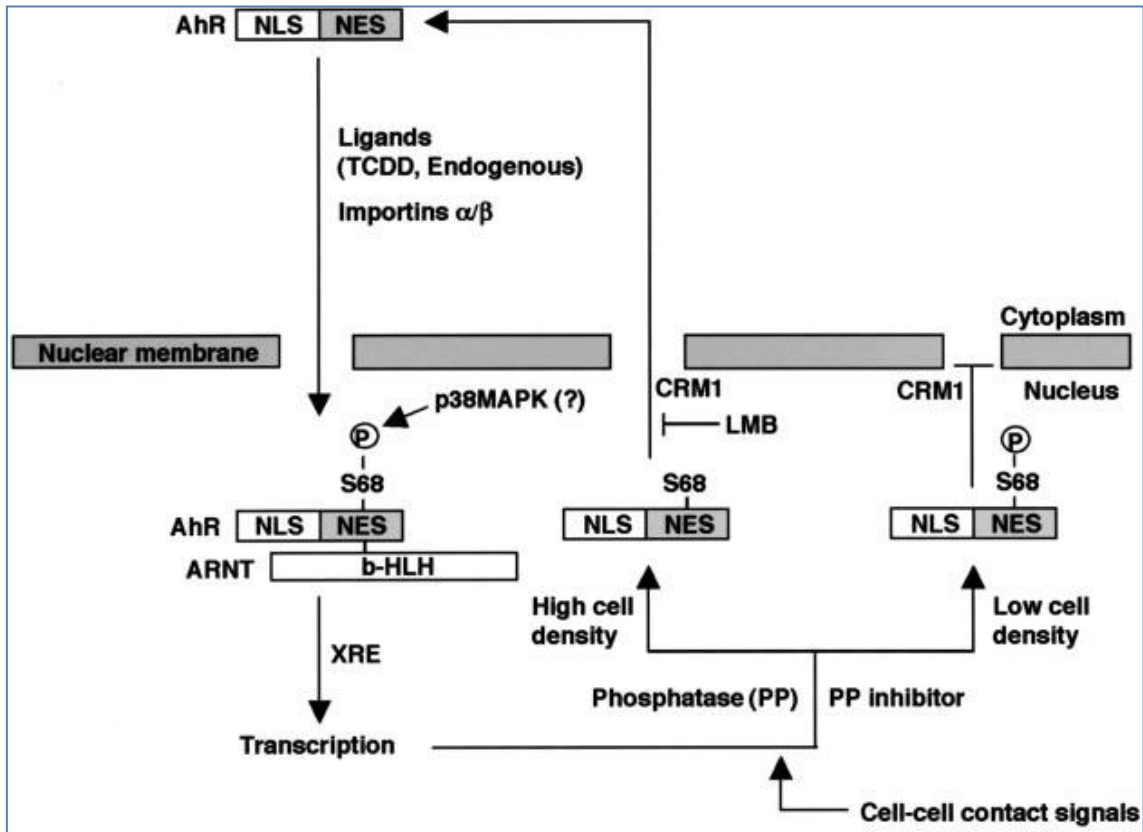


Figure 3.5. Proposed hypothesis for nuclear localization of AhR caused by loss of cell-cell contact. Nuclear accumulation of the AhR occurs in response to lack of cell-cell contact. Ikuta et al. hypothesise that this is via sparse confluency causing decreased phosphatase activity which results in phosphorylated NES, blocking nuclear export. Figure modified from (Ikuta et al., 2004).

Sadek et al hypothesise that changes of cell shape and adhesion when primary keratinocytes are in suspension, may disrupt AhR/hsp90 binding, causing AhR nuclear translocation through lack of chaperone molecules as discussed earlier (Sadek and Allen-Hoffmann, 1994b).

To confirm the basic observation from Ikuta et al. that confluency affects AhR localisation in primary keratinocytes, primary keratinocytes were seeded at differing densities on coverslips and IHC was performed with an anti-AhR antibody, fluorescently tagged secondary antibody and nuclear stain Topro-3, as described in materials and methods. Confocal images of immunostained keratinocytes are shown in Figure 3.6. Green staining shows AhR, blue shows nuclei. Similar to HaCaT cells, in sparse cultures AhR was mainly nuclear and in confluent cells the AhR became predominantly cytoplasmic. These findings are consistent with the literature and show that cell contact mediated AhR relocalisation is a conserved mechanism from HaCaTs to primary

keratinocytes (Ikuta et al., 2004) and also suggests that CYP1A1 induction by lack of cell-cell contact in primary keratinocytes may be caused by this effect in our culture model (Sadek and Allen-Hoffmann, 1994a). We did not study effects of confluency on activation of AhR by luciferase or Western blot, but it would be interesting to explore this in studies where activation of AhR in sparse populations is relevant, for example wound healing. In our project, we have taken this into consideration and all experiments were carried out in confluent cells (>80%). Not only does keep background AhR activation low and variation to a minimum, but it also provides a more physiologically relevant model to un-wounded, normal human skin.

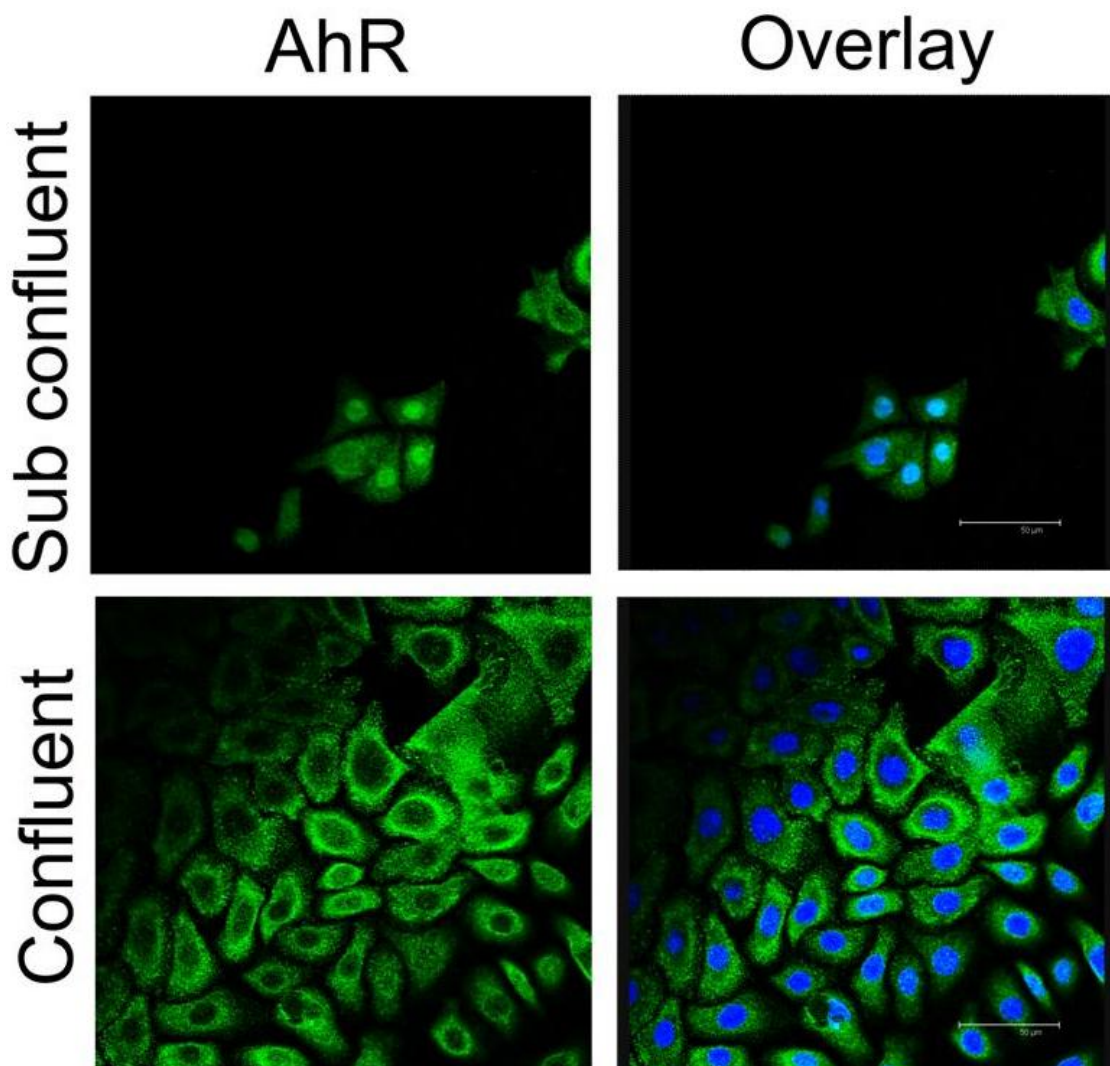


Figure 3.6. Sparse cell confluency can induce AhR translocation to the nucleus. Primary keratinocytes were grown seeded at different densities on glass coverslips for 24h and fixed (in parallel) maintaining different confluencies. Cells were fixed with 4% PF and IHC was performed using an anti-AhR antibody (green) and topro-3 nuclear stain (blue). Confocal images were captured on a Leica SP2 confocal microscope at mid Z stack and are representative of 3 donors. Scale bar = 50µm.

3.2.1.6 Western blotting and antibody optimisation

Antibodies used for Western blots were optimised and chosen based on antibody specificity and reproducibility. Two anti-CYP1A1 antibodies were tested for specificity on Western blots. The antibody that was excluded for use in the project (clone H-70, SantaCruz) showed more non-specific bands around the correct molecular weight, making distinguishing the specific CYP1A1 band difficult. The CYP1A1 antibody that was chosen (clone B-4, SantaCruz) was optimised for the time of incubation and protein block used resulting in the clearest specific bands and lowest non-specific binding. The AhR antibodies originally tested for Western blot were both discarded due to high background and non-specific binding after optimising dilutions and incubation conditions. A third AhR antibody was chosen and took little optimisation apart from the dilution used and time of incubation.

The antibodies chosen finally were anti-CYP1A1 (clone B-4, Santacruz), anti- AhR (MA1-415, Biomol) as describe in section 2.5 of materials and methods. The anti- β -actin was already optimised and used in our group. Appendix X shows the optimised antibodies in complete blots with protein standard ladder as run on each blot. Both images in Appendix X show the same membrane, probed first with anti-CYP1A1 (A) and secondly with AhR (B), so CYP1A1 bands are visible on the lower blot too – they are both anti-mouse antibodies. As shown, the primary antibodies produced clean blots, with one non-specific band for anti-CYP1A1 (although a faint thicker band was sometimes present ~10kDa above the CYP1A1 band as shown in the lower blot for anti-AhR) and no non-specific bands for anti-AhR or anti- β -actin. The results from different experiments did vary sometimes in that the background binding could be variable with CYP1A1 and AhR antibodies but all Western blots were run in duplicate to discount this type of variation. The AhR and CYP1A1 blots in Appendix X have been shown in Appendix G and Figure 3.16 D.i to demonstrate the effect of α -NF on ITE-induced AhR activation.

3.3 Main Studies

After the preliminary studies it was clear that all 3 agonists showed induction of AhR activity. In chronological order, the next phase of the study focussed on α -NF, but for clarity this is presented later (section 3.3.2). Moreover, in the next series of experiments, α -NF was included in parallel as a potential AhR inhibitor but for clarity, these data are also presented later (section 3.3.2).

The full time courses presented for the activation of the AhR by the 3 agonists and the inhibition of agonist induced AhR activation by α -NF (sections 3.3.3.1, 0, 3.3.3.2) are quite complex, so the complete time courses have been presented in the appendix with detailed description of the data and summary figures showing data at days 2 and 8 in the main text.

3.3.1 AhR activation by TCDD, β -NF and ITE

3.3.1.1 AhR transcriptional activation by agonists

To compare AhR activation potential of each ligand in primary keratinocytes, luciferase assays were performed following transfection of primary keratinocytes with pXRE4-SV40-Luciferase as described in materials and methods, and treatment of keratinocytes with ranges of doses of TCDD, β -NF or ITE as indicated for 48h. The doses chosen were based on preliminary studies of ligand solubility, quenching of luciferase, pharmacological AhR activity and toxicity as described earlier in the chapter. Figure 3.7 shows that all ligands induced AhR activation significantly in a dose dependent manner (one-way ANOVA vehicle compared to each ligand $P < 0.0001$, analysis of linear trend compared vehicle to increasing doses each ligand, TCDD and ITE: $P < 0.0001$. β -NF: $P = 0.0003$).

The dose ranges tested in the luciferase assay varied over a 1000 fold range and did not necessarily overlap. Therefore, to compare the AhR agonist activity of the ligands in keratinocytes, we plotted the normalised luciferase activity versus log concentration. When we normalised to a dose of 50nM assuming a linear response the relative luciferase values were TCDD = 5, α -NF = 2, β -NF = 1.5, ITE = 1. Alternatively, normalising to an equivalent increase in relative luciferase, TCDD was at the lowest dose compared to β -NF and then ITE. This correlated with the literature which ranked

TCDD as the highest affinity, followed by β -NF and ITE at similar affinities (but ITE slightly less) (Song 2002, Henry 2006), activation by α -NF remained at levels lower than TCDD, β -NF and ITE up to 24 μ M, the maximum dose tested.

As described in the introduction (section 1.1.4.2) and the paper by Henry et al., ITE exhibits a similar potency for the AhR as TCDD. Maximal induction of AhR activity was to a similar level by ITE (at concentrations 1000 fold higher than TCDD), but whereas TCDD induced AhR activation (by AhR degradation and CYP1B1 induction) that persisted for 24h, ITE induced activation in parallel had decreased by 24h (Henry et al., 2006; Henry et al., 2010). The authors suggested that this was due to clearance of ITE by metabolism compared to persistent TCDD levels. The comparison of TCDD to ITE corresponds to the normalised ranking of luciferase induction shown in Figure 3.7. Song et al. describe that ITE has a similar binding affinity for the AhR, which would also correlate with the ranking of AhR-activation by agonists described here.

To try and achieve higher AhR activation than 20nM β -NF without quenching, keratinocytes were treated with 50nM β -NF as shown in Figure 3.7, however no increased activity was shown and the response plateau had been reached. Maximal stimulation of XRE-luciferase by β -NF was achieved at 20nM β -NF (Figure 3.3 and Figure 3.7), at higher doses reduced levels of XRE luciferase was observed, as described earlier (Figure 3.3 A).

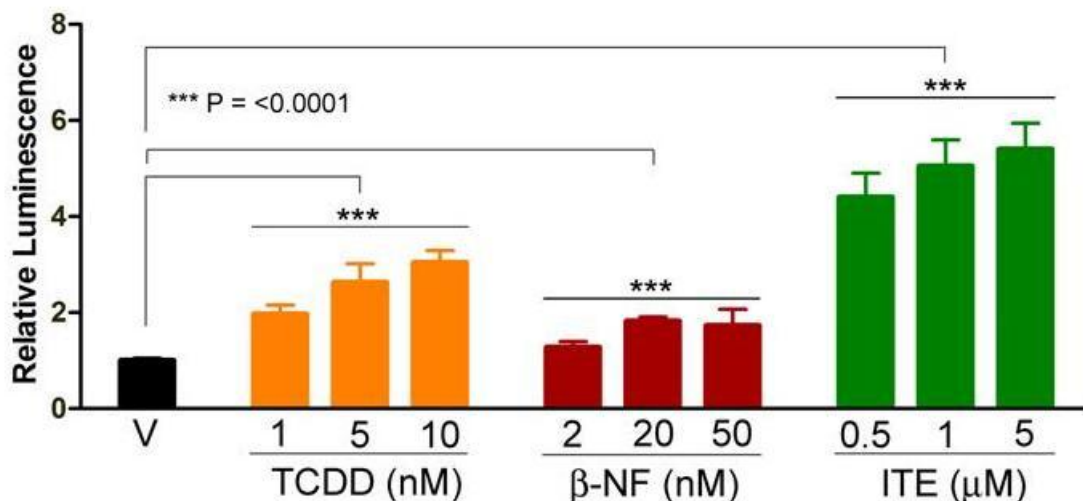


Figure 3.7. AhR transcriptional activity in keratinocytes is induced by treatment with TCDD, β-NF and ITE. Primary keratinocytes were treated with concentrations of ligand as indicated for 48h and XRE luciferase activity was then measured. Values represent mean firefly luciferase/renilla ratios (\pm sem) normalized to vehicle. $n \geq 9$, triplicate wells from ≥ 3 independent donors. One-way ANOVA was performed comparing vehicle to ligand ($P < 0.0001$) with analysis of trend compared to vehicle as post hoc test. TCDD and ITE $*** P < 0.0001$. β-NF $*** P = 0.0003$.

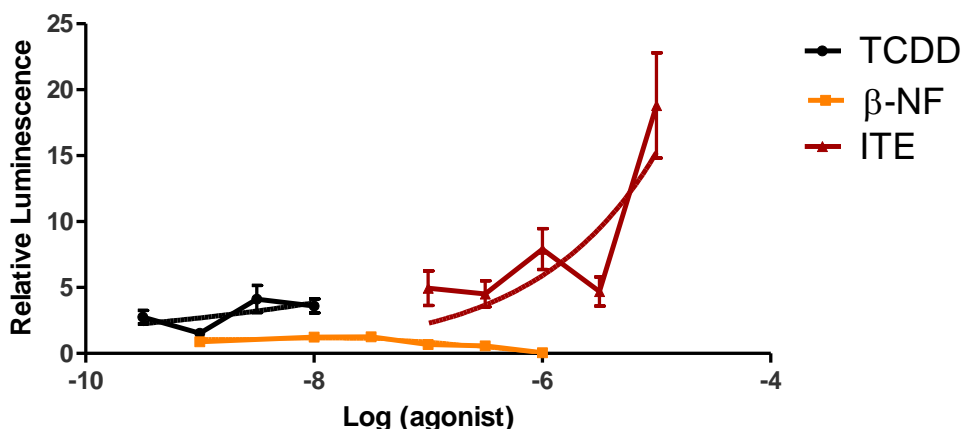


Figure 3.8. Log dose response curve for AhR-agonists. Data from luciferase assays were plotted on a log scale to allow normalisation of results to 50nM for all agonists. Non linear regression curves were fitted between points using Graphpad Prism 5.

3.3.1.2 Induction of AhR activation measured by AhR degradation and CYP1A1 induction

One of the aims of the project was to identify differential downstream effects of AhR activation by physiological and non-physiological agonists, including assessment of AhR transcriptional activities and differential induction of CYP1A1 protein and degradation of AhR protein. Previous literature on AhR activation in primary cultured keratinocytes reported that treatment of keratinocytes with 10nM TCDD or 30μM β-NF induced AhR

activation by Western blot (induced CYP1A1 and AhR degradation) after 6 and 8 days. Differentiation markers were also up regulated in time and TCDD treatment dependent manners (loricrin and TGM-1 expression and activation) (Du et al., 2006a). Ray and Swanson showed an increase in basal pro-filaggrin in primary keratinocytes over time (days 2, 6 and 8) which was increased further by treatment with 1nM TCDD. This correlates with AhR protein degradation induced by 1nM TCDD treatment at days 2, 6 and 8 (Ray and Swanson, 2003). Sutter et al. showed up-regulation of CYP1A1 mRNA in primary keratinocytes by a range of 0.1 - 10nM TCDD treatment at 24h (Sutter et al., 2009). Ray and Swanson showed immortalisation of primary human keratinocytes by treatment with 0.01-10nM TCDD. This paper also showed AhR down-regulation by TCDD treatment at 2, 6 and 8 days (Ray and Swanson, 2004) . These papers all show AhR activation in primary keratinocytes by 1 or 10nM TCDD. Based on these results in the literature, SRB assays (Figure 3.1) and preliminary dose response studies (Figure 3.2 and Figure 3.7), primary keratinocytes were treated with ligands as indicated for up to 8 days with time points every 48h. Samples were lysed and Western blotting performed. Antibodies against AhR, CYP1A1 and β -actin (see Table 3 for details) were used to probe membranes and bands were quantified by densitometry and presented as ODU normalised to β -actin, as described in materials and methods

3.3.1.3 TCDD

Figure 3.10 and Figure 3.11 show dose dependent degradation of AhR by TCDD treatment that was present at days 2 and 8 and a dose dependent increase in CYP1A1 at day 8. For complete timecourses see Appendix B and Appendix C. Two-way ANOVA was performed to compare vehicle with TCDD treated cells at each time point. At all time points, the effects of TCDD on AhR degradation were significant ($P < 0.007$). The effects of TCDD and duration of incubation on CYP1A1 were not significant and there was no significant interaction between TCDD and duration of incubation (time).

AhR is known to be more inducible in differentiated cells and that is shown by the increased induction of CYP1A1 at day 8 (Figure 3.11) compared to day 2 (Figure 3.10). Du et al show an increase in CYP1A1 induction in differentiated human primary keratinocytes in monolayer, as do Jones and Reiners in murine keratinocytes (Du et al., 2006b; Jones and Reiners, 1997). Ray and Swanson showed that CYP1A1 expression in 1nM TCDD treated primary keratinocytes increased with passage number from p2 to

p16; CYP1A1 mRNA increased 3 fold, but AhR mRNA remained unaffected. Interestingly, TCDD dependent AhR degradation occurred from day 2, whereas CYP1A1 induction only occurred at days 6 and 8 (Appendix C). As TCDD resulted in maximal induction of CYP1A1 and maximal degradation of AhR at days 6 and 8, further studies focussed on these time points.

Figure 3.2 A shows that 0.5nM TCDD induced high levels of AhR transcriptional activation that was higher than 1 and 5nM TCDD but not 10nM TCDD at 24 and 48 h. This could have been caused by a decrease in solubility of TCDD at higher concentrations. To investigate the effect of 0.5nM TCDD on AhR degradation and CYP1A1 induction, primary keratinocytes were treated for up to 8 days with 0.5, 1, 2 or 5nM TCDD. Figure 3.9 shows that 0.5nM TCDD induced AhR degradation and low levels of CYP1A1 induction at 6 and 8 days. The levels of AhR degradation were similar to those induced by 1, 2 or 5nM TCDD. Comparing the results from the luciferase assay (Figure 3.2) to Western blot (Figure 3.9), levels of AhR activation were not as high as expected. Levels of activation shown by Western blot were consistent with the TCDD dose dependent increase in AhR activation shown in Figure 3.10 and Figure 3.11. The time points used (day 6 and 8) were based on the observations from Appendix B and Appendix C that AhR dependent effects on protein occur at the later time points studied, day 8.

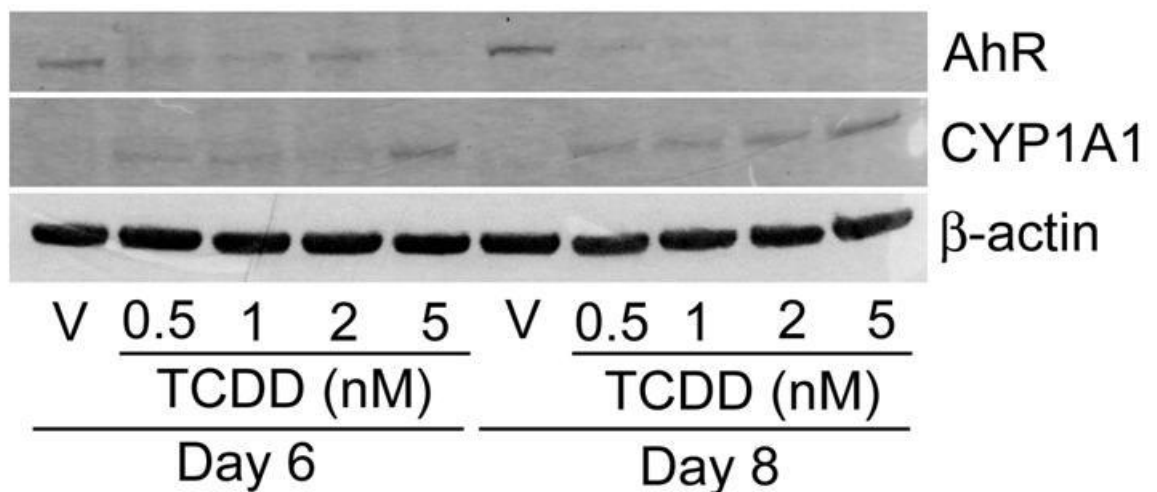


Figure 3.9. Dose dependent induction of AhR degradation and CYP1A1 by TCDD in primary keratinocytes. Primary keratinocytes were treated with vehicle or concentrations of TCDD as indicated for up to 8 days. Western blots were performed and probed with anti-AhR, anti-CYP1A1 and anti- β -actin antibodies.

3.3.1.4 β -NF

Time course studies of AhR degradation and CYP1A1 induction were also carried out following treatment of keratinocytes with β -NF. Figure 3.11 shows that AhR was degraded by β -NF treatment at day 8, Appendix D and Appendix E show AhR degradation occurred from days 4 to 8. CYP1A1 was induced by β -NF treatment at all time points, but did not correlate well with AhR levels. Figure 3.10 and Figure 3.11 showed that the classical AhR agonist TCDD induced AhR degradation from days 2 to 8 but only induced CYP1A1 at days 6 and 8 (Appendix C). CYP1A1 levels induced by β -NF did appear from day 2, but the increase was low (note the scale on the y axis). Despite this, CYP1A1 appeared to be induced at all time points by 15 μ M β -NF. Two-way ANOVA was performed to compare vehicle with β -NF treated cells at each time point. At all time points, the effects of β -NF on AhR degradation were significant ($P = 0.02$). The effects of β -NF and time on CYP1A1 were not significant and there was no significant interaction between β -NF and duration of incubation (time).

3.3.1.5 ITE

To test the effects of the relatively new physiological ligand ITE on induction of CYP1A1 and degradation of AhR, primary keratinocytes were treated with vehicle or concentrations of ITE for up to 8 days. Figure 3.10 and Figure 3.11 show dose dependent AhR degradation induced by ITE from day 2 to day 8, most markedly at day 2. Despite robust AhR degradation at days 2, 4, 6 and 8, ITE-induced CYP1A1 was very low at all time points (Appendix F and Appendix G). Low levels of ITE-dependent induction of CYP1A1 were observed on Western blots from some donors but levels were low and inconsistent.

Two-way ANOVA was performed to compare vehicle with ITE treated cells at each time point. At all time points, the effects of ITE on AhR degradation were significant ($P = 0.0002$). The effects of ITE and time on CYP1A1 were not significant and there was no significant interaction between ITE and duration of incubation (time).

AhR degradation occurred at both early time points and later time points, with little induction of CYP1A1. This indicated that ITE may be distinct in its mechanism of activation of AhR or the conformational changes that ITE binding induced on the AhR. One potential mechanism is that some genes have distinct XRE domains that require specific traits in the induced conformation of ligand-activated AhR. For example, CTSD

has an imperfect XRE domain which when bound by TCDD-activated AhR can induce inhibition of CTSD (Wang et al., 1998; Wang et al., 1999). Even though this elicits inhibitory responses, there is no reason why this mechanism may not be applied to ligand specific induction of proteins too. ITE may not provide these required activation characteristics.

3.3.1.6 Summary and comparison of AhR ligands on AhR and CYP1A1 protein levels

Treatment of primary keratinocytes with TCDD, β -NF and ITE showed significant degradation of AhR from days 2 to 8. CYP1A1 induction was most clearly induced by TCDD. There was some clear but variable induction of CYP1A1 in some experiments by β -NF, with only slight amounts of CYP1A1 induction by ITE. This data convincingly shows that all ligands induced AhR activation, although ITE differentially activated the AhR, not inducing CYP1A1 protein.

Figure 3.10 and Figure 3.11 shows a summary of ligand induced AhR activation measured by AhR degradation and CYP1A1 activation at day 2 (Figure 3.10) and day 8 (Figure 3.11) to demonstrate the significant effects of duration of incubation of ligand on CYP1A1 and AhR levels. At day 2 there was degradation of AhR induced by TCDD and ITE, while there was slight induction of CYP1A1 by β -NF. AhR activation (AhR degradation and CYP1A1 induction) by TCDD, β -NF and ITE occurred maximally and more reproducibly at the later time points studied, day 8.

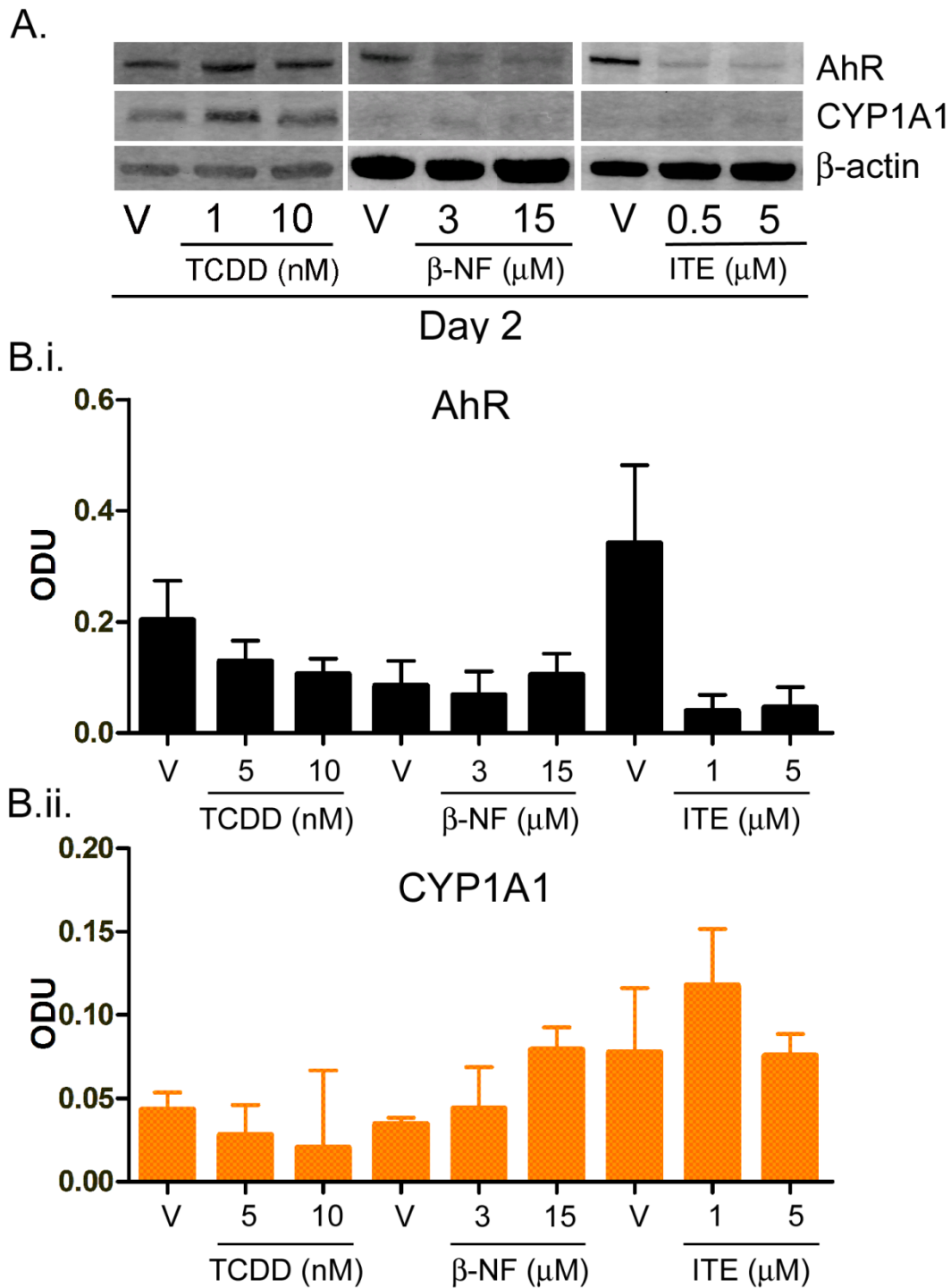


Figure 3.10. Comparison of AhR activation by TCDD, β -NF and ITE at day 2.

Primary keratinocytes were treated with vehicle or concentrations of AhR ligands (TCDD, β -NF and ITE) as indicated. After 2 days keratinocytes were lysed and Western blotting performed (**A**). Membranes were probed with anti-AhR (black bars) or anti-CYP1A1 (orange bars) antibodies and β -actin as a loading control. **B**) Western blots were analysed by densitometry. Optical density units of AhR (B.i) and CYP1A1 (B.ii) bands were normalized to β -actin. Western blot is representative of duplicate blots in 3 donors. Densitometry represents mean \pm sem. Statistical analysis is described in Figure 3.11.

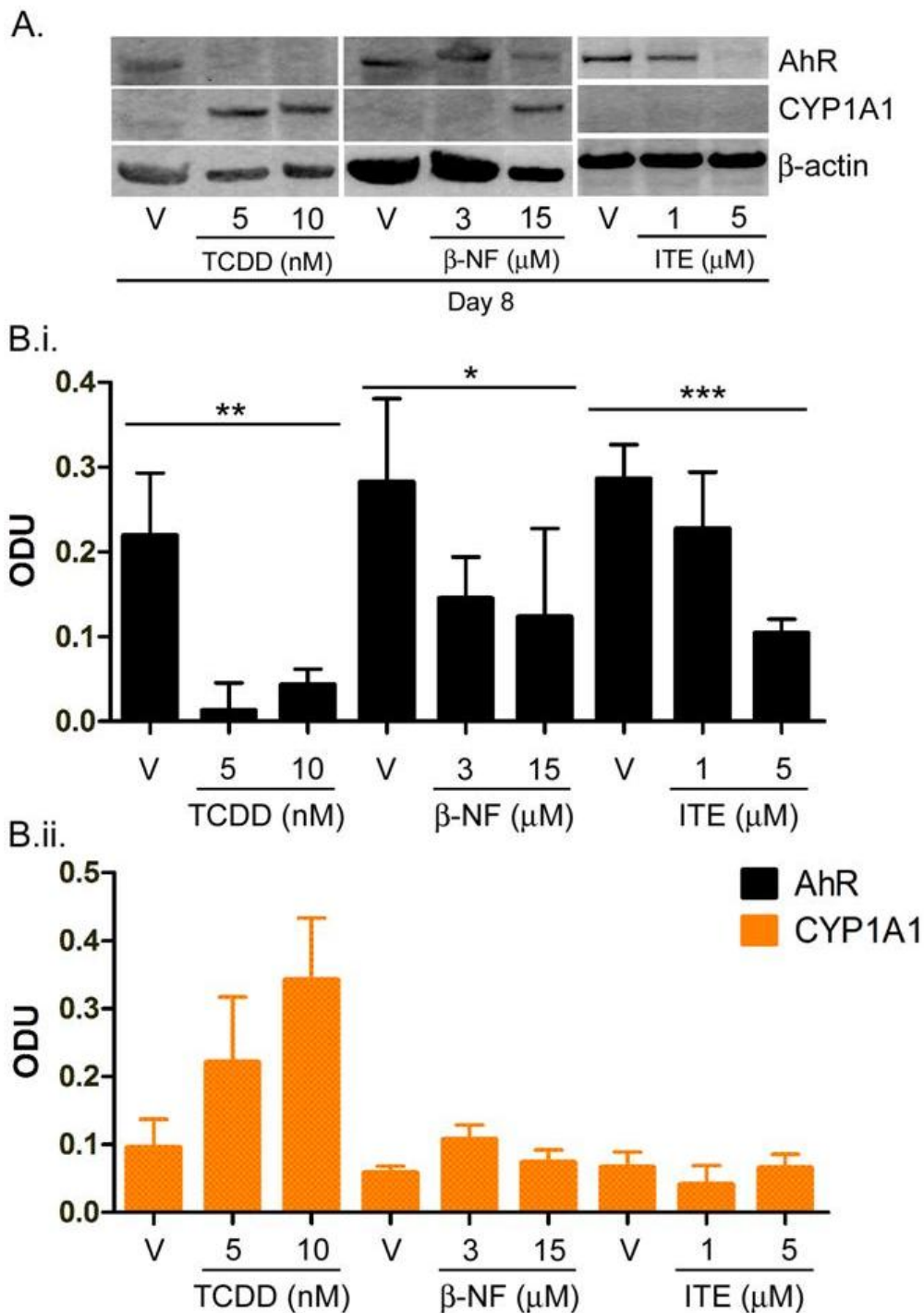


Figure 3.11. Comparison of AhR activation by TCDD, β-NF and ITE at day 8.

Primary keratinocytes were treated with vehicle or concentrations of AhR ligands (TCDD, β-NF and ITE) as indicated. After 8 days keratinocytes were lysed and Western blotting performed (**A**). Membranes were probed with anti-AhR (black bars) or anti-CYP1A1 (orange bars) antibodies and β-actin as a loading control. **B**) Western blots were analysed by densitometry. Optical density units of AhR (B.i) and CYP1A1 (B.ii) bands were normalized to β-actin. **B**) Two-way ANOVA was performed comparing vehicle to the effects of time and ligand. Effects of ligand on AhR degradation were significant for all ligands, TCDD: ** $P < 0.007$, β-NF: * $P = 0.02$, ITE: *** $P = 0.0002$. The effects of time and ligand did not induce significant changes in CYP1A1 levels. Western blot is representative of duplicate blots in 3 donors. Densitometry represents mean \pm sem.

3.3.1.7 Effects of low β -NF (nM) on AhR degradation and CYP1A1 induction

To allow direct comparisons between the effect of β -NF on AhR activation by protein levels (CYP1A1 induction and AhR degradation) and transcriptional activation, primary keratinocytes were treated with nM concentrations of β -NF for up to 8 days (days 2 and 8: Figure 3.12, complete timecourse: Appendix H). Western blots were performed on keratinocyte lysates and probed with anti-AhR, anti-CYP1A1 and anti- β -actin as described in materials and methods.

AhR degradation was consistent with our previous data (Figure 3.10 and Figure 3.11). Rather surprisingly, levels of CYP1A1 were decreased by 200 and 2000nM β -NF treated samples from day 4-8 as opposed to the normal increase of CYP1A1 induced by agonist treatment. Consistent with data shown in previous Western blotting data AhR degradation consistently occurred from day 2 but CYP1A1 degradation occurred at days 4 and 8 (Appendix H). There are no reports in the literature of down-regulation of CYP1A1 by AhR activation, however it occurred transiently in the dose responses summarised in Appendix H. The CYP1A1 data is not robust – it is representative of only two donors, but mainly the levels of CYP1A1 are very low on the blots and may well represent not much more than noise (Figure 3.12 A). Concentrations of nM β -NF induced AhR activation (luciferase assays Figure 3.7) and AhR degradation by Western blot (Figure 3.12) but activation was apparently too low to induce CYP1A1. This suggests that a certain level of AhR activation may be required before CYP1A1 can be induced, nM β -NF and ITE induced AhR activation (Figure 3.1) may not reach this CYP1A1 inducing threshold.

It is clear from the blot in Figure 3.12 that β -NF induced AhR degradation at days 2 and 8 in a dose dependent manner. There is an increase in AhR compared to vehicle at days 2 and 6 (Appendix H). This has been reported in rat hepatocytes; recovery of AhR mRNA and protein after TCDD-induced activation can result in a ~2 fold increase from basal levels (Franc et al., 2001; Sloop and Lucier, 1987).

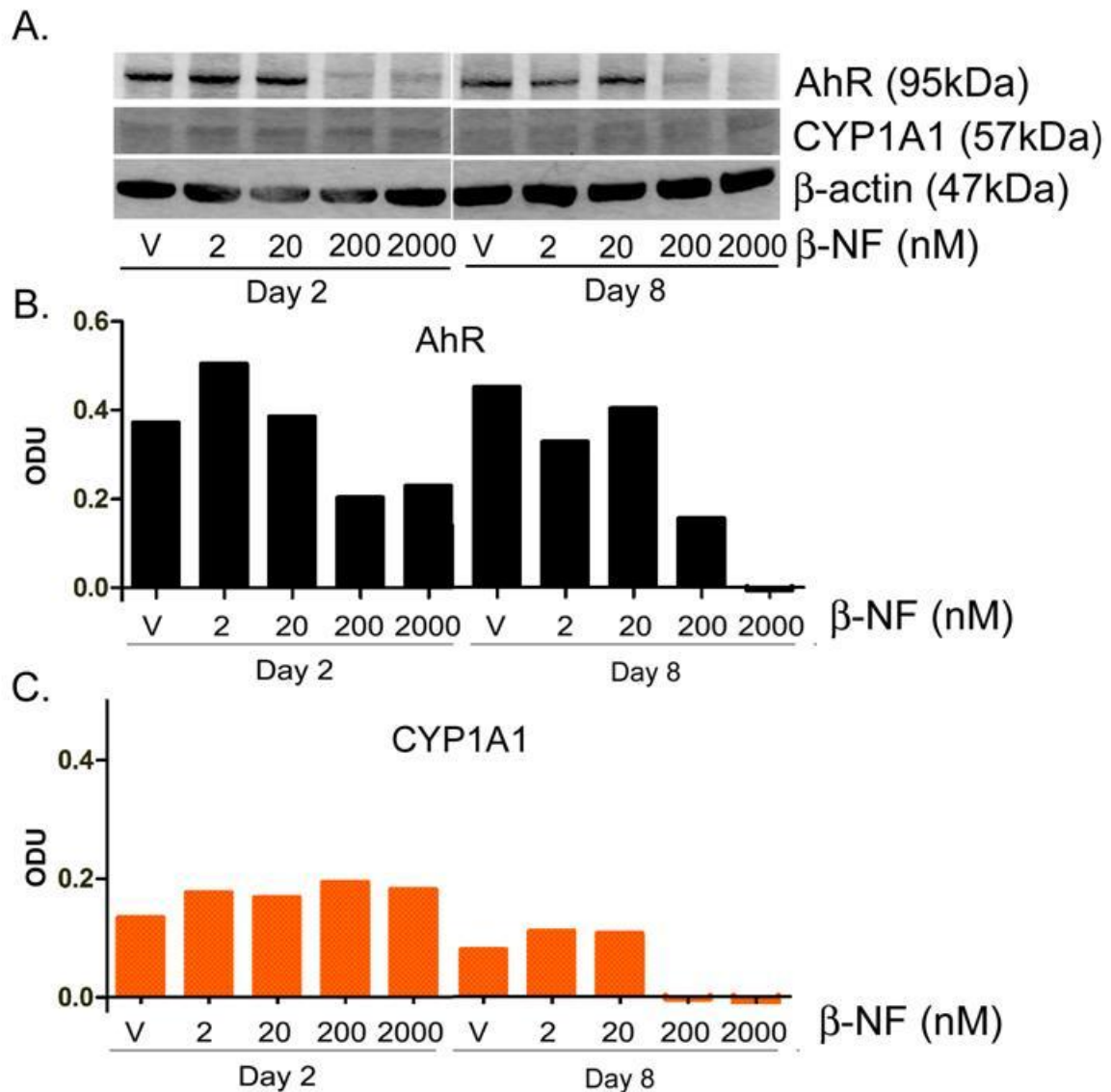


Figure 3.12. β -NF (nM) induced AhR and CYP1A1 degradation in a time and dose dependent manner. Primary keratinocytes were treated with vehicle or concentrations of β -NF as indicated from 2 to 8 days. **A)** Western blotting was performed and membranes were probed with anti-AhR and anti-CYP1A1 antibodies and β -actin as a loading control. **B)** Western blots were analysed by densitometry. Optical density units of AhR (B.i) and CYP1A1 (B.ii) bands were normalized to β -actin. Western blot is representative of duplicate blots in 2 donors. Densitometry represents mean. No statistical analysis was performed due to low sample number.

3.3.2 Inhibition of agonist induced AhR-activation by α -NF

To further validate that the chosen AhR agonists (TCDD, β -NF, ITE) were exerting their effects in keratinocytes through AhR, we utilised α -naphthoflavone, a partial AhR agonist that inhibits AhR activation at low concentrations and induces AhR activation at high concentrations (Ferraris et al., 2005; Merchant et al., 1990). A dose response curve was performed to test its potential agonistic activity in primary keratinocytes; doses were based on those used in a study by Ferraris et al. in the HepG2 cell line (Ferraris et al., 2005). Figure 3.13 shows primary keratinocytes transfected with pXRE4-SV40-luciferase and treated with varying concentrations of α -NF for 48h. α -NF did not reproducibly induce significant AhR dependent transcriptional activation in keratinocytes (one-way ANOVA; $P < 0.3$).

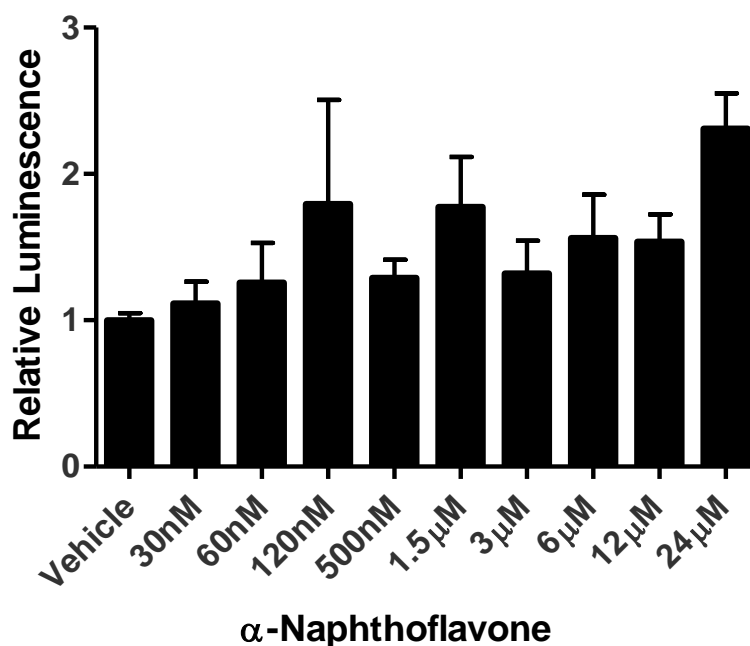


Figure 3.13. Partial agonist α -Naphthoflavone induces AhR transcriptional activity at high concentrations. Primary keratinocytes were transfected with XRE-luciferase and treated with vehicle or concentrations of α -NF as indicated for 48h. XRE-luciferase activity was measured and mean firefly:renilla luciferase ratio was normalised to vehicle \pm sem. $n=9$, triplicate wells from 3 donors. Values showed no significant changes by one-way ANOVA (vehicle compared to treated samples $P = < 0.3$) but did show a significant increase in linear trend ($P = < 0.02$).

To correlate the effect of α -NF on transcriptional activation to protein levels, primary keratinocytes were grown and treated for up to 8 days with α -NF. Figure 3.15 and Figure 3.16 a shows the effect of α -NF alone on AhR degradation and CYP1A1 induction at days 2 and 8 (Complete time courses shown in (Appendix I)). As described in the Western blot time courses previously, effects of AhR activation were seen maximally and most reproducibly at late time points, however certain agonists showed effects at earlier time points (β -NF induced CYP1A1 induction at day 2, see Figure 3.10). Therefore, I studied the effects of α -NF on AhR and CYP1A1 protein expression. At day 2 some minor AhR degradation was apparent, but was more marked at days 4 and 6, minor CYP1A1 induction occurred at all time points. There was a lack of high CYP1A1 induction at day 8 suggesting that α -NF only exerted weak agonistic effects at these concentrations. In contrast to ITE which also did not induce high CYP1A1, α -NF did not induce robust AhR degradation.

This data was consistent with the literature; Merchant et al. showed a low increase of CYP1A1 by 1 μ M α -NF by Northern blot in mouse hepatoma cell line (Merchant et al., 1990), while Gasiewicz et al. showed that 1 and 5 μ M α -NF induced low levels of AhR/XRE binding in mouse hepatoma cells (Gasiewicz, 1991). These concentrations were both shown to inhibit AhR activation induced by 1000 fold lower concentrations of TCDD. Ferraris et al. showed that inhibition of CYP1A1 inducer iprodione - induced XRE-luciferase assay by 120nM, 1.2 μ M or 2.4 μ M α -NF. The dose range used in Figure 3.13 was based on the Ferraris paper because it was one of the few papers found treating human cells with high doses of α -NF to show inhibition of an XRE-luciferase (Ferraris et al., 2005).

Taken together, these data indicate that at early time points (2 days), α -NF demonstrated minimal agonist activity in keratinocytes, however at later time points (8 days) clear evidence of agonist activity by α -NF was observed at 5 and 10 μ M. Two-way ANOVA was performed to compare vehicle with α -NF treated cells at each time point. At all time points, the effects of α -NF on AhR degradation were significant ($P < 0.05$). There was no significant interaction between α -NF and duration of incubation (time). Therefore use of α -NF as a potential antagonist at later time points should be interpreted with caution but

Gasiewicz et al. and Merchant et al. both showed that the most efficient AhR-inhibition was induced by levels of α -NF that alone acted as an AhR-agonist (Gasiewicz, 1991; Merchant et al., 1990).

To determine whether α -NF may act as an AhR antagonist in keratinocytes, luciferase assays were carried out following treatment of primary keratinocytes concurrently with vehicle or specified ligand \pm α -NF for 48h (Figure 3.14). Figure 3.14 A shows that 5 and 10 μ M α -NF significantly inhibited TCDD induced AhR transcriptional activation at 1, 5 and 10nM TCDD. Not surprisingly the inhibitory effects of α -NF were more marked at higher concentrations of TCDD. Results and statistics for vehicle compared to ligand are presented in Figure 3.7, but data and statistics are duplicated in Figure 3.14 for clarity. Statistical analysis was carried out on keratinocytes treated with ligand alone compared to ligand plus 5 or 10 μ M α -NF (one-way ANOVA 1nM TCDD: P <0.007, 5nM TCDD: P <0.02, 10nM TCDD: P <0.0001. Dunnett's post hoc test 1nM TCDD plus 5 μ M α -NF: ** and 5nM TCDD plus 5 or 10 μ M α -NF: *. Linear trend 10nM TCDD: P <0.0001). 5 μ M α -NF inhibited TCDD-induced AhR activation more efficiently than 10 μ M α -NF (at 1 and 5nM TCDD). This could be caused by 10 μ M α -NF beginning to show agonist activity in presence of low levels of TCDD, while AhR dependent transcriptional activation induced by 10nM TCDD was strong enough to block α -NF agonist activity and ensure its performance as an inhibitor, as discussed in the last section, the most efficient inhibition by α -NF was at concentrations where it induced AhR-activity when alone (Gasiewicz, 1991; Merchant et al., 1990).

β -NF induced AhR transcriptional activation was inhibited at 20 and 50nM β -NF significantly by both 5 and 10 μ M α -NF (one-way ANOVA, ligand alone compared to ligand plus α -NF, 20nM β -NF: P = 0.0006, 50nM β -NF: P = 0.0006. Linear trend, 20nM β -NF: P < 0.003, 50nM β -NF: P = 0.0002). ITE induced AhR activation was also significantly inhibited by α -NF at 0.5 and 1 μ M ITE, but was not significant at 5 μ M ITE (P <0.09) although reached significance by analysis of linear trend (P <0.03) (one-way ANOVA, 0.5 μ M ITE: P = 0.0001 and 1 μ M ITE: P <0.0003. Linear trend, 0.5 μ M ITE: P <0.0001, 1 μ M ITE: P = 0.0007, 5 μ M ITE: P <0.004).

Thus at concentrations that resulted in minimal AhR activation (Figure 3.13), α -NF significantly inhibited XRE-luciferase activity induced by all 3 agonists. However 5 μ M α -NF showed greater inhibition of TCDD-induced transcriptional activation. These data confirm that TCDD, β -NF and ITE effects on XRE-luciferase are induced mechanistically by AhR activation.

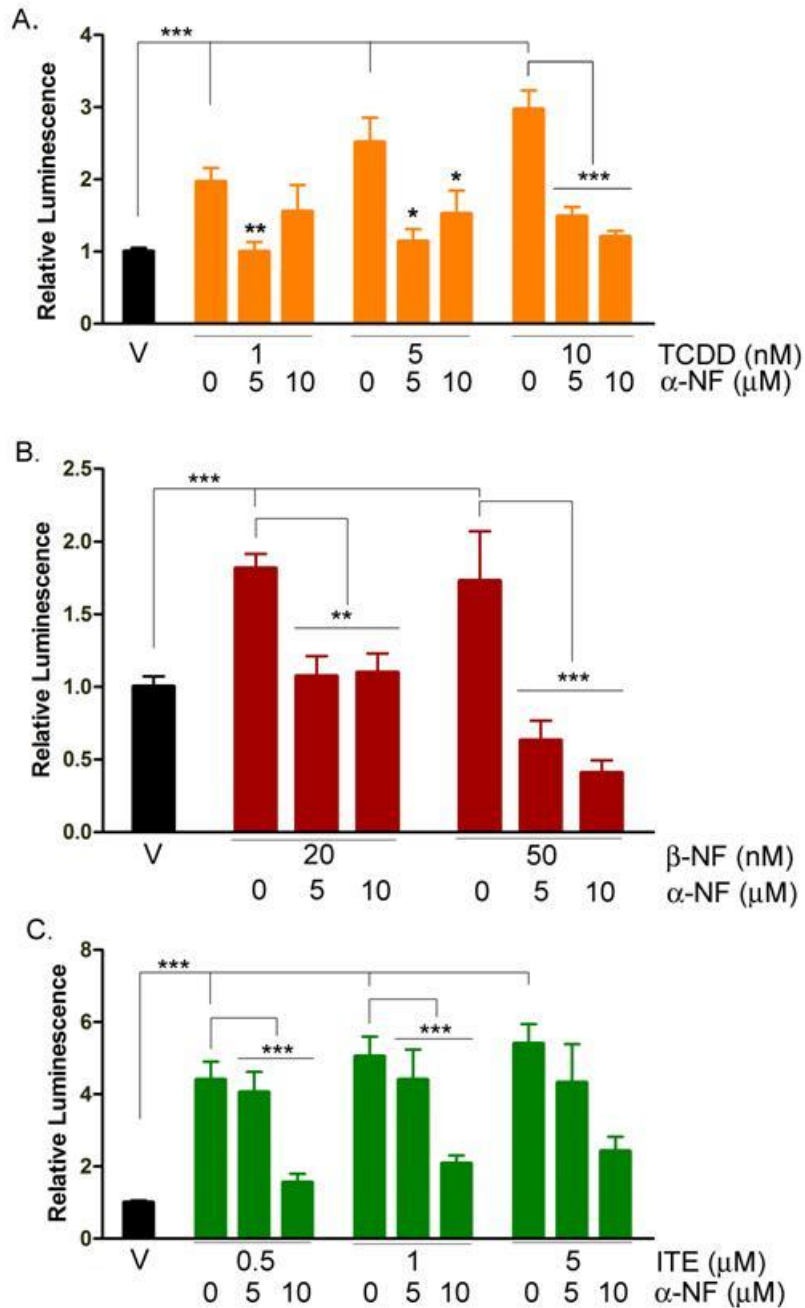


Figure 3.14. α -Naphthoflavone inhibits ligand induced AhR transcriptional activity.

Primary keratinocytes were co-transfected with XRE-luciferase and Renilla internal control. After 24h, keratinocytes were treated with vehicle or **A)** TCDD, **B)** β -NF or **C)** ITE at concentrations shown plus 0, 5 or 10 μ M α -NF for 48h. Values shown as firefly:renilla ratio normalised to vehicle. $n \geq 9$, from ≥ 3 donors carried out in triplicate \pm sem. One-way ANOVA was performed, with analysis of trend compared to ligand treated alone as post hoc test. **A)** One-way ANOVA; 1nM TCDD: ** $P < 0.001$, 5nM TCDD: * $P < 0.02$, 10nM TCDD: *** $P < 0.0001$. Linear trend; 10nM TCDD: *** $P < 0.0001$. Stars with no bars indicate significance with Dunnett's post hoc test, comparing ligand to each concentration of α -NF. **B)** One-way ANOVA; 20nM β -NF: *** $P = 0.0006$, 50nM β -NF: *** $P = 0.0002$. Linear trend 20nM β -NF: *** $P < 0.003$, 50nM β -NF: *** $P = 0.0002$. **C)** One-way ANOVA, 0.5 μ M ITE: *** $P < 0.0001$, 1 μ M ITE: *** $P < 0.0003$. Analysis of trend; 0.5 μ M ITE: *** $P < 0.0001$, 1 μ M ITE: *** $P = 0.0001$, 5 μ M ITE: * $P < 0.03$. Statistics bars from vehicle to ligand treated bars represent significance of AhR activation by ligand alone as in Figure 3.7.

3.3.3 The effects of α -NF on ligand induced AhR activation

To investigate whether α -NF also blocked AhR agonist-induced AhR degradation and CYP1A1 induction, primary keratinocytes were co-treated with AhR ligand plus α -NF (in parallel) for 2, 4, 6 and 8 days and Western blotting performed. As described earlier, these experiments were carried out in parallel with the AhR activation studies earlier in the chapter (section 3.3.1) but are being presented here for clarity. The data for agonists with no co-treatment with α -NF is duplicated from the data shown in section 3.3.1. To briefly recap, by Western blot α -NF treatment alone induced AhR degradation at days 4, 6 and 8 with only slight CYP1A1 induction at days 2 and 4. α -NF induced slight transcriptional activation by luciferase assay at the highest dose tested, 24 μ M. At similar doses to those used for inhibition studies, low activation was induced at higher concentrations (Figure 3.13). In summary, α -NF induced low AhR activation at days 6 and 8.

3.3.3.1 TCDD

As previously shown (Figure 3.10 and Figure 3.11) treatment with 5 or 10nM TCDD induced AhR degradation at all time points and induced CYP1A1 at day 8. TCDD-induced AhR-transcriptional activation was blocked dose dependently by 5 and 10 μ M α -NF (Figure 3.14 A).

Appendix B and Appendix C shows complete time courses of co-treatment of primary keratinocytes with TCDD plus α -NF. TCDD-induced AhR degradation was blocked consistently at each time point with 5 and 10 μ M α -NF in dose dependent manner. In contrast to the α -NF inhibition of TCDD-induced XRE-luciferase activity shown in Figure 3.14, TCDD induced CYP1A1 was further increased by α -NF co-treatment at days 2, 4 and 6 by 5nM TCDD plus 5/10 μ M α -NF. CYP1A1 induction by 10nM TCDD was also up regulated by addition of 5/10 μ M α -NF at day 2. Apart from these time points and dose combinations, α -NF robustly inhibited TCDD-induced CYP1A1 induction at days 4, 6 and 8 with 10nM TCDD plus 5/10 μ M α -NF and day 8 only with 5nM TCDD plus 5/10 μ M α -NF.

AhR degradation induced by TCDD treatment at day 8 was partially blocked by 5 μM $\alpha\text{-NF}$ and maximally blocked by 10 μM $\alpha\text{-NF}$. CYP1A1 induction was blocked by co-treatment induced by 10nM TCDD at 8 days with 5 or 10 μM $\alpha\text{-NF}$. Two-way ANOVA was performed to compare TCDD treated cells with cells co-treated with TCDD and $\alpha\text{-NF}$ at each time point. In cells treated with 5nM TCDD, $\alpha\text{-NF}$ induced significant recovery of AhR ($P < 0.002$), and in cells treated with 10nM TCDD alone or in combination with $\alpha\text{-NF}$ the duration of incubation (time) showed a significant effect on CYP1A1 response to treatment ($P = 0.0001$). The interaction between time and $\alpha\text{-NF}$ was not significant.

Considering the $\alpha\text{-NF}$ activation data, the time points that induced the most AhR activation (AhR degradation at day 8, Figure 3.16 A) also showed the most efficient inhibition (AhR degradation and CYP1A1 activation, day 8, Figure 3.16 B), returning AhR and CYP1A1 to similar levels as those in vehicle treated samples at day 8.

These data suggest that combined with TCDD, $\alpha\text{-NF}$'s antagonist activity was predominant, especially at late time points. 10nM TCDD induced degradation of AhR and induction of CYP1A1 was consistently blocked in each donor, at each time point (except day 2) and dose dependently by $\alpha\text{-NF}$, showing robust inhibition of TCDD-induced AhR activation by $\alpha\text{-NF}$. Figure 3.10 and Figure 3.11 shows AhR activation induced by μM $\beta\text{-NF}$; AhR degradation occurred at days 2-8, while low CYP1A1 activation was induced at days 6 and 8. Appendix D and Appendix E show complete time courses of the effects of $\alpha\text{-NF}$ on $\beta\text{-NF}$ -induced AhR activation. At days 2 and 6, co-treatment of $\beta\text{-NF}$ plus $\alpha\text{-NF}$ had no effect on AhR degradation. At days 4 and 8, $\beta\text{-NF}$ induced AhR degradation alone, and AhR was degraded further with co-treatment of $\alpha\text{-NF}$. The effects of $\alpha\text{-NF}$ on $\beta\text{-NF}$ induced CYP1A1 were more variable; CYP1A1 levels in samples treated with 3 μM $\beta\text{-NF}$ were increased by $\alpha\text{-NF}$ treatment at days 2, 4, 6 and 8. CYP1A1 levels in 15 μM $\beta\text{-NF}$ treated samples were increased by $\alpha\text{-NF}$ treatment at day 4 and partially at day 8. Inhibition of $\beta\text{-NF}$ -induced activation by $\alpha\text{-NF}$ co-treatment occurred at day 2 (15 μM $\beta\text{-NF}$), partially at day 4 (3 μM $\beta\text{-NF}$ plus 10 μM $\alpha\text{-NF}$) and day 8 (3/15 μM $\beta\text{-NF}$ plus 10 μM $\alpha\text{-NF}$).

Two-way ANOVA was performed to compare β -NF treated cells with cells co-treated with β -NF and α -NF at each time point. In cells treated with $3\mu\text{M}$ β -NF alone or in combination with α -NF the duration of incubation (time) showed a significant effect on CYP1A1 response to treatment ($P < 0.03$). The effects of α -NF and the interaction between time and α -NF were not significant.

Day 8 showed robust induction of CYP1A1 with co-treatment of β -NF and α -NF, as expected for AhR-dependent effects. Gelardi et al. show the inhibition of $15\mu\text{M}$ β -NF-induced CYP1A1 activity dose dependently by 1, 5, 10 and $150\mu\text{M}$ α -NF in a human keratinocyte cell line. $1\mu\text{M}$ inhibited CYP1A1 induction by ~50%, while $5\mu\text{M}$ inhibited CYP1A1 induction to ~25% and $10\mu\text{M}$ inhibited CYP1A1 induction to ~20% after 48h treatment (Gelardi et al., 2001). This percentage of knock down is similar to that shown by luciferase activity induced by $20/50\text{nM}$ β -NF by $5/10\mu\text{M}$ α -NF at 48h (Figure 3.14).

As previously shown (Figure 3.10, Figure 3.11 and Figure 3.12), β -NF alone did not reproducibly induce CYP1A1 apart from at day 2. However in this experiment we saw clear induction of CYP1A1 by the combination of β -NF and α -NF. These data indicate that in the presence of β -NF, α -NF showed partial agonist activity and together acted synergistically to activate AhR, resulting in AhR degradation and CYP1A1 induction at increased levels than achieved by either β -NF or α -NF alone.

To conclude, co-treatment of primary keratinocytes with α -NF plus β -NF mainly resulted in increased AhR activation. Some β -NF-induced AhR activation was blocked by α -NF, but this was sporadic and showed no consistent time or dose dependence. This conclusion was consistent in 3 donors.

3.3.3.2 ITE

To summarise ITE induced AhR activation, Figure 3.10 and Figure 3.11 showed robust AhR degradation from day 2 to 8 by 1 and $5\mu\text{M}$ ITE. Despite strong AhR knock down there was little or no CYP1A1 induction at any time point.

Appendix F and Appendix G show complete time course data of α -NF induced inhibition of ITE induced AhR activation. At days 2 and 4 (Appendix F), α -NF had little effect on ITE-induced AhR degradation. At days 6 and 8 (Appendix G

and Figure 3.16), co-treatment of ITE plus α -NF consistently knocked down AhR further than ITE alone. Notably, co-treatment with ITE plus α -NF consistently induced CYP1A1 over dose and time. ITE alone did not induce CYP1A1 at any time point or concentration and data presented in Figure 3.15 and Figure 3.16 show that α -NF alone did not significantly induce CYP1A1.

Two-way ANOVA was performed to compare ITE treated cells with cells co-treated with ITE and α -NF at each time point. In cells treated with 1 μ M ITE, α -NF induced significant decrease in CYP1A1 ($P < 0.02$), and in cells treated with 5 μ M ITE alone or in combination with α -NF the duration of incubation (time) showed a significant effect on AhR response to treatment ($P < 0.0001$). The interaction between time and α -NF was not significant.

ITE has not previously been used in inhibition studies with α -NF, so the data here in Figure 3.14, Figure 3.15 and Figure 3.16 are novel. From this data, we can conclude that co-treatment of primary keratinocytes with ITE plus α -NF induced further AhR activation than treatment with ITE alone. This occurred consistently in 3 donors, with all dose combinations and at all time points.

3.3.3.3 Summary of data showing effect of α -NF on agonist induced AhR activity

Summary figures comparing the effects of TCDD, β -NF and ITE on AhR activation at days 2 and 8 have been shown in Figure 3.15 and Figure 3.16. The effects of α -NF on CYP1A1 induction and AhR degradation is also shown to enable direct comparison of α -NF-induced AhR activation with the effect that it has on the agonists. Complete time courses have been shown from Appendix B to I.

α -NF consistently blocked TCDD-dependent AhR degradation and CYP1A1 induction, showing that TCDD-induced effects on the AhR and CYP1A1 were AhR dependent. The effects of α -NF on β -NF-induced CYP1A1 and AhR degradation were varied, but α -NF often induced AhR activation to higher levels than β -NF alone. Co-treatment with ITE and α -NF consistently resulted in AhR activation (CYP1A1 induction) to a higher level than ITE alone.

These data have revealed two differential effects between TCDD and ITE (the effects of β -NF lie in between). The first is that ITE alone did not induce CYP1A1, the second was that further AhR activation was induced by co-treatment of ITE plus α -NF. This suggests a differential mechanism of AhR activation between TCDD and ITE. Reports of differential levels of activation have been well documented with α -NF. The mechanism of activation of α -NF is based on the form of AhR that α -NF induces upon binding. TCDD binding to the AhR induced conformational changes of the AhR that increased its affinity for the ARNT and DNA, inducing strong dimerisation to ARNT and binding to the XRE to induce transcriptional activation of the AhR-dependent battery. α -NF however induced a form of the AhR that has low-affinity for DNA and high-affinity for the ligand, reducing its induction of transcriptional activation (Henry et al., 1989; Merchant et al., 1990). ITE could potentially induce a low DNA affinity form of AhR that does not have the capacity to bind the XRE either strongly enough to induce CYP1A1, or provide all of the required elements to induce CYP1A1. Differential activation has been shown with TGM-1 between TCDD and β -NF (Du et al., 2006a), and although this has yet to be explained, shows that differential activation between AhR ligands does occur. AhR translocation and degradation has been shown to be induced by even non-AhR agonists, for example geldanamycin dimerises with hsp90 (Grenert et al., 1997), inducing translocation of the AhR and degradation without XRE binding (Pollenz and Buggy, 2006; Song and Pollenz, 2002). This suggests that AhR degradation does not necessarily correlate with levels of AhR-activation and that the robust ITE-dependent AhR degradation may be caused by the ITE-induced changes inferring efficient removal of chaperone molecules or modifying nuclear localisation or export signals increasing nuclear translocation and the efficiency of AhR degradation (Ikuta et al., 2004).

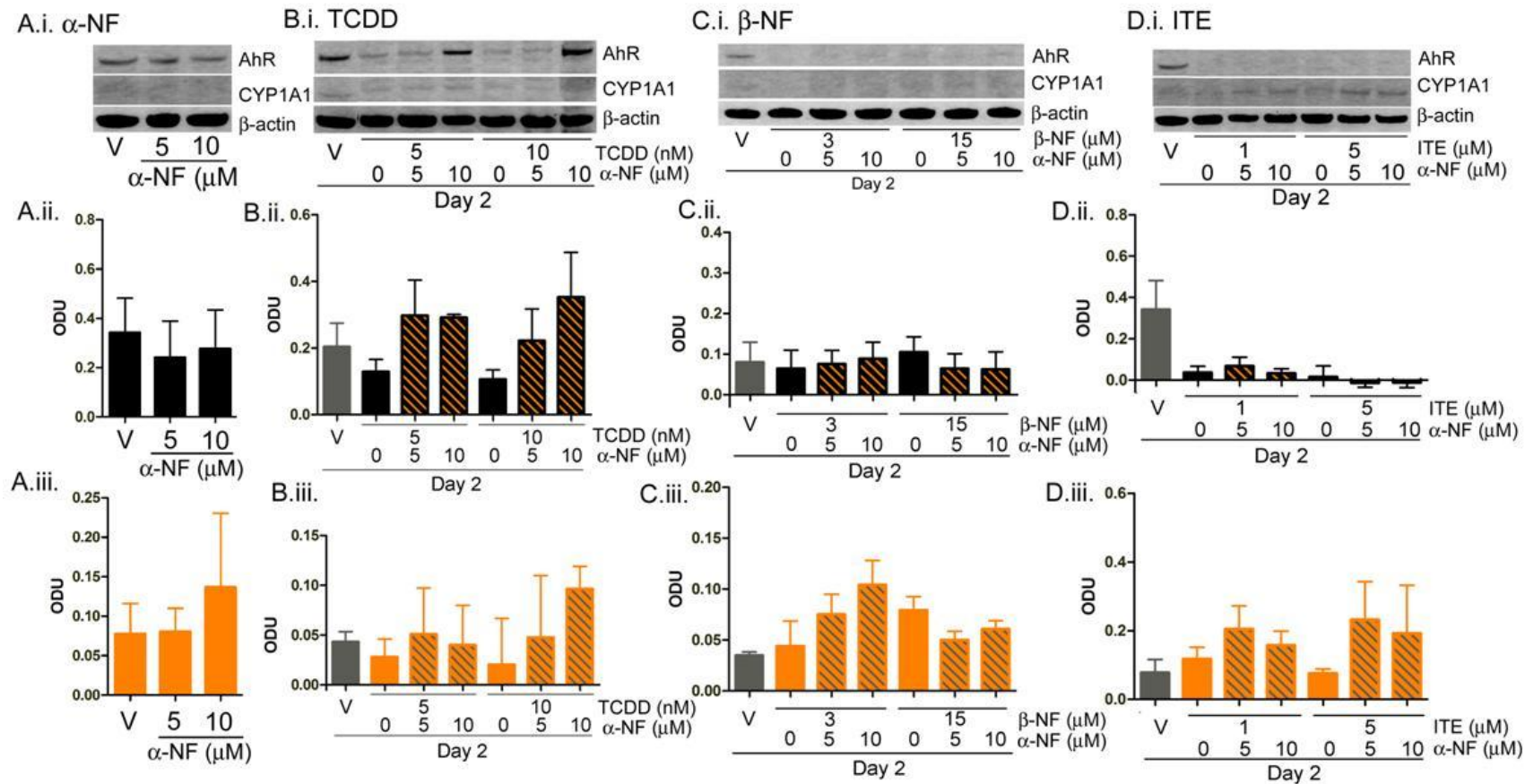


Figure 3.15. The effects of α -Naphthoflavone on ligand induced AhR activation. Primary keratinocytes were treated with vehicle or **A)** α -NF, **B)** TCDD, **C)** β -NF or **D)** ITE as indicated. After 2 days cells were lysed and Western blotting performed. Blots were probed with Anti-AhR (black bars), anti-CYP1A1 (orange) and anti- β -actin antibodies and bands were quantified using densitometry, presented as optical density units (ODU) normalised to β -actin. Western blot is representative of duplicate blots in 3 donors. Values for densitometry represent means \pm sem for 3 blots taken from 3 donors. Two-way ANOVA compared ligand treatment to co-treatment of ligand and α -NF treatment at each time point, results are explained in the previous paragraph.

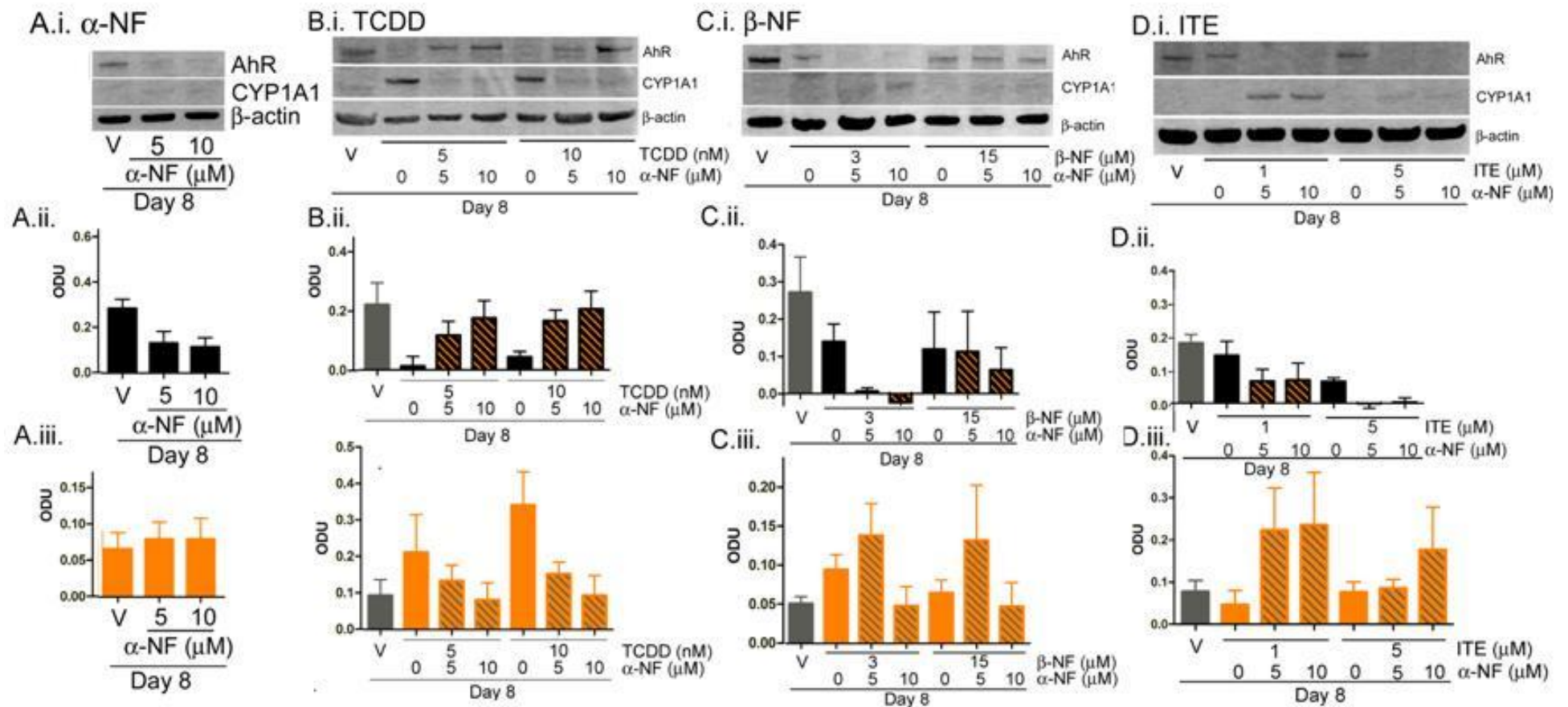


Figure 3.16. The effects of α -Naphthoflavone on ligand induced AhR activation. Primary keratinocytes were treated with vehicle or **A)** α -NF, **B)** TCDD, **C)** β -NF or **D)** ITE as indicated. After 8 days cells were lysed and Western blotting performed. Blots were probed with Anti-AhR (black bars), anti-CYP1A1 (orange) and anti- β -actin antibodies and bands were quantified using densitometry, presented as optical density units (ODU) normalised to β -actin. Western blot is representative of duplicate blots in 3 donors. Values for densitometry represent means \pm sem for 3 blots taken from 3 donors. Two-way ANOVA compared ligand treatment to co-treatment of ligand and α -NF treatment at each time point, results are explained in the previous paragraph.

3.4 Discussion

3.4.1 Summary of AhR activation and inhibition

During this project I compared the classic AhR agonist TCDD, the low-affinity AhR agonist β -NF and a highly potent physiological AhR agonist ITE. Our hypothesis was that ligand affinity for the AhR would cause differential effects on transcription of genes and downstream effects on primary keratinocyte proliferation, differentiation and cell death. Utilising assays measuring transcriptional activation of AhR (dual luciferase assays) and downstream regulation of proteins (Western blot and IHC) we aimed to test this hypothesis.

In this chapter I have aimed to define levels of AhR activation by 3 agonists with different characteristics: chloracnegenic high-affinity TCDD, endogenous high-potency ITE and low-affinity β -NF. I have used 3 readouts of AhR activation: AhR degradation, CYP1A1 activation and AhR transcriptional activation. Dose and time responses have been initially defined and showed that 1, 5 and 10nM TCDD; 2, 20 and 50nM or 3 and 15 μ M β -NF; or 0.5, 1 and 5 μ M ITE all activated AhR-dependent transcription, which was inhibited by the addition of partial AhR agonist α -NF. All 3 ligands induced AhR degradation and TCDD and β -NF induced CYP1A1 protein, but ITE did not. As expected, α -NF blocked TCDD-dependent AhR degradation and CYP1A1 induction, but induced further activation in ITE treated samples and induced mixed results in β -NF treated keratinocytes. These results showed that although all agonists elicited their effects by AhR, co-treatment with a partial agonist could induce higher AhR activation than either agonist (or partial agonist) alone.

	TCDD 5/10nM	β -NF 3/15 μ M	ITE 1/5 μ M	α -NF alone 5/10 μ M
AhR luciferase D2	+++	++	+	+
AhR degradation	--- D2-8	--- D4-8	--- D2-8	- D4-8
CYP1A1 induction	+++ D6/8	+ D2/6/8	0	0
AhR luciferase Plus α -NF D2	---	---	---	
AhR degradation Plus α -NF	+++ D2-8	-- D4/8	--- D6/8	
CYP1A1 induction Plus α -NF	-- D4-8	+ D2-8	+++ D2-8	

Table 5. A summary of AhR activation by ligands and inhibition by co-treatment with agonist plus α -NF. +/- indicates effect of treatment on level of AhR activation readout. Green figures represents AhR activation, red figures represents AhR inhibition.

3.4.2 AhR activation by TCDD, β -NF and ITE

I have shown that TCDD was a strong ligand for AhR, inducing transcriptional activation (Figure 3.2 A and Figure 3.7) AhR degradation and CYP1A1 induction (Figure 3.10 and Figure 3.11) all in a dose dependent manner. β -NF induced transcriptional activation (Figure 3.2 B and Figure 3.7) to a lower degree than TCDD but induced AhR degradation to a similar degree as TCDD (Figure 3.10 and Figure 3.11). The β -NF results were not directly comparable between luciferase and Western blot due to the quenching affect that β -NF had on firefly luciferase (Figure 3.3). Western blotting was also carried out using lower doses of β -NF and like TCDD, ITE and μ M β -NF, nM β -NF induced degradation of AhR from days 2 to 8. Like ITE, nM β -NF failed to induce CYP1A1, so Western blots were performed for the rest of the project using μ M β -NF to show levels of AhR activation (AhR degradation and CYP1A1 induction) comparable to levels of AhR activation induced by TCDD. The firefly luciferase quenching assay was not carried out at nM doses, so we cannot be certain of levels of onset of the quenching effect. As discussed in the results text, Wang 2002 showed an EC₅₀ of 0.1 μ M β -NF (Wang, 2002). This would suggest that the maximal response of 20nM β -NF (Figure 3.7 B) could be due to β -NF inducing quenching at concentrations above this. I showed that

AhR activation increased with concentrations higher than this by Western blot (Figure 3.12). Doses used in the quenching assay (Figure 3.3 B, C and D) were 15 and 30 μ M β -NF. To compare the quenching induced by β -NF treated cells (Figure 3.3 A) and directly adding β -NF to the lysate, the levels of β -NF in keratinocyte lysates from treated cells should be considered. As reported by Williams et al., the cells should contain the same concentration of ligand as the medium did (or slightly more depending on solubility of the compound) (Williams et al., 1991), so the final concentrations of β -NF in assayed samples by both methods should be similar.

3.4.2.1 AhR degradation and CYP1A1 induction

As described in the last section, AhR degradation did not correlate well with the potency of the ligand and was easily induced (even after short time periods of treatment) as demonstrated by non-AhR ligands inducing AhR degradation (Pollenz and Buggy, 2006; Song and Pollenz, 2002). CYP1A1 induction proved more difficult to induce, requiring longer periods of treatment (6 or 8 days) with higher potency ligands (TCDD or β -NF). To compare α -NF to the full AhR-agonists, its activation of XRE-luciferase was less than TCDD, β -NF and ITE, and CYP1A1 was not induced by Western blot, although as expected, AhR was degraded.

CYP1A1 induction correlated with the ranking of AhR-activation potential of AhR-agonists in Figure 3.7 and Figure 3.8, with TCDD inducing highest AhR-activation, β -NF inducing less AhR activation than TCDD (as shown by induction of CYP1A1 levels) and ITE inducing the lowest levels of AhR activation (no CYP1A1 induction). This was reported by Pushparajah et al., by comparing the levels of CYP1A1 induced by different PAHs with different binding affinities in liver and lung from humans and rats (Pushparajah et al., 2008). ITE has been shown to up-regulate CYP1A1 in a human hepatic cell line at 0.1, 1 and 5 μ M after 24h treatment (Henry et al., 2006). This may be a cell-type dependent observation, or that the hepatoma cell line was more sensitive to AhR activation than keratinocytes. ITE was originally isolated from the lung which contains large amounts of epithelium and therefore is more similar to skin, than a murine liver cell line is, suggesting that studying ITE in an epidermal system (primary keratinocytes) may represent a more physiologically relevant model than liver, to elucidate the role of ITE in lung.

Induction of CYP1A1 is often used as a primary readout of AhR activation (although developments are being made to create more thorough high throughput screening assays (Garside et al., 2008)). Industrial screening of novel compounds in drug development utilises CYP1A1 as an indicator of AhR activation and AhR-mediated toxicity. As our principle concern is that CYP1A1 induction may reflect chloracnegenic potential, we have studied the effect of AhR agonists on keratinocytes. Consistent with earlier literature I have shown TCDD to induce CYP1A1. However, robust induction was variable and time and dose dependent. Moreover, I have also shown that non-chloracnegen β -NF induces CYP1A1 although again this was variable. The aim of this project was to correlate CYP1A1 induction with the other readouts of AhR activation: AhR degradation and transcriptional activation, to look for differential effects, indicating toxicity in a compound. The experimental data in this chapter clearly shows differential effects of TCDD, β -NF and ITE. However they are not as we would have expected; β -NF (a non-chloracnegen) induced CYP1A1, while ITE strongly induced AhR degradation and AhR transcriptional activation without CYP1A1 induction. ITE has been shown to induce CYP1A1 in other systems for example mouse hepatoma cell lines (Henry et al., 2006; Henry et al., 2010), so this may be a species specific effect. In the papers reporting ITE use (in cell lines more sensitive to AhR activation than human keratinocytes), maximum concentrations used *in vitro* were 2.5 μ M ITE. It is possible that higher doses of ITE would elicit CYP1A1 induction, but higher concentrations caused high levels of toxicity in keratinocytes (Figure 3.1 C), resulting in concentrations of ITE not being viable *in vitro* or presumably *in vivo*. If ITE was compared to β -NF, which also induced robust AhR degradation but low CYP1A1 activation, concentrations of $\geq 15\mu$ M induced toxicity in primary keratinocytes. CYP1A1 induction was induced with 3 μ M β -NF at 8 days. As ITE is thought to have a similar affinity for the AhR as β -NF but is 5 times more potent, it would have been presumed that ITE would elicit its responses at lower concentrations than β -NF but we did not observe this. In conclusion, higher concentrations of ITE should have been tested for CYP1A1 activation despite high toxicity but these results would have not been relevant to the physiological role of the AhR.

In interpreting these results, I have utilised TCDD, a chloracnegenic AhR agonist. There are reports of chloracne being caused by other PAH/HAHs (Gawkrodger et al., 2009; Smith et al., 2008), and it is constantly under discussion as to which characteristics of an AhR agonist may cause chloracne, as discussed in the introduction. One hypothesis

is that high-residency is a required characteristic of a chloracneagen and that if residency were increased in other agonists that they too would become chloracneagenic. I have not tested this hypothesis in this study, however considering that our results were in an *in vitro* cell culture model alone, one possible interpretation is that because of low ligand metabolism (eg. CYP1A1 metabolism of β -NF), the residency of β -NF would be increased resulting in effects similar to TCDD.

This is possible, but Berghard et al. showed that transient activation of AhR by β -NF in human keratinocytes was prolonged by the co-treatment CYP1A1 inhibitor 1-ethynylpyrene. This suggests that in regards to β -NF metabolism, CYP1A1 activity may be lower in cell culture than *in vivo*, and β -NF clearance not as fast (which is likely, considering the lack of systemic clearance *in vitro*) but it is still high enough in cultured keratinocytes to metabolise β -NF quickly. A second consideration is the ligand-dependent induction of their own metabolism. This introduces the possibility that by later time points that showed CYP1A1 induction, this would also increase ligand clearance. It would be interesting to test the effects of inhibited CYP1A1 activity on induced CYP1A1 expression, if β -NF efficiently induced its own metabolism then this assay would result in a big increase in induced CYP1A1.

3.4.2.2 AhR activation

Overall, classical protein biomarkers of AhR activation occurred at the later time points (days 6 and 8) in protein assays. AhR degradation was induced from day 2 by all agonists, but CYP1A1 induction did not occur until days 6 and 8 (Figure 3.10 and Figure 3.11). Late induction of biomarkers of AhR activation in cultured keratinocytes and epidermal equivalent models has been reported previously in the literature (Du et al., 2006a; Geusau et al., 2005; Loertscher et al., 2002; Loertscher et al., 2001b) and is different to the time course seen in liver; where effects of AhR activation occur at earlier time points (Henry et al., 2006; Henry et al., 2010), suggesting higher AhR activity in liver based systems.

To use a more quantifiable method of transcriptional up-regulation of specific genes, PCR or microarrays could help to define which genes are being regulated by AhR activation. Interestingly, preliminary studies on 0.5nM TCDD showed similar results – high transcriptional activation by luciferase assay but low activation by AhR degradation and CYP1A1 induction, due to its nature, the luciferase assay is more sensitive than Western blot. This supports the possibility that higher concentrations of ITE may induce

CYP1A1. Alternatively, a differential mechanism may be involved; the XRE domains in some genes are distinct, which may lead to specific criteria being required for induction of certain proteins, for example Cathepsin D. CTSD is shown to have an imperfect XRE domain that upon TCDD-induced AhR binding inhibits CTSD expression (Wang et al., 1998; Wang et al., 1999). It is not certain, but these domains may require characteristic conformational changes of AhR that are only induced by certain AhR-agonists (and may not necessarily be only inhibitory), providing a mechanism for ligand-specific effects of AhR activation. The genes regulated by XRE domains are not fully defined and at the present time, work is being carried out to elucidate more proteins directly regulated by AhR (Sutter et al., 2011). Therefore, alternative XRE regulatory mechanisms may be shown to regulate many more genes. There are examples in the literature where 2 promoter regions are required for maximal induction of a certain protein, for example the Sp1 binding domain in CTSD and the oestrogen receptor (Wang et al., 1999). Maximal basal levels of CTSD are only induced when both the Sp1 binding domain and the XRE are present. The AhR/ARNT dimer can interact with the Sp1 protein, resulting in higher induction of CTSD. The Sp1 protein can also bind the XRE. The conclusions from this are that proteins such as CTSD are regulated by the “housekeeping” promoter (including Sp1) and also the “inducible” promoter (including XRE), resulting in maximal induction when both are present/activated. Sp1 is known to interact with the AhR in other cases too (Mulero-Navarro et al., 2006; Santiago-Josefat and Fernandez-Salguero, 2003). This could be a possible hypothesis for differential CYP1A1 activation that low-affinity AhR agonists do not provide high enough affinity AhR/ARNT dimers to interact with other required proteins or promoters to induce CYP1A1.

Keratinocyte differentiation has been shown to increase AhR response to agonists (Ray and Swanson, 2004), but CYP1A1 is not thought to be induced by differentiation alone. The CYP1A1 induction time courses shown in Appendices B to H showed increased CYP1A1 expression over time basally and AhR-induced, consistent with the literature (Ray and Swanson, 2004). Interestingly, time-dependent increase in CYP1A1 in vehicle treated cells only occurred in the vehicle treated samples on the TCDD treated Western blots (Appendix B and Appendix C) and from days 2 to 4 on vehicle treated samples on β -NF Western blots (Appendix D). This result was not significant and may represent a variable that we have not controlled for, or it could demonstrate the variation seen by Western blot, indicating the need to perform each blot in duplicate.

3.4.2.3 Inhibition of ligand induced AhR activation by α -NF

I went on to modulate the AhR pathway using partial AhR agonist α -NF. The aim was to inhibit readouts of AhR activation (transcriptional activation and AhR degradation/CYP1A1 induction) with co-treatment of α -NF plus TCDD, β -NF or ITE, to show AhR dependence of the effects of each ligand. As α -NF is known to have agonist activity at high concentrations (Ferraris et al., 2005; Swanson and Perdew, 1993), we measured its AhR-activation potential and corresponding to the literature, α -NF induced low levels of AhR activation. α -NF is known to inhibit TCDD (Gasiewicz, 1991; Merchant et al., 1990) and β -NF (Gelardi et al., 2001; Swanson and Perdew, 1993) but studies with ITE had not been carried out. The literature shows that the most effective concentrations of α -NF to inhibit AhR activation were also those that induced AhR activation alone. This suggests that the low levels of α -NF-dependent AhR activation shown in Figure 3.13, Figure 3.15 and Figure 3.16 should not be a concern (Gasiewicz, 1991). Inhibition of TCDD-induced AhR activation by α -NF occurred as expected (Figure 3.14 A) whereas inhibition of ITE and β -NF-induced AhR activation was more complex; β -NF- and ITE- induced transcriptional activation was inhibited by α -NF (Figure 3.14 B and C) in a dose dependent manner, however Western blotting showed an increase in AhR activation by co-treatment of β -NF plus α -NF, higher than that induced by β -NF alone (Figure 3.15 and Figure 3.16) and also increased further AhR activation with co-treatment of ITE plus α -NF (Figure 3.15 and Figure 3.16). The consistent increase in AhR activation by co-treatment with β -NF or ITE and α -NF suggests an alternative mechanism of action with co-treatment of the AhR, which corresponds with the alternative mechanisms suggested for differential CYP1A1 induction in the previous paragraph. Additionally, it has recently been shown that human AhR has 4 ligand binding domains which contain different binding sequences, allowing the possibility of different binding dynamics for different ligands. It is not known but hypothesised that this may also provide the capacity for more than one ligand to bind concurrently, which would provide a mechanism for the wide ranging variability in responses to ligands, and suggest possible differential effects by interaction of ligands (Salzano et al., 2011).

In retrospect, it would have been useful to include transcriptional activation assays at longer time points with 5 and 10 μ M α -NF to allow more directly comparable results to the Western blot time courses. However, as we have shown in Figure 3.15 and Figure 3.16, the time points at which α -NF exerted low AhR agonist activity (day 8, Figure 3.13)

induced the most efficient inhibition of TCDD-induced AhR degradation and CYP1A1 inhibition. It would also be useful to include a full antagonist in inhibition studies with TCDD, β -NF and ITE, to conclusively show the blocked effects of β -NF- and ITE-induced activation.

Ligand binding to the AhR causes conformational changes of the AhR which can affect its interactions with chaperone proteins and DNA (Gasiewicz and Bauman, 1987; Henry et al., 1989). AhR agonists induce conformational changes that increase AhR affinity for DNA, aiding binding to the promoter XRE and AhR affinity for ARNT. In the case of the AhR antagonist, α -NF, binding is thought to lower AhR affinity for DNA and increase affinity for any endogenous or exogenous AhR ligand, in the case of low concentrations of α -NF, forming a low activity complex. This change can be reversed by TCDD treatment, but once TCDD has induced the high DNA affinity AhR, α -NF cannot reverse that (Gasiewicz, 1991). This is thought to occur during TCDD inhibition (Gasiewicz and Bauman, 1987) but other mechanisms have been reported. Henry et al. showed that α -NF competitively binds AhR at the ligand binding site, stopping TCDD binding. They showed that α -NF not only blocked TCDD-dependent AhR activation but also blocked TCDD-induced translocation to the nucleus and consequent AhR degradation (Henry et al., 1999). As I show that co-treatment of β -NF/ ITE plus α -NF induced further AhR degradation and CYP1A1 activation (Figure 3.16), it would suggest that the Henry theory does not apply to co-treatment of β -NF/ ITE plus α -NF, as AhR degradation is not blocked by α -NF co-treatment. Another mechanism must therefore be involved. A simple possibility is that low concentrations of ligand (for example nM β -NF) do not saturate the AhR ligand binding sites available and co-treatment with α -NF allows α -NF to bind the free AhR, inducing further AhR activation, independent of ITE, but inducing synergistic effects. However, the recent paper by Salzano et al. presents a convincing hypothesis that AhR may have the potential to concurrently bind more than one agonist.

Increased AhR activation by co-treatment of β -NF/ITE plus α -NF suggests that the low-affinity agonist alone does not have the capacity to fully activate the AhR. Co-treatment of keratinocytes by ITE/ β -NF plus α -NF inhibited luciferase induction, but induced CYP1A1 induction. Co-activation of AhR by ITE plus α -NF also induced high AhR degradation.

The role of the AhR physiologically should also be considered. It is known to mediate many toxicities when activated by exogenous compounds, but its role in the absence of exogenous ligands is not well known. It is obviously highly involved in development, but its activation in its physiological roles is not by high concentrations of exogenous compounds, but physiologically relevant concentrations of endogenous ligands (not concentrations that would cause toxicity *in vitro*) and ligand-independent mechanisms (eg. cell-cell contact). CYP1A1 has been studied as a marker of exogenous ligand induced AhR activation, which physiologically, has only been shown to cause toxicity.

From this, we can hypothesise that endogenous ligands should not cause toxicity (ie. CYP1A1) unless used at concentrations *in vitro* that would not be physiologically relevant (because of high toxicity), but elicit milder effects on cellular processes such as differentiation through AhR activation, as represented by AhR degradation. Experiments on the AhR should be characterised into studies into effects of AhR activation in a physiological role, or AhR as a mediator of toxic responses from exogenous compounds.

4 AhR activation in epidermal equivalents

4.1. Introduction

The physiological roles of the AhR in skin are poorly understood and the endogenous ligand(s) and environmental-derived ligands that activate AhR in skin have not been characterised. One important aim of this project was to increase understanding of the pathobiology of chloracne. The AhR is susceptible to activation by ligand-independent mechanisms such as confluency (Ikuta et al., 2004) and differentiation status of the cell causing increased AhR activation potential (Coomes et al., 1983; Du et al., 2006a; Jones and Reiners, 1997; Pohl et al., 1984), so monolayer studies are not an ideal model for AhR activation. Epidermal equivalents allow primary keratinocytes to differentiate, providing more physiological conditions for AhR activation to be studied.

4.1.1 Models exerting chloracne-like effects

Although TCDD causes chloracne (Geusau et al., 2001; May, 1973; Sorg, 2009) and AhR deficient mice develop localised hyperplasia and hyperkeratosis (Fernandez-Salguero et al., 1997), the relationship between agonist-induced AhR activation and the pathophysiology and dermatological changes associated with chloracne remain incompletely understood. There is no suitable *in vivo* model for chloracne (as listed in the following paragraph) but an AhR knock out model is too crude; the exact involvement of AhR degradation in chloracne has not been elucidated and may still be partially dependent on AhR expression. Moreover, as mouse skin differs significantly from human skin by being considerably thinner and bearing hair, studies in mouse skin cannot be readily applied to human skin. Moreover, it is noted in chloracne case studies that follicles involved in chloracne are vellus follicles only, not involving follicles on the scalp (Hambrick, 1957). Interestingly, AhR null mice exhibiting chloracne-like lesions show early alopecia (Fernandez-Salguero et al., 1997). This highlights the importance of the type of the follicle involved in chloracne, indicating that many models reported to show a chloracne-like phenotype (primates, the rabbit ear model and hairless mice, reviewed in (Panteleyev and Bickers, 2006)) should be regarded with caution. AhR also shows high levels of interspecies variability in regards to affinity, making it harder again to extrapolate non human data to a human disease (Henry et al., 1989; Koyano et al., 2005).

A similar phenotype was also produced in ARNT knock out mice. As described in section 1.1.1.5, they exhibited defects in desquamation and barrier function caused by defective lipid metabolism, and a thickened stratum corneum. Overall, the effects appeared similar to the group of epidermal diseases named retention hyperkeratosis, which is explained in detail in Chapter 7.

4.1.2 The epidermal equivalent model

We therefore conducted studies using human epidermal equivalents which have been shown to closely follow differentiation patterns of human skin in vivo (Auxenfans et al., 2009; Eckhart et al., 2000; Stark et al., 1999) and exhibit inducible metabolic activity by AhR agonists (Harris et al., 2002a; Harris et al., 2002b). We tested the hypothesis that the changes in epidermal equivalent differentiation and stratum corneum compaction observed in response to TCDD are associated with the potency and/or residency of the AhR ligand. We also aimed to test whether these changes could be blocked by AhR knock down and whether we could develop a system to test how these changes relate to AhR degradation.

Previously human epidermal equivalents have been used in studies of AhR activation by 1 or 10nM TCDD (Geusau et al., 2005; Loertscher et al., 2001b). Loertscher et al show early induction of terminal differentiation in epidermal equivalents formed with a spontaneously immortalized human keratinocyte cell line NIKS, which were shown to have the same differentiation and apoptosis pathways as normal primary keratinocytes (Allen-Hoffmann et al., 2000). They show histological changes resulting from treatment with 10nM TCDD for 7 days by showing early development of the cornified layer and by IHC, early and aberrant expression of filaggrin, involucrin and TGM-1. They also observed an increase in thickness in the ratio of keratinized layers to non-keratinized layers, which they attribute to increased and early onset of terminal differentiation resulting from TCDD treatment. To rule out the effects of cell death on culture thickness, the authors used IHC staining for active caspase-3 and TUNEL assays, which showed no evidence of TCDD-dependent increase in apoptosis. They concluded that early onset of terminal differentiation was the main mechanism for phenotypic effects in their epidermal equivalent model (Loertscher et al., 2001b). However, this paper is based on an epidermal equivalent model consisting of immortalised keratinocytes as opposed to primary keratinocytes. The author claims to have carried out the phenotypic

experiments on epidermal equivalents from primary keratinocytes showing the same results, but these data are not shown. Conclusions on terminal differentiation and cell death cannot be reliably extrapolated from a model consisting of immortalized keratinocytes, as they may not undergo normal cell death, they have been characterised for differentiation and apoptosis, but not necrosis or autophagy. This must be kept in mind while considering the conclusions from this paper. Geusau et al. show similar effects as Loertscher et al. but in epidermal equivalents produced using primary human keratinocytes. Again, they show that TCDD treatment resulted in increased thickness of the stratum corneum and parakeratosis, decreased VCL thickness (basal, spinous and granular layer as indicated in Figure 4.1) and loss of granular layer. However, differentiation markers did not consistently indicate increased/early differentiation; Western blots were used to show increased involucrin, but also an accumulation of profilaggrin, resulting from a block in processing to filaggrin, and decreased caspase 14 (and processing to its mature form), a protease involved in terminal differentiation. This paper concludes that TCDD induced aberrant differentiation and blocked final stages of terminal differentiation. The model described in this paper was more relevant to chloracne because it consisted of primary cells, but some of the results are not consistent with other literature. These inconsistencies may be because of cell and species variability in extrapolating results in the literature to this primary human keratinocyte model. Loertscher et al. suggest that TCDD induced non-apoptotic cell death may contribute to the phenotype, but did not define the mechanism of cell death. We go on to confirm that apoptosis was not induced by TCDD in epidermal equivalents and show novel data that autophagy, a mechanism of both cell survival and cell death, is induced by TCDD.

The metabolic capacity of human epidermal equivalents has been studied, but has not been correlated to phenotype, differentiation or homeostasis in the cells (Harris et al., 2002a; Harris et al., 2002b). Harris et al showed that treatment of epidermal equivalents, primary human keratinocytes in monolayer culture and *ex vivo* follicles and epidermis with β -NF or 3-MC induced CYP1A1 and glutathione-s-transferase (GST) activity. GST activity was higher in epidermal equivalents compared to *ex vivo* samples, and CYP1A1 activity in epidermal equivalents was batch dependent but CYP1A1 could be induced in *ex vivo* samples and keratinocyte cultures (but was not present in non-induced samples). CYP1A1 and GST activity increased with keratinocyte monolayer

confluence, in agreement with the literature (Harris et al., 2002a). These papers confirm metabolic function in epidermal equivalents and that it is inducible by AhR activation.

One of the primary benefits for using the epidermal equivalent model in this project is to allow treatment of *ex vivo* human keratinocytes in a model relevant to human skin, with AhR ligands. The characteristics of this model allow cell differentiation and homeostasis to be observed by development and phenotype (H&E)(Ponec et al., 2000). Formation of the epidermal equivalent is dependent upon normal homeostasis in cell culture, with a normal balance of proliferation, differentiation and cell death. Any changes in this homeostasis can be seen in changes to the epidermal equivalent phenotype by H&E (thinner VCL, parakeratosis, holes in cell layers) and these can be further defined by IHC to provide specific measurement and localisation of proteins.

4.3 Results

In this chapter, we show novel data on the phenotypic changes and effects on keratinocyte differentiation in human epidermal equivalents treated with β -NF or ITE and show direct comparisons between effects of AhR activation by different ligands on the epidermal equivalent phenotype. We also show effects of AhR activation on induction of well defined differentiation markers filaggrin, involucrin and TGM-1 by AhR ligands and preliminary data showing effects of AhR knock down on epidermal equivalent phenotype.

4.3.1 Effects of AhR ligands on epidermal equivalent phenotype

The epidermal equivalent model used here as defined in materials and methods (Jans and Reynolds, 2012)(unpublished data) was based on the protocol from Poumay et al. with modifications (Poumay, 2004). The time point chosen for treatment of epidermal equivalents was 7 days, based on the Geusau paper (Geusau et al., 2005). H&E staining was performed to visualise the phenotypic effects of agonist treatment (Figure 4.1). The discrete layers of the viable cell layer (VCL: basal, spinous and granular) were present, with a cornified layer showing the open basket weave phenotype characteristic of healthy epidermis (Figure 4.1 A). The black lines on A and B indicate the VCL and stratum corneum (SC) as labelled (Figure 4.1). Figure 4.1 B and Figure 4.2 showed that as expected, TCDD treatment significantly decreased viable cell layer thickness (one-way ANOVA comparing vehicle to TCDD treated $P = <0.0001$) and as previously shown

in epidermal equivalents using human keratinocyte cell line or primary keratinocytes (Geusau et al., 2005; Loertscher et al., 2001b). In contrast however, β -NF or ITE treatment did not cause a significant change in VCL thickness (Figure 4.1). The effects of TCDD on the VCL could be caused by increased cell death or early onset of terminal differentiation; TCDD is known to cause a decrease in keratinocyte number, independent of apoptosis in primary human keratinocyte monolayers and human keratinocyte cell line epidermal equivalents (Loertscher et al., 2001a; Loertscher et al., 2001b) although we observed no decrease in ODU in SRB assay; TCDD is also known to induce early onset of terminal differentiation in primary keratinocyte monolayers (Osborne and Greenlee, 1985; Ray and Swanson, 2003) and epidermal equivalents (Geusau et al., 2005; Loertscher et al., 2001b). This suggests that at doses that induce AhR activation in keratinocyte monolayers, neither β -NF nor ITE induce the mechanism causing the decrease in VCL thickness in epidermal equivalents, that it is a TCDD specific effect. The novel data shown here are the effects of β -NF and ITE on keratinocyte differentiation in the epidermal equivalent model and the direct comparisons between TCDD, β -NF and ITE.

Another observation in the TCDD treated epidermal equivalent model was that the stratum corneum became compact and thicker (SC, upper right black line). This occurred to a lesser extent in β -NF and ITE treated epidermal equivalents, suggesting that β -NF and ITE induced the mechanisms leading to stratum corneum compaction but to a lesser extent than TCDD. Parakeratosis was also present in TCDD, β -NF and ITE treated samples. This often occurred because of disrupted differentiation, causing nuclei to persist in cells instead of being degraded in the normal course of differentiation. Notably, these two main changes (VCL decrease and stratum corneum compaction) in epidermal equivalent phenotype are characteristic of chloracne within vellus follicles and comedones, as is parakeratosis. The VCL within the follicle becomes thinner and stratum corneum becomes compacted and thicker causing a follicular plug which leads to comedone formation, as shown in (Hambrick, 1957; Pastor et al., 2002).

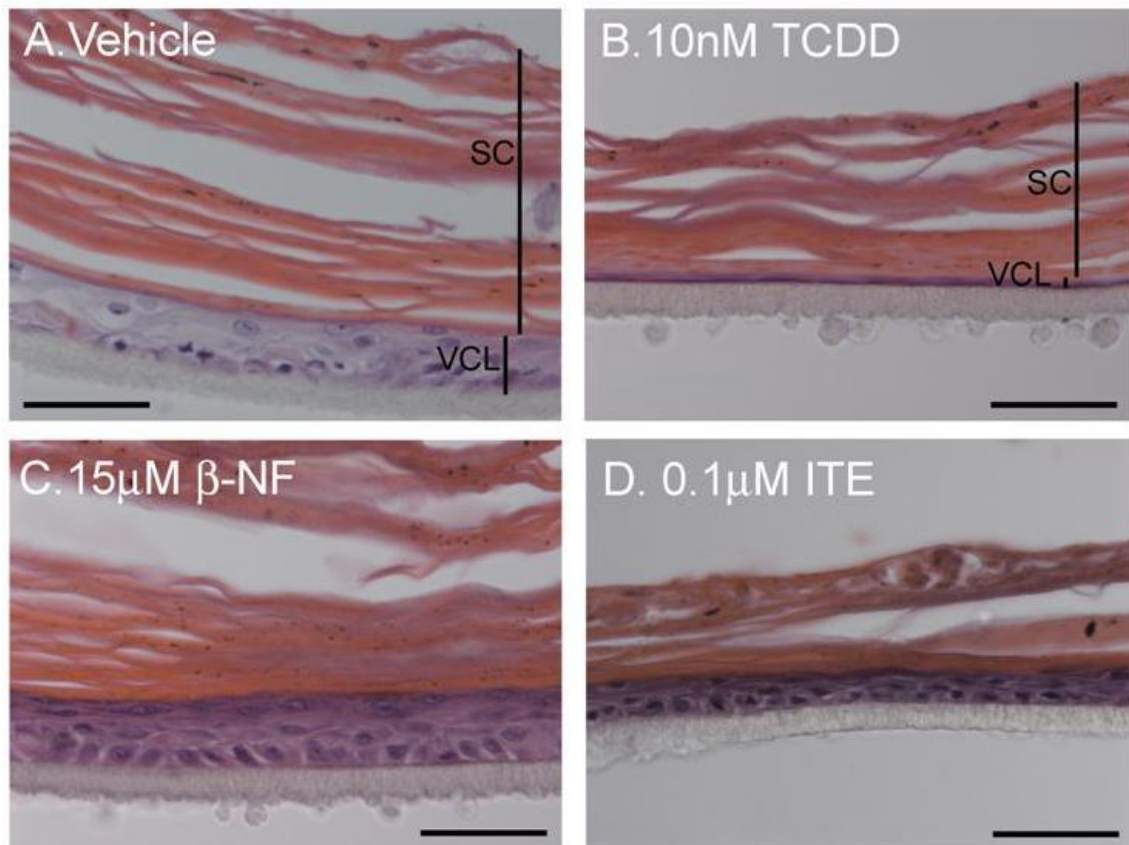


Figure 4.1. TCDD caused decreased thickness of the viable cell layer and compaction of the stratum corneum in the epidermal equivalent model. Epidermal equivalents were grown as described in materials and methods and treated with vehicle, TCDD, β -NF or ITE every 48h for 7 days. After 7 days, equivalents were fixed, embedded in paraffin and stained with H&E. The VCL consists of discrete layers – basal, spinous and granular, all of which are present. VCL and SC (stratum corneum) are marked by labelled black lines in A and B. Images **A**, **C** and **D** are representative of effects in 3 donors, **B** shows maximal decrease in VCL thickness seen in epidermal equivalents in 3 donors. Scale bar = 50 μ m.

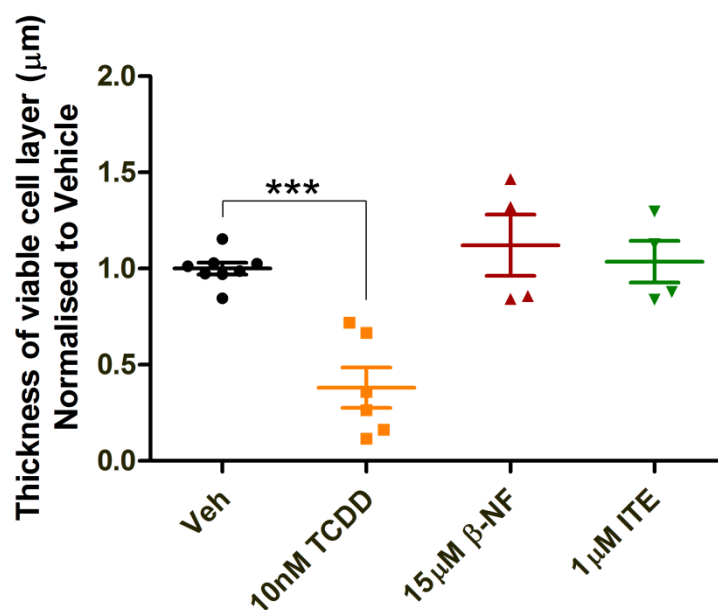


Figure 4.2. TCDD caused a significant decrease in viable cell layer thickness. Epidermal equivalents were grown and treated with vehicle, TCDD, β -NF or ITE every 48h for 7 days. H&E staining was performed and images captured by light microscopy. Using Image J, 6 measurements of the viable cell layer were taken from 2 images per treatment for each donor. Individual values and means (\pm sem) are shown for 3 independent donors (Vehicle/TCDD) and 2 donors (β -NF/ITE). One way-ANOVA was performed comparing vehicle to ligand, *** P = <0.0001.

From this data we can conclude that neither β -NF nor ITE treatment induced the mechanism by which TCDD induced the effects on VCL thickness. We next went on to investigate the possible mechanisms for these effects and whether TCDD, β -NF and ITE did induce differential effects.

4.3.2 The effects of AhR ligands on differentiation

The proposed mechanisms of TCDD-induced decreased VCL thickness were increases in cell death or differentiation (Loertscher et al., 2001b). We used immunohistochemistry to investigate any differential effects of TCDD, β -NF or ITE on differentiation, using markers filaggrin, involucrin and TGM-1 (Figure 4.3) and apoptosis (active caspase-3 Figure 4.4, cleaved lamin A Figure 4.5). Apoptosis was studied to confirm that it was not occurring in our epidermal equivalent model; Loertscher et al. defined this in a keratinocyte cell line epidermal equivalent model and primary keratinocyte monolayers, while Geusau et al. did not study cell death in their primary keratinocyte epidermal equivalent model (Geusau et al., 2005; Loertscher et al., 2001b).

To assess the effect of AhR activation on keratinocyte differentiation, immunohistochemical analysis of filaggrin, involucrin and TGM-1 was carried out. Involucrin and profilaggrin are both precursors of the cornified envelope, and TGM-1 is one of the main enzymes that forms cross links with precursors of the cornified envelope to the cell membrane. Involucrin is a direct substrate for TGM-1, while profilaggrin is not (reviewed in (Eckert et al., 2005; Sandilands et al., 2009)). Profilaggrin is one of the main components of keratohyalin granules seen as puncta in the granular cell layer. It is broken down by proteolysis and phosphorylation to filaggrin during terminal differentiation. Loertscher et al. reported that TCDD caused filaggrin staining to become patchy, and present in cells in closer proximity to the basal layer (Loertscher et al., 2001b). Figure 4.3 (left column) shows that punctate staining was even throughout the granular layer in vehicle treated samples. β -NF treatment caused staining to become uneven throughout the granular layer, and expressed in cells in closer proximity to the basal layer, while TCDD and ITE caused an overall decrease and irregularity (as with β -NF) in filaggrin staining. Loertscher et al. reported that TCDD caused dysregulation (similar effects to filaggrin) and increased involucrin staining. In vehicle treated samples, involucrin was expressed in the spinous and granular layers (Figure 4.3 middle column). In TCDD-, β -NF- and ITE-treated samples, levels of involucrin expression were increased and aberrantly expressed in cells in closer proximity to the basal layer, often including the basal layer. Loertscher et al. showed that TCDD caused TGM-1 staining to become irregular around the inner edge of the cell membrane. In vehicle treated samples, TGM-1 was expressed evenly and continuously around the inner edge of the cell membrane. In TCDD treated samples this staining became increased and irregular around the cell membrane. β -NF and ITE treated epidermal equivalents showed slight increased staining but expression did not appear aberrant. This TCDD-specific effect on TGM-1 is consistent with the literature; Du et al. showed that in primary human keratinocytes, TCDD up regulated expression and activation of TGM-1, but β -NF did not (Du et al., 2006a). Egberts et al. showed that TGM-1 expression correlated well with activation, so we can presume that the dysregulation of staining for TGM-1 correlated with dysregulated TGM-1 expression and activation, causing the downstream effects associated with increased TGM-1 activation, which are increased involucrin and loricrin, and crosslinking forming the cornified cell layer (Egberts et al., 2004).

To summarise, filaggrin expression in human epidermal equivalents was dysregulated by TCDD, β -NF and ITE. TCDD and ITE also induced decreased overall staining of filaggrin. Involucrin expression was increased and also expressed in cells in closer proximity to the basal layer, by TCDD, β -NF and ITE treatment, but the increase in staining was higher in TCDD treated samples than the other ligands. TGM-1 expression was increased and dysregulated by TCDD treatment, but staining in β -NF and ITE treated samples only appeared slightly upregulated with no signs of dysregulation. From this we can conclude that AhR activation by all 3 ligands induced early onset of terminal differentiation, but the effects were most prominent with TCDD, and that TCDD was the only agonist to induce dysregulation of TGM-1 expression.

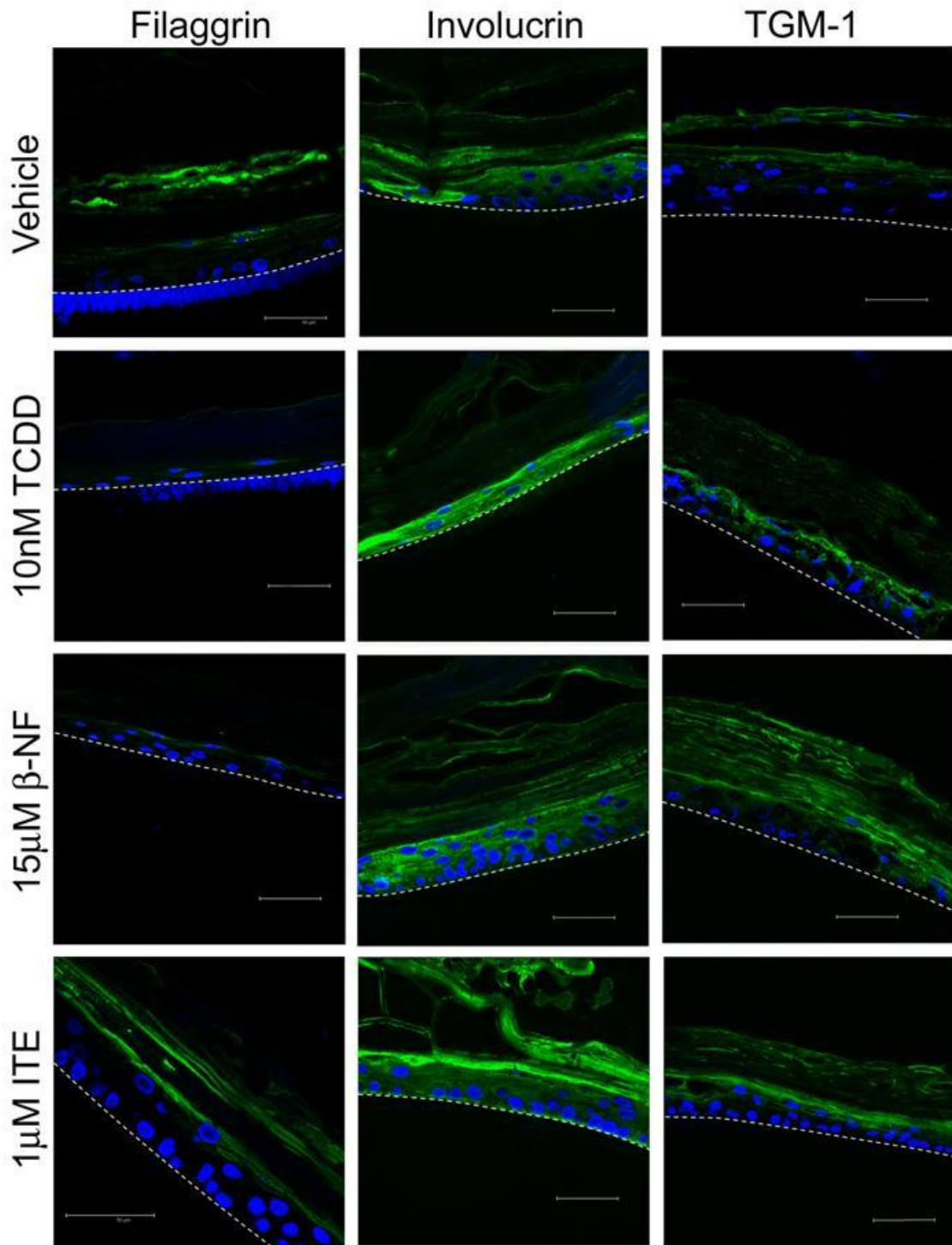


Figure 4.3. AhR activation caused dysregulated expression of differentiation markers. Human epidermal equivalents were grown and treated with vehicle, 10nM TCDD, 15µM β-NF or 1µM ITE every 48h for 7 days. Immunohistochemistry was carried out using anti-filaggrin (left column), anti-involucrin (middle column) or anti-TGM-1 (right column)(all green) antibodies with Oregon green (488) tagged secondary antibody and topro-3 (blue) nuclear stain. Mid z section images were captured by confocal microscopy and are representative of epidermal equivalents from 3 donors. Dotted white lines represent junction between basal layer and polycarbonate membrane. Scale bars = 50µm.

4.3.3 The effects of AhR ligands on apoptotic cell death

Apoptosis is a complex process of regulated programmed cell death that can be activated by many intra- and extracellular pathways, including DNA damage, lysosomal stress and activation of death receptors. Upon activation of any caspase-dependent pathways, a cascade of proteolytic reactions is initiated, activating a combination of cell specific caspases. The common effector is Caspase-3; it is widely expressed in most cells and tissues (including skin and keratinocytes (Eckhart et al., 2000; McGill et al., 2005; Weatherhead et al., 2011)) and its activation is involved in many apoptotic pathways, making it a good biomarker for apoptosis (reviewed in (Ulukaya et al., 2011)). Although caspase-3 activation is common in apoptosis, it is not involved in every apoptotic pathway, so other markers (further downstream in the apoptotic pathway than caspases) should also be studied, for example cleaved lamin A or cleaved PARP. Lamin A is a substrate for caspase 6 and cleavage must occur for chromatin condensation to occur during apoptosis (Ruchaud et al., 2002). This makes cleaved Lamin A a good candidate for use as a complementary biomarker to active caspase-3 and this is why it has been studied here (reviewed in (Arnault et al., 2010)).

Loertscher et al. showed that in primary keratinocytes in monolayer and in human keratinocyte cell line epidermal equivalents, TCDD treatment did not induce apoptosis (Loertscher et al., 2001a; Loertscher et al., 2001b). This suggests that epidermal equivalents containing primary keratinocytes would also show no increase in apoptosis. To rule apoptotic cell death out of the possible mechanisms for decreasing VCL thickness and to confirm that TCDD did not induce apoptotic cell death in our primary keratinocyte epidermal equivalent model, we used IHC against anti-active caspase-3 (Figure 4.4) and anti-cleaved lamin A (Figure 4.5) on TCDD, β -NF and ITE treated epidermal equivalent sections.

Firstly, IHC was performed on epidermal equivalents treated with vehicle, TCDD, β -NF or ITE, using anti-active caspase-3 (green) and topro-3 (blue) as described in materials and methods. UV treated skin was used as a positive control and showed active caspase-3 positive cells in the epidermis, whereas low numbers of positive cells were seen in vehicle, with no increase in active caspase-3 staining in TCDD, β -NF or ITE treated epidermal equivalents. These data were consistent in epidermal equivalents from 3 donors. There was slight variation in basal levels of active caspase-3 between

donor, but no induction of active caspase-3 by AhR agonists was present in any samples. This suggests that apoptosis was not induced by AhR in primary human keratinocyte epidermal equivalents at the time points studied.

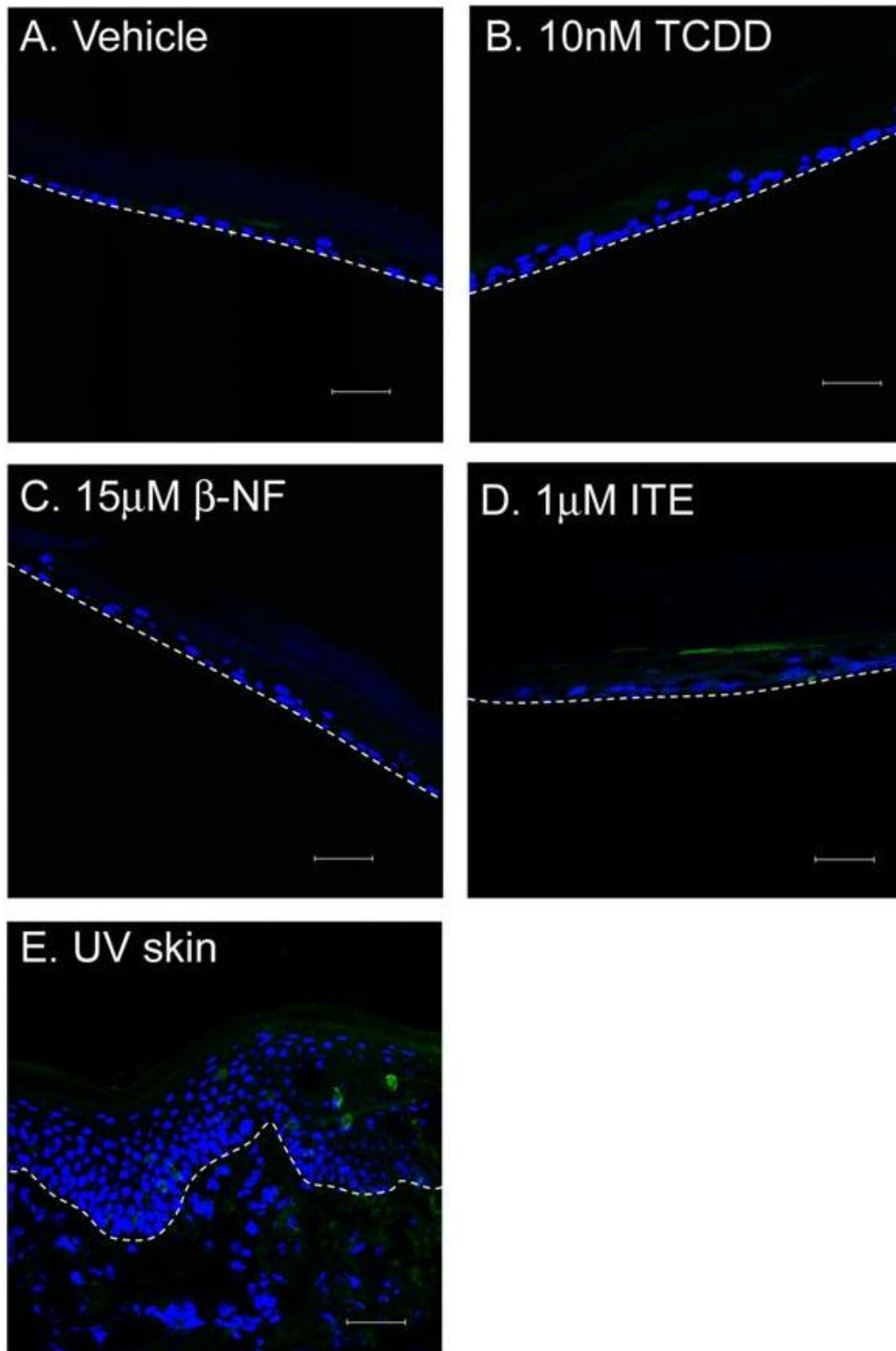


Figure 4.4. AhR activation does not induce Caspase-3 activation. Epidermal equivalents were treated with vehicle, 10nM TCDD, 15µM β -NF or 1µM ITE every 48h for 7 days. IHC was carried out using anti-active caspase 3 (green) and Oregon green 3 fluorescently tagged secondary antibody, topro-3 (blue) was used to stain nuclei. UV treated human skin was used as positive control. Mid z section images were captured by confocal microscopy. Images are representative of 3 donors. Dotted white line represents junction between epidermis and dermis (E) or basal layer and polycarbonate membrane (A-D). Scale bars = 50µm.

To test whether apoptosis may be occurring through a caspase-3 independent pathway, we performed IHC using anti-cleaved lamin A primary antibody (brown staining) with a Dako Envision plus HRP labelled secondary and DAB staining, with haematoxylin co-stain (blue) as describe in materials and methods (Figure 4.5). DAB staining was used in this experiment instead of fluorescence because of logistical considerations: the assay had been set up in a lab with this method, no confocal microscope was available. The positive control was normal human skin of a sample from a donor known from previous staining for apoptotic markers to have high cleaved Lamin A positivity. The origin of the sample was not clear so may have undergone treatment previously, as normal human epidermis does not normally contain high levels of cleaved Lamin A. No positive staining was seen in vehicle and it was not induced by TCDD, β -NF or ITE treatment. As with staining for active-caspase 3, minor variation was present in basal levels between donors, but no induction of cleaved lamin A by any agonist treatment was present in any donor.

Considering that neither active caspase-3 nor cleaved lamin A were induced in any donor sample by the 3 agonists, this suggests that apoptotic cell death was not induced by TCDD, and we show novel data that neither β -NF nor ITE induced apoptosis in human epidermal equivalent.

This is consistent with the literature and provides evidence that decreased VCL is not caused by apoptosis (Loertscher et al., 2001b). However, the literature shows a decrease in numbers of primary human keratinocytes treated with TCDD (Loertscher et al., 2001a), and non-apoptotic cell death could still be a mechanism contributing to decreased VCL. This is not defined here, but is investigated in the following chapter.

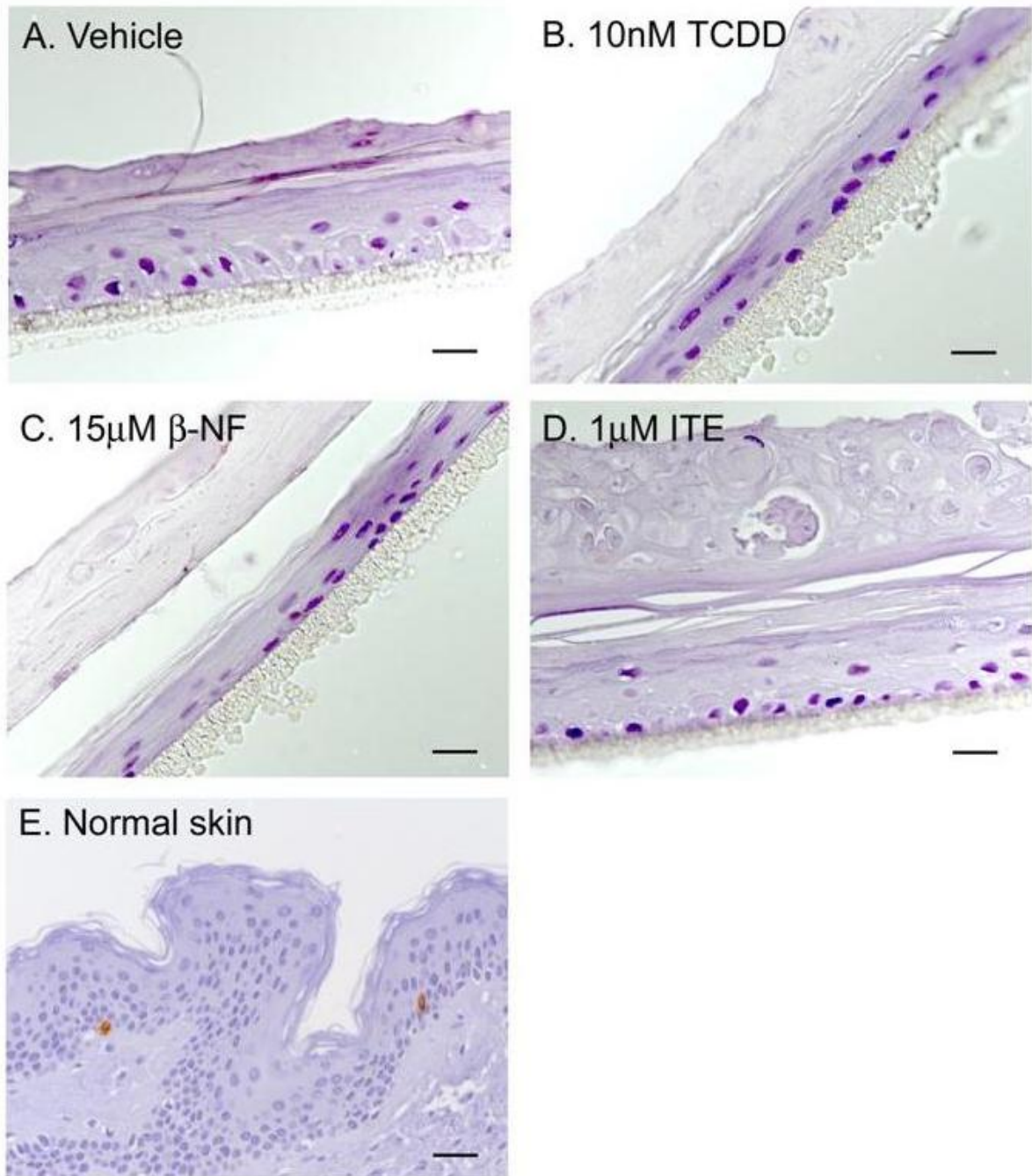


Figure 4.5. AhR activation does not increase cleaved Lamin A staining in epidermal equivalents. Epidermal equivalents were treated with vehicle, 10nM TCDD, 15µM β -NF or 1µM ITE every 48h for 7 days. Equivalents were fixed, embedded in paraffin and immunostained with anti-active caspase 3 antibody (brown) and Dako envision conjugated secondary antibody with DAB staining. Sections were counterstained with haematoxylin (blue). Human skin was used as the positive control. Images were captured by light microscopy and are representative of 3 donors (vehicle and TCDD) or 2 donors (β -NF and ITE). Scale bars = 20µm (A-D), 40µm (E).

4.3.4 AhR induction in epidermal equivalents

AhR activity has been characterised in human epidermal equivalents (Harris et al., 2002a; Harris et al., 2002b) and keratinocyte monolayers at different stages of differentiation (Du et al., 2006a; Greenlee et al., 1985; Ray and Swanson, 2003) and confluency (Ikuta et al., 2004; Sadek and Allen-Hoffmann, 1994b) but AhR levels and localisation have not been studied in epidermal equivalents.

Ligand residency has been shown to affect duration of AhR activation and therefore down-regulation of AhR in primary keratinocytes. Berghard et al showed that in primary human keratinocytes, maximal levels of AhR activation (CYP1A1 mRNA induction) by TCDF (2,3,7,8-tetrachlorodibenzofuran, a similar halogenated aromatic hydrocarbon to TCDD) and β -NF were similar after 8h treatment, persisting for at least 5 days (TCDF) or 4 days (β -NF) in human keratinocytes, showing that β -NF induction was transient compared to sustained activation by TCDF. This paper concluded that transient activation was caused by the fast metabolism of β -NF by CYP1A1, because blocking CYP1A1 activation resulting in sustained β -NF-induced AhR activation (Berghard et al., 1992). Similar effects of transient AhR activation were seen by ITE treatment in a mouse hepatoma cell line. ITE induced AhR to a similar degree as TCDD at 6h but by 24h in ITE treated samples AhR levels had recovered and CYP1B1 levels had started to decrease (Henry et al., 2010). It would be interesting to study a time course of AhR levels in keratinocytes or epidermal equivalents (practically, this would be more difficult) to follow the patterns of degradation and recovery of AhR caused by the ligands. This may also help to decipher the results from the varied time course effects I have shown in Chapters 3, 5 and 6.

The amount of time for ligand-induced AhR degradation to occur depends on cell type and ligand (Pollenz and Buggy, 2006; Swanson and Perdew, 1993). To study AhR levels and localisation in epidermal equivalents, IHC was performed using a primary anti-AhR antibody on epidermal equivalents treated with vehicle, 10nM TCDD (high-residency) or 15 μ M β -NF (low-residency) to see the effects of AhR activation on AhR levels and localisation in epidermal equivalents. ITE has not been included here because its metabolism has not been defined, but literature shows that in regard to transient activation, both β -NF and ITE induced AhR degradation had recovered by 24h, suggesting similar speed of clearance by metabolism. Figure 4.6 (top row) shows that in vehicle treated epidermal equivalents, AhR was present in both the cytoplasm and

nucleus, but was mainly nuclear. Overall expression did not appear to change throughout the course of keratinocyte differentiation. Figure 4.6 (middle row) showed epidermal equivalents treated with 10nM TCDD for 7 days. There was a decrease in nuclear AhR expression and localisation appeared at the nuclear membrane. AhR expression also appeared at slightly higher levels in the granular cell layer too. Figure 4.6 (lower row) shows epidermal equivalents treated with β -NF. AhR levels appeared slightly higher than those seen in vehicle treated cells, and we presume that the levels were decreased by β -NF treatment but have recovered since the last agonist treatment of the culture. There are reports of increased levels of AhR after ligand-dependent degradation in the literature. Franc et al. show that in rat hepatocytes, a single dose of TCDD induced AhR degradation at day 1, but AhR protein and mRNA recovered by days 4 and 10 to above basal levels. This was independent of strain sensitivity and the authors suggested that pre-translation mechanisms of regulation may have been responsible (Franc et al., 2001). Similar results were seen in rat liver after chronic dosing over 22 weeks, with an increase in TCDD binding to cytosolic AhR (Sloop and Lucier, 1987). Both papers reported increases of ~2 fold compared to basal AhR levels. Interestingly, samples of involved chloracne epidermis were tested for CYP1A1 and AhR mRNA levels ~6 years after a group of men had been chronically exposed to dioxins for an unknown length of time, in an industrial setting. Unexpectedly, both AhR and CYP1A1 levels were shown to be increased (Tang et al., 2008), corresponding potentially with the reported increased AhR from recovery both acute and chronic doses of TCDD (Franc et al., 2001; Sloop and Lucier, 1987). These three studies were carried out *in vivo* over chronic dosing or 1 acute dose and without detailed time course studies (in animals) and with little exposure history (in humans). Localisation of AhR in vehicle and β -NF epidermal equivalent samples appeared patchy (Figure 4.6), this could represent clustering or localisation specific to nuclear structures, but to draw any conclusions from this, more studies would be required to confirm any colocalisation or sequestering.

In summary, AhR localisation in epidermal equivalents was predominantly nuclear, with slightly lower levels in the cytoplasm. TCDD treatment appeared to induce down-regulation of the AhR after 7 days of treatment (consistent with Western blot data in monolayer studies (section 3.3.1.3)) and induced localisation to the nuclear membrane. β -NF samples showed high levels of AhR (again, predominantly nuclear) which when the literature is taken into account, we hypothesise has recovered from transient β -NF

dependent down-regulation, or is an effect of chronic treatment over 7 days. Because this assay has been performed on fixed epidermal equivalents it only shows a snapshot in time and therefore the time and activation dependent degradation and recovery of AhR needs to be studied with a complementary assay to confirm the data – Western blots have been performed in monolayer keratinocyte cultures but to truly confirm this result, protein lysates from epidermal equivalents should be run by Western blot.

Considering AhR localisation in monolayer cultured keratinocytes and its strong localisation to the cytoplasm at high keratinocyte confluency (Figure 3.6), we might have expected to see cytoplasmic AhR localisation in epidermal equivalents. In the literature there is little information on the localisation of AhR in normal skin; because AhR localisation is affected by so many factors, endogenous and exogenous, any papers reporting AhR localisation showed conditions where the AhR might be activated. For example, Zhou et al. showed cytoplasmic AhR in rat liver 20h post sham operation but the AhR is thought to play a role in wound healing (Zhou et al., 2008), by increased CTSD inducing proliferation and migration as shown in HaCaTs (Vashishta et al., 2007) and Abbot et al showed nuclear AhR in embryonic mouse tissue, where the AhR is thought to be activated during its role in development (Abbott et al., 1995). Because of the variability between tissue and conditions reported in these papers and our work, the literature does not help to clarify whether nuclear AhR in untreated epidermal equivalents is a normal state or induced state. The cause of nuclear AhR in the epidermal equivalent model can only be speculated on; however it suggests that ligand-independent AhR activation may be occurring in the epidermal equivalent model. Unpublished data from the Reynolds group has shown AhR to be mainly cytoplasmic in normal human skin, suggesting that epidermal equivalent culture may induce AhR activation by a ligand-independent mechanism.

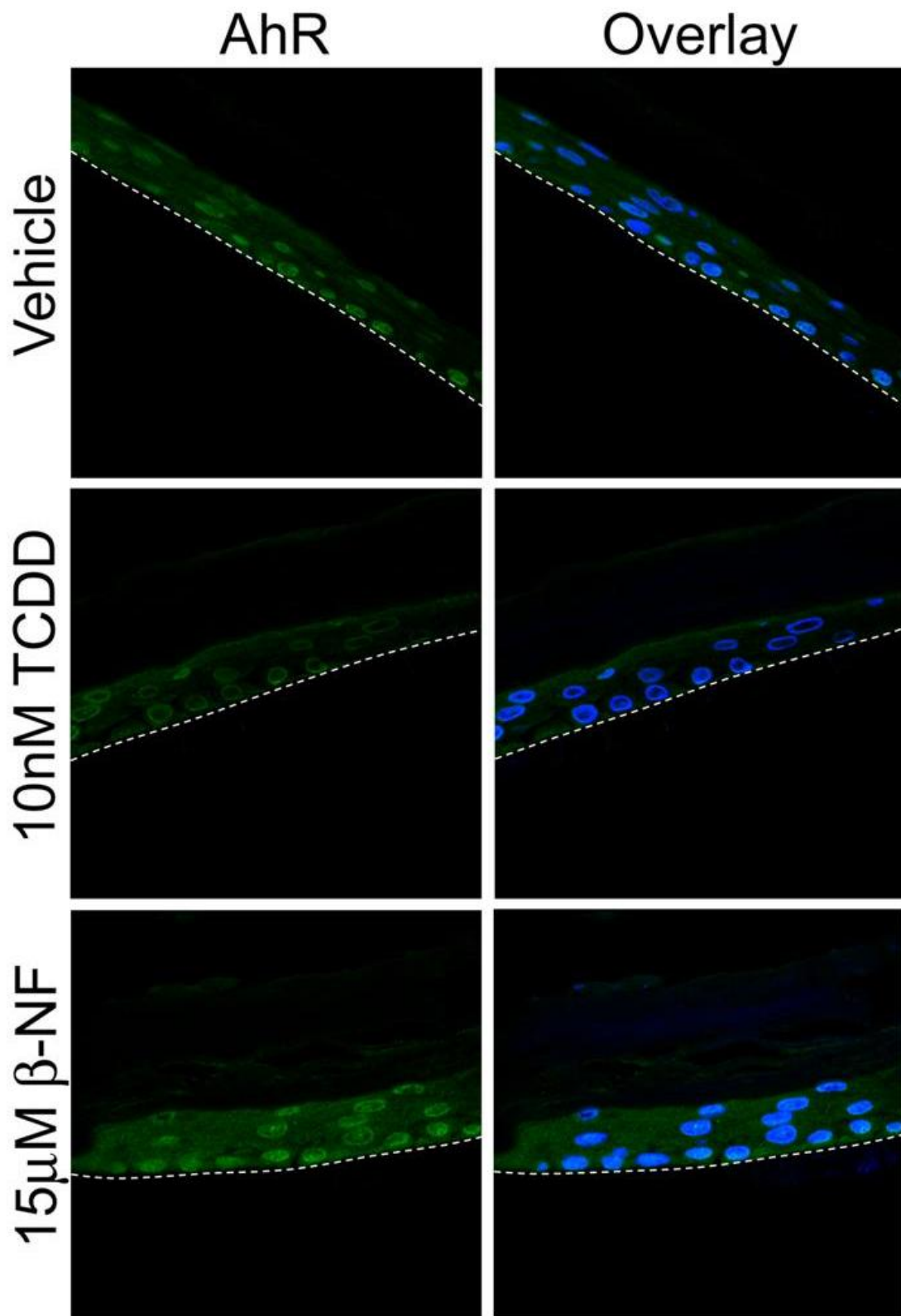


Figure 4.6. TCDD treatment causes a decrease in nuclear AhR expression in epidermal equivalents. Human epidermal equivalents were grown and treated with vehicle, 10nM TCDD, 15μM β-NF or 1μM ITE every 48h for 7 days, so at time of harvesting had not been treated for 24h. IHC was carried out using anti-AhR (green) with Oregon green tagged secondary antibody and topopro-3 nuclear stain (blue). Images are mid sections captured by confocal microscopy, representative of epidermal equivalents from 3 donors. Dotted white lines represent junction between basal layer and polycarbonate membrane. Scale bars = 50μm.

4.3.4.1 AhR Knock down

It is unclear whether the effects of AhR activation on epidermal differentiation are caused by downstream regulation of certain proteins, the sequestering of ARNT from other PAS pathways or the lack of AhR caused by activation-dependent degradation. The last hypothesis possibly would contribute to the hypothesis of increased residency of ligands causing a compound to be chloracnegenic. With a view to utilising AhR knock down as proof of concept for the down stream effects of AhR activation (eg. CYP1A1 up-regulation and dysregulated differentiation), 2 methods for AhR knockdown were developed in primary keratinocytes; transient transfection with siRNA targeting AhR and lentiviral transduction of shRNA targeting AhR.

Protocols for transfection of primary human keratinocytes with siRNA targeting AhR were optimised. Two protocols were tested: lipofectamine and plus or nucleofection (both protocols had been developed previously in the lab for siRNAs targeting different proteins). Nucleofection with siRNA to AhR resulted in very low keratinocyte viability, so was not suitable for use. The lipofectamine and plus protocol resulted in little visible decrease in cell viability (by light microscopy) so was chosen for use in future studies.

Primary keratinocyte monolayers were transfected in parallel with each of 4 siRNAs targeting AhR separately, the 4 siRNAs combined, or a scrambled siRNA control using lipofectamine and plus. Non-transfected keratinocytes were cultured in parallel. 24h or 48h post transfection, keratinocytes were either lysed for Western blotting or seeded at high confluency for epidermal equivalents. See materials and methods for details.

Figure 4.7 A shows a Western blot of primary keratinocytes transfected with siRNA constructs targeting AhR (labelled 5-8, see materials and methods for details), combined AhR constructs (5,6,7 and 8) or scrambled control siRNA for 24h (upper blot) or 48h (lower blot). After transfection cells were lysed and Western blotting performed. At 24h, AhR appeared to be partially knocked down by constructs 5-8, with construct 6 showing most efficient knockdown. By 48h AhR levels had recovered partially in all siRNA transfected samples. These data show the maximal knock down seen out of 2 donors.

Figure 4.7 B shows epidermal equivalents made using primary keratinocytes transfected with siRNA constructs; scrambled (Figure 4.7 a and c) or construct 6 (Figure

4.7 b and d). The 4 epidermal equivalents were cultured for 5 days and then treated for 7 days with vehicle (a and b) or 10nM TCDD (c and d). Cultures were harvested, fixed in 4% PF overnight, paraffin embedded and H&E staining performed.

Interestingly, instead of blocking the TCDD phenotype in epidermal equivalents, AhR knockdown itself caused a TCDD-like phenotype. Epidermal equivalents transfected with scrambled siRNA and treated with vehicle (Figure 4.7 a) resembled the normal phenotype: thick VCL and basket weave stratum corneum. Figure 4.7 c shows scrambled siRNA epidermal equivalents treated with 10nM TCDD and as expected, the normal TCDD induced phenotype was present: thinner VCL and compacted stratum corneum. Epidermal equivalents transfected with siRNA 6 targeting AhR and treated with vehicle (Figure 4.7 b) showed slight stratum corneum compaction and thinner VCL, compared to vehicle treated scrambled samples, but when treated with 10nM TCDD (Figure 4.7 d) exacerbated the phenotype further, resulting in a more compacted stratum corneum and thin VCL.

It is difficult to predict levels of AhR knock down that can be expected in cells 12 days post transfection. siRNA remains in the cell for a short time period (see partial recovery of AhR levels at 48h in Figure 4.7 A and (McManus and Sharp, 2002)) however because cell proliferation decreases in epidermal equivalents and differentiation occurs, siRNA is thought to be conserved for longer (Mildner et al., 2006).

This assay shows that siRNA-induced AhR knock down resulted in a TCDD-like phenotype in vehicle treated samples. TCDD treatment of AhR knock down epidermal equivalents increased this effect, this may have been caused by TCDD activating any remaining AhR and causing its degradation, resulting in minimal levels of AhR in the culture. This assay alone suggests that the TCDD phenotype described in this chapter may be caused by the lack of AhR resulting from TCDD-induced AhR degradation. Because this is only preliminary information, the experiment should be repeated in 2 more donors to confirm these results and AhR knock down in epidermal equivalents confirmed by Western blot and IHC. To investigate the affect of AhR knock down on epidermal equivalents further, IHC could be performed using antibodies against filaggrin, involucrin and TGM-1 to show the effects of AhR knock down on differentiation, and by Western blot to show blocked induction of CYP1A1.

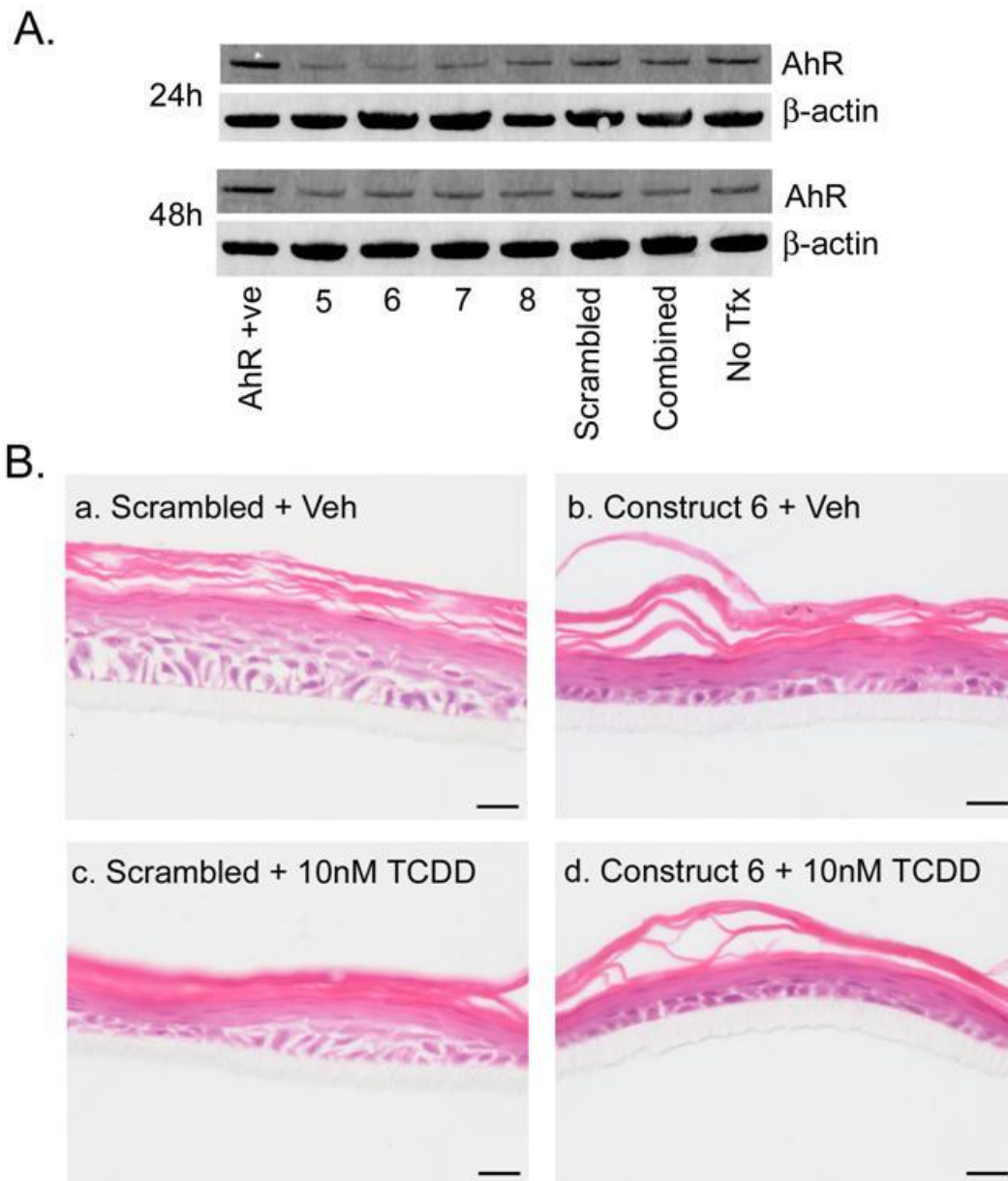


Figure 4.7. AhR knock down induces TCDD-like phenotype in epidermal equivalents. Primary keratinocytes were transfected with siRNAs against AhR, combined siRNAs (5, 6, 7 and 8) or scrambled control sequence. **A)** 24h or 48h after transfection cells were lysed for Western blot and probed with anti-AhR and anti- β -actin antibodies. **B)** Immediately after transfection with siRNA construct 6 cells were seeded onto polycarbonate membranes to form epidermal equivalents. Epidermal equivalents were treated with vehicle (a, b) or 10nM TCDD (c,d) for 7 days and medium changed with fresh TCDD every 48h, fixed in 4% PF, sectioned and stained with H&E. Western blot shows maximal knock down from 2 donors, epidermal equivalents show results from 1 donor. Scale bar = 20 μ m.

SiRNA constructs only last over short time points in dividing cells and also only dividing cells are successfully transfected with the constructs due to the replication dependent production of the short interfering RNA. This means that stem cells are not efficiently transduced with siRNA and therefore contribute to the rapid loss of siRNA knockdown in a monolayer. As AhR levels from siRNA knock down in primary keratinocytes had recovered by 48h, this does not result in enough time to perform many types of assay, therefore we utilised lentiviral shRNA vectors against AhR to induce stable AhR knock down in primary keratinocytes, which also efficiently transduces stem cells, producing a wider range of assays and time points in which to study AhR knock down.

The lentiviral vectors against AhR and control sequences (non-silencing and EGFP) were purchased from Open Biosystems, based on pGIPZ constructs that conferred resistance to puromycin and GFP positivity (through an IRES). shRNA lentiviral constructs were packaged and produced by transfecting 293T packaging cells with control or AhR shRNA and packaging vectors. 3 days post transfection, lentiviral particles were harvested from the 293T cells. Primary keratinocytes were then transduced with the shRNA lentivirus using polybrene and spin transduction as described in materials and methods. After 48h incubation, GFP expression had reached its maximum (as shown in Figure 4.8) and keratinocytes were put into selection media (complete epifluorescence containing 1 µg/ml puromycin) for 5 days. After 5 days selection, cells were either lysed for Western blotting or seeded to form epidermal equivalents.

Figure 4.8 shows images taken by fluorescence microscopy of primary keratinocytes 48h after transduction. Images show GFP and bright field images overlaid to show the number of cells present and the transfection efficiency for each construct. Levels of GFP expression varied greatly between transduced cells within construct, but even cells with faint GFP positivity appeared to express the construct to high enough levels to confer puromycin resistance. 48h post transfection, keratinocytes were put into selection media for 5 days and over this time were passaged once to ensure dead (untransduced) cells were removed from the culture. After 5 days in selection media, fluorescence was checked again and ~90% of cells were GFP positive. Once keratinocytes had reached this stage they were then seeded to form epidermal equivalents or lysed for Western blotting.

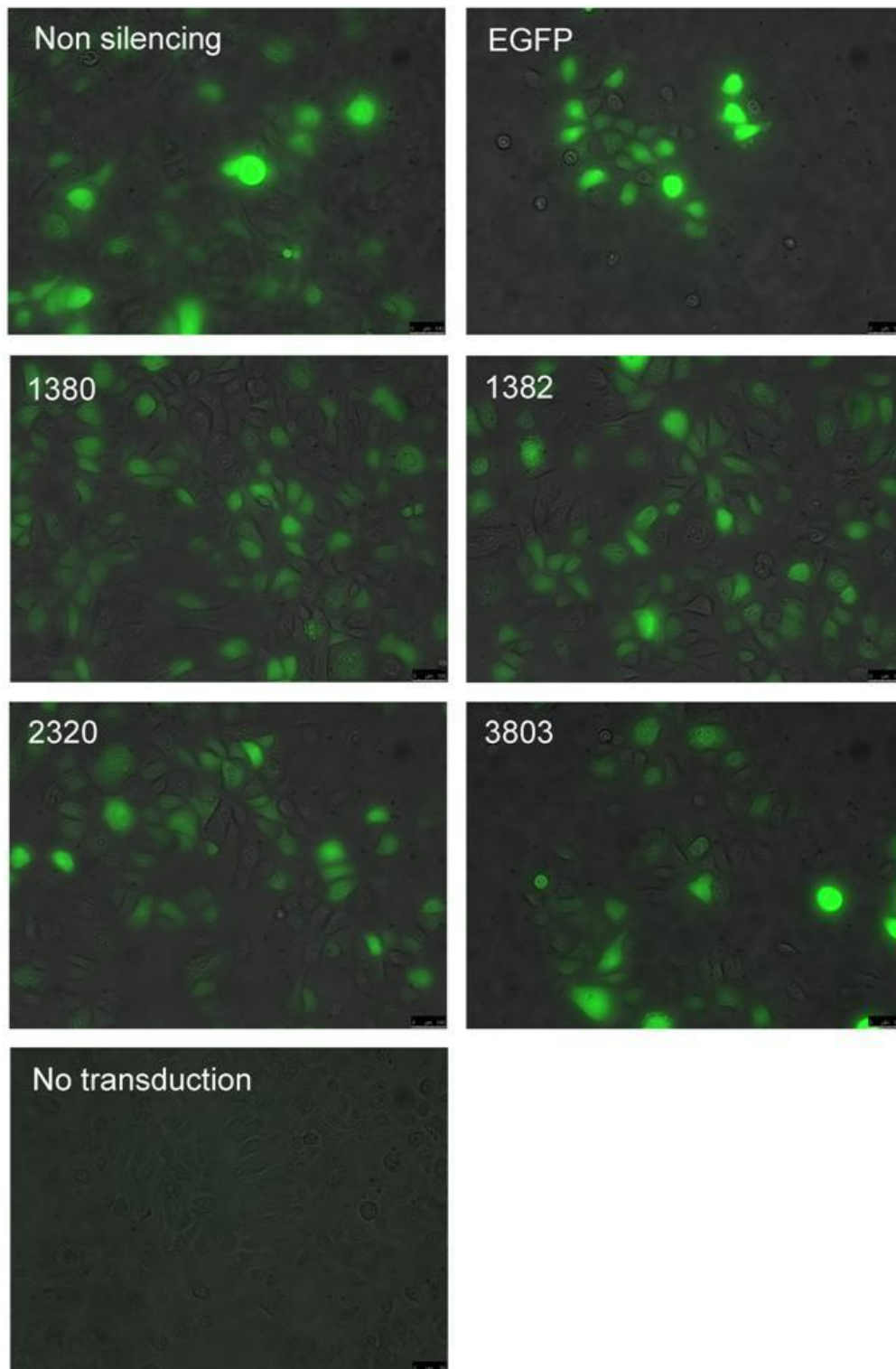


Figure 4.8. GFP expression 48h after transduction of primary keratinocytes with lentiviral shRNA. Primary keratinocyte monolayers were transduced with control (non-silencing or EGFP) or AhR shRNA (1380, 1382, 2320 or 3803) or left untransduced and cultured for 48h. Fluorescent and bright field images were taken and overlaid to show efficiency of transduction. Images are representative of 2 donors. Scale bars = 100 μ m

Figure 4.9 shows a Western blot of lysates from primary keratinocytes transduced with control or shRNA constructs against AhR. Partial knock down of AhR was achieved by constructs 2320 and 3803 compared to controls sequences, empty GFP (EGFP) and non-silencing. Construct 2320 induced the most efficient knockdown compared to control sequences. This Western blot shows the most robust knock down out of 3 donors.

Figure 4.10 shows H&E stained sections of epidermal equivalents grown from primary keratinocytes transduced with EGFP or AhR shRNA constructs 1382, 2320 or 3803. These epidermal equivalents were from the same transduction experiment and donor as those lysed for Western blotting in Figure 4.9, grown and selected in parallel. The epidermal equivalent containing EGFP (A) showed a normal phenotype with the stratum corneum showing a thick and open basket weave pattern VCL. Epidermal equivalents grown from primary keratinocytes transduced with EGFP or AhR shRNA constructs 1382 (B), 2320 (C) or 3803 showed a TCDD like phenotype of compacted stratum corneum and thinner VCL. This is consistent with the phenotype present in AhR knock out mice (Fernandez-Salguero et al., 1997). Epidermal equivalent 3803 (D) appeared to show a different phenotype, with a thinner VCL but open stratum corneum phenotype. There were visible gaps in the VCL of EGFP (A) and 3803 (D) epidermal equivalents. This suggests that long term (~3 weeks overall) culture of lentivirally transduced cells may affect homeostasis in epidermal equivalents. This could be a result of many different factors, both donor-dependent and independent but before this was studied in detail, the experiment should be repeated in cells from at least one more donor. TCDD-like phenotypes were maximally expressed by construct 1382 and 2320, to a similar extent. As 2320 induced the most AhR knock down by Western blot (Figure 4.9) the maximal effect would be expected here. Although 1382 showed little, if any knock down by Western blot the epidermal equivalent generated from AhR shRNA (1382) keratinocytes showed a more compact stratum corneum than 2320. The increase in presumed knock down (that must have been present to cause the phenotypic changes) could have been caused by the increased amount of time that epidermal equivalents were cultured for, as shown in the protocol flow diagram (Figure 2.2) in materials and methods. Keratinocytes were lysed for Western blotting on the day that other cells were seeded for epidermal equivalent culture, giving epidermal equivalents an extra 12 days to express shRNA and induce AhR knock down. This could exacerbate the knock down seen from the Western blot. The increased compaction in 1382 epidermal equivalents

as opposed to 2320 could be the result of differing construct sequence, but as these epidermal equivalents are only an example of one donor and experiment, they need to be repeated before conclusions are drawn. The 1380 construct epidermal equivalent became infected during epidermal equivalent culture and is therefore not included in Figure 4.10. Fortunately, no AhR knock down was achieved by this construct in Western blot, so we were not expecting to see any knock down in the epidermal equivalent.

Epidermal equivalents expressing siRNA or shRNA knock down of AhR both show compacted stratum corneum and thinner VCL (the TCDD-like phenotype, Figure 4.1). Even though both sets of epidermal equivalents only represent one donor each, this would suggest that the TCDD-like phenotype and therefore chloracne, could be linked to the lack of AhR caused by activation dependent degradation.

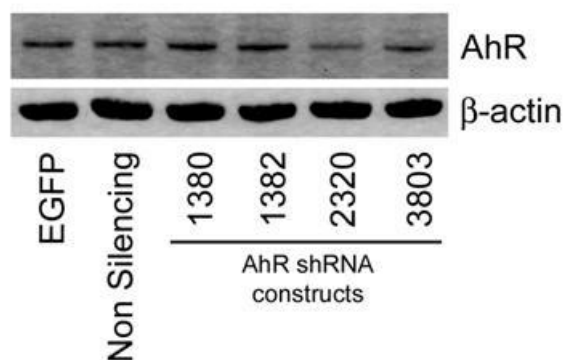


Figure 4.9. AhR is knocked down by shRNA in monolayer primary keratinocytes. Primary keratinocytes were transduced with lentiviral shRNA control sequences (EGFP or non silencing), or targeting AhR (4 constructs: 1380, 1382, 2320 or 3803). Cells were selected for 5 days with puromycin and lysed. Western blotting was performed and probed with anti-AhR and anti- β -actin antibodies. Western blot shows clearest blot out of 3 donors

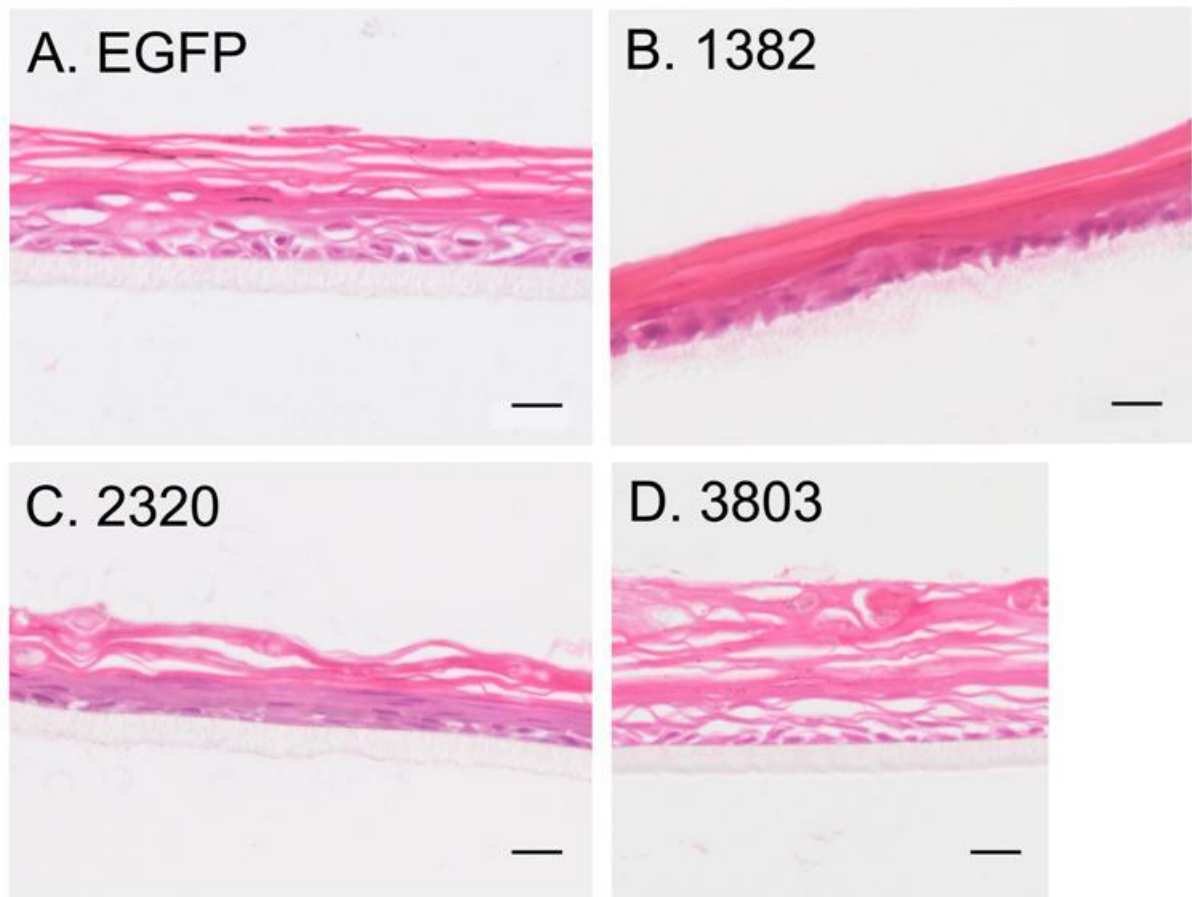


Figure 4.10. AhR knock down by shRNA induces a TCDD-like phenotype. Primary keratinocytes were transduced with lentiviral shRNA with no targeting sequence (A. EGFP) or targeting AhR (B 1382, C 2320, D 3803). Transduced keratinocytes were seeded into epidermal equivalents and cultured 12 days. Samples were harvested, fixed and paraffin embedded and H&E staining performed. Scale bar = 20 μ m. Images show 1 set of epidermal equivalents from 1 donor.

Throughout the development of these protocols, we observed that if cells that had expressed a high percentage of GFP positivity after 5 days selection were then grown in normal medium, the percentage of GFP positive cells would not propagate itself and would decrease. This is a well known but little reported phenomenon and is thought to be caused by epigenetic modification by the cell itself to “turn off” the shRNA construct and therefore the GFP. To avoid this and keep the GFP population high, cells must be put under constant (or regular) selection pressure to keep the shRNA expressed as a method of survival. The epidermal equivalents were carried out before this problem was observed and solved, so epidermal equivalents were not cultured in selection media. This may be responsible for the lack of GFP positivity present in cells of the VCL in shRNA epidermal equivalents.

Figure 4.11 shows sections from paraffin embedded shRNA epidermal equivalents that were stained with topro-3 as a nuclear marker and imaged at mid z section by confocal microscopy. GFP positive cells were only present in the stratum corneum. This could have been caused by the loss of shRNA expression when cultured out of selection medium and suggests that shRNA is not longer being transcribed by the cell. This would not account for the visible TCDD-like effects of AhR knock down in the epidermal equivalents (Figure 4.10), although due to time constraints, AhR staining was not carried out on shRNA epidermal equivalents, so we cannot make any conclusions about the efficiency or persistence of knock down in the model. In subsequent experiments using lentiviral mediated shRNA transduction and production of epidermal equivalents our group has gone on to use selection media for the complete culture time, and in future work, shRNA epidermal equivalents would be stained for AhR by IHC to measure the levels of AhR knock down and any effects of lentiviral shRNA transduction on AhR localisation in the cell or in the epidermal equivalent.

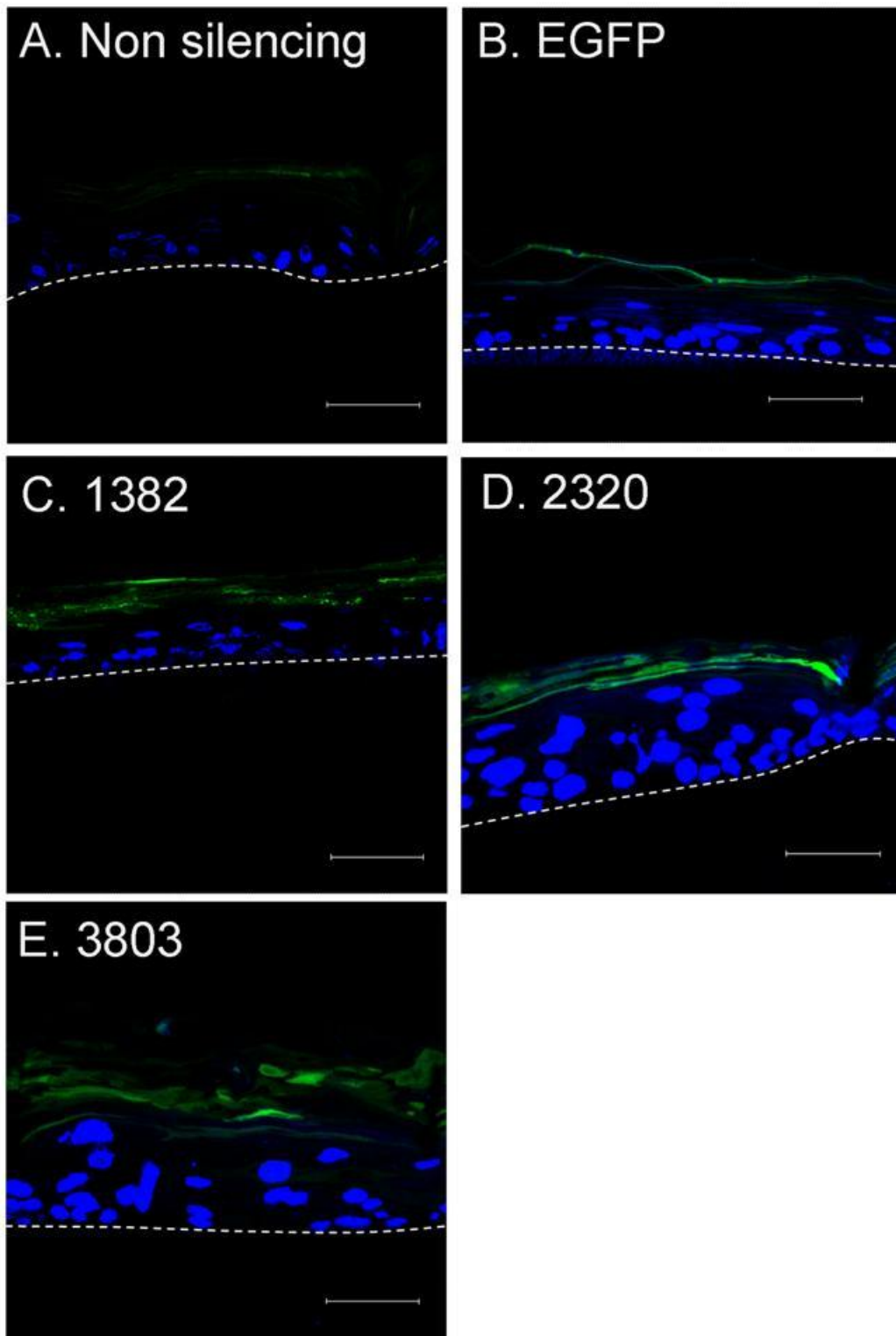


Figure 4.11. GFP expression in epidermal equivalents cultured with shRNA transduced keratinocytes. Primary keratinocytes were transduced with shRNA as indicated and cultures in puromycin selection medium for 5 days. Keratinocytes were seeded into epidermal equivalents and cultured for 12 days. Samples were fixed in 4% PF and paraffin embedded. GFP was expressed in the cells and nuclei were stained with topro-3 (blue). Images were captured by confocal microscopy, at mid z section. Images are representative of 1 donor, dotted white line represents junction between basal layer and polycarbonate membrane. Scale bars = 50µm.

4.4 Discussion

4.4.1 Summary

During this project we aimed to investigate the effects of AhR activation in a physiologically relevant human skin model. In this chapter epidermal equivalents were produced using normal human keratinocytes to investigate the effects of AhR activation on phenotype, cell differentiation and death, by using AhR ligands with distinct binding affinities and AhR characteristics (chapter 3). Our aim was to investigate differential effects of AhR ligands with distinct AhR binding affinities and potencies and with a view to identify potential biomarkers for AhR induced human toxicity.

The results reported in this chapter showed that TCDD induced degradation of AhR in an epidermal equivalent model treated for 7 days, whereas β -NF treatment induced higher levels of AhR (compared to vehicle), presumably after recovery from β -NF-dependent AhR degradation (Figure 4.6). TCDD treatment induced chloracneform effects in epidermal equivalents (Figure 4.1); thinner VCL and thickened and compacted stratum corneum as previously reported in human chloracne samples (Hambrick, 1957; Pastor et al., 2002). Neither β -NF nor ITE induced a thinner VCL (Figure 4.2), although both β -NF and ITE treatment appeared to cause slight compaction of the stratum corneum. TCDD, β -NF and ITE all induced parakeratosis in the stratum corneum, which is also characteristic of chloracne. Parakeratosis is a commonly observed effect of dysregulated homeostasis in epidermal models and disease (Geusau et al., 2005; Hambrick, 1957) and although consistent with TCDD-induced pathology in chloracne, is not a specific biomarker of TCDD-induced toxicity. Early differentiation was induced in our model by TCDD, confirming reports of this in the literature (Du et al., 2006a; Loertscher et al., 2002; Osborne and Greenlee, 1985). β -NF and ITE induced similar effects on filaggrin and involucrin but to a lesser extent (Figure 4.3). TGM-1 was dysregulated by TCDD treatment but not β -NF or ITE, which may be a potential biomarker relevant to chloracne, which would be expected to result in downstream effects on protein cross linking during terminal differentiation, which includes direct regulation of involucrin activity (Eckert et al., 2005; Yaffe et al., 1993). This suggested that TCDD-induced early onset of terminal differentiation may be a contributing factor to the decreased VCL and may account at least in part for the pathological features observed in chloracne - specifically within vellus follicles and comedone epithelial linings. We showed that the thinner VCL was not caused by caspase-3 dependent cell

death induced by TCDD treatment (Figure 4.4)(Loertscher et al., 2001a), but another form of cell death still may contribute to this phenotype and is investigated in the following chapter. We also showed 2 sets of preliminary data showing that knock down by 2 different methods (siRNA and shRNA) induced a TCDD-like phenotype. This supports the hypothesis that the effects of AhR activation are AhR degradation dependent, and corresponds with AhR knock out mice exhibiting chloracne like lesions of the skin (Fernandez-Salguero et al., 1997).

4.4.1.1 AhR activation

AhR activation is reported to increase as cells differentiate in the VCL (Du et al., 2006a; Harris et al., 2002a; Ray and Swanson, 2003). Ray and Swanson reported that AhR protein levels increased (by Western blot) as cells differentiated (Ray and Swanson, 2003), but Du et al. showed no increase at days 6 and 8 of AhR in vehicle treated cells (Du et al., 2006a). AhR localisation was also reported to be affected by cell confluency (Figure 3.6 and (Ikuta et al., 2004; Sadek and Allen-Hoffmann, 1994a)). We looked at AhR levels and localisation in the epidermal equivalent model by IHC (Figure 4.6). AhR expression did not appear to vary through the layers of the VCL. As described in section 1.1.2, the AhR activation can be modulated by a number of factors including expression of AhRR, so the increased activity of AhR reported in differentiating keratinocytes may be caused by increased levels of potential activity of the AhR, not necessarily increased AhR expression. As described in section 1.1.2, AhR activity can be affected by factors other than AhR expression, such as expression of the AhR repressor protein. When we looked at AhR localisation in the epidermal equivalent, AhR was predominantly nuclear. This opposes our observations in monolayer culture, that confluent cells show a predominant cytoplasmic localisation of the AhR (Figure 3.6 Figure 3.7) suggesting that extrapolation from monolayer to epidermal equivalent culture is not as straight forward as previously thought; there may be another mechanism of ligand-independent AhR activation that we are not aware of that has been activated during epidermal equivalent culture. Rather surprisingly, there is little reported IHC staining for AhR in normal tissue samples in the literature and because of the variability of tissues studied (eg the liver has far higher exposure to xenobiotics) and culture or treatment conditions used, it is difficult to compare the data directly to ours. The antibody used was optimised by testing fixation techniques and concentrations and the same fixation method and conditions were used for both monolayer and epidermal

equivalent studies, and even though nuclear AhR localisation may not have been expected, it is possible that the AhR is nuclear in this model, as described throughout this thesis, nuclear translocation of AhR can occur ligand-independently. The staining also decreased in response to TCDD treatment as expected. After TCDD induced AhR activation, nuclear AhR levels decreased, leaving AhR staining around the nuclear membrane and in the cytoplasm (cytoplasmic levels did not appear to change between vehicle and TCDD treated samples)(Figure 4.6). Thus, as expected TCDD induced AhR degradation. Directly contradicting the effects of TCDD, β -NF appeared to *induce* nuclear and cytoplasmic expression of the AhR. Reports in the literature on primary rat hepatocytes have shown that β -NF induced down-regulation of AhR at day 1 but by day 4 AhR levels had recovered to levels ~2 fold higher than basal levels, and the same observation was made in chronically TCDD treated rats (Franc et al., 2001; Sloop and Lucier, 1987).

Considering these papers, we can hypothesise that β -NF caused decreased levels of AhR at shorter time points, but because of the fast metabolism of β -NF by CYP1A1 (Berghard et al., 1992), AhR had recovered by ~48h to a higher level. Increased AhR was reported after both acute (Franc et al., 2001) and chronic (Sloop and Lucier, 1987; Tang et al., 2008) dioxin treatment of rats *in vivo*, but it would be interesting to define the time responses of AhR degradation and recovery in epidermal equivalents by all TCDD, β -NF and ITE AhR-agonists; Previously this phenomenon has only been reported *in vivo* and with dioxins. As these data are only representative of one donor, they should be repeated to enable robust conclusions to be drawn.

In this chapter, we have considered that the effects of β -NF in epidermal equivalents may be exacerbated because of the possibility that metabolism was impaired in this model. However the recovery of AhR levels shown here suggests that CYP1A1 metabolism is active. As high-residency is one of the main characteristics hypothesised to be required for a chloracneagen, it would also be interesting to see the correlation of prolonged β -NF and ITE AhR-activation on the epidermal equivalent phenotype. Berghard et al. showed that transient AhR activation by β -NF in primary human keratinocytes was increased by the addition of CYP1A1 inhibitor 1-ethynylpyrene. To increase residency of ligands, activity of the cytochrome P450s must be inhibited because of the ligand-independent induction of their own metabolism through the AhR.

4.4.1.2 TCDD-induced phenotype in the epidermal equivalent model

Some of the defining characteristics of the chloracne phenotype are the decrease in viable cell layer thickness and compaction of the stratum corneum within the follicle. (Figure 1.8) (Hambrick, 1957; Pastor et al., 2002). This causes development of the follicular plug and leads to comedone formation. The TCDD phenotype observed in epidermal equivalents, thinner viable cell layer (specific to TCDD treatment, Figure 4.2 and (Geusau et al., 2005; Loertscher et al., 2001b)) and thickened and compacted stratum corneum, showed significant similarities to chloracne (Figure 4.1) and was TCDD-specific; neither β -NF nor ITE induced a thinner VCL. Cell death and differentiation are likely causes of this phenotype, so were investigated by IHC. No up-regulation of active caspase-3 or cleaved lamin A was present in TCDD, β -NF or ITE treated samples, suggesting AhR activation does not increase apoptosis.

TCDD induced AhR activation is known to induce early onset of aberrant terminal differentiation as shown in Figure 4.3 and the literature (Du et al., 2006a; Geusau et al., 2005; Loertscher et al., 2002; Loertscher et al., 2001b). An interesting link between AhR activation and increased differentiation was the TCDD-dependent induction of TGM-1 (Du et al., 2006a), which crosslinks involucrin and loricrin during terminal differentiation. Increased TGM-1 has also recently been shown to be increased in lesional chloracne skin samples (Liu et al., 2011). This direct link, as well as the recently identified presence of an XRE domain upstream of filaggrin, provide a robust link between AhR activation and decreased VCL thickness in chloracne, but it does not explain the link to the compacted stratum corneum.

Stratum corneum compaction characteristic in ichthyoses and Sjogren-Larsson syndrome. It is known to be caused a lack of lamellar lipid contents or malformation of lamellar bodies (Rizzo et al., 2010), causing a deficiency in lipids and proteases to form lipid rafts and a normal stratum corneum (Sando et al., 2003). This is investigated further in the following chapter.

4.4.2 Is the TCDD/chloracne phenotype caused by AhR knock down?

One of the main hypotheses is that ligand-dependent AhR down-regulation is a main contributing factor of the chloracne phenotype (section 1.6). Considering this, there may

be two potential outcomes of AhR knockdown; 1) blocking the phenotypic effects of TCDD (thinner VCL/compacted stratum corneum) or 2) resembling TCDD like effects. The first possibility would suggest that TCDD/chloracne like effects were caused by transcriptional up-regulation of AhR regulated proteins, the second would suggest that TCDD like effects were caused by lack of AhR due to activation-dependent down-regulation of AhR. As shown in Figure 4.7 and Figure 4.10, AhR knock down in epidermal equivalents resulted in a phenotype that resembled TCDD treated epidermal equivalents, and AhR null mice (Fernandez-Salguero et al., 1997) suggesting that the effects were caused by lack of AhR, resulting from persistent TCDD treatment, or intervention by siRNA or shRNA.

The AhR pathway was modulated with siRNA or shRNA targeting the AhR. Using siRNA transfected keratinocytes (Figure 4.7), Western blots showed efficient knockdown of AhR with construct 6 at 24h but levels of AhR had recovered well at 48h. Epidermal equivalents formed with siRNA (construct 6) transfected keratinocytes showed a partial TCDD-like phenotype in vehicle treated samples which when treated with TCDD, was exacerbated further. This suggests that AhR knock down alone contributes to the TCDD-like phenotype, but as shown by Western blot (Figure 4.7 A), siRNA does not persist in dividing keratinocytes. In epidermal equivalents, proliferation is tightly regulated (as in human skin). Thus keratinocytes generally proliferate only in the basal layer, becoming transit amplifying cells in suprabasal levels, which are post mitotic keratinocytes that enter a program of differentiation. This is thought to increase the amount of time that siRNA persists in the cells (Mildner et al., 2006). The exacerbated effects of TCDD treatment of AhR knock down epidermal equivalents could be a result of AhR knock down not being 100% efficient. TCDD would activate and degrade the remaining AhR, causing an epidermal equivalent with a hypothetical 100% knock down. To support these preliminary results, AhR knock down by shRNA also induced a TCDD/chloracne phenotype. Even though both sets of data are preliminary, taken together it strongly suggests that AhR down-regulation is responsible for TCDD like effects.

5 Differential effects of AhR activation on autophagy

5.1 Introduction

Autophagy represents the major 'lysosomal' mediated process for targeting, sequestering and degrading cellular material (including whole organelles) that are damaged or no longer required by the cell.

As a catabolic process autophagy principally provides energy and recycled cellular material for cells to continue with their normal cellular processes (Settembre and Ballabio, 2011). It is primarily a cell survival process but can also cause cell death and is basally active in all cells. Because of its function in degradation of damaged proteins and organelles, autophagy stops persistence of any mutated or damaged cells and is therefore an important mechanism in inhibiting disease. This means that aberrant autophagy has recently been implemented in many disease pathways, including neurodegenerative diseases, cystic fibrosis and melanoma (Armstrong et al., 2011; Luciani et al., 2010; Nixon et al., 2008). The autophagic process is described in more detail in section 1.5.

Autophagy involves the formation of double membraned autophagosomes which sequester proteins or organelles for degradation by the lysosomes (Eskelinen, 2005; Longatti and Tooze, 2009). Proteins are first targeted for degradation by ubiquitination. p62 (the "cargo receptor") then binds to the ubiquitinated motif on the protein/organelle and by also binding to LC3 II (with which it colocalises) brings the proteins/organelle together with the autophagosome for encapsulation (Itakura and Mizushima, 2011; Kraft et al., 2010). The autophagosome fuses with the lysosome, which contains a cocktail of proteases to degrade the cellular material (Settembre et al., 2011).

This is not a static process; autophagic flux is the term given to the dynamic increase and degradation of autophagosome formation causing changes in the rate of LC3 I to II conversion and p62 degradation (Huang et al., 2010; Shvets and Elazar, 2009). As described in section 5.2.5 autophagy can become blocked. This can cause an accumulation of LC3 that may incorrectly suggest increased autophagy. Because of this, active autophagy cannot be confirmed using a single assay at a single time point. Many methods of following "active" autophagy have now been characterised, these include: measuring LC3 I and II expression by Western blot or IHC (Mizushima and

Yoshimori, 2007), measuring degradation of p62 by Western blot or IHC, following conversion of LC3 I to II during recruitment to the autophagosome by using an RFP-GFP-LC3 construct, and transmission EM which is the gold standard measure of active autophagy, showing characteristic structures of autophagy (primarily the double membrane of the autophagosome) in the cytoplasm. Methods of confirming active autophagy are reviewed here (Klionsky et al., 2008; Tasdemir et al., 2008).

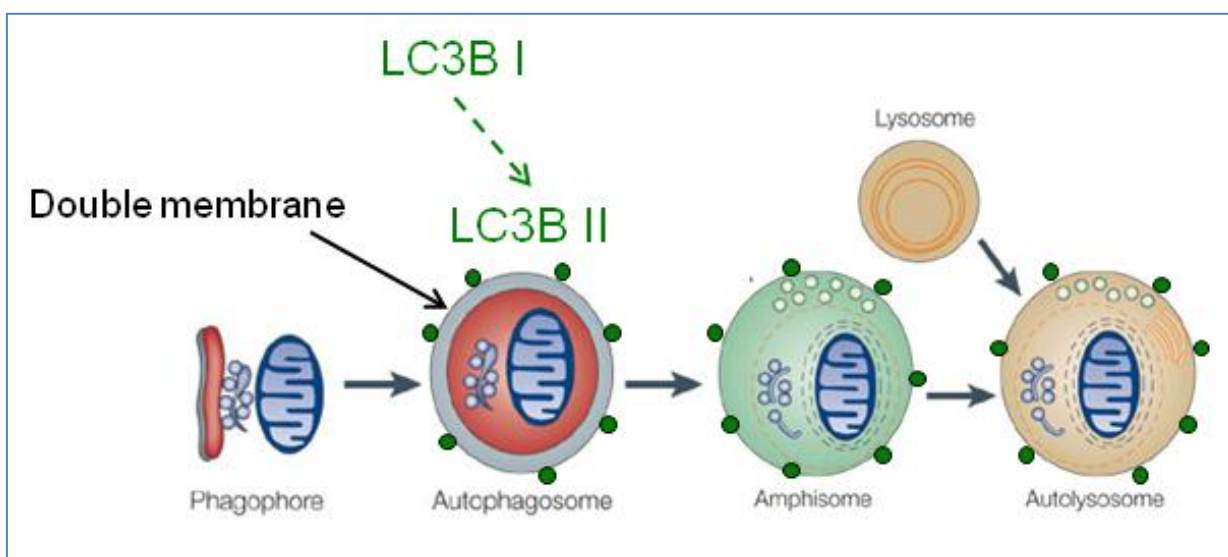


Figure 5.1. Formation of the autolysosome and recruitment of LC3 II to the membrane of the autophagosome. Formation of the degradative autolysosome involves 2 steps to note: 1) the conversion of LC3 I to II and recruitment to the autophagosome membrane; 2) fusion of the lysosome to the autophagosome forming the degradative autolysosome. Image modified from (Kroemer and Jaattela).

The main methods used in this chapter are measuring levels of LC3 I and II induction, p62 degradation, and accumulation of LC3 and p62 after autophagic block by bafilomycin A1 (by Western blot). Transmission EM is also used to show characteristic signs of active autophagy and novel observations in epidermal equivalents treated with AhR agonists.

Microtubule-associated protein light chain 3 (LC3) is a protein involved in autophagosome formation. During active autophagy, cytoplasmic LC3 I is recruited to the autophagosome membrane and converted to LC3 II through post translational modification by conjugation with phosphatidylethanolamine, a ubiquitin mediated event (Kabeya et al., 2000; Kabeya et al., 2004). This can be used as a marker for autophagy by Western blot and immunochemistry. Because LC3 II is highly hydrophobic, it migrates faster on Western blots (despite its slightly larger molecular weight),

distinguishing the 2 forms at 16kDa (LC3 I) and 14kDa (LC3 II). Increased levels of LC3 II are taken to indicate increased autophagy. An induction in both can demonstrate either transcriptional up-regulation or a block in autophagy, causing an accumulation of LC3 I and II (Mizushima and Yoshimori, 2007). To distinguish between these very different outcomes, LC3 II up-regulation can be correlated with p62, the “cargo receptor”, which is also degraded by autophagy (sections 5.2.3 and 5.2.5). During active autophagy p62 expression is low, however should LC3 up-regulation be caused by autophagic block, p62 is no longer degraded and hence accumulation is indicated by increased expression (Yoon et al., 2010).

5.2 Results

5.2.1 The effects of AhR activation on LC3 II induction

This sections introduces the novel concept of AhR activation inducing autophagy (by LC3 induction and p62 degradation), which has not previously been reported. The antibodies used in this chapter for Western blotting were previously optimised by Jane Armstrong based on the manufacturers recommendations and complete blots are presented in Appendix Z to show the justification of selected bands for p62 and LC3 antibodies.

To test whether AhR activation increased autophagy in primary keratinocytes, we treated cells grown in monolayer with vehicle, TCDD, β -NF or ITE for up to 8 days as described in materials and methods. As shown in chapter 3, doses of 1-10nM TCDD were used in AhR activation assays. This was decided based on levels of AhR activation potential, solubility and comparisons in the literature. 0.5nM TCDD was not utilised because although it showed strong transcriptional activation by luciferase assay (Figure 3.2) it showed no increased AhR activation by Western blot (Figure 3.9). To see any correlation between this high transcriptional activation (that only induces low AhR activation by AhR degradation and CYP1A1 induction) and LC3 induction, the blot used in Figure 3.9 was re-probed for LC3. Figure 5.2 shows that interestingly, 0.5nM TCDD induced the highest levels of LC3 II activation, compared with treatment up to 5nM TCDD. This occurred at days 6 and 8, the later time points. At day 2 only very low levels of LC3 II induction were evident (Figure 5.2). The pattern of transcriptional induction in Figure 3.2 showed a high activation at 0.5nM TCDD that was roughly equal to 5nM TCDD but less than with 10nM TCDD, the lowest activation was at 1nM TCDD. This

transcriptional activation did not correlate with LC3 II induction, because 5nM TCDD did not induce high levels of LC3 II or equal 0.5nM TCDD. This pattern was observed in only one donor, although results from other donors followed similar patterns.

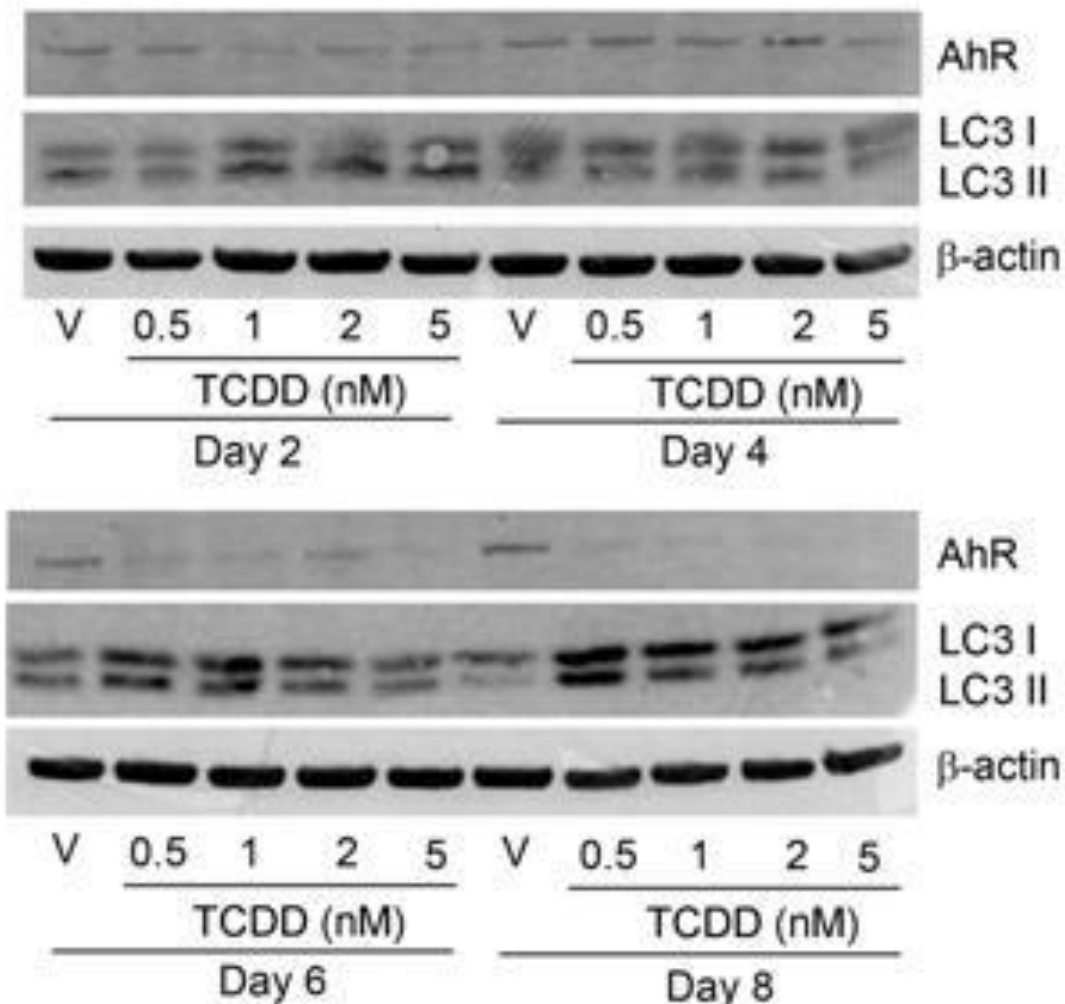


Figure 5.2. LC3 II is induced by TCDD treatment in primary human keratinocytes. Primary keratinocytes were treated with vehicle or concentrations of TCDD as indicated. Samples were lysed and Western blotting performed. The Western blot is representative of data from one donor with these specific doses, but LC3 levels were observed in 3 separate donors at different concentrations.

5.2.2 The effects of AhR activation on p62 degradation

The effect of TCDD- or ITE-induced AhR activation on p62 (combined with the effects observed on LC3 II) provides evidence that AhR activation results in autophagy (Figure 5.3 left and right columns). However, the effect of β -NF-induced AhR activation on p62 (Figure 5.3 middle column) indicates the blocking of autophagy. These data demonstrate the importance of using multiple readouts of autophagy in one system. Taking into consideration both the LC3 II induction results and p62 degradation results,

it shows that TCDD and ITE induced levels of LC3 II and induced degradation of p62, suggesting that TCDD and ITE induced autophagy in keratinocytes. β -NF induced levels of LC3 II but also induced higher levels of p62, suggesting these results indicate that the proteins are accumulating due to blocked autophagy and autophagic degradation.

5.2.3 The correlation of p62 and LC3 II

As stated above, autophagy is a complex process to measure by static assays. Induction of LC3 II may not relate to increased active autophagy, but could indicate autophagic block. p62, a protein involved in and degraded by autophagy, can be used as a secondary marker to LC3 II to indicate active autophagic degradation. As explained at the start of the chapter, I ran Western blots with lysates from primary keratinocytes treated with TCDD, β -NF or ITE. Blots were probed for both LC3 II and p62 and bands were measured by densitometry; densitometry for LC3 II represents 3 donors, while p62 only represents 1-3 donors because of time constraints, statistical analysis was therefore not carried out. Images of bands from Western blots presented together for each treatment are from the same blot.

5.2.3.1 TCDD

As shown in Figure 5.3 and Figure 5.4, TCDD induced dose dependent p62 degradation from day 2 to day 8 (Appendix J and Appendix K show TCDD-induced degradation occurred at all time points assayed). Figure 5.4 shows that TCDD induced LC3 II levels maximally at day 8 (Appendix J shows that LC3 II was not induced by TCDD at day 4 but LC3 II levels were induced by TCDD at day 6 - Appendix K).

The complete time course data in Appendix K shows rough correlation of LC3 II induction and p62 degradation. This is consistent with the hypothesis that TCDD activates autophagy, increasing LC3 II levels as numbers of autophagosomes increase, leading to an autophagy-dependent degradation of p62.

p62 and AhR degradation correlated well with each other as well as with increased TCDD concentration. This is an interesting observation because as discussed by Kraft et al., degradation of material by the 26s proteasome (like AhR (Song and Pollenz, 2002)) is closely linked to autophagic degradation, the mechanism of p62 degradation (Jaakkola and Pursiheimo, 2009; Kraft et al., 2010).

In densitometry from pooled donors, TCDD reliably caused degradation of p62, although sample size was small. LC3 II was increased at days 6 and 8 most effectively by 0.5nM TCDD (Figure 5.4 and Appendix K). Two-way ANOVA was performed to compare vehicle to TCDD and duration of incubation on LC3 II expression. The data were not significant, but the overall results (decreased p62 and increased LC3 II) were consistent between donors but time and dose responses varied, causing pooled data to mask the individual effects and patterns of flux that was caused by autophagy (Huang et al., 2010).

This would suggest that there is another variable affecting the time responses and autophagic flux seen at each time point, for example the time that the cells have spent in cell culture, the age of the donor (affecting levels of proliferation), or the cell cycle (TCDD increased the number of cells in G1/G0 phase (Loertscher et al., 2001a; Ray and Swanson, 2003)).

Despite only showing preliminary p62 data, taken together with LC3 II this suggests convincingly that TCDD induces active autophagy.

5.2.3.2 β -NF

Figure 5.3 and Figure 5.4 shows the effect of β -NF treatment on p62 and LC3 II expression in primary keratinocytes at 2 and 8 days. As with TCDD, the number of donor replicates for p62 is between 1 and 3 donors and therefore no statistical analysis was carried out. 15 μ M β -NF induced LC3 II at days 2 and 4 (Figure 5.3 and Appendix L), but p62 levels were also increased at these time points. Increased LC3 II and p62 levels did not correlate with AhR degradation.

Densitometry pooled from 3 donors (Figure 5.3, Figure 5.4, Appendix L and Appendix M B.ii.) showed a dose dependent increase in LC3 II at days 2, 4 and 6 and an increase at day 8, suggesting that β -NF induced active autophagy. However when compared to the increase in p62 at days 2, 4 and slightly at days 6, this suggests accumulation of both LC3 II and p62 resulting from blocked autophagy. This represents data from only 1-3 donors, therefore further experiments are required to confirm this.

LC3 II induction didn't correlate well with AhR degradation; at day 6, AhR appeared degraded maximally but only slight LC3 II was induced by 15 μ M β -NF. At days 2 and 8, high levels of LC3 II were induced by one dose of β -NF and not the other (15 μ M β NF induced LC3 at day 2, 3 μ M β -NF induced LC3 at day 8) and AhR degradation did not correlate with up regulated LC3 II.

Two-way ANOVA was performed to compare vehicle to β -NF treated cells at each time point. β -NF induced a significant increase in LC3 II across time points ($P < 0.004$) and duration of incubation also had a significant effect on LC3 II expression in β -NF treated samples ($P < 0.04$). The interaction between β -NF and duration of incubation were not significant.

5.2.3.3 ITE

Figure 5.3 and Figure 5.4 shows keratinocytes treated with vehicle or concentrations of ITE as indicated for 2 and 8 days (full time course is shown in Appendix N and Appendix O). As shown in β -NF treated samples, levels of increased LC3 II did not correlate completely with AhR degradation; days 4 and 6 show equal AhR degradation to day 2 but little LC3 I or II was induced.

Levels of p62 did not show much variation, although in vehicle treated samples (where levels of p62 should be relatively high), especially at days 2 and 4 (Appendix N), the basal levels of p62 were not high. Despite this, p62 degradation occurred at day 8. AhR and p62 levels did not correlate well, AhR degradation occurred at days 2, 4 and 6 with no or little effect on p62.

Figure 5.3 and Figure 5.4 shows increased LC3 II levels by ITE treatment at days 2 and 8. Appendix O shows that increased LC3 II levels occurred at day 8 only, but as previously stated, even though ITE induced LC3 II levels were consistent between donors, time and dose dependency varied. Interestingly, Appendix N and Appendix O shows ITE-independent variation in LC3 II levels in vehicle treated samples, suggesting basal autophagic flux between days (as described in (Shvets and Elazar, 2009)). Densitometry for p62 staining at days 2 and 4 is only representative of one donor, but days 6 and 8 are representative of 2 donors. Results demonstrate p62 expression was slightly decreased at days 6 and 8 with 5 μ M ITE, but the increase shown at day 4 is not convincing, this data only represents one donor and the actual increase of p62 on the blot is not high (Appendix N and Appendix O).

Two-way ANOVA was performed to compare vehicle to ITE treated cells at each time point. Duration of incubation also had a significant effect on LC3 II expression in ITE treated samples ($P < 0.04$). The interaction between β -NF and duration of incubation were not significant. Overall, the increase in LC3 II at day 8 and decrease in p62 at days 6 and 8 were convincing, suggesting that ITE induced active autophagy.

To summarise these results, all AhR agonists (TCDD, β -NF and ITE) induced LC3 II to a high level, while p62 was degraded by TCDD and ITE (day 8 only) and increased by β -NF treatment. Patterns of LC3 II induction and p62 degradation in regards to dose and time point varied across agonist and donor, but all donors showed an increase in LC3 II. Some LC3 I induction occurred too, but LC3 II measurements alone are not enough to conclude the cause, for example an increase in autophagy overall, transcriptional up-regulation or autophagic block. This will be discussed later in the chapter.

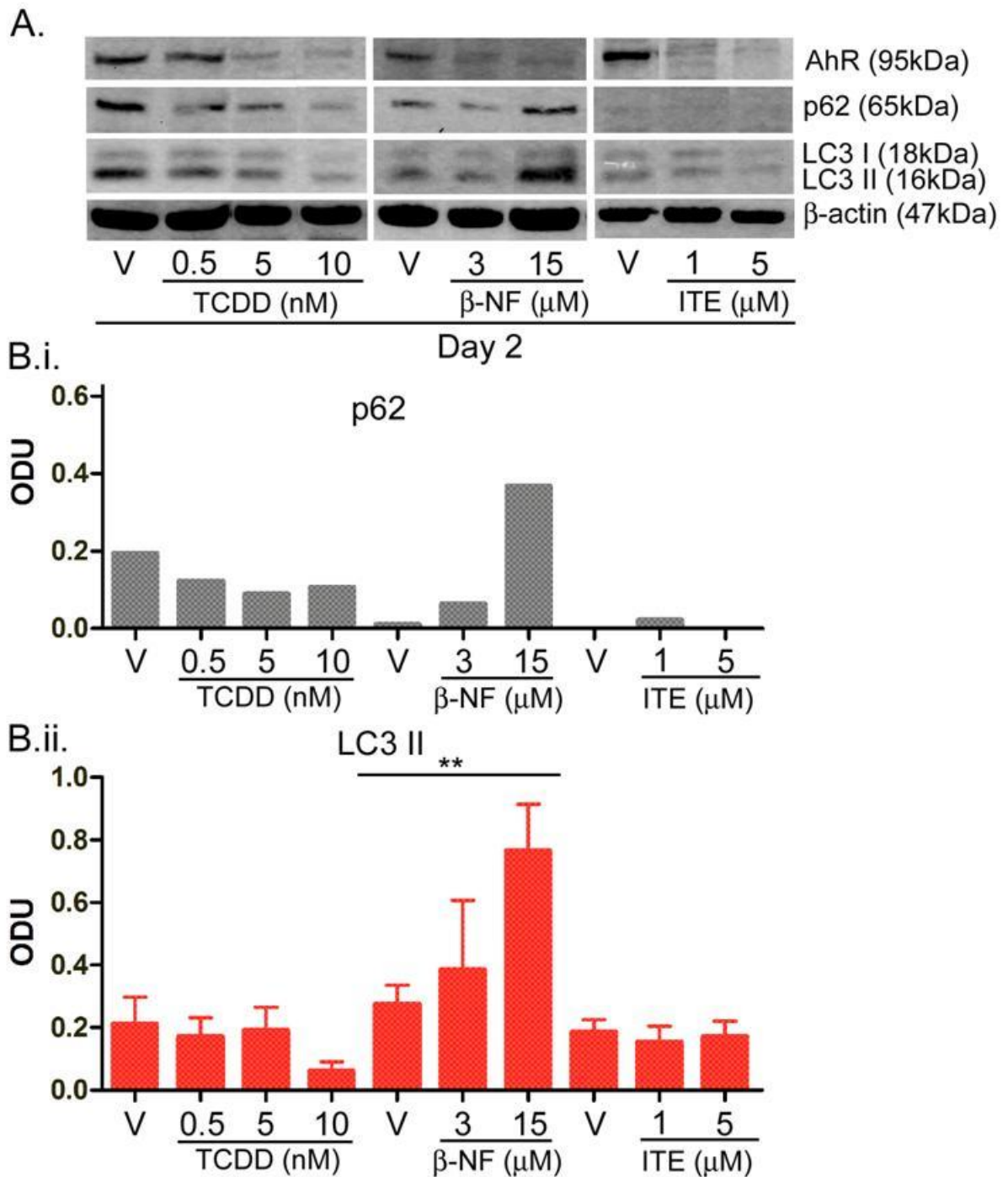


Figure 5.3. Comparison of the effects of TCDD, β -NF and ITE on p62 and LC3 II at day 2. Primary keratinocytes were treated for 2 days with vehicle or concentrations of TCDD, β -NF or ITE as indicated. Samples were lysed and Western blotting performed (**A**). Densitometry was carried out on Western blots probed for **B.i.**) anti-p62 and **B.ii.**) anti-LC3 antibodies normalised to β -actin. Statistical analysis was performed as described in Figure 5.4.

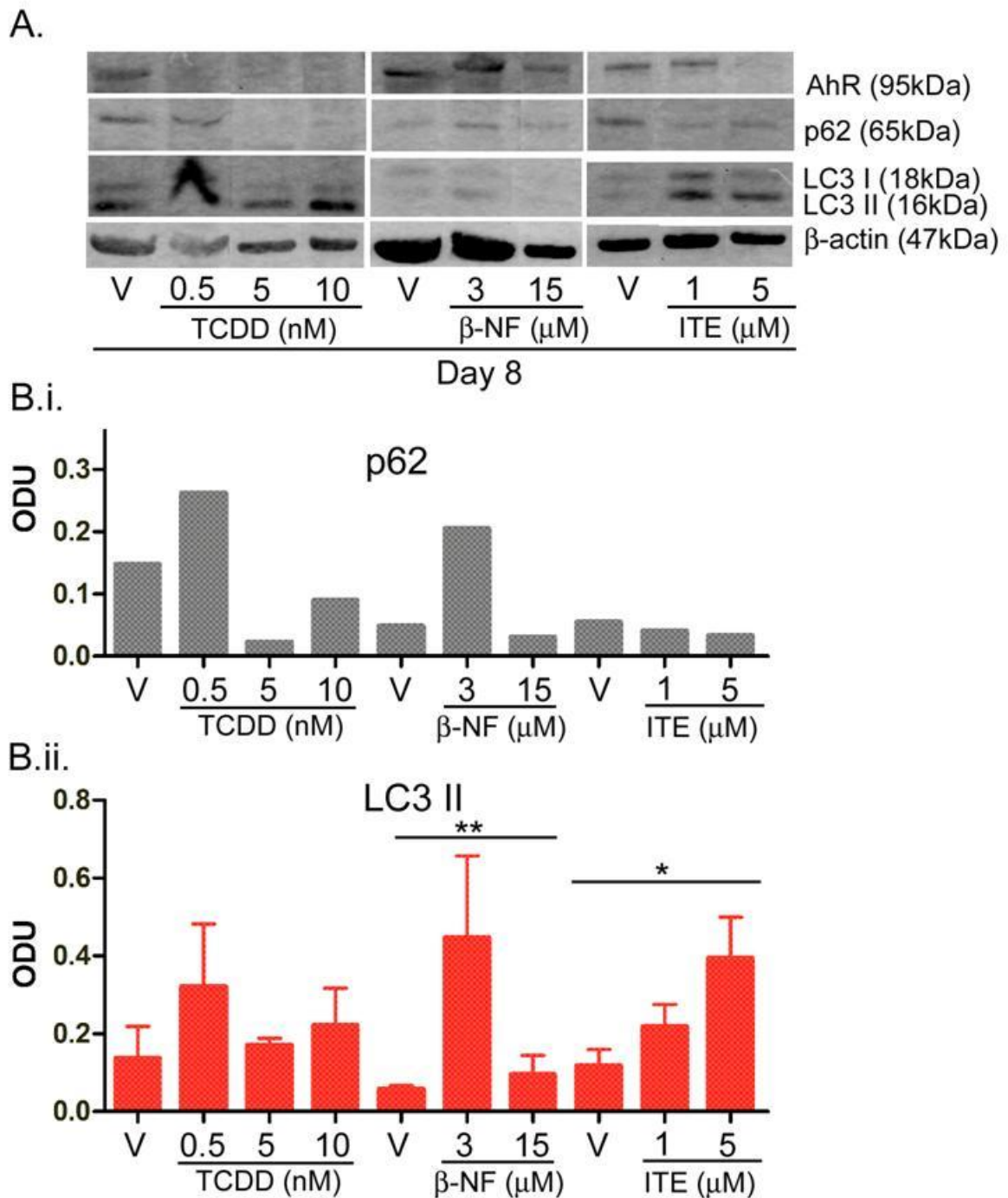


Figure 5.4. Comparison of the effects of TCDD, β-NF and ITE on p62 and LC3 II at day 8. Primary keratinocytes were treated for up to 8 days with TCDD, β-NF or ITE as indicated. Samples were lysed and Western blotting performed (**A**). Densitometry was carried out on blots probed with **B.i.)** anti-p62 and **B.ii.)** anti-LC3 antibodies normalised to β-actin. **B.i)** No STATs have been carried out on p62 due to small sample size (n = 2/3 donors days 2 and 4, n = 1/2 donors days 6 and 8). **B.ii.)** 2-way ANOVA was performed comparing vehicle to ligand at each time point, results were not significant for TCDD treated samples. β-NF and time induced significant effects (P < 0.004 and P < 0.04 respectively). ITE: Time had a significant effect, increasing LC3 II response to ITE treatment (P < 0.04). LC3 II densitometry is representative of mean ± sem from 3 donors.

5.2.4 Effects of α -NF on AhR induced autophagy

5.2.4.1 α -NF

α -NF is a partial AhR agonist and can therefore activate AhR at low concentrations and inhibit AhR activation at high concentrations, as demonstrated in the previous chapter by transcriptional activation (Figure 3.14) and CYP1A1 induction or AhR degradation (Figure 3.15 and Figure 3.16). As TCDD and ITE induced active autophagy in keratinocytes (shown in this chapter) we looked at the potential of partial agonist α -NF to induce autophagy by induction of LC3 II and degradation of p62 (Figure 5.5 and Figure 5.6). α -NF decreased levels of p62 at days 6 and 8 (Appendix P), the later time points that agonist-induced AhR effects on protein levels have been shown previously (Figure 3.15 and Figure 3.16). At days 6 and 8 α -NF also exhibited mild AhR agonistic effects on AhR degradation and CYP1A1 induction α -NF treatment resulted in slight degradation of LC3 II at days 4, 6 and 8, and day 2 was the only time point to show increased LC3 II (Appendix P). p62 was increased at days 2 and 4, but decreased at days 6 and 8. These results suggest that 10 μ M α -NF at day 2 could induce autophagic block (accumulated LC3 II and p62 caused by blocked autophagic degradation) but p62 was more consistently decreased at days 4, 6 and 8 which seems a more convincing result. Densitometry is only representative of 1 donor in Figure 5.5 and Figure 5.6, so more replicates are required to draw a solid conclusion from this.

The effects of α -NF and time on LC3 II levels were analysed by 2-way ANOVA, comparing vehicle to α -NF concentration at each time point. These results were not significant, suggesting that 5 and 10 μ M α -NF had little direct agonistic effect on the AhR compared to full AhR agonists inducing LC3 II and degrading p62 in a correlated and time dependent manner (section 5.2.4). Considering the previously shown low levels of α -NF-dependent AhR activation (Figure 3.13, Figure 3.15 and Figure 3.16) it seems reasonable to conclude that α -NF induced low levels of autophagy at days 6 and 8.

We therefore proceeded to utilise α -NF as a potential AhR antagonist to examine the AhR dependence of the TCDD, β -NF and ITE induced effects on autophagy, considering the low levels of AhR and autophagic activation induced by α -NF.

5.2.4.2 TCDD

Figure 5.5 and Figure 5.6 show primary keratinocytes treated with vehicle or concentrations of TCDD \pm α -NF for 2 and 8 days. As shown in Appendix J and Appendix K, TCDD induced levels of LC3 II at days 6 and 8 and degraded p62 at all time points. Chapter 3 showed that TCDD-induced AhR activation was inhibited consistently over time and dose (in all donors) by α -NF (Figure 3.15 and Figure 3.16). To test whether TCDD-induced LC3 II and degraded p62 were AhR dependent, the inhibitory effects of partial AhR agonist α -NF on TCDD-dependent AhR activation were thus evaluated.

At early time points (day 2), TCDD did not induce LC3 II and only induced low levels of p62 degradation (Figure 5.5). α -NF co-treatment appeared to either have no effect on or increase p62 levels. Most marked increase of p62 occurred with 10nM TCDD plus 5 or 10 μ M α -NF, but α -NF did not block TCDD-induced degradation of p62. Co-treatment with α -NF appeared to cause a decrease in LC3 II expression except at day 4 where LC3 II was increased by 10nM TCDD plus 10 μ M α -NF, equating to inhibited AhR activation (Appendix J), although these effects were small. Taking this into consideration, α -NF in combination with TCDD appeared to block autophagy at days 2 and 4.

At days 6 and 8 p62 levels appeared to be increased by co-treatment with α -NF and TCDD compared to either agent alone (Appendix K). Interestingly, co-treatment with α -NF and TCDD resulted in higher p62 levels than basal levels in vehicle treated samples. This could suggest that α -NF blocks autophagy. On the other hand, addition of α -NF appeared to block TCDD-induced increase in LC3 II protein levels. This data is confusing and as there were some signs that α -NF blocked autophagy, further studies are needed to clarify the effects of co-treatment with α -NF and TCDD on autophagy.

Two-way ANOVA was performed to compare TCDD treated cells with cells co-treated with TCDD and α -NF at each time point. In cells treated with 5nM TCDD, α -NF induced significant down-regulation of LC3 II ($P < 0.02$). The interaction between time and α -NF were not significant. Analysis was not carried out on p62 due to small sample size.

5.2.4.3 β -NF

Surprisingly, β -NF was shown to increase levels of both LC3 II and p62, indicating inhibition of autophagy. Figure 5.3 and Figure 5.4 showed that β -NF treatment induced higher levels of p62 at both early and late time points, along with an increase in LC3 II at each time point that correlated well with increased p62 (for the complete time course see Appendix L and Appendix M). In the previous chapter, I showed that α -NF inhibited β -NF-induced transcriptional activation (Figure 3.14), but α -NF exacerbated β -NF-induced AhR activation by AhR degradation and CYP1A1 induction (Figure 3.15 and Figure 3.16).

Figure 5.5 and Figure 5.6 shows that the effects of α -NF on β -NF-blocked autophagy were transient; p62 levels were variably effected at days 2 and 4, with an increase induced by α -NF at day 2 by 15 μ M β -NF. 15 μ M β -NF plus α -NF at days 2 and 4 showed down-regulation of p62, suggesting an inhibition of blocked autophagy by α -NF co-treatment, p62 levels were not decreased to basal levels (vehicle), so activation of autophagy was not the case. This did not correlate with α -NF-dependent increase in LC3 II though, at days 2 and 4 treatment with 15 μ M β -NF plus α -NF induced down-regulation of LC3 II.

These results are difficult to interpret; p62 down-regulation with α -NF/ β -NF co-treatment suggests that additional treatment with α -NF caused activated autophagy as opposed to the autophagic block induced by β -NF alone. But at the time points and dose combinations that induced p62 degradation, LC3 II levels were also decreased, which suggested inhibition of β -NF induced autophagic block, but no induced active autophagy. This raises the possibility that even though β -NF differentially blocked autophagy (as opposed to TCDD and ITE's induced autophagy), it was AhR-dependent and could be inhibited by α -NF.

At day 8 (Figure 5.6), the effects of α -NF on p62 again were varied. α -NF either increased or did not affect LC3 II, exacerbating the β -NF-dependent autophagic block. The effects of time and co-treatment with β -NF and α -NF on LC3 II levels were analysed by 2-way ANOVA, comparing ligand treated samples to α -NF co-treatment and time. Time had a significant effect on the effects of co-treatment by β -NF and α -NF (* $P < 0.02$) (Appendix L and Appendix M), consistent with the expected time points for AhR-dependent effects. These effects were varied in donors, with each donor showing

mixed effects of increased/decreased LC3 II and p62 over time. α -NF could either be inhibiting β -NF-dependent autophagic block or inducing further autophagic block, but it did not induce autophagy, which was its effect (although low) alone.

Two-way ANOVA was performed to compare β -NF treated cells with cells co-treated with β -NF and α -NF at each time point. In cells treated with 15 μ M β -NF, duration of incubation induced significant effects on LC3 II ($P < 0.02$). The interaction between time and α -NF were not significant. Analysis was not carried out on p62 due to small sample size.

5.2.4.4 ITE

Results from this chapter demonstrate that ITE induced autophagy at day 8 by increased LC3 II and decreased p62 (Figure 5.4). In the previous chapters I showed that α -NF did not block ITE-induced AhR activation, but exacerbated it, inducing further AhR degradation and CYP1A1 activation than ITE alone (Figure 3.15 and Figure 3.16).

Figure 5.5 shows that p62 was increased at day 2 (and day 4 - Appendix N) by co-treatment with ITE plus α -NF. ITE appeared to induce up-regulation of p62 alone, but the changes were on a very small scale. This suggests that the combination of ITE plus α -NF may result in a block of autophagy. LC3 II was slightly up regulated by ITE plus α -NF treatment at day 2, which would suggest blocked autophagy. Considering the increased AhR activation in chapter 3 with combined treatment of ITE and α -NF, this would suggest that induced AhR activation by combined ITE and α -NF may induce autophagy.

Figure 5.5 and Figure 5.6 shows that p62 levels were increased by combined treatment of α -NF plus ITE. This suggests decreased autophagy (and correlates with LC3 II levels), which would in turn suggest AhR inhibition, presuming AhR activation resulted in induction of autophagy. However, this would not correlate with the AhR bands, both AhR and LC3 I and II were decreased in α -NF treated samples, suggesting active AhR and decreased autophagy. p62 correlated well with LC3 II, indicating that autophagy was activated in this case. The pattern of response in the donor shown in the Western blot is strong, and exerted a definite pattern of decreased LC3 II by α -NF treatment which correlates with p62 and AhR, suggesting that this was a true pattern of response in this donor. This response varied between donors and therefore as suggested

previously, pooled densitometry does not represent the pattern of effects of treatment well. p62 and LC3 II did not correlate well, demonstrating the variability of α -NF treatment. Because of this, the pooled effects of combined α -NF and ITE on LC3 II were varied, day 8 showed induction of higher levels of LC3 II by 1 μ M ITE plus 5 μ M α -NF, but lower levels were induced by 1 μ M ITE plus 10 μ M α -NF and 5 μ M ITE plus 5/10 μ M α -NF.

Again this data is difficult to interpret, showing a combination of possible blocked autophagy and inhibited activation of autophagy. p62 levels were increased and correlated with down-regulation of LC3 II, suggesting that combined ITE and α -NF resulted in inhibition of autophagic activation during AhR activation. But p62 levels in α -NF treated samples were far higher than vehicle suggesting blocked autophagy, which as LC3 II levels were not consistently down regulated by α -NF, cannot be ruled out.

These data were analysed by 2 way ANOVA, but were not significant. As explained above, robust patterns of effects in each donor could be masked by pooling data from donors.

5.2.4.5 Summary

Figure 5.5 and Figure 5.6 show that co-treatment with TCDD and α -NF induced variable effects on autophagy, and because of increased p62, possibly induced autophagic block. β -NF induced autophagic block and that in combination with α -NF induced further AhR activity (shown by CYP1A1 induction and AhR degradation in chapter 3) exacerbating the AhR-dependent effects of β -NF and blocking autophagy further. Like β -NF, ITE-induced AhR activation was shown to be exacerbated by α -NF in chapter 3, but like TCDD, ITE-dependent AhR activation was shown in this chapter to induce active autophagy. The effect of co-treatment with ITE plus α -NF resulted in exacerbated AhR activation that possibly caused autophagic block. As indicated by β -NF compared to TCDD, AhR activation can possibly either induce or block active autophagy.

Figure 5.5 and Figure 5.6 A showed that α -NF alone induced low levels of autophagy at days 4, 6 and 8 by p62 degradation but only induced LC3 II at day 2. This increase in LC3 II correlated with induction of higher levels of p62. This suggests α -NF dependent autophagic block. If α -NF could induce autophagic block, then this may be a causative

factor of the effects of co-treatment with ligands and α -NF also inducing a possible autophagic block. It would be interesting to test the potential of α -NF on activation of autophagy further. If the autophagic block shown at day 2 in Figure 5.5 was a true result, we could hypothesise that flavone-dependent AhR activation blocked autophagy directly opposing TCDD- and ITE- dependent induction of active autophagy. Autophagic flux assays (described later in the chapter) could be used for α -NF \pm TCDD, β -NF or ITE to show resulting increased or blocked autophagy and another AhR antagonist could be utilised in LC3 induction/p62 degradation assays to confirm whether AhR-dependently blocked autophagy was flavone specific or a result of inhibition of AhR-dependent TCDD-induced autophagy.

As described at the start of the chapter, autophagy is a dynamic process that is difficult to measure by static biomarkers. These data provide a good indication of the effect that AhR agonists TCDD, β -NF and ITE have on autophagy (more so in clearly defined cut cases such as TCDD), but to define the effects of β -NF and ITE on autophagy and the mechanisms behind this, more experiments are required. I hypothesise that AhR activation by TCDD and ITE may activate autophagy and that this contributes to the phenotype observed in epidermal equivalents.

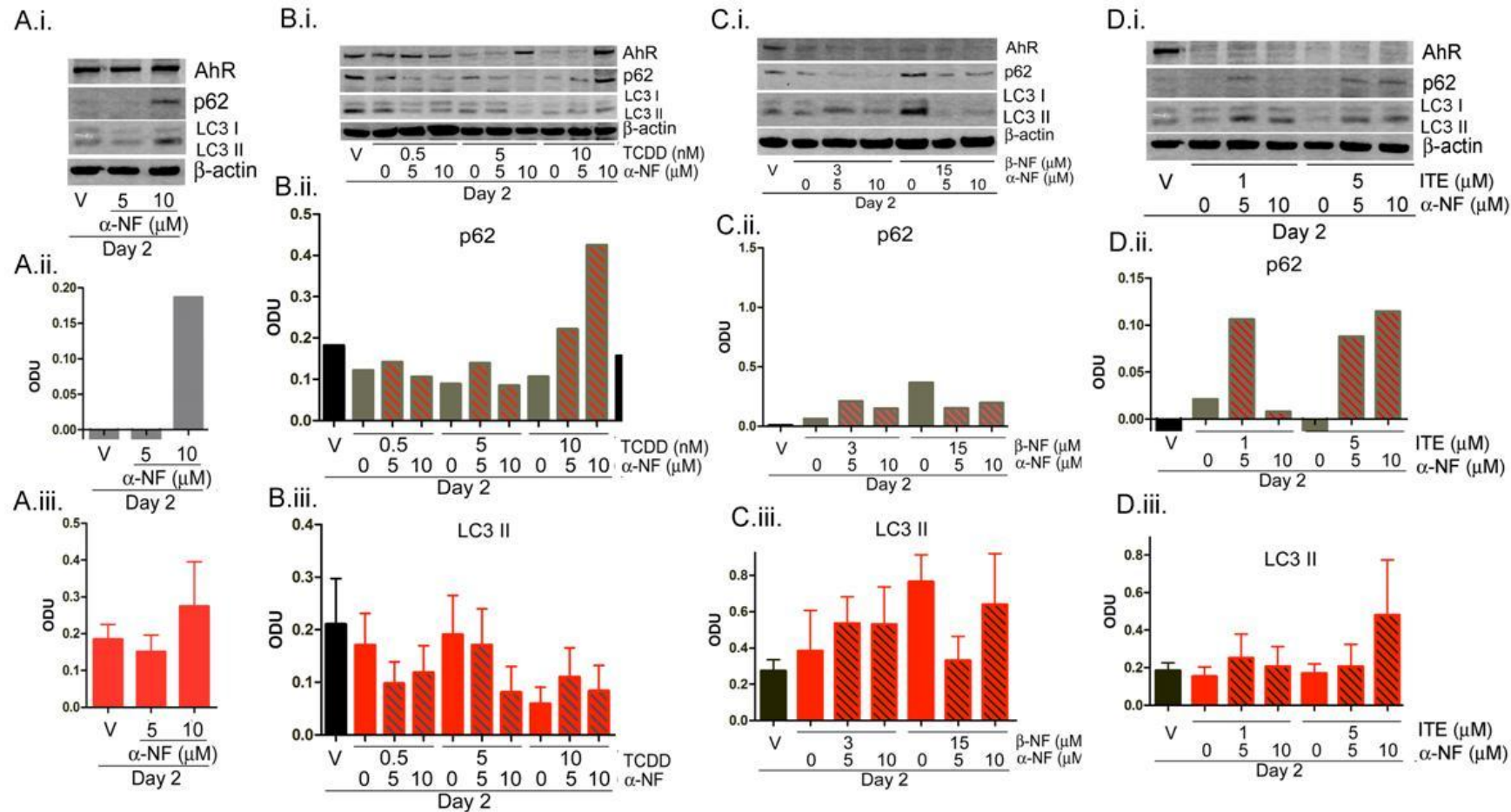


Figure 5.5. The effects of co-treatment with TCDD, β -NF or ITE plus α -NF on autophagy in primary keratinocytes. Primary keratinocytes were treated with vehicle or ligand \pm α -NF as indicated. After 2 days cells were lysed and Western blotting performed (A). Densitometry was performed on Western blots probed with B.i) p62 and B.ii) LC3 II. Black bars represent vehicle treated keratinocytes, plain bars indicating ligand alone and hatching on bars indicates co-treatment of keratinocytes with α -NF. Densitometry from LC3 II and p62 was normalised to β -actin. B.i.) Values are represented as mean ODU from 1-3 donors. No analysis was performed on p62 due to low sample size. Statistical analysis is included in Figure 5.6.

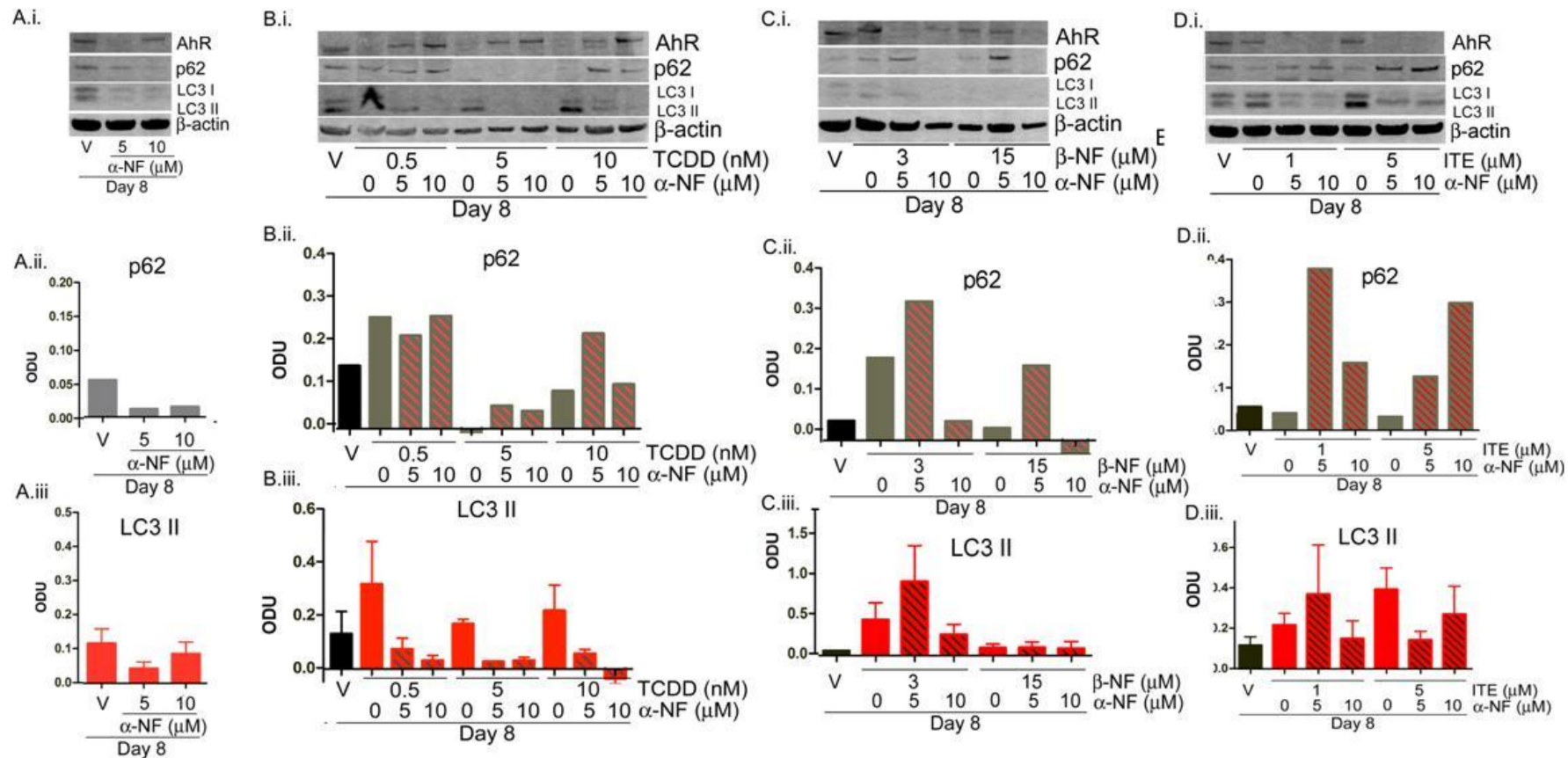


Figure 5.6 The effects of co-treatment with TCDD, β -NF or ITE plus α -NF on autophagy in primary keratinocytes. Primary keratinocytes were treated with vehicle or ligand \pm α -NF as indicated. After 8 days cells were lysed and Western blotting performed (A). Densitometry was performed on Western blots probed with B.i) p62 and B.ii) LC3 II. Black bars represent vehicle treated keratinocytes, plain bars indicating ligand alone and hatching on bars indicates co-treatment of keratinocytes with α -NF. Densitometry from LC3 II and p62 was normalised to β -actin. B.i.) Values are represented as mean ODU from 1-3 donors. No analysis was performed on p62 due to low sample size. Two-way ANOVA was used to compare the effects of ligand treatment with α -NF and time. TCDD: α -NF had a significant effect on LC3 II ($P = 0.002$), β -NF: Time had a significant effect on the effects of β -NF/ α -NF on LC3 II. In ITE treated cells, neither ITE, α -NF nor time had a significant effect on LC3 II.

5.2.5 The effects of autophagic block on LC3 II and p62

To address the potential involvement of autophagic block induced by TCDD, β -NF or ITE causing up-regulation of LC3 II and p62, primary keratinocytes were treated with bafilomycin A1, a compound which blocks autophagy by inhibiting the fusion of lysosomes to the autophagosome by inhibiting ATPase which mediates acidification of the lysosomes upon which lysosome-autophagosome fusion is dependent (see Figure 5.7) (Lukacs et al., 1990). As shown in Figure 5.6, LC3 II and p62 expression were determined by Western blots and densitometry. Treatment with Bafilomycin A1 resulted in blocked autophagy which allowed an accumulation of LC3 I and II. If a compound induced active autophagy, the combination of compound plus Bafilomycin A1 would result in increased levels of LC3 I and II equalling the combination of LC3 I and II induced by the compound and bafilomycin A1. However, if the compound blocked autophagy, bafilomycin A1 co-treatment would induce no further LC3 I and II because it has already all accumulated.

As expected, bafilomycin A1 treatment alone caused up-regulation of LC3 I and II, and increased levels of p62 (Carew et al., 2011)(Figure 5.7). TCDD alone induced LC3 II protein levels (the relatively low expression levels seen here may relate to Western blot development to allow visualisation of high levels seen in bafilomycin A1 treated samples), but after co-treatment of TCDD and bafilomycin A1, an accumulative effect was seen (although slight), suggesting that TCDD induced active autophagy (Figure 5.7).

β -NF and ITE did not visibly induce LC3 I or II alone, so co-treatment with bafilomycin A1 only resulted in levels equal to that induced by bafilomycin A1 alone. Therefore the presence or absence of autophagic block in these samples cannot be determined. p62 levels in all bafilomycin A1 treated samples (alone or co treated with ligand) were high as expected, as bafilomycin A1 induced autophagic block which inhibited degradation of p62 as well. p62 levels were slightly reduced by TCDD treatment (as in Figure 5.3 and Figure 5.4) but expression in samples treated with β -NF or ITE alone did not appear lower than vehicle treated samples. In Figure 5.3 and Figure 5.4, TCDD and ITE treatment induced p62 degradation to levels lower than those in vehicle. Inhibition of TCDD- or ITE-dependent p62 degradation by α -NF resulted in p62 levels being equal to

or higher than vehicle in many cases (Figure 5.5 and Figure 5.6). The lack of LC3 II induction by ligand alone could be caused by the short time point used, data shown in Figure 5.7 is at day 2, whereas the figures in the chapter showing AhR-dependent effects on autophagy are at days 6 and 8 (Figure 5.3 and Figure 5.4). No statistical analysis was performed because data from only 2 donors was used.

Pepstatin A, an inhibitor for aspartic protease Cathepsin D, was included in Figure 5.7 to test the effects of CTSD inhibition CTSD protein levels by Western blot. The effect of pepstatin A on CTSD protein levels is discussed in the next chapter.

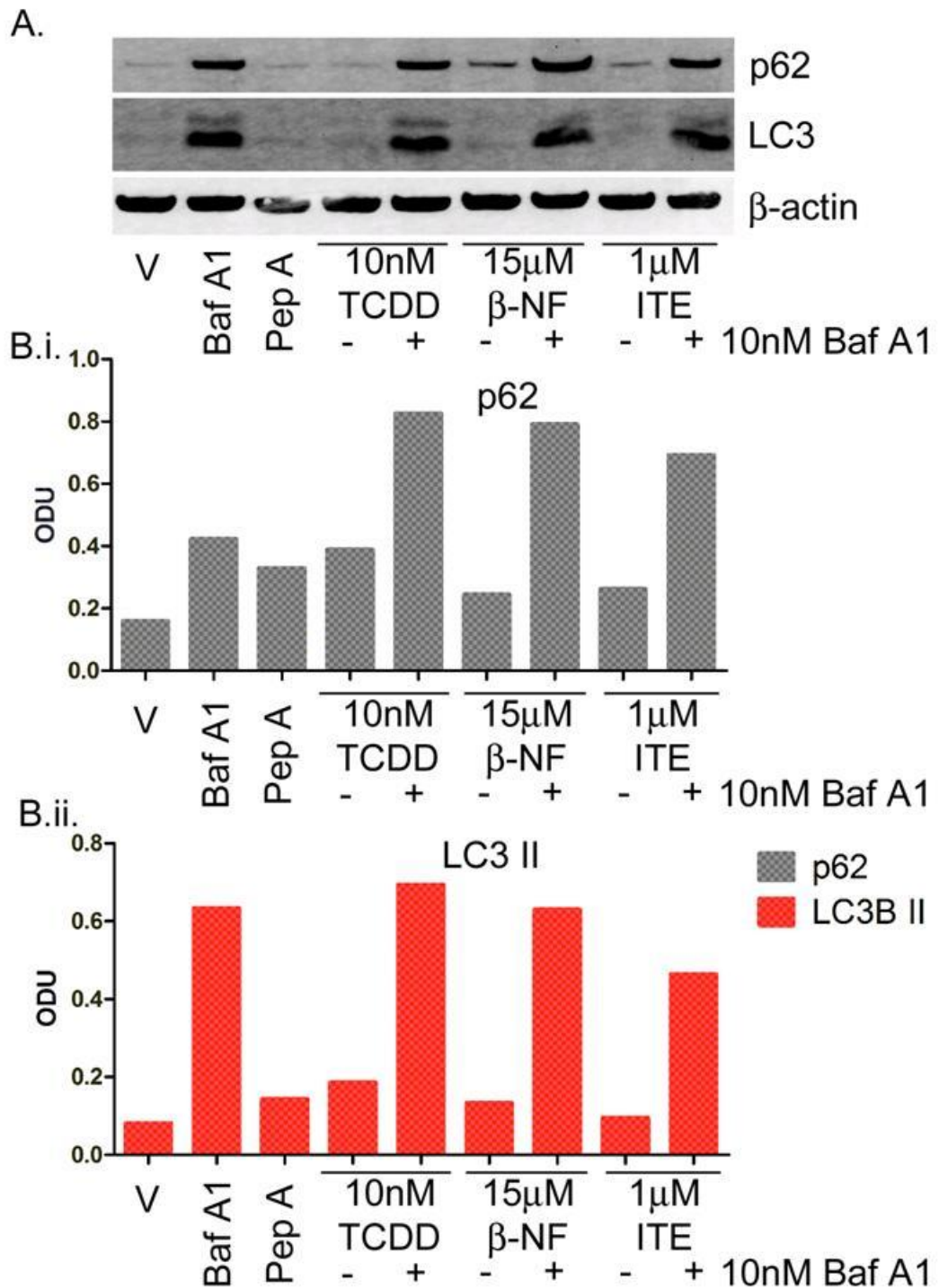


Figure 5.7. Bafilomycin A1 induced levels of LC3 II and p62 in primary keratinocytes. Primary keratinocytes were treated with vehicle, 10nM TCDD, 15µM β-NF or 1µM ITE ± 10nM bafilomycin A1, or Bafilomycin A1 alone. After 2 days cells were lysed and Western blotting performed. Blots were probed with anti-p62, anti-LC3 antibodies and β-actin as a loading control. **A)** Western blot is representative of blots from 2 donors. **B)** Densitometry is shown as mean average from 2 donors, normalised to β-actin and presented as optical densitometry units. No statistical analysis was performed due to small sample size.

5.2.6 Active autophagy in epidermal equivalents

As described at the start of this chapter and in the introduction, autophagy is a complex and dynamic process involving the formation of autophagosomes, before fusion with lysosomes. Because of the characteristic double membrane formed during maturation (indicated in Figure 5.1) to contain proteins and organelles for degradation during active autophagy, the process can be visualised by following the formation of the autophagosome and its degradation of cellular organelles. Transmission EM (EM) is the ideal tool to do this because of its clarity of images at high magnification (Eskelinen, 2005). EM is commonly used to look for autophagy in tissues (Carew et al., 2011; Eskelinen, 2005; Gunzel et al., 1991) and it has also been used to validate the epidermal equivalent model itself (Ponec et al., 2000). As shown throughout this chapter by Western blot, static measurements of autophagic biomarkers LC3 II and p62 can produce misleading or difficult to interpret results. For example, increases in LC3 II levels can indicate either an increase in active autophagy (as opposed to basal autophagy) or blocked autophagy but measurements of autophagic flux show the increased frequency of LC3 I to II conversion and their degradation, providing a real time measurement of the increased turnover of autophagy. One flux assay uses an mRFP-GFP-LC3 construct to follow autophagosome maturation. The progress of LC3 I to LC3 II conversion as it is recruited to the autophagosome is followed by the accumulation of green and red puncta before association with the acidic autolysosome which quenches the GFP, leaving only RFP and indicating maturation of the autolysosome (Kimura et al., 2007). This protocol was under development in Dr Lovat's group during this project, but due to time constraints it was not possible to develop any data for this project.

EM indicates active autophagy mainly by the presence of vacuoles and increased numbers of double membraned autophagic vacuoles (the more general term "autophagic vacuole" is often used in regard to microscopy because of the difficulty associated with identifying the stage of maturation of the organelle), low levels of autophagic vacuoles are present in most samples because of its basal role in cells. Because of the "gold standard" status of autophagy identified by EM (Carew et al., 2011; Eskelinen, 2005) and the well characterised EM in human skin and epidermal equivalents (Gunzel et al., 1991; Ponec et al., 2000), EM proved the ideal process to

understand levels of active autophagy in our TCDD, β -NF and ITE treated epidermal equivalents.

Epidermal equivalents were cultured as described in materials and methods and treated with vehicle, 10nM TCDD, 15 μ M β -NF or 1 μ M ITE for 7 days. Epidermal equivalents were harvested and fixed in 2.5% glutaraldehyde in 0.1M Sodium cacodylate solution. EM was performed at AstraZeneca, Macclesfield with the help of Simon Brocklehurst. At low magnification (\sim x3000), images spanned the whole section from polycarbonate membrane (marked with a black line) to stratum corneum (σ) (Figure 5.8 and Figure 5.9, A and B). The vehicle treated sample (Figure 5.8 A) showed well characterised VCL, including the rounded columnar basal cells, then flattening out in the lower and upper spinous layers. A degree of spongiosis was present in the vehicle treated sample (Figure 5.8 A, white arrows) however this has been observed commonly in validated epidermal equivalents previously by Ponec et al (Ponec et al., 2000). Keratin fibres formed visible clusters in the spinous layer (keratins are present in all layers: K5/K14 basal; K1/K10 suprabasal) and cells became enucleated and flattened further as they reached the granular layer. At higher magnification (x100,000), cellular structures were present, including groups of lamellar bodies at the upper spinous/granular membranes with their characteristic lamellar contents visible (Figure 5.10 A and B and Figure 5.11) and well formed keratohyalin granules were present in the granular layer (Figure 5.11). Terminal differentiation in the granular layer was impressively defined (Figure 5.10 C and Figure 5.11), with fusion of lamellar bodies to the cell membranes and their extrusion of lamellar structures into the extracellular areas of the stratum corneum also visible (Figure 5.10 C and D). These images help to validate the presence of well formed and complete differentiation process in the epidermal equivalent model. Ponec et al validated the barrier function in commercially available epidermal equivalents, explaining these features further and offering a comparison between commercially available epidermal equivalents and models grown in the lab (Ponec et al., 2000).

Examining the treated epidermal equivalents was equally as interesting; an obvious observation was the high numbers of vacuoles present in TCDD treated epidermal equivalents (Figure 5.8, B). Low numbers were present in vehicle treated samples (Figure 5.8 A) consistent with autophagy being a survival pathway present basally in all cells. β -NF (Figure 5.9 A) and ITE (Figure 5.9 B) treated samples had relatively low numbers of vacuoles, but these were higher in number than basal levels. Vacuolation is

commonly a characteristic of apoptosis, but it is known to be present in autophagy. As described in the introduction, this is hypothesised to either represent a connection between autophagy and apoptosis or be a sign of autophagy induced cell death, by inducing such high levels of degradation that the cell dies (Gonzalez-Polo et al., 2005).

Mitochondria are a common target for autophagy (mitophagy), and autophagic vacuoles are often in close proximity to mitochondria in the same areas in the cell (Wang et al., 2011). Intact mitochondria were present in all samples, suggesting mitophagy was not activated by these AhR agonists (Figure 5.8 A.i. and Figure 5.9 A.i). High numbers of early (Figure 5.8 B.i.) and late degradative (Figure 5.8 B.ii.) autophagic vacuoles (*) were seen in TCDD treated samples, showing high levels of organisation. ITE treated samples contained evidence of active autophagy (early autophagic vacuoles, Figure 5.9 B.i.) higher than basal levels but less than TCDD.

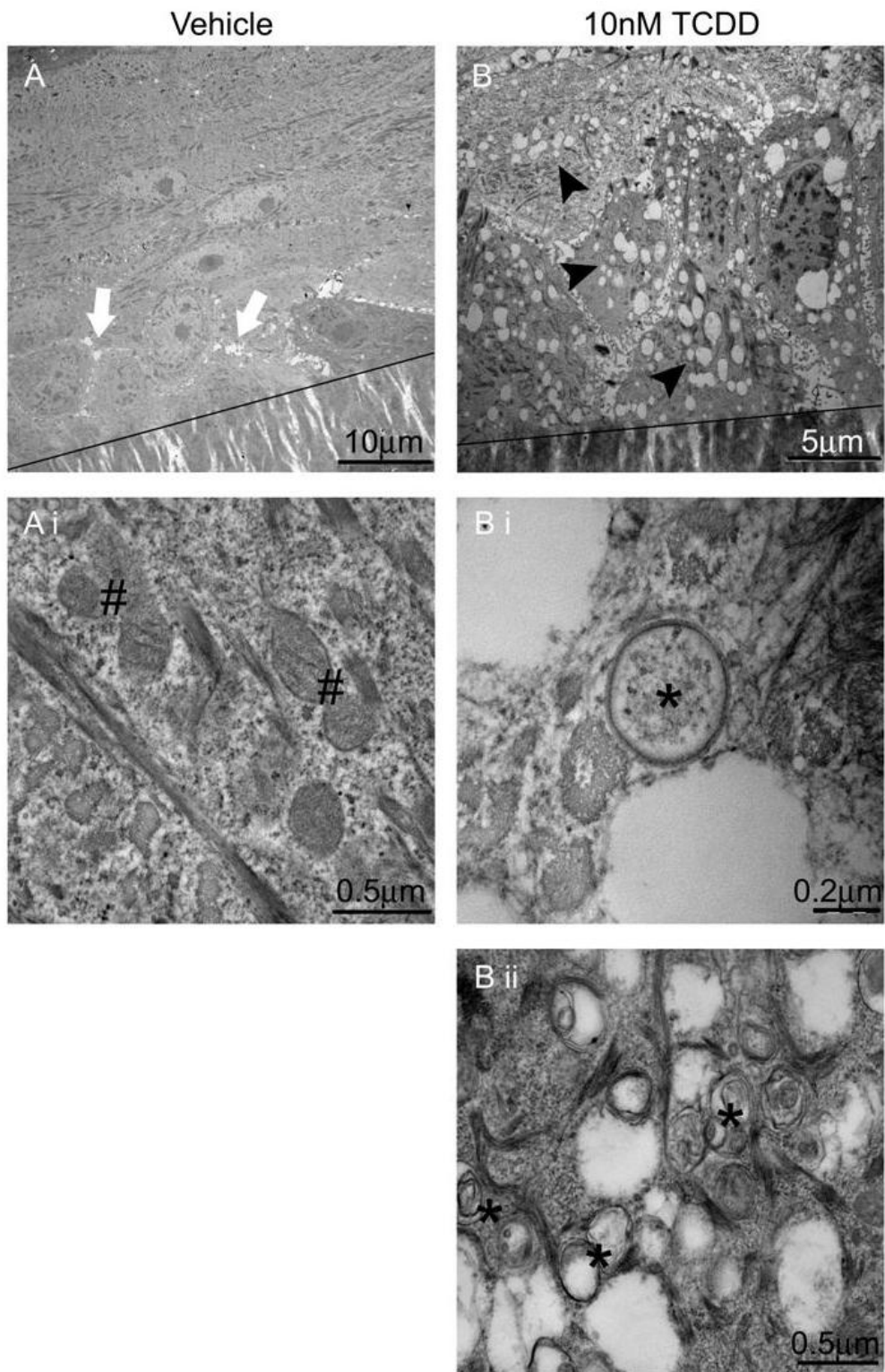


Figure 5.8. Characteristic signs of autophagy in TCDD treated epidermal equivalents. Epidermal equivalents were treated with **A**) vehicle or **B**) 10nM TCDD. After 7 days, equivalents were fixed in 2.5% glutaraldehyde in 0.1M Sodium cacodylate solution. Transmission electron microscopy was performed on a JEOL JEM-1400 electron microscope. Top panels show low magnification (**A** - x3000, **B** - x6000) epidermal equivalent sections from polycarbonate membrane (black line) to stratum corneum (**A**) or spinous layer (**B**). Black arrow heads indicate vacuolisation; white arrows indicate spongiosis; # indicate intact mitochondria; * indicate early (**B.i.**) and late degradative (**B.ii.**) autophagic vacuoles.

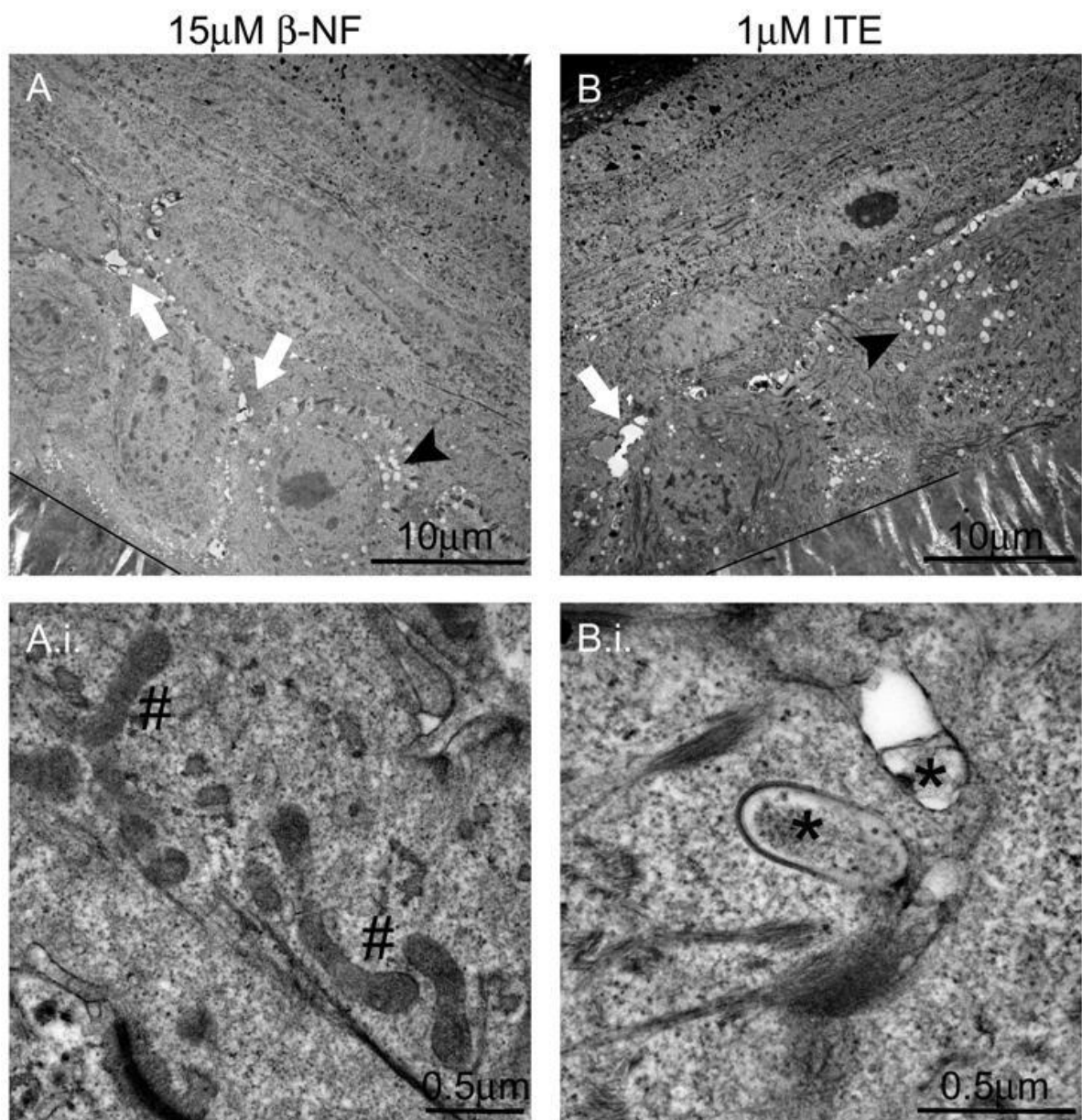


Figure 5.9. ITE induced low levels of active autophagy in epidermal equivalents. Epidermal equivalents were treated with **A)** 15µM β-NF or **B)** 1µM ITE. After 7 days, equivalents were fixed in 2.5% glutaraldehyde in 0.1M Sodium cacodylate solution. Transmission electron microscopy was performed on a JEOL JEM-1400 electron microscope. Top panel shows low magnification (x4000) epidermal equivalent section from polycarbonate membrane (black line) to stratum corneum. Black arrow heads indicate vacuolisation; white arrows indicate spongiosis, # indicates intact mitochondria (**A.i.**); * indicates autophagic vacuoles (**B.i.**).

Lamellar bodies are organelles found in the epidermis (and other cornified epithelia - similar organelles also in lung where secrete surfactant) containing lipids and their processing enzymes required for barrier function (described in more detail in section 1.2.1 and (Raymond et al., 2008)). Like lysosomes, they contain proteases (including Cathepsin D) and protease inhibitors, but instead of expressing LAMP-1 like

lysosomes, they express caveolin, a cholesterol scaffold protein, which facilitates formation of lipid rafts (Fartasch, 2004; Raymond et al., 2008). Empty, misformed or low numbers of lamellar bodies can contribute to diseased states such as ichthyoses, where barrier function is compromised and stratum corneum can become compacted causing scaling and inflexibility of the epidermis (Ponec et al., 2000; Rizzo et al., 2010).

The only certain identification of lamellar bodies is through EM, where the membrane bound organelle can be identified by its characteristic lamellar contents (Figure 5.10 B)(Rassner et al., 1999). Expression is normally in the upper spinous/granular layer of the epidermis and from here the organelles move to the apical membrane of the outermost granular cell where it fuses to the membrane (Fartasch, 2004; Raymond et al., 2008)(Figure 5.10 C and D) causing deep invaginations in the membrane allowing its contents (mainly sphingolipids, cholesterol and acid hydrolases (Raymond et al., 2008; Sando et al., 2003)) to be secreted into the junction of the granular and cornified cells. Processing enzymes convert lipids to form lamellar sheets in the intercellular spaces (these are visible by EM, Figure 5.10 D), contributing to the open basket weave phenotype. Ponec et al studied barrier function and formation of the cornified envelope in epidermal equivalents and comparable EM images showing detailed stratum corneum are included in the paper (Ponec et al., 2000).

The addition of vitamin C to the epidermal equivalent culture allows the formation of lamellar bodies which are present in high numbers in vehicle treated samples (Figure 5.11A). After TCDD treatment, this number appeared decreased (Figure 5.11 B), ITE treatment also appeared to decrease numbers of lamellar bodies (Figure 5.11 D) however β -NF did not (Figure 5.11 C). When we first considered the compacted stratum corneum phenotype in our TCDD treated epidermal equivalent cultures, we drew parallels with ichthyosis and Sjogren Larsson syndrome, which characteristically produces a compact and thickened stratum corneum. This is caused by a mutation in the ALDH3A2 gene which encodes for fatty aldehyde dehydrogenase and results in low and aberrant lipid metabolism. This causes lamellar bodies to be empty and causes a deficiency in lipids extruded into the stratum corneum, causing compaction and a deficient epidermal barrier. (Rizzo et al., 2010). Therefore, a low number of lamellar bodies (resulting in lipid deficiency as in Sjogren Larsson syndrome) present in the TCDD treated epidermal equivalents could be a main contributing factor to the compacted stratum corneum phenotype. There are also reports of “lipophagy” in the

liver; autophagy targets and degrades fat droplets to efficiently produce high levels of energy (Singh et al., 2009b; Weidberg et al., 2009). Interestingly, we saw evidence in the TCDD treated epidermal equivalent cultures of targeted degradation of lamellar bodies (Figure 5.12 B), suggesting that autophagy may contribute to the observed decrease in lamellar bodies in TCDD and ITE treated epidermal equivalents, directly causing compacted stratum corneum.

Decreased lamellar bodies caused by TCDD treatment have not been reported in the literature and targeted degradation of lamellar bodies by autophagy has not been either. These novel observations may be preliminary, but are very exciting. During this project, EM of epidermal equivalents from only one donor was performed. Further studies are required to confirm this observation.

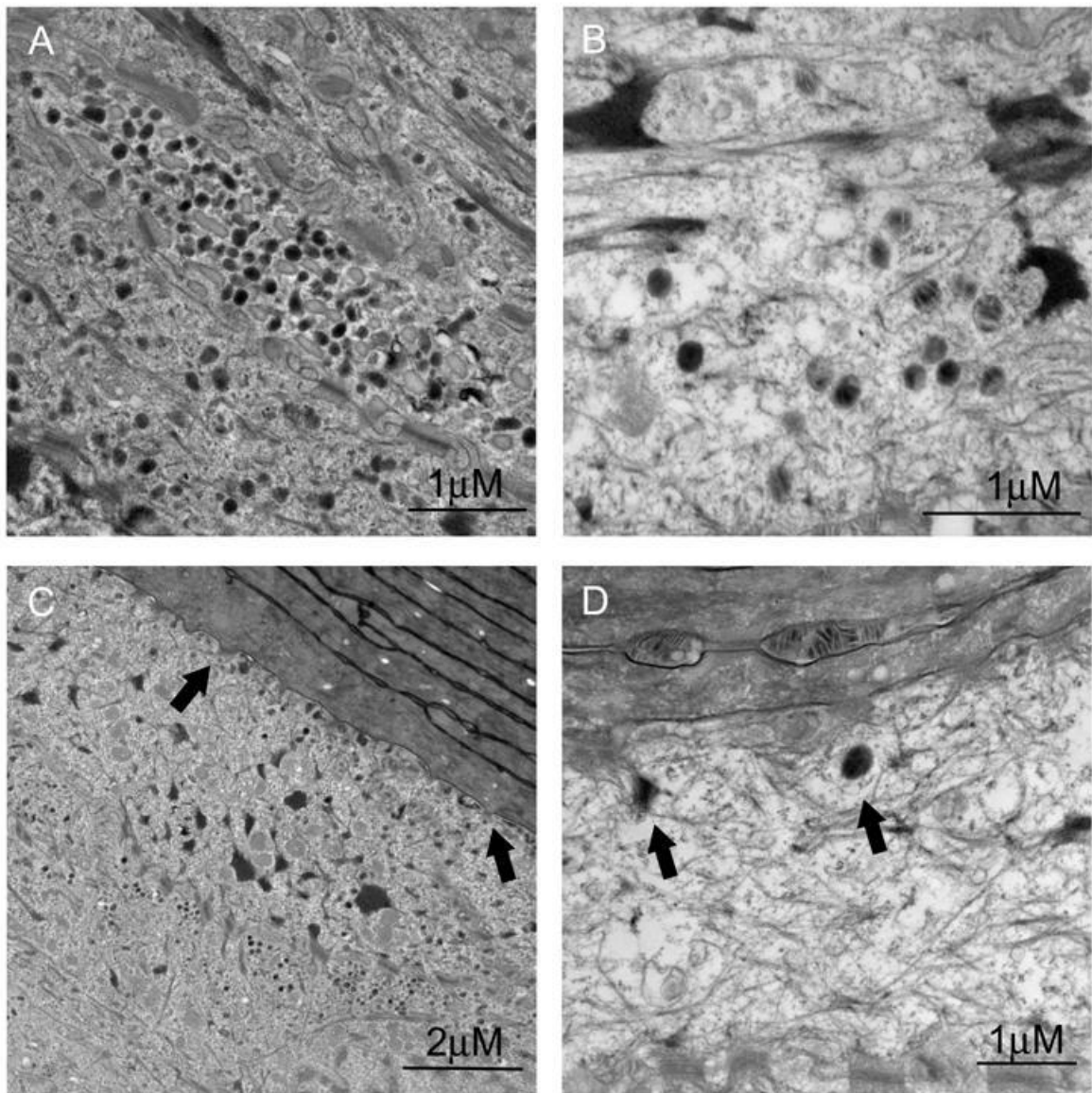


Figure 5.10. Lamellar bodies fuse with membrane structures in the stratum corneum. Electron micrographs of epidermal equivalents treated with **A/C)** vehicle or **B/D)** 10nM TCDD for 7 days. **A)** Normal expression of lamellar bodies in vehicle treated sample. **B)** Characteristic structure seen by EM used to define lamellar bodies. **C and D)** Lamellar body contained lipids are secreted into the stratum corneum by fusion of lamellar bodies to membranes of cells in transition between granular and cornified layers. These structures can be seen contained in the stratum corneum in **D**. Black arrow heads represent the fusion of lamellar bodies with the membrane cornified layer.

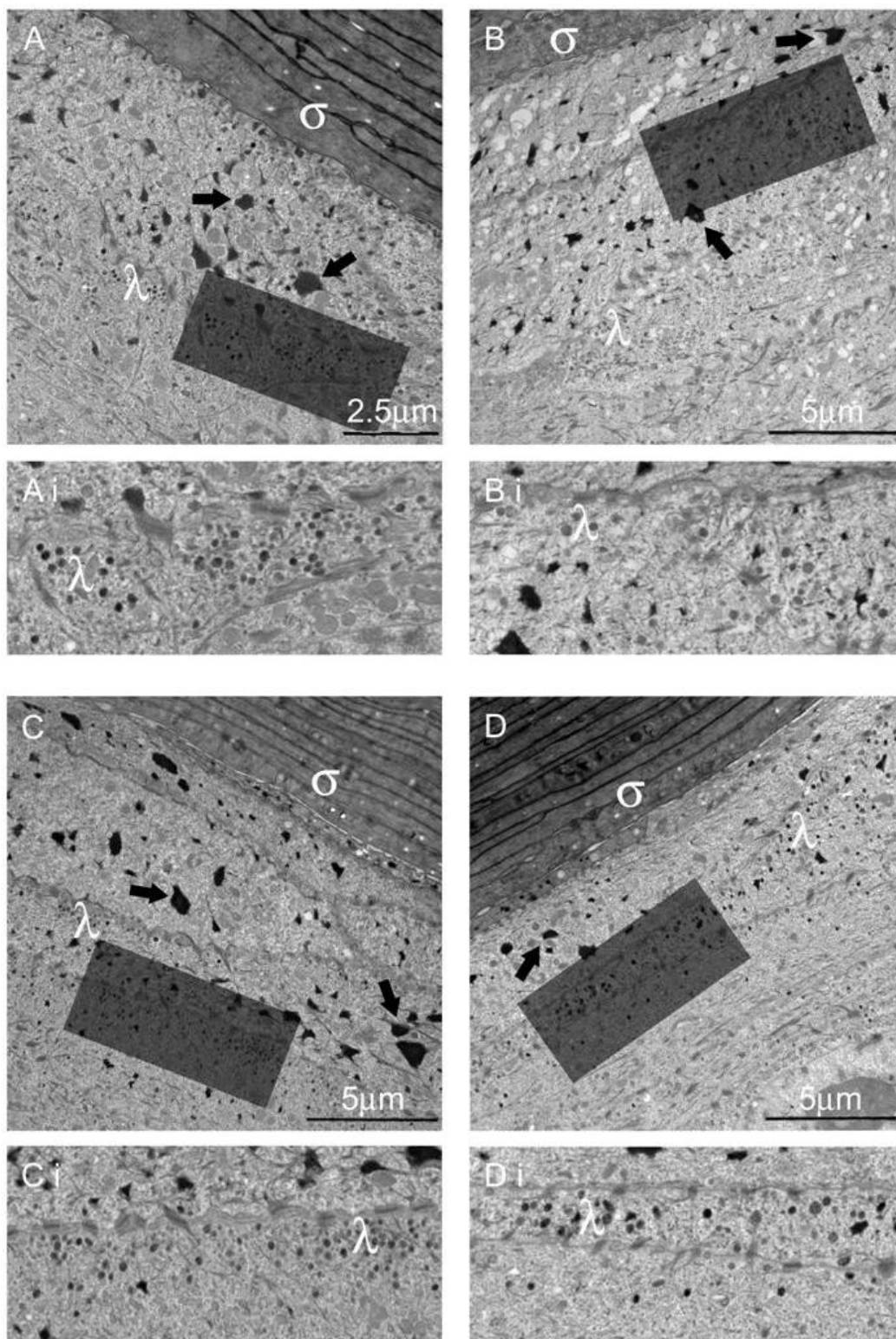


Figure 5.11. TCDD and ITE treatment leads to decreased numbers of lamellar bodies in epidermal equivalents. Electron micrographs of epidermal equivalents treated with **A)** Vehicle, **B)** 10nM TCDD, **C)** 15µM β-NF or **D)** 1µM ITE for 7 days. **A** shows high numbers of lamellar bodies at the upper membrane of a cell of the upper spinous/granular layer. **B/D)** TCDD/ITE treatment appears to decrease numbers of lamellar bodies. Clusters of lamellar bodies become uneven. **C)** Numbers of lamellar bodies appear normal in β-NF treated cells, but clusters become uneven. Shaded area shows area shown at higher magnification. Arrows indicate keratohyalin granules, λ indicates clusters of lamellar bodies, σ indicates stratum corneum.

After observing the decreased numbers of lamellar bodies in TCDD-treated epidermal equivalents, I hypothesised that autophagy may cause this down-regulation. As demonstrated in the liver, autophagy targets fat droplets to release ATP in cells during starvation. I found evidence of targeted lamellar bodies in the electronmicrographs, as shown in Figure 5.12. Lamellar body-like structures were observed within vacuoles in the granular layer (Figure 5.12 A) but more defined images were also found, showing double membraned autophagosomes apparently engulfing lamellar bodies (Figure 5.12 B). To confirm this, further studies would have to be undertaken to repeat this in other donors, and also use a method of fixation specific for imaging lipid structures that would produce more defined images of lamellar bodies (Rassner et al., 1999; Raymond et al., 2008). The white arrows indicate the electron dense cornified envelope, which is formed by TGM-1 activation crosslinking proteins including involucrin and filaggrin, which is vital for barrier function. This is characteristic in classification of diseases exerting hyperkeratinisation such as psoriasis and lamellar ichthyosis and is explained further in chapter 6 and the general discussion.

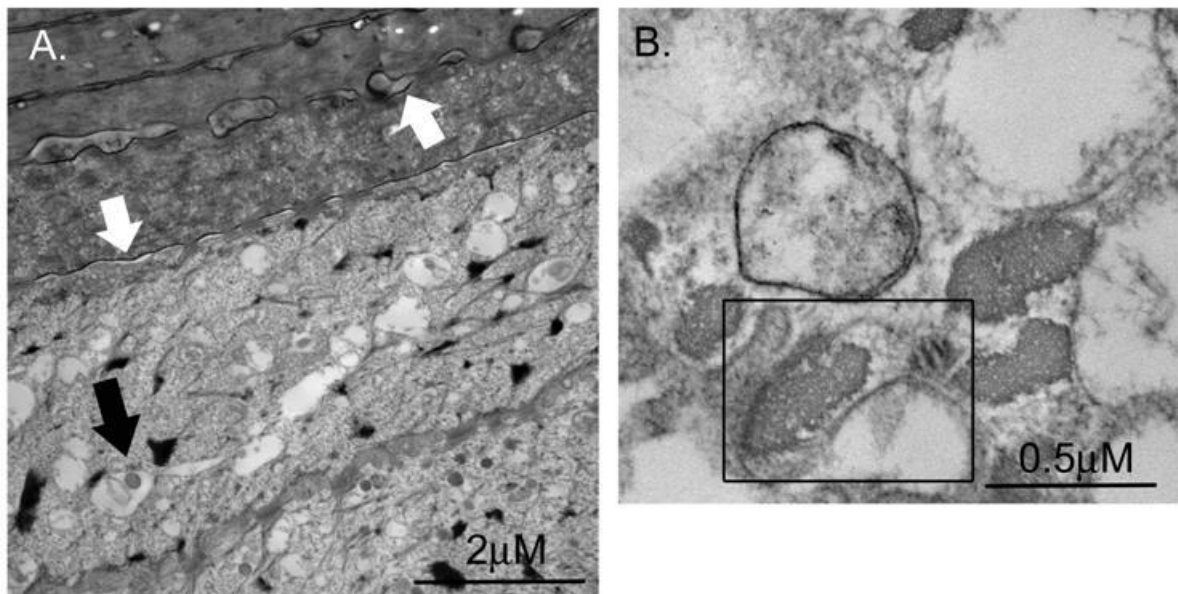


Figure 5.12. Evidence of autophagy targeting lamellar bodies. Electron micrographs showing sections of epidermal equivalent treated for 7 days with 10nM TCDD. **A)** Black arrows indicate a possible vacuole containing a lamellar body. White arrows represent the electron dense areas of the cornified envelope formation where lamellar bodies visibly fuse with the membrane secreting their contents into the granular/cornified extracellular area. **B)** A double membrane autophagic vacuole engulfing a lamellar body (marked by the black box) characteristically marked with lamellar stripes. The autophagic vacuole possibly contains material for degradation.

Further observations have been made in the electronmicrographs; desmosomes appear to be reorganised in TCDD and ITE treated epidermal equivalents (Figure 5.13 A and B). In vehicle and β -NF treated samples the desmosomes run along the cell membranes in the viable cell layers, however in samples where autophagy is activated (including dithranol treated samples) the desmosomes become spindle like. Long intermediate filaments appear to stretch from the desmosomes into the cytoplasm of neighbouring cells. This has not been previously reported in the literature and the only diseased states seem to be connected to loss of desmosomes causing blistering phenotypes (described further in the introduction section 1.2.1)

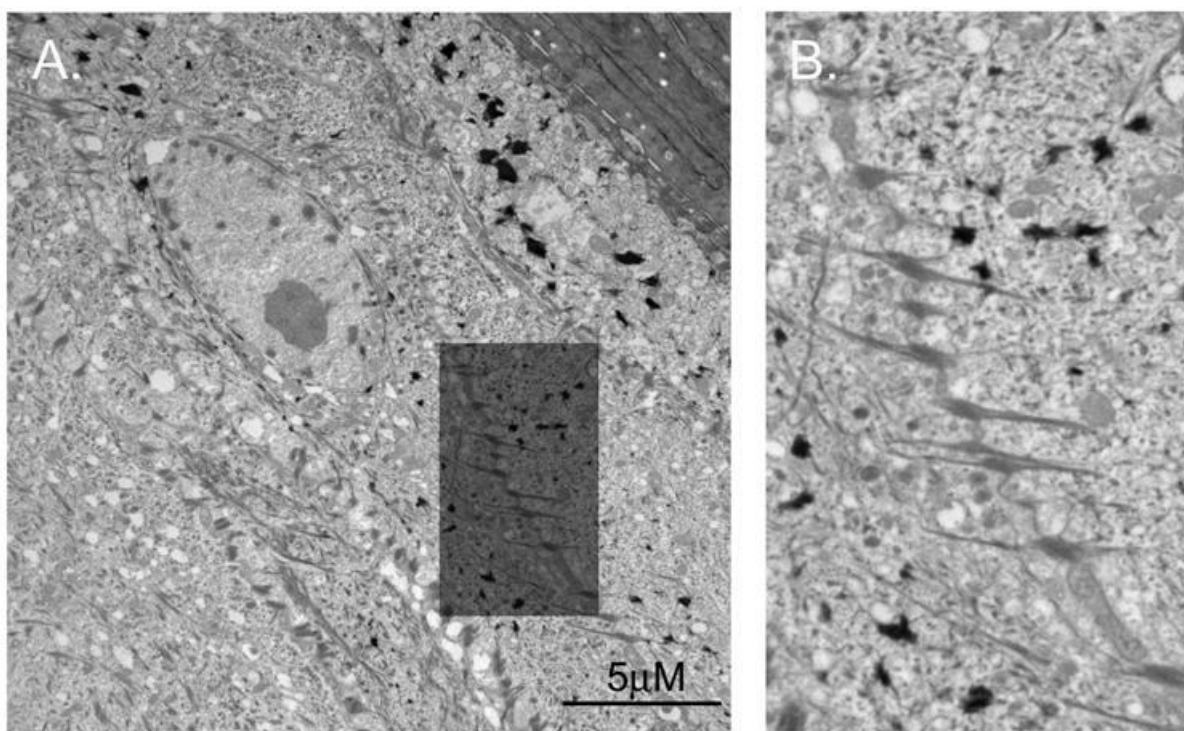


Figure 5.13. AhR activation causes desmosomal re-arrangement. Electron micrographs of epidermal equivalents treated with 10nM TCDD for 7 days. **A)** A nucleated cell in the upper spinous layer shows rearranged desmosomes that have turned perpendicular to the cell membrane and extended into the cytoplasm of the neighbouring cells. **B)** Higher magnification shows desmosomes along the cell membrane forming spindle like structures stretching into the cytoplasm of neighbouring cells.

5.3 Discussion

5.3.1 Summary

In this chapter I have shown novel data linking AhR activation to autophagy in keratinocyte monolayers and epidermal equivalents. Using classic biomarkers LC3 II, p62 and EM, I have shown TCDD and ITE to induce autophagy and in contrast, β -NF to block autophagy. I attempted to prove AhR dependence of autophagic induction, but α -NF, the partial agonist used to inhibit AhR, showed signs of inducing blocked autophagy by treatment itself and in combination with all ligands.

	TCDD 0.5-10nM	β-NF 3/15μM	ITE 1/5μM	α-NF alone 5/10μM
p62 degradation	+++ D2-8	--- D2-8	+++ D6/8	- / + Varied
LC3 II induction	++ D6/8	+++ D2-8	++ D8	+ / - D2 D4-8
p62 degradation + α-NF	--- D2-8	+/- Varied	-- D2-8	
LC3 II increase + α-NF	-- D2-8	+/- Varied	+ D2/8	
EM	+++	0	++	

Table 6. A summary of autophagic activation by AhR ligands and inhibition by co-treatment with agonist plus α -NF. +/- indicates effect of treatment on level of AhR activation readout. Green figures represents autophagic activation, red figures represent autophagic inhibition.

Autophagy has not been linked to the AhR in the literature so far. The induction of autophagy by TCDD and ITE and the possible blocking of autophagy by β -NF (and possibly α -NF) is novel (section 5.2.3). Electron micrographs of TCDD treated epidermal equivalents have been published previously (Loertscher et al., 2001b) but no connection to lamellar bodies or autophagy is reported or discussed. β -NF has not previously been linked to autophagy or its effects on the phenotype induced in epidermal equivalents. There are few publications on ITE and its use in epidermal equivalents and its effects on autophagy are also novel. The observations of decreased

numbers of lamellar bodies in TCDD treated epidermal equivalents and the evidence for their possible targeting by autophagy is also a novel observation, allowing us to make new and exciting hypotheses combining the role of autophagy in stratum corneum compaction (section 5.2.6).

5.3.2 TCDD and ITE induce active autophagy but β -NF blocks autophagy

LC3 alone is not a good autophagic marker because of the complex mechanisms involved in active autophagy. Here, it is paired with expression of p62 which together are indicative of the induction of active autophagy (described in detail in the introduction section 1.5.1). Although p62 expression is taken to inversely correlate with active autophagy, it is also regulated by other factors, and this should be considered. As TCDD treated keratinocytes showed an inverse correlation between increased LC3 II and decreased p62 in an inverse dose response; as TCDD induced active autophagy, p62 was degraded more, indicating the induction of active autophagy (Figure 5.3 and Figure 5.4). This was confirmed by co-treatment with ligands and bafilomycin A1 and EM of TCDD-treated epidermal equivalents; Figure 5.8 shows TCDD induced vacuolation of epidermal equivalents and the presence of early and late autophagic vacuoles. As EM is the gold standard method of identifying the presence of active autophagy, this shows conclusive evidence that TCDD induced active autophagy in keratinocytes, which showed signs of cell death by the presence of increased autophagic vacuoles.

β -NF induced both LC3 II and p62 (Figure 5.3 and Figure 5.4), suggesting a block in autophagy. LC3 II induction was present at day 2, which may possibly suggest an AhR-independent, or differential AhR-dependent mechanism for β -NF induced effects on autophagy as most AhR dependent effects are seen at later time points, or that β -NF is a potent autophagic blocker. EM showed little evidence of autophagy, only a low number of vacuoles were present, similar to levels present in vehicle treated epidermal equivalents (Figure 5.9). From this we can conclude that β -NF does not induce autophagy, but may block it. Unfortunately, the bafilomycin A1 autophagy blocking assay that would have helped to confirm this result (Figure 5.7) did not provide conclusive data.

ITE up regulated LC3 II in a time and dose dependent manner while causing a slight decrease in levels of p62 at day 8, the time point associated with the protein effects of AhR activation (Figure 5.6 and Figure 5.4). The Bafilomycin A1 assay, as with β -NF, did not show conclusive results due to lack of LC3 II up-regulation and p62 down-regulation by ITE alone. EM showed increased vacuolation in ITE samples compared to vehicle treated samples and evidence of double membraned autophagic vacuoles (Figure 5.9), strongly suggested that ITE induced active autophagy.

These data do not conclusively show the effects of β -NF or ITE on autophagy (although evidence for TCDD induced autophagy is robust). Autophagy is a dynamic process and is difficult to measure conclusively with static assays. Both Western blotting and EM are stationary measures of autophagy, and therefore do not show changes in flux. Despite the high status of EM in autophagic identification, it is still a static measurement at a set time point and therefore may miss the induction of autophagy at certain time points. We therefore cannot conclude from EM performed on β -NF or ITE treated samples that autophagy was not induced, only that it did not occur at that specific time point. The autophagic flux assay described in this chapter could be utilised to define the effects of β -NF and ITE on the increased or decreased levels of active autophagy, and to define the contribution of the AhR pathway in autophagy further using TCDD and genetic or pharmacological inhibition and intervention. By using confocal fixed or live cell imaging, the mRFP-GFP-LC3 construct can be transfected into cells and conversion of LC3 I to II and recruitment to the autophagosome and the autophagosome maturation can be followed. As described in section 5.1, the maturation of autophagosomes is represented by the colocalisation of green and red puncta before fusion of the autophagosome and lysosomes, which decreases the pH quenching the GFP signal and leaving RFP puncta marking mature autolysosomes (Armstrong et al., 2011; Kimura et al., 2007) and would be a useful method for future studies.

5.3.3 Modulation of autophagy by α -NF

As in chapter 3, the partial AhR agonist α -NF was used in co-treatment with ligands to modulate the AhR pathway and observe effects on autophagy (Figure 5.5 and Figure 5.6). Treatment of primary keratinocytes with α -NF alone had little effect on LC3 II induction (levels appeared slightly lower but this was not significant) and slightly decreased p62 levels (Figure 5.5 and Figure 5.6). Previous papers have reported the

use of α -NF at concentrations that induced its own (minor) AhR agonistic effects, to inhibit AhR activation by TCDD (Gasiewicz, 1991). As the agonistic effects shown here are very minor (no LC3 II induction apart from at day 2), its use as an AhR antagonist would have been thought to be its main effect. However at day 2, α -NF did exert blocked-autophagy like effects, p62 and LC3 II induction. The first thing to consider here is that the densitometry and Western blot shown in Figure 5.5 and Figure 5.6 A are only representative of 1 donor and therefore require repeating to indicate any conclusive data. The second is that the induced LC3 II and p62 was at an early time point and as mentioned earlier, this is not the typical time point to observe AhR-dependent effects. The third is the possibility of α -NF inducing blocked autophagy. It is a flavone similar to β -NF (although they do exert different effects, for example β -NF quenches firefly luciferase activity while α -NF does not, see section 3.2.1.3) and it is possible that AhR-dependently blocked autophagy could be a flavone specific trait. Considering all of these points, the effects of α -NF on autophagy and AhR activation are low but should be taken into consideration when studying the results involving co-treatment with α -NF and AhR agonists.

Co-treatment of TCDD plus α -NF blocked LC3 II induction and consequent p62 degradation, often with p62 levels recovering to higher levels than basal. This suggested that TCDD induced autophagy was AhR dependent, but also that α -NF may have autophagic blocking properties in co-treatment with TCDD. This was not robust data, the effects were small and inconsistent over dose and donor. α -NF also blocked up-regulation of LC3 II and p62 by β -NF, suggesting inhibition of blocked autophagy and that the autophagic block induced by β -NF was also AhR dependent. α -NF appeared to inhibit the blocked autophagy but did not induce active autophagy. The results obtained with ITE co-treatment with α -NF are however more complex to interpret; LC3 II was induced and p62 degraded by treatment with ITE alone. Co-treatment with all combinations of ITE plus α -NF blocked both LC3 II induction and p62 degradation (except 1 μ M ITE plus 5 μ M α -NF which induced LC3 II further) which suggests inhibition of ITE-induced autophagy; however co-treatment of ITE and α -NF induced p62 to levels higher than vehicle. Interestingly this occurred in all cases of co-treatment of α -NF plus TCDD, β -NF and ITE, and suggests that α -NF may cause a block in autophagy. The varied responses of LC3 II induction and p62 degradation resulting from α -NF plus agonist co-treatment may be a result of combined agonistic properties of α -NF when paired with an agonist at an unbalanced dose combination,

favouring agonistic activity and not antagonistic activity. High-affinity properties of ITE, it may be caused by induction of autophagic block, it could also be an aberrant result because only one Western blot is available, this p62 blot was carried out once due to time constraints. To study AhR dependence of autophagy more thoroughly and without complications of compound interactions, cells transfected with shRNA against AhR could be co-transfected with the mRFP-GFP-LC3 construct and effects of AhR knock down on autophagic flux studied.

5.3.4 AhR activation effects lamellar bodies and desmosomes

The electron micrographs taken of the epidermal equivalents provided interesting histology of the keratinocytes and epidermal equivalent formation. A novel observation was the re-organisation of desmosomes in TCDD and ITE treated samples (Figure 5.13). Intermediate filaments appeared to elongate and form spindle like structures into the cytoplasm of neighbouring cells. There are no reports of this desmosomal reorganisation in the literature, only that a deficiency results in loss of adhesion between epidermal layers and the formation of blisters (Pigors et al., 2011).

Not only did EM provided confirmation of active autophagy, it has also shown interesting effects of AhR activation on the epidermal equivalents. Lamellar bodies were present in the upper spinous/granular layer in all samples, however numbers were lower in TCDD and ITE treated samples (Figure 5.10 and Figure 5.11). There are reports indicating the targeting of fat droplets in the liver by autophagy (Singh et al., 2009b; Weidberg et al., 2009) which lead us to consider the degradation of lamellar bodies, also lipid containing organelles, by autophagy. We consequently found evidence of autophagic targeting of lamellar bodies in the epidermal equivalents. As shown by Rizzo et al in their study of mechanisms contributing to the compacted stratum corneum in Sjogren-Larsson syndrome, a deficiency in the availability of lamellar lipids for extrusion into the granular layer/stratum corneum junction caused compacted stratum corneum and poor barrier function (Rizzo et al., 2010). This suggests that the cause of compacted stratum corneum in our epidermal equivalent model is most likely a result of lipid deficiency caused by low numbers of lamellar bodies. We have not tested for compromised barrier function in epidermal equivalents, and state of barrier function has not been commented on in the literature in chloracne, but as indicated in Figure 5.12, the cornified envelope

can be seen by EM. This could be used as an identifying factor of malformed cornified envelopes, and indicate whether barrier function would be compromised in an *in vivo* model. If autophagy does target lamellar bodies then this forms a novel mechanistic link between AhR, autophagy and disease and differentiation.

6 AhR activation regulates Cathepsin D

6.1 Introduction

6.1.1 CTSD Regulation

As described in section 1.1.1.6, CTSD is known primarily to be regulated by the oestrogen receptor (ER) and expression is induced by the ER ligand 17 β -estradiol (E2) inducing ER binding to the oestrogen response element (ERE), the promoter for the ER upstream of CTSD (Cavaillès et al., 1993; Porter et al., 1997; Wang et al., 1998). TCDD is known to elicit anti-oestrogenic effects in breast cancer cell lines; Gierthy et al. showed TCDD-dependent growth suppression in MCF-7 cells, while Chen et al. showed inhibition of a battery of ER-induced proteins including hsp 27 and epidermal growth factor α by TCDD in MCF-7 cells (Chen et al., 2001; Gierthy et al., 1993). AhR can inhibit ER activity by inducing its degradation through the proteasome, by increasing ubiquitination of ER α , the tagging of proteins for recognition by proteasomal degradation (Wormke et al., 2003) or disrupting the ER-Sp1 complex at the Sp1 promoter (Khan et al., 2006; Wang et al., 1998; Wang et al., 1999). Because of the anti-oestrogenic effects of TCDD treatment on CTSD in breast cancer, CTSD has been studied to demonstrate the anti-oestrogenic properties of TCDD by the Safe laboratory.

CTSD comprises of 3 major forms; the translated form 52 kDa pre-pro CTSD, 48 kDa pro CTSD in the endosome which is active and mainly involved in CTSD secretion in cancers (Ohri et al., 2008; Rochefort et al., 1989) and 34 kDa active CTSD which is lysosomal and has roles in degradation of material sequestered by autophagosomes (Raymond et al., 2008) and in activation of TGM-1 in terminal differentiation (Zeeuwen et al., 2010).

6.1.1.1 CTSD in epidermis

Section 1.4.3 describes the important role of CTSD in keratinocyte differentiation. Expression and activation of CTSD is increased as keratinocytes differentiate (Egberts et al., 2004) and active CTSD activates TGM-1, one of the main enzymes of the cornified envelope (Zeeuwen et al., 2010). TGM-1 forms the cross links in proteins, mainly involucrin and loricrin, to the cell membrane where they form the insoluble and hydrophobic structures of the cornified envelope (Egberts et al., 2004). Diseased states

that have been shown to arise from dysregulation of TGM-1 are grouped into two categories. Retention hyperkeratosis and hyperproliferation associated hyperkeratosis. Retention hyperkeratosis is characterised by decreased barrier function caused by decreased TGM-1 not cross linking involucrin and loricrin, which Egberts et al. has shown to be induced by CTSD knock out mice, and is recognised in lamellar ichthyosis. Hyperproliferation associated hyperkeratosis is the exact opposite and results from increased CTSD (Kawada et al., 1997) increasing TGM-1 cross link forming activity for involucrin and loricrin.

6.1.1.2 Ingenuity pathway analysis

The observation that stratum corneum compaction was caused by TCDD treatment in the epidermal equivalent model allowed parallels to be drawn between the effects in this model and stratum corneum compaction observed in chloracne follicles and comedones and the well researched disease group of ichthyosis, specifically Sjogren-Larsson syndrome. To explore the extensive literature efficiently, a bioinformatical approach was taken. Ingenuity pathway analysis was carried out to determine known direct and indirect interactions between the AhR pathway and genes or phrases implemented in the phenotypic characteristics of ichthyosis and the mechanisms behind these. This technique was performed on our behalf by Stephanie Roberts at Alderley Park, AstraZeneca. Two methods were involved in this, text mining and pathway analysis. Text mining was used to identify the relationship between set phrases for the AhR and proteins that were involved in stratum corneum compaction, for example “AhR-ARNT” and “CTSD promoter” were linked by the word “binds”. Pathway analysis linked “set A”, a set of proteins involved in the AhR pathway, to intermediate proteins and “set B”, the proteins identified in the linked pathway. The hits were referenced forming a bibliography of literature verbally linking AhR to stratum corneum compaction phrases.

The main paper identified, Wang et al., located an Sp1 binding site and XRE promoter domain upstream of CTSD (Wang et al., 1999). Regulation by the Sp1 protein and binding site by nuclear receptors such as the ER and AhR is quite complex, and described in more detail in section 1.4.1.1 of the introduction. They have shown that CTSD is regulated by 3 regions, the ERE, Sp1 and XRE. Figure 1.3 demonstrates the promoter regions and receptor interactions forming the complex regulation of CTSD (Wang et al., 1998). AhR-dependent regulation of CTSD is not only by the XRE, but

also via interactions with the Sp1 protein (Wang et al., 1998). This is not thought to be cell specific, but has mainly been studied in breast cancer cell lines such as MCF-7 cells, due to their dependence *in vivo* on oestrogen. CTSD regulation has not been studied in keratinocytes in regards to TCDD inhibition of ER regulated CTSD before. In the presence of an ERE and E2 ligand, ER binds to the promoter, up regulating CTSD protein expression. However, the ER also binds to Sp1 protein, which in turn binds to the Sp1 binding site, inducing basal activity; the Sp1 protein often requires binding of another nuclear receptor to induce activity and is unable to do so alone. The AhR also binds to the Sp1 protein and in the presence of TCDD breaks ER-Sp1 binding, inhibiting ER-dependent induction of CTSD (Chen et al., 2001; Gierthy et al., 1993; Khan et al., 2006; Krishnan et al., 1995; Porter et al., 1997). Interestingly, and of relevance to keratinocytes, Wang et al. also described the relevance of inactive AhR inducing maximal CTSD basal activity, providing a physiological role for the AhR (Wang et al., 1998; Wang et al., 1999).

Not only is CTSD known to be induced in breast cancer, endometrial cancer (both oestrogen dependent (Westley and May, 1987)) (Masson et al., 2011; Rochefort et al., 1988; Rochefort et al., 1989) and lung cancer (Vashishta et al., 2006) but its levels are also induced during development (Zuzarte-Luis et al., 2007) in wound healing, demonstrated mainly in the skin (Hernandez-Cueto et al., 1987; Lorente et al., 1987; Vashishta et al., 2007). Vashishta et al. demonstrate that under stress conditions including heat shock or oxidative stress and wound healing, HaCaTs secreted increased amounts of pro-CTSD (corresponding with CTSD secretion in tumours (Ohri et al., 2008)). Levels of pre-pro and active CTSD in the lysates remained stable but pro CTSD was decreased. This is thought to have an autocrine effect of increased proliferation and migration (Vashishta et al., 2007). Increased CTSD in breast cancer cell lines has been shown to specifically induce proliferation, invasion and metastasis, which when considered with the anti-oestrogenic effects of AhR activation, suggests that AhR agonists may be a useful therapeutic tool (Zhang et al., 2009), and that hyper proliferation and mobility are the characteristics required in wound healing too.

6.2 Results

6.2.1 Regulation of Cathepsin D by AhR activation

In order to show the functional link between AhR and CTSD expression in keratinocytes, we treated epidermal equivalents with 10nM TCDD, 15 μ M β -NF or 1 μ M

ITE for 7 days as described in materials and methods and cut paraffin embedded sections for IHC (section 2.2.3). An anti-CTSD antibody was used with DAB linked secondary antibody which was specific to a region of CTSD present in all 3 forms of CTSD, pre-pro CTSD, pro CTSD and active CTSD. Therefore it is difficult to distinguish the forms of CTSD by IHC. Pre-pro and pro CTSD are found in the Endoplasmic reticulum and endolysosome (respectively) and as CTSD moves to the lysosome it is processed to its mature or active form. CTSD staining can be cytoplasmic (associated with apoptosis as described in section 1.4.2.1 in the introduction) or punctate within the lysosome.

Different CTSD antibodies were used in the project for DAB IHC and probing Western blotting membranes. The CTSD antibody for IHC (Abd serotec) recognised a sequence present in all forms of CTSD and was optimised and staining performed with the help of Kate Brown at AstraZeneca, Macclesfield. The antibody used in Western blotting (Calbiochem) was optimised for concentration and conditions of incubation based on manufacturers instructions, but was a clean antibody as shown in Appendix AA. The different forms of CTSD were all recognised apart from the small active chain of 14 kDa and were deciphered by their relevant sizes compared to each other and the protein standard. The antibody was chosen based on its use in the literature (Egberts et al., 2004; Heinrich et al., 2004).

Vehicle treated samples showed low levels of punctate CTSD staining confined to the granular layer. In TCDD, β -NF and ITE treated samples, increased punctate CTSD staining was present throughout the VCL, including aberrant expression in the basal and spinous layers (Figure 6.1). The effects seemed more marked for TCDD. It is unclear from these data whether this staining represented an increase in size or number of CTSD containing lysosomes, or a fusion of lysosomes. The increased and aberrant CTSD by AhR agonist treatment is consistent throughout the donors and AhR agonist.

Interestingly, an AhR agonist-induced increase in CTSD is opposite to what would be expected considering the TCDD-inhibition of oestrogen receptor induced CTSD as described in the previous paragraphs. Because of the major post translational modifications that CTSD undergoes and localisation of specific forms of CTSD, this may well not represent transcriptional up-regulation of CTSD but could suggest an accumulation of CTSD caused by mechanisms such as blocked secretion (as a

response to stress or in tumours (Vashishta et al., 2006; Vashishta et al., 2007)), or increased post translational modification to lysosomal or punctate CTSD that may relate to an increase in lysosomes. In relation to apoptosis, lysosomes are permeabilised allowing secretion of CTSD into the cytoplasm (described in section 1.4.2.1 and (Baumgartner et al., 2007; Guicciardi et al., 2004)). This would almost certainly cause an opposite effect to that shown in Figure 6.1, showing decreased punctate staining and an increase in cytoplasmic staining. Even though the data here may be difficult to interpret fully, we can conclude (along with Figure 4.4 and Figure 4.5) that CTSD-dependent apoptosis had not been induced.

Liu et al. have recently shown TGM-1 mRNA levels to be increased in chloracne (discussed in Chapter 4). In diseased states with increased TGM-1, increased CTSD is normally the causative factor, because of its direct role in TGM-1 activation (Figure 1.5). This shows that increased CTSD in epidermal equivalents does correspond with the group of hyperproliferation associated hyperkeratosis, described in Chapter 7 (Figure 7.2), although it is contradictory to the Western blot data in monolayers.

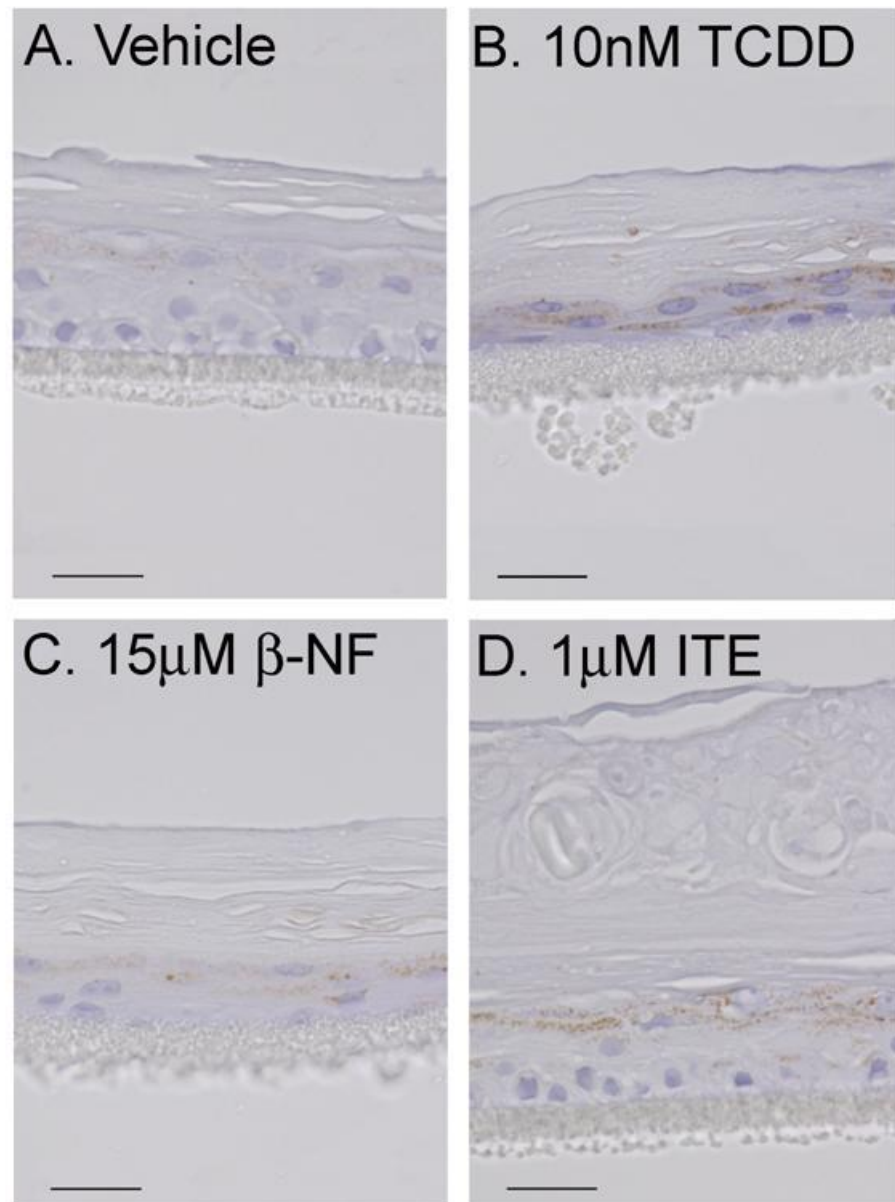


Figure 6.1. Cathepsin D staining increased and became dysregulated with AhR activation. Epidermal equivalents were treated with vehicle or AhR agonists as indicated. After 7 days, epidermal equivalents were fixed, embedded in paraffin and immunostained with anti-cathepsin D (CSTD) antibody, anti-mouse secondary and DAB staining (brown), and counterstained with haematoxylin. Images are representative of equivalents from 3 (Vehicle and TCDD) or 2 (β -NF and ITE) separate donors. Scale bar = 20 μ m.

To define any alterations in expression or maturation, Western blotting was used to distinguish the effects of AhR activation on pre-pro and pro CTSD compared to active CTSD. Different forms of CTSD can be distinguished by Western blot because the post-translational modifications during CTSD maturation result in different sized molecules for each form. CTSD maturation is a complex process and described in more detail in

section 1.4.1.2, but as an overview, low pH causes dissociation of receptors and phosphates from the synthesized 54 kDa pre-pro-CTSD in the golgi body to form 48kDa pro-CTSD in endolysosomal compartments, then it is cleaved by cathepsins B and L to the double chain mature CTSD of 34kDa and 14kDa located to the lysosomes. In section 6.2.1, densitometry has been carried out on combined pre-pro and pro-CTSD (“pro-CTSD” here will indicate pre-pro- and pro-CTSD including any smaller intermediate molecules formed during normal processing), with active CTSD separately analysed. Only the processing from golgi/endosomal pro-CTSD to the active lysosomal CTSD will be discussed here, as this is the main form involved in autophagy and there are other forms of pre CTSD intermediate molecules formed during processing, that characterising all of them would require far more specific assays.

Primary keratinocytes were treated for up to 8 days with TCDD, β -NF or ITE, lysed and Western blotting performed. Membranes were probed with anti-CTSD and anti-AhR primary antibodies with anti- β -actin as loading control. As in previous chapters, α -NF co-treated samples were run in parallel, but this data is presented later in the chapter for clarity.

6.2.1.1 TCDD

Figure 6.2 and Figure 6.3 show primary keratinocytes treated with vehicle or concentrations of TCDD for 6 and 8 days respectively. In contrast to the data observed in epidermal equivalents analysed by IHC (Figure 6.1), TCDD treatment did not appear to increase levels of CTSD in monolayer culture. However, these results are consistent with the literature that showed that TCDD decreased CTSD by inhibiting ER-dependent processing (Chen et al., 2001; Safe and Wormke, 2003; Zhang et al., 2009). Both antibodies used here detected all forms of CTSD but they can be distinguished only by Western blot. As previously reported, TCDD effects were most marked at 8 days (Figure 6.3), and consistent with this, TCDD-induced degradation of AhR was most pronounced at this time point. Figure 6.2, Figure 6.3, Appendix Q and Appendix R show that pro-CTSD was slightly decreased by TCDD treatment at days 2, 4 and 8. Figure 6.2, Figure 6.3, Appendix Q and Appendix R also show a decrease in active CTSD caused by TCDD treatment at days 2, 4 and 8. Basal levels of active CTSD appeared higher at days 6 and 8 in primary keratinocytes, and at day 8 TCDD exerted its greatest effect on active CTSD. This corresponds to the rest of our data in previous chapters, showing

AhR-dependent effects on proteins often occurred at the later time points and could be caused by increased CTSD levels as keratinocytes begin to differentiate in monolayer culture.

The CTSD densitometry did not give a clear result as the error bars were large compared to the scale and the induced effects were not large. Two-way ANOVA was performed to compare vehicle to TCDD treatment at each time point, but as expected no effects were significant. Based on previous data, results at days 6 and 8 are more likely to be AhR-dependent. However it is difficult to decipher a single effect of TCDD on pro CTSD because of its variable effects. Concentrating on day 6 and 8, TCDD appeared to induce up-regulation of pro CTSD at day 6 but down-regulation at day 8, although if the error bars are considered, these effects may not be real. Considering Figure 6.2, Figure 6.3 and Appendix Q, no similar patterns of pro or active CTSD induction were shown by single donors; for example, one donor showed decreased active CTSD by co-treatment with TCDD and α -NF, while another showed increased active CTSD with co-treatment and the third showed no discernable pattern. Active CTSD densitometry data appear more convincing because of the more definite pattern of down-regulation at day 8. Despite this inconclusive data, the CTSD antibody does seem valid, there is a general increase in CTSD levels (more prominent in active CTSD) over time which would correlate with the increased expression of CTSD in differentiated keratinocytes, which would be occurring at days 6 and 8.

The main point we can conclude from this data is that Western blots on monolayer keratinocyte cultures may not be the ideal model to study CTSD levels and activation. Because of the complex post translational modification of CTSD, in future studies it may be better to study a defined form of CTSD with a specific readout, for example CTSD activation studies. Western blots provide strong data when post translational modifications or transcriptional regulation are prominent (for example autophagic block in Figure 6.6), but Western blots may not have been sensitive enough to show differences in levels in this case. AhR activation would be likely to exert higher effects in differentiating cells or epidermal equivalents. This may be a contributing factor to the differential effects of AhR-agonists on CTSD in epidermal equivalents and Western blots, there are more effects visible in epidermal equivalents due to differentiated keratinocytes. The antibodies are different too, but validated antibodies should provide the same results.

6.2.1.2 β -NF

Figure 6.2 and Figure 6.3 show primary keratinocytes treated with β -NF for 2 and 8 days respectively, then lysed and Western blotting performed. As previously reported, β -NF effects were most marked at 2-4 days (Figure 5.3 and Appendix L) and consistent with this, β -NF-induced degradation of AhR was most pronounced at this time point. As previously discussed this may relate to β -NF inducing its own metabolism (section 3.4.2.1). Levels of pro CTSD increased with β -NF treatment most markedly at days 2 and 4 with 15 μ M β -NF (Appendix S). There was a slight increase in active CTSD levels in both basal and β -NF treated keratinocytes at days 6 and 8, the increase in basal levels could be a result of differentiation in the keratinocytes in monolayer culture, as in Figure 6.2 and Figure 6.3. Active CTSD showed a slight decrease with 3 μ M β -NF then a slight increase with 15 μ M β -NF at days 2, 4 and 8. Day 6 shows a dose dependent decrease in active CTSD. There were 2 possible causes for this decrease, it corresponded with the literature showing AhR-dependent down-regulation of CTSD, but also may be an effect of β -NF-dependent autophagic block. Pro CTSD may accumulate resulting from blocked autophagy and maturation to active CTSD in the lysosomes. This is described in more detail in Figure 6.6. This data is inconclusive due to the varied responses and is only repeated in 2 donors so no statistical analysis was performed. To confirm these results the experiments should be repeated in further donors and alternative endpoints used, for example CTSD activity assays.

6.2.1.3 ITE

Figure 6.2 and Figure 6.3 show primary keratinocytes treated with vehicle or concentrations of ITE for 2 and 8 days, lysed and Western blotting performed. Pro CTSD was decreased by ITE treatment at days 2 and 4, but increased slightly at days 6 and 8 (Appendix Q and Appendix R). As previously described, AhR-dependent effects often occurred at days 6 and 8 (although ITE induced AhR degradation at all time points, and no CYP1A1 at any time points) and as Figure 6.3 and Appendix V represents replicates in 3 donors at days 6 and 8 (data from only 2 donors was available at days 2 and 4), this data is more reliable. Based on data at days 6 and 8, Figure 6.3 shows slight up-regulation of pro CTSD and also that active CTSD was decreased by ITE, dose dependently and at all time points (Appendix U and Appendix

V). This suggests that ITE may block processing of pro to active CTSD, although little accumulation of pro CTSD occurred.

In summary, Figure 6.3 show that TCDD treatment of monolayer keratinocytes caused the trend of a decrease in pro and active CTSD at day 8, corresponding to the literature described previously in this chapter. ITE also appeared to cause a decrease in active CTSD, although pro CTSD was decreased at days 2 and 4 but increased at days 6 and 8. β -NF appeared to induce the opposite effects to TCDD, increasing both pro and active-CTSD. These variable responses between TCDD and β -NF were shown in chapter 5 in regards to TCDD induced autophagy and β -NF blocked autophagy. This would suggest that blocked autophagy and increased CTSD could be linked. Carew et al. report that chemically blocked autophagy induced an increase in CTSD by Western blot, however only one band of CTSD is shown and it does not distinguish which form of CTSD this is (Carew et al., 2011). The effects of blocked autophagy on CTSD are shown in Figure 6.6. No statistical analysis was performed due to small sample size.

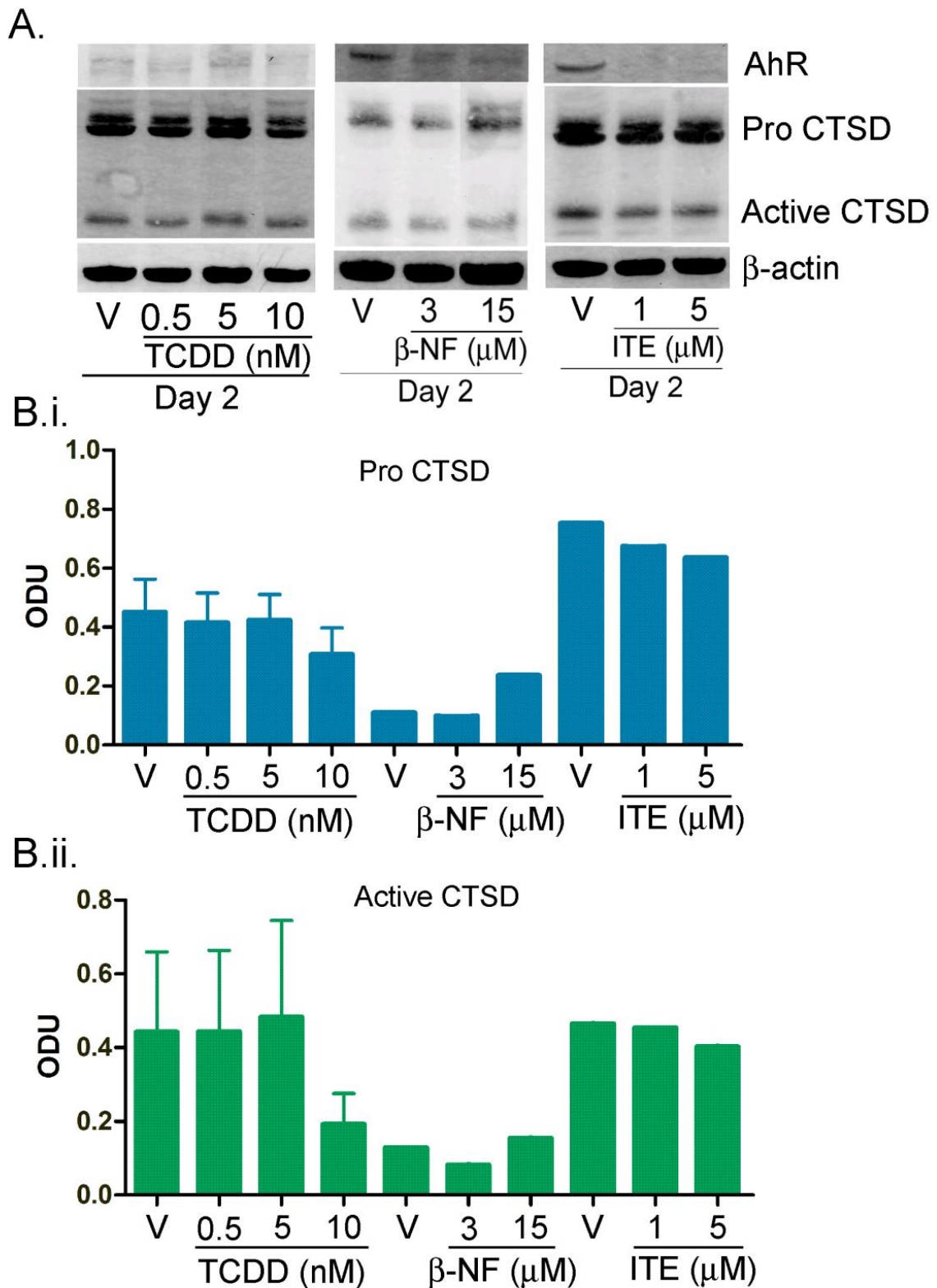


Figure 6.2. Summary of the effects of AhR activation on CTSD at day 2. Primary keratinocytes were treated for 2 days with vehicle or concentrations of ligand as indicated. Samples were lysed and Western blotting performed (A). Densitometry was carried out on blots probed with an anti-CTSD antibody showing B.i) pre-pro and pro-CTSD bands and B.ii) active-CTSD bands normalised to β -actin. Two-way ANOVA was performed to compare vehicle to ligand treated samples at each time point, but no effects were significant.

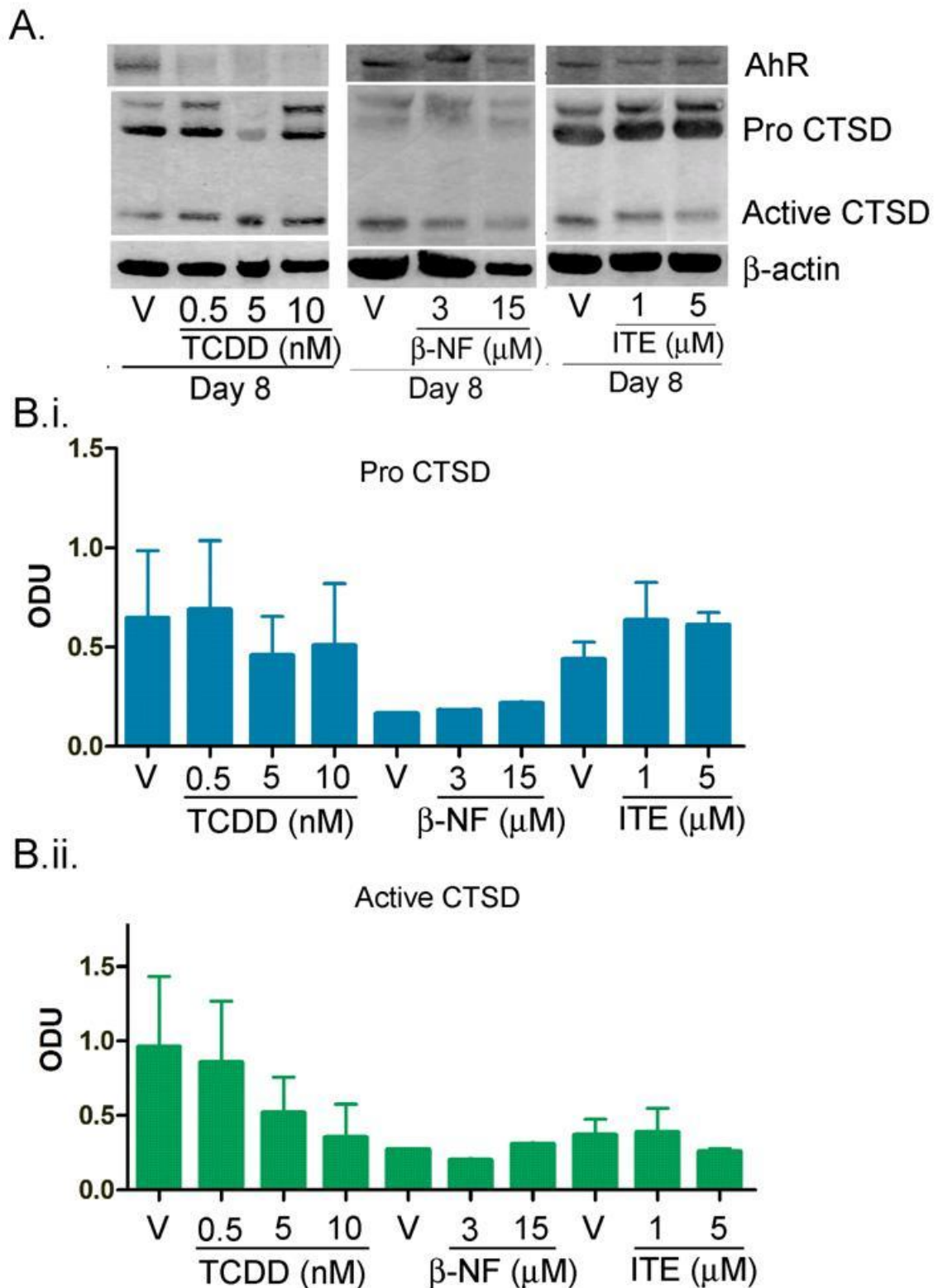


Figure 6.3. Summary of the effects of AhR activation on CTSD at day 8. Primary keratinocytes were treated for 8 days with vehicle or concentrations of ligand as indicated. Samples were lysed and Western blotting performed (**A**). Densitometry was carried out on blots probed with an anti-CTSD antibody showing **B.i**) pre-pro and pro-CTSD bands and **B.ii**) active-CTSD bands normalised to β -actin. Two-way ANOVA was performed to compare vehicle to ligand treated samples at each time point, but no effects were significant.

6.2.1.4 α -NF

To test the effects of partial AhR agonist α -NF alone on CTSD, we treated primary keratinocytes with vehicle or concentrations of α -NF as indicated for up to 8 days. As previously reported, α -NF agonistic effects were most marked at 6-8 days (Figure 3.13 and Appendix I), and consistent with this, α -NF-induced degradation of AhR was pronounced at 2-8 days. A trend towards up-regulation of pro CTSD was shown by α -NF treatment at days 2, 6 and 8 was observed most prominently at the later time points associated with AhR activation (Figure 6.5 and Appendix W). Active CTSD was slightly up regulated at day 2 by α -NF treatment, but at days 4, 6 and 8 the trend was towards down-regulation. Due to the small changes and variable effects, these results are not convincing, and more specific assays (eg CTSD activation assays) may be more sensitive to α -NF induced changes. The up-regulation of pro CTSD by α -NF did not correspond with TCDD-induced effects but is more similar to β -NF-induced effects. This would suggest (as in chapter 5) that α -NF, like β -NF, may block autophagy. Compared to β -NF, these affects were very low (Figure 5.5 and Figure 5.6 A). The varied effects of α -NF-dependent degradation of active CTSD would also correspond with β -NF-induced effects, although α -NF induced slight degradation of active CTSD at days 4, 6 and 8 so this appears to be the prominent response, corresponding more with TCDD induced effects.

Chapter 3 showed that α -NF induced low AhR activation at days 6 and 8 by AhR degradation and CYP1A1 induction (Figure 3.15 and Figure 3.16 A), which suggested a correlation with increased pro CTSD and decreased active CTSD in Figure 6.2 and Figure 6.3. This could suggest a slight blocking in conversion of pro to active CTSD, as suggested too by ITE. If these data are real, it may suggest that low levels of AhR activation blocks CTSD activation.

6.2.2 Modulation of ligand induced AhR-dependent effects on Cathepsin D by α -NF

6.2.2.1 TCDD

Data previously presented in this thesis showed inhibition of TCDD-induced AhR activation by α -NF, specifically α -NF blocked TCDD-induced AhR degradation and CYP1A1 induction (see summary Figure 3.15 and Figure 3.16). TCDD also induced autophagy that was shown to be AhR dependent by co-treatment with α -NF which resulted in inhibition of LC3 II induction, although p62 degradation was blocked resulting in higher levels than vehicle, suggesting a possible autophagic block (Figure 5.5 and Figure 5.6).

Figure 6.3, Appendix Q and Appendix R show that TCDD appeared to induce some degradation of both pro and active CTSD at 4, 6 and 8 days, consistent with previous reports in the literature in the MCF-7 cell line (Krishnan et al., 1995). However this did not reach statistical significance. Figure 6.4 B shows that TCDD induced down-regulation of pro CTSD was inhibited at day 2 mainly by 5 μ M α -NF, returning levels of pro CTSD to higher than basal levels. Day 4 showed more varied effects, with both increased and decreased levels of pro-CTSD by α -NF co-treatment depending on TCDD concentration (Appendix Q). Again, TCDD induced some degradation of active CTSD (most consistent at day 4) which appeared to be blocked by α -NF co-treatment. TCDD induced degradation of AhR at days 2, 4, 6 and 8, and CYP1A1 induction at days 6 and 8. This was consistently blocked by α -NF at all time points and dose combinations (Appendix B and Appendix C). This suggests that the effects of TCDD co-treatment with α -NF are caused by inhibition of AhR activation, which is the predominant effect of this compound combination.

As described previously in chapter 5, the patterns of expression on the blots shown do not always correspond to the patterns shown by pooled data from 3 donors. This could be caused by the individual effects induced by each donor being masked by data from other donors that do not follow the same time dependent expression. This is one of the issues with pooling data, but I have considered patterns of expression in each donor and included observations on the consistency between donors.

Appendix R shows that at day 6, co-treatment of TCDD plus α -NF induced up-regulation of pro CTSD, returning levels of pro CTSD to higher than basal levels. Day 8 showed

some up-regulation of pro CTSD by TCDD and α -NF, but this was more varied and levels were not increased higher than basal levels (Figure 6.5). TCDD and α -NF had a small and variable effect on active CTSD at day 6, whereas at day 8, co-treatment of TCDD (0.5 and 5nM) and α -NF induced further down-regulation of active CTSD. 10nM TCDD plus α -NF at day 8 induced active CTSD from 10nM TCDD alone, but did not restore levels to basal levels.

Considering the literature and the results shown in Figure 6.5, Appendix Q and Appendix R, we hypothesise that α -NF did not block TCDD-dependent inhibition of CTSD because α -NF may induce the conformational changes leading to ER-dependent CTSD inhibition too. Other typical AhR agonists have not been tested for ER inhibition but diindolylmethane (DIM), a known anti-oestrogen (Chen et al., 2001) and compounds with similar structures to TCDD were shown to also inhibit ER-induced CTSD or CTSD in ER null models (Zhang et al., 2009). α -NF may or may not have potential to inhibit ER-Sp1 binding or it may depend upon the concentrations of α -NF and whether it is acting primarily as an agonist or antagonist. However α -NF is likely to induce AhR degradation regardless of agonist or antagonistic activity because of its mechanism of action inducing translocation and degradation independent of XRE binding (Song and Pollenz, 2002) resulting in a deficiency of inactive AhR available to induce maximal basal CTSD expression in conjunction with Sp1 (Wang et al., 1999). Therefore, to test the AhR dependence of TCDD-induced CTSD down-regulation, an AhR inhibitor that would stop AhR activation but allow the persistence of inactive AhR to induce maximal basal CTSD expression would be required. Instead of pharmacological intervention, this may be possible by molecular intervention; making a constitutively inactive AhR could be achieved by removing the ligand binding domain of the AhR, but nuclear shuttling would still be required because Sp1 binding requires nuclear AhR in an inactive conformational. Alternatively (and more easily) an alternative AhR inhibitor such as 3-MNF could be used to block ligand-activated effects of AhR.

6.2.2.2 β -NF

Section 3.3.2 showed that β -NF-dependent AhR activation was partially increased by co-treatment with α -NF (this result varied across time and dose response). β -NF was shown to block autophagy, which was directly opposite to the effects of TCDD-induced AhR activation of autophagic induction (section 5.2.3). β -NF-dependent autophagic block was inhibited by α -NF, but no autophagy was induced at days 2 and 4 (section 5.2.4.3, Appendix L), while at days 6 and 8 co-treatment with α -NF and β -NF did induce further autophagic block (Appendix M).

β -NF treatment alone induced levels of pro-CTSD as shown in Figure 6.4 and Figure 6.5 and exerted variable effects on active CTSD throughout doses. These figures also show that co-treatment with β -NF and α -NF at most dose combinations and at both time points consistently induced levels of both pro and active CTSD at days 2 and 4 often to levels higher than basal levels. β -NF data is only representative of 2 donors, but patterns of increased active CTSD in β -NF and α -NF co-treated samples were apparent in both donors. Moreover, these results are in line with the effects of α -NF on β -NF-induced responses as described in Chapter 3.

As shown in chapter 5, co-treatment of α -NF and β -NF did not result in further induction of autophagic block at days 2 and 4 (Figure 5.5 and Appendix L), but instead suggested AhR dependent inhibition of β -NF-induced autophagic block. Co-treatment of β -NF and α -NF also variably induced AhR activation to higher levels than β -NF alone, but with no induction of autophagy. If this occurred, we would have expected to see a decrease in pro CTSD (the accumulation of pro CTSD caused by blocked autophagy would be expected to decrease) and increase in active CTSD as processing of pro to active CTSD occurred once more (it became inhibited during autophagic block, see Figure 6.6). This is not the case, as increased pro CTSD was the trend, and probably indicates that this data is not robust enough to draw specific conclusions from. These results may be clarified in further work using a different AhR inhibitor that does not confuse the results by causing increased AhR activation in combination with other AhR ligands.

Appendix T shows varied effects of co-treatment with α -NF and β -NF on pro CTSD at days 6 and 8. However, active CTSD was down regulated by α -NF consistently at days 6 and 8 by all dose combinations. This is opposite to the effects observed at days 2 and 4 (Appendix S). Taken together, co-treatment with α -NF and β -NF induced either no

effect or an increase in pro-CTSD levels. Active CTSD was increased at days 2 and 4 quite consistently but the effects were low, and at days 4 and 6 co-treatment with α -NF and β -NF induced consistent down-regulation of active CTSD. This direct contrast is interesting and suggests that the effects seen at early time points may be AhR-independent mechanisms, because AhR-dependent effects have been shown mainly at days 6 and 8.

The differential effects between days 2/4 and 6/8 could be a result of β -NF inducing its own metabolism by CYP1A1. I have shown that β -NF induced CYP1A1 at days 6 to 8 in chapter 3, and Berghard et al. show the functional effects (prolonged AhR activation) of inhibited CYP1A1 in keratinocytes (Berghard et al., 1992). This would lower the available concentration of β -NF, causing α -NF to elicit the predominant effects on CTSD, which I have shown in Appendix W, where α -NF alone at days 6 and 8 induced slight increase in pro CTSD and slight decrease in active CTSD.

6.2.2.3 ITE

As previously described, ITE induced AhR activation by transcriptional activation (Figure 3.7) and consistently degraded AhR at all time points studied (days 2-8) but did not result in CYP1A1 induction (Figure 3.10 and Figure 3.11). ITE-induced transcriptional activation measured by luciferase assay was inhibited by α -NF (Figure 3.14) but co-treatment of α -NF consistently increased ITE-induced AhR activation as assessed by AhR degradation on Western blotting. Moreover, CYP1A1 induction was only induced by co-treatment with ITE and α -NF (Figure 3.15 and Figure 3.16). ITE induced active autophagy as assessed by p62 degradation and LC3 II up-regulation (Figure 5.3 and Figure 5.4), and EM (Figure 5.9). Co-treatment of ITE and α -NF showed increased p62 and LC3 II which (as the levels were higher than basal levels in α -NF treated samples) suggested blocked autophagy.

Figure 6.3 showed that ITE treatment of primary keratinocytes induced pro CTSD at day 8, and decreased active CTSD at days 2-8 (Appendix U and Appendix V). Figure 6.4 D shows that the ITE induced down-regulation of pro CTSD was inhibited by α -NF consistently through time and dose at day 2. The levels that pro CTSD recovered to were slightly higher than basal levels. α -NF also consistently blocked the ITE-dependent down-regulation of active CTSD levels, returning them to similar levels to

basal levels. Taken together with the increased AhR degradation caused by co-treatment of ITE and α -NF, (as shown in Figure 3.16 D) this suggests that increased AhR activation by ITE and α -NF blocked the activation of CTSD.

Figure 6.4 D is consistent with Figure 6.5 D showing co-treatment of α -NF and ITE at days 2 and 8 induced levels of pro CTSD consistently over time and dose. Figure 6.5 D shows that α -NF decreased levels of active CTSD at days 6 and 8, the opposite effect to that seen at days 2 and 4 (Figure 6.4 D). As in Figure 6.4 C and Figure 6.5 C (the effects of β -NF) the active CTSD data is contradictory between early and late time points. This has not occurred with co-treatment of TCDD and α -NF, but has with β -NF, which suggests that the differential effects may be caused by changes to the balance of ITE/ α -NF that may be caused by increased metabolism of ITE.

As discussed previously the metabolism of ITE is not defined but like other AhR agonists (especially physiological ones), it is expected to be quick and induced by AhR activation. The effects at days 6 and 8 may be a result of increased metabolism of ITE, which would mean that the effects shown in Figure 6.5 D are more dependent on α -NF, which would correspond with the effects of α -NF alone on increased pro CTSD and decreased active CTSD (Figure 6.5 A).

6.2.2.4 Summary of effects of AhR activation on CTSD

In summary, TCDD induced down-regulation of pro and active CTSD. TCDD-dependent down-regulation of pro-CTSD was inhibited by α -NF, but this data was variable (Figure 6.4 B and Figure 6.5 B). TCDD-induced down-regulation of active CTSD was consistently further down regulated by α -NF treatment, suggesting that α -NF exacerbated TCDD-dependent effects on CTSD.

β -NF alone induced up-regulation of pro CTSD and down-regulation of active CTSD, suggesting it was accumulated due to inhibited processing of pro CTSD to active CTSD by blocked autophagy. Co-treatment of β -NF with α -NF resulted in exacerbated β -NF-dependent effects and further accumulation of pro CTSD (Figure 6.4 C and Figure 6.5 C). The effects of α -NF on β -NF-dependent effects at days 2 and 4 showed consistent additional induction of active CTSD (Appendix S) but at days 6 and 8, α -NF treatment consistently down regulated active CTSD levels, thereby further exacerbating the effects of β -NF (Appendix T). This suggests β -NF dependent autophagic block was

induced further by α -NF, inducing pro CTSD accumulation and blocked processing to active CTSD.

α -NF alone consistently induced pro CTSD, which at days 2 and 4 inhibited ITE induced down-regulation (Appendix U) and at days 6 and 8 exacerbated ITE induced up-regulation of pro CTSD (Appendix V). Like β -NF, active CTSD was effected by α -NF differentially over time; days 2 and 4 showed increased active CTSD with α -NF treatment (Appendix U), while days 6 and 8 showed decreased active CTSD with α -NF treatment (Appendix V). The common characteristic between β -NF and ITE is their quick metabolism, which is induced by AhR activation. After 6 and 8 days treatment, this is likely to be the mechanism behind the differential effects, although interestingly, only active CTSD is affected. This could be studied further by inhibiting the metabolism of β -NF and ITE and testing whether the effects shown (increased active CTSD) would persist at days 6 and 8.

Overall, α -NF did not block AhR agonist-induced inhibition of CTSD perhaps in part because the mechanism of α -NF as an antagonist still exerts the effects required for CTSD inhibition via ER inhibition. α -NF induces AhR degradation as other agonists and non-agonists can (geldanamycin), by inducing nuclear translocation and degradation independent of DNA binding (Song and Pollenz, 2002). This may still result in decreased levels of AhR, inhibiting maximal basal expression of CTSD via Sp1. This may account for the results observed when co-treatment with TCDD and α -NF induced AhR-dependent CTSD inhibition further.

ITE and β -NF showed variable effects on CTSD over time. Both AhR agonists were shown to induce AhR activation at days 6 and 8 in chapter 3 (Figure 3.11 C and D), although AhR degradation did occur from days 2-8 for TCDD, β -NF and ITE (see Table 5). As this data set showed large differences between the effects of AhR activation and inhibition at early and late time points, the later time points have been considered to be more robust based on the consistent protein markers of AhR activation showing signs of AhR activation at days 6 and 8 in the previous chapters.

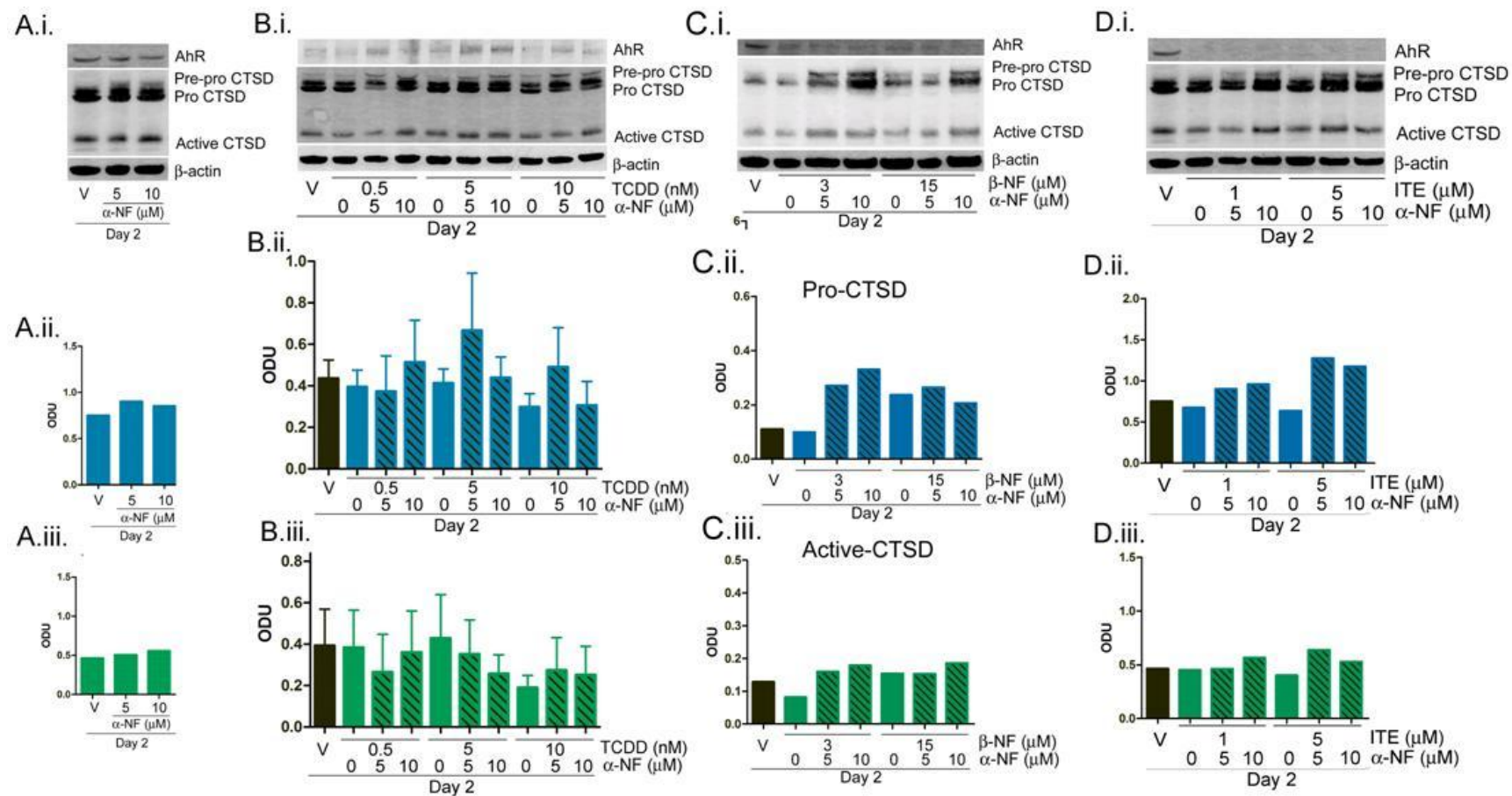


Figure 6.4. Summary of the effects of AhR-agonists and α -NF on Cathepsin D. Primary keratinocytes were treated with vehicle of concentrations of **A)** TCDD, **B)** β -NF or **C)** ITE as indicated. After 2 days cells were lysed and Western blotting performed using an anti-CTSD antibody and β -actin as loading control. Bands were analysed by densitometry and presented as optical density units normalised to β -actin. Western blot is representative of duplicate blots in 2 or 3 donors. Values for densitometry represent means of 2 blots (B) or mean \pm sem for 3 blots (A and C). Two-way ANOVA was performed to compare TCDD treatment to vehicle and time. **B)** Analysis was not significant. **A, C, D)** No statistical analysis was carried out due to low sample size.

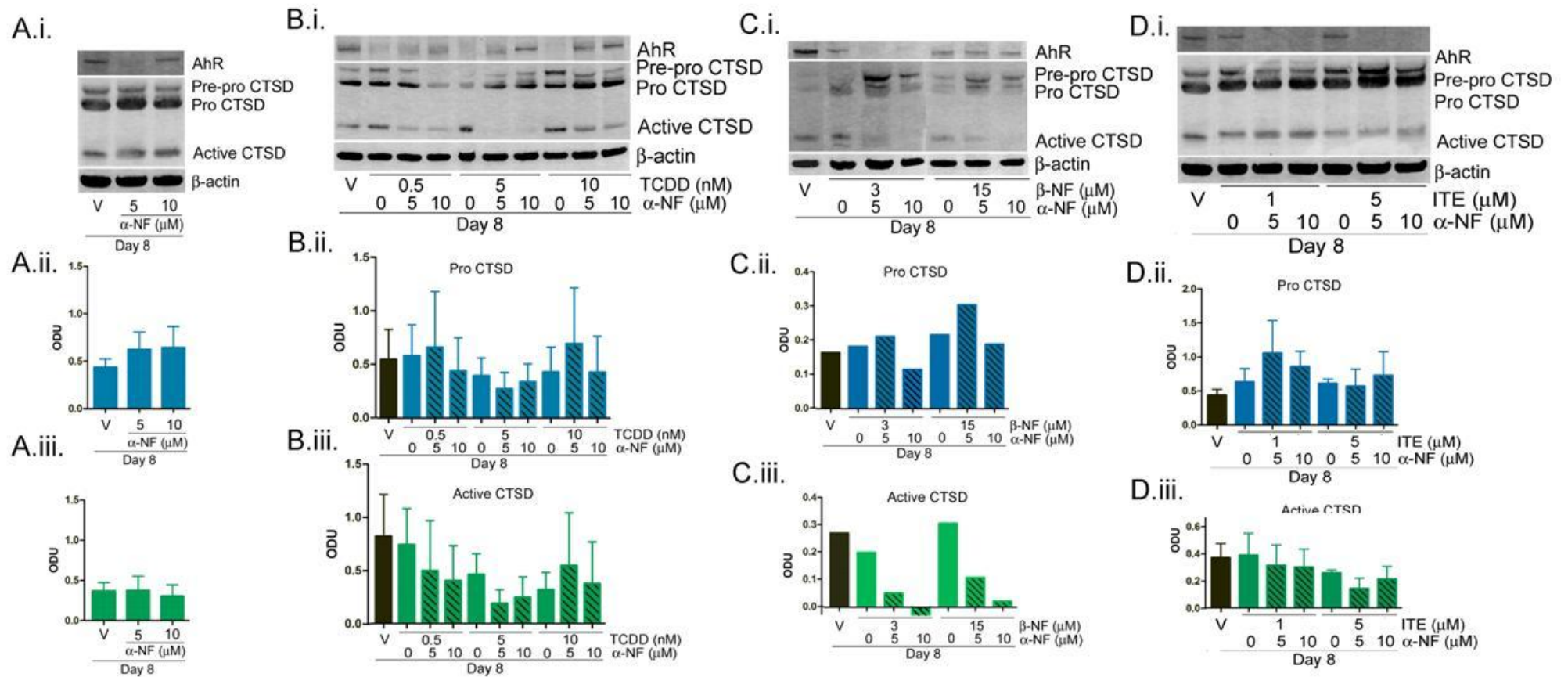


Figure 6.5. Summary of the effects of AhR-agonists and α -NF on Cathepsin D. Primary keratinocytes were treated with vehicle or concentrations of **A)** TCDD, **B)** β -NF or **C)** ITE as indicated. After 8 days cells were lysed and Western blotting performed using an anti-CTSD antibody and β -actin as loading control. Bands were analysed by densitometry and presented as optical density units normalised to β -actin. Western blot is representative of duplicate blots in 2 or 3 donors. Values for densitometry represent means of 2 blots (B) or mean \pm sem for 3 blots (A and C). Statistical analysis is described in the previous figure.

6.2.3 Effects of autophagic block on CTSD

Despite the close links between lysosomes and autophagy, (lysosomes process the main degradative material in the autophagy pathway described in section 1.5.1, there is little known data on the effects of CTSD on autophagy. Carew et al showed evidence that autophagic block increased levels of CTSD, however the form of CTSD presented in the paper was not defined (Carew et al., 2011). Blocked autophagy was also reported to increase apoptosis by pro CTSD accumulation and lysosomal disruption, resulting in cytoplasmic CTSD which activated apoptosis via caspase-8 or Bid (as described in section 1.5.1.3) (Baumgartner et al., 2007; Boya et al., 2005; Heinrich et al., 2004).

We hypothesized therefore that agonist-activated AhR regulated CTSD, that AhR activation induced autophagy and that there may be a functional regulatory link between autophagy and CTSD. This was also suggested by the differential effects of AhR activation by TCDD and β -NF, active autophagy was induced by TCDD while β -NF blocked autophagy and TCDD-induced effects were stable over time, while β -NF (and ITE) induced opposite effects on active CTSD during days 2 and 4 compared to days 6 and 8.

To test the effects of autophagic block on CTSD, Bafilomycin A1 was utilised to induce autophagic block as shown in Figure 5.7. Bafilomycin A1 is a compound that inhibits the acidification of lysosomes that allows fusion between lysosomes and autophagosomes, resulting in blocked autophagy (as described in section 5.2.5). Primary keratinocytes were treated with either bafilomycin A1, pepstatin A (a specific CTSD inhibitor) or ligand, or co-treated with ligand and Bafilomycin A1. Pepstatin A is an inhibitor of CTSD activity (specific to aspartyl proteases) (McAdoo et al., 1973). Cells were treated with this to see the effects of the inhibition of CTSD activity on autophagy and any effects of blocked CTSD activity on autophagy (by LC3 II and p62). Western blotting was performed with anti-CTSD, anti-p62 and anti-LC3 antibodies to identify the effects of autophagic block on CTSD maturation. Because of the exaggerated and defined effect of autophagic block on pre-pro CTSD, pre-pro and pro CTSD bands were analysed by densitometry separately for this experiment.

Notably, blockage of autophagy by treatment with Bafilomycin A1, caused a marked reduction in processing of CTSD to active CTSD (Figure 6.6). CTSD appeared to

accumulate in pre-pro CTSD, while pro CTSD levels remained unaffected consistent with previous findings of (Baumgartner et al., 2007; Boya et al., 2005; Heinrich et al., 2004). The block of pro CTSD processing to active CTSD suggests that autophagy is required for CTSD processing to the lysosomes, or that the mechanism by which Bafilomycin A1 blocked autophagy (by inhibition of lysosomal acidification) is required for the final steps of CTSD maturation, which corresponds to reports in the literature (described in section 1.4.1.2 and reviewed in (Zaidi et al., 2008)). In contrast, Pepstatin A did not affect LC3 I or II, or p62, suggesting that inhibition of CTSD activation did not affect autophagy, or that inhibited CTSD activity did not inhibit its own maturation. The effects of blocked autophagy on CTSD here are clear, however unfortunately, TCDD, β -NF and ITE have not clearly up-regulated LC3 II as shown previously (section 5.2.4), so it is difficult to decipher the AhR-dependent effects. I believe that this is probably caused by the high effects of autophagic block masking the smaller ligand-induced effects. It could also be due to the time point chosen which was at 2 days, and I have shown many ligand induced effects on LC3 II/p62 at later time points. In future work I would run a time course using Bafilomycin A1 treated and co-treated cells to investigate this effect further.

The hypothesis that active autophagy is coupled with increased processing of pro CTSD to active CTSD would correspond with the IHC data showing increased punctate (lysosomal) CTSD staining in TCDD and ITE treated epidermal equivalents (Figure 6.1). Western blots in Figure 5.3 to Figure 5.6 do not correspond with this hypothesis. However, β -NF also induced up-regulation of punctate CTSD staining by IHC, suggesting that this result is not specific to activated autophagy and because all ligands induced CTSD punctate staining in epidermal equivalents (Figure 6.1), this may represent the differential effects of AhR activation in epidermal equivalents compared to keratinocytes. Considering that autophagy blocked by Bafilomycin A1 inhibited the processing of active CTSD, it could be presumed that induction of active autophagy would upregulate active CTSD. There are reports in the literature suggesting that CTSD levels regulate autophagy, by increasing the amount of protein degradation in the cell via increased numbers of lysosomes and therefore increasing the required numbers of autophagosomes to remove the degraded material (Settembre and Ballabio, 2011; Settembre et al., 2011).

The link between autophagic block and CTSD accumulation in primary keratinocytes is a novel observation. Carew et al have reported increased levels of an unidentified form of CTSD in MCF-7 cells that lead to lysosomal permeabilisation (Carew et al., 2011) and AhR has also been linked to lysosomal fragility (Caruso et al., 2004).

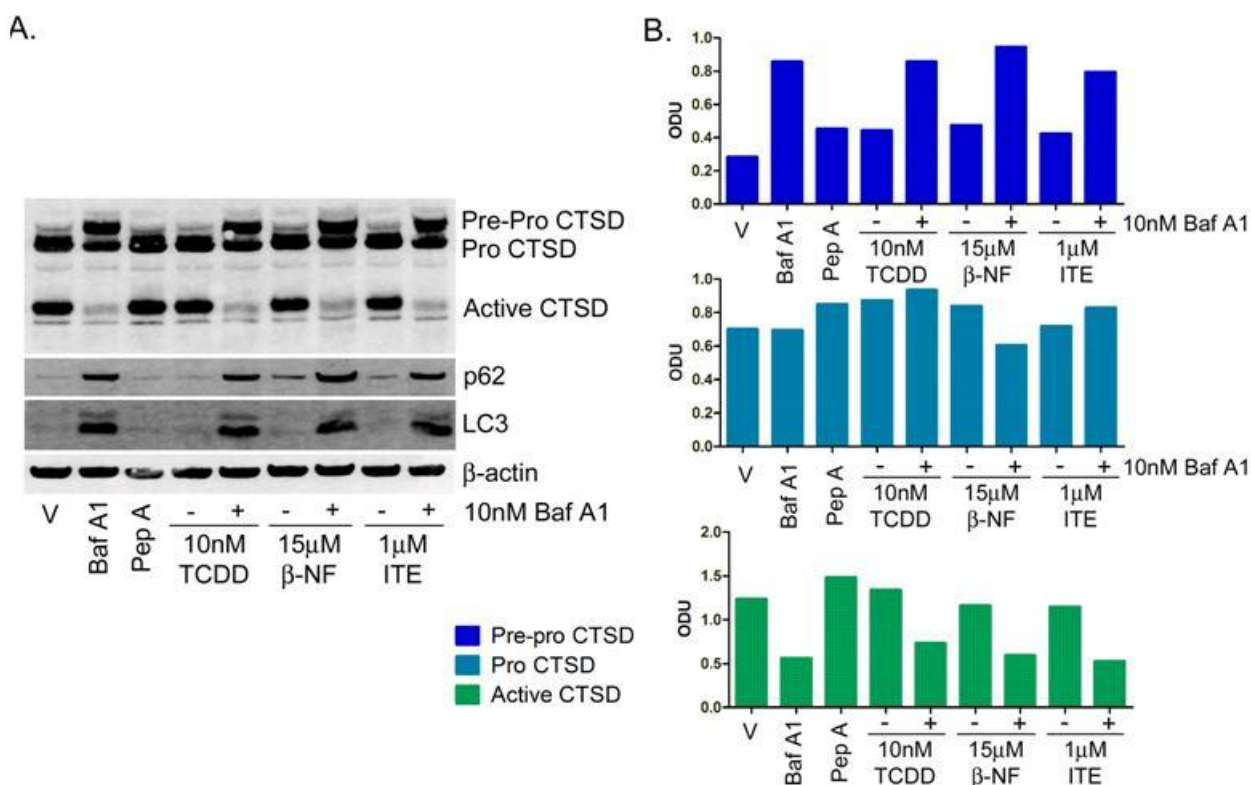


Figure 6.6. Blocked autophagic by Bafilomycin A1 inhibits Cathepsin D processing. Primary keratinocytes were treated with vehicle, ligand, bafilomycin A1, pepstatin A or cotreated with ligand plus bafilomycin A1. After 24h cells were lysed and Western blotting performed. Blots were probed with antibodies against CTSD, p62, LC3 and β-actin as loading control. **A)** Western blot is representative of blots from 2 donors. **B)** Densitometry was carried out on CTSD bands for pre-pro CTSD, pro CTSD, and active CTSD and presented as optical density units (ODU) normalised to β-actin. Mean values are shown from 2 donors. Statistical analysis was not carried out due to low sample size.

6.2.4 Live cell localisation of CTSD

As described in this chapter and in section 1.4, CTSD has many different functions in the cell and localisation can depend upon which function is being undertaken. To observe the changes in lysosomal (active) CTSD with following AhR activation and induction of autophagy, a CTSD specific fluorescent marker, BODIPY PA was utilised to visualise CTSD in lysosomes for live cell confocal image analysis (Figure 6.7). BODIPY FI-Pepstatin A (referred to as “BODIPY PA” in this thesis) specifically binds to active

CTSD in the lysosome at pH 4.5, when the conformation of CTSD reveals the active site. BODIPY PA also fluoresces in an unbound state at higher non-acidic pH.

Dithranol was used as a positive control for inducing autophagic activation. It has been shown previously in our group (Milner and Reynolds, 2012)(unpublished data) that treatment of primary keratinocytes with 5 μ M dithranol for 24h induced autophagy, as measured by the biomarker LC3 II induction by Western blot and other markers.

Primary keratinocytes were pre-treated for 1h with vehicle, 10nM TCDD or 5 μ M dithranol and 1 μ M BODIPY PA. CTSD responses to AhR-activation were expected to be fast, due to the quick responses showed by Menon et al., that CTSD containing lamellar bodies began regenerating 30 minutes after barrier stress (tape stripping or acetone) and by 6 h, numbers of lamellar bodies had returned to normal (Menon et al., 1992a) , so we started using this time frame to measure early effects on CTSD. Keratinocytes were imaged overnight (up to ~11h). Live cell imaging is included on a disc (Appendix BB) and selected frames are included in Figure 6.7.

Vehicle treated cells (Figure 6.7 top row) showed lysosomal staining that was predominantly perinuclear but lysosomes were seen to travel to the outer cell membrane. The staining intensity was constant throughout, with no apparent changes in speed or pattern of lysosomal movement.

Dithranol treated keratinocytes at early time points (1h 30 mins, Figure 6.7 second row), showed that puncta were more widely distributed than the perinuclear region. At ~4h, a large increase in staining was seen in every cell and the development of membrane blebbing occurred. These membranes were lined with BODIPY PA fluorescence, and developed in all cells shortly after the cell wide increase in BODIPY PA fluorescence. Taking into consideration that CTSD specific BODIPY PA fluorescence only occurs at lysosomal pH, this may represent either non-CTSD specific binding with BODIPY locating to the cell membrane, or membrane localisation of lysosomes. We believe that this may represent final stages in autophagic cell death.

At early time points (2h 15 mins) TCDD treated samples (Figure 6.7 bottom row) showed strong punctate staining in the perinuclear region of the cell but compared to vehicle, more puncta were spread throughout the cytoplasm. At ~6h cells began to

show an increase in BODIPY PA fluorescence similar to that seen in dithranol treated samples, but not including every cell. These cells then went on to produce the spreading and blebbing of the BODIPY PA lined membrane that preceded cell death. This data showing use of the BODIPY PA in primary keratinocytes in relation to autophagy is novel. However the data is not conclusive and must be tested further. LAMP staining could be used to define which staining relates to lysosomal CTSD and if the membrane staining represents non-specific or lysosomal CTSD fluorescence. Once optimised further, other AhR ligands such as ITE and β -NF could be tested to define if this observation is specific to autophagy.

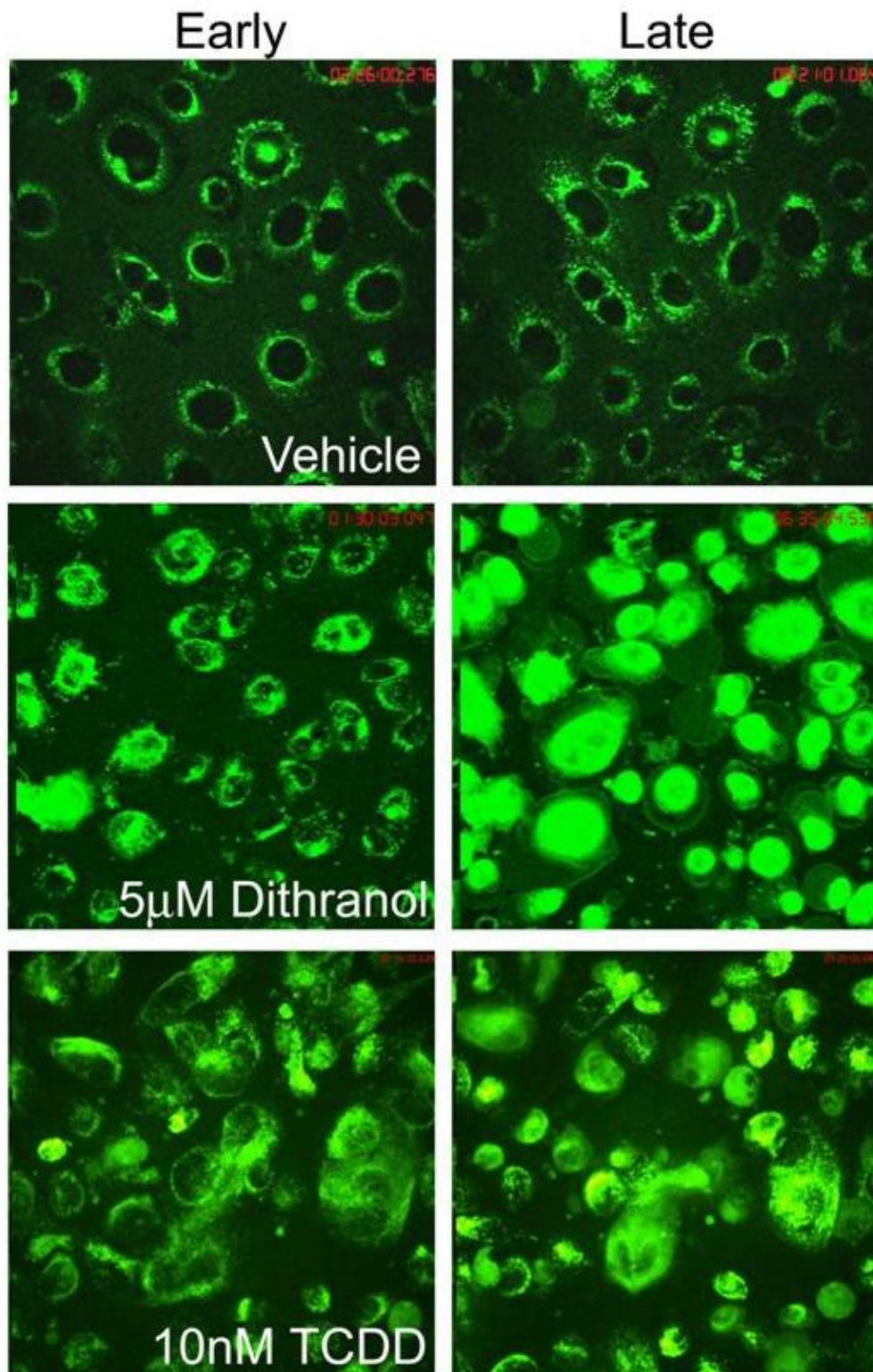


Figure 6.7. Autophagy causes Cathepsin D expression to increase and recruited to the membrane. Primary keratinocytes were treated with vehicle, 5μM Dithranol or 10nM TCDD for 1h pre imaging and the duration of live cell imaging. 1μM BODIPY PA was added to the medium for 30 minutes and cells imaged by confocal live cell microscopy for up to 11h. Left hand column shows images taken early in the timecourse; vehicle at 2 h 26 mins, dithranol at 1 h 30 mins, TCDD at 2 h 15 mins. Right hand column shows images taken at later time points; vehicle at 9 h 21 mins, dithranol at 6 h 30 mins, TCDD at 9 h 20 mins. Images are representative of 3 donors (dithranol) and 2 donors (TCDD).

6.3 Discussion

6.3.1 Summary

In summary, TCDD decreased levels of pro and active CTSD, corresponding with the literature. α -NF-induced AhR inhibition resulted in the reversal of TCDD-induced decreased levels of pro CTSD but further decreased levels of active CTSD. β -NF induced levels of pro CTSD and had little effect on active CTSD with some increased and decreased levels shown. Co-treatment with α -NF consistently caused further increased levels of pro CTSD by β -NF but active CTSD was up regulated at days 2 and 4 and strongly down regulated at days 6 and 8 by α -NF plus β -NF. ITE induced down-regulation of pro CTSD at days 2 and 4, and up-regulation of pro CTSD at days 6 and 8. Active CTSD was down regulated by ITE. Co-treatment with α -NF consistently up regulated pro CTSD, while active CTSD was up regulated by α -NF plus ITE at days 2 and 4, and down regulated at days 6 and 8.

Immunohistochemistry for CTSD showed consistently increased punctate staining across ligand and donor, in epidermal equivalents treated with TCDD, β -NF and ITE, with expression aberrantly in the basal and spinous layers too.

	TCDD 0.5/5/10nM	β-NF 15/30 μ M	ITE 1/5 μ M	α-NF alone 5/10 μ M	Blocked autophagy
Pro CTSD decrease	+ D2/4/8	-- D2/8	+ / - D2/4 D6/8	- D2/4/8	- - -
Active CTSD decrease	++ D2-8	- / + D2/4/8 D6	+++ D2-8	+ D4/6/8	+ + +
Pro CTSD decrease plus α-NF	- / + Varied	- - - D2-4	- - - D2-8		
Active CTSD decrease plus α-NF	+ D2/4/8	- - / + + + D2/4 D6/8	- - / + D4 D6/8		
CTSD in epidermal equivalents	+++	+	+++		

Table 7. A summary of the effects of AhR activation on CTSD. Plus represents concurrence with the row title, minus represents opposite effect to the row title. Green figures represent AhR activation, red figures represent AhR inhibition from chapter 3.

6.3.2 CTSD expression is regulated by AhR

CTSD transcriptional regulation is complex and mainly dependent on the oestrogen receptor (ER) binding the ER responsive element (ERE) and inducing transcriptional activation of CTSD. CTSD is also known to be regulated as a housekeeping gene, by Sp1 protein binding the Sp1 binding site (Figure 1.3). The Sp1 binding site is known to interact with many other nuclear receptors as it often cannot induce transcriptional activation alone (Krishnan et al., 1995; Wang et al., 1998). Ingenuity pathway analysis of papers linking the compacted stratum corneum in ichthyosis (representing the TCDD-induced effects in epidermal equivalents) to the AhR pathway indicated the link shown in the papers by Wang et al (Wang et al., 1998; Wang et al., 1999). These papers reported the presence of an XRE promoter upstream of CTSD and showed that CTSD was regulated by the AhR. AhR does not induce straight forward transcriptional up-regulation of CTSD (as explained in section 6.1) but activated AhR causes inhibition of CTSD, while inactive AhR is required for maximal basal activity (Khan et al., 2006; Wang et al., 1999).

Using IHC to show localisation of CTSD (punctate or cytoplasmic), we showed that AhR activation by all ligands induced punctate staining throughout the VCL (Figure 6.1). This was thought to represent an increase in the post-translational maturation of CTSD (as the literature showed that active AhR inhibited levels of CTSD transcription). Both antibodies used recognised all forms of CTSD by IHC and Western blot. The ligand induced effects on CTSD were not robust, and should be investigated further, but patterns of effects were shown. The results from the Western blots for TCDD and ITE did not correspond with the IHC, but did correspond with the literature; TCDD induced possible down-regulation of pro and active CTSD while β -NF and ITE induced varied CTSD results, although β -NF did appear to induce levels of active CTSD, which would correlate with IHC (Figure 6.2 and Figure 6.3). Opposite to TCDD, β -NF was previously shown to induce autophagic block (chapter 5) and has been shown here to possibly induce pro and active CTSD. This suggests that the differential effects of β -NF on autophagy and CTSD regulation may stem from a similar mechanism.

The contrasting results from IHC in Figure 6.1 to Western blots from Figure 6.2 to 6.5 could be caused by the difficulty of defining the stages and molecular identity of increased CTSD by IHC. These images were not detailed enough to track the progress

of CTSD through each compartment or to conclude which forms of CTSD were increased. To define the effects on each form of CTSD, further IHC could be performed, co-staining for CTSD with LAMP-1, a lysosomal marker to confirm that puncta are lysosomes and therefore that the DAB puncta represent active CTSD. Confocal microscopy or EM with immunostaining could be used to show detailed cellular localisation of CTSD and the effects on each form of CTSD. Western blotting has only been performed here in monolayer cultures, which as CTSD is expressed more in differentiated cells of the granular layer, is not an ideal model. Western blotting could be carried out on epidermal equivalents to correlate increased levels of CTSD seen in IHC with the identification of maturation by Western blot band size.

IHC for CTSD was performed on primary keratinocyte monolayers using the antibody validated in epidermal equivalents, however no staining was present. As shown in IHC on epidermal equivalents (Figure 6.1), CTSD puncta were expressed mainly in the granular layer. Proliferating monolayers represent basal cells, unless grown under differentiating conditions. There are different protocols for differentiating cultures – addition of high calcium into the medium which induces fast differentiation, missing out specifically defined intermediate stages in the VCL or culturing the cells to confluency to try to achieve the correct stage of differentiation. IHC was performed on granular cells grown at high confluency, but still no punctate staining was visible. Considering this in context of Western blot cultures, there was a time dependent increase in basal CTSD (increased pro and active CTSD in Appendix Q and Appendix R, and increased active CTSD in Appendix S and Appendix T) and differential effects were seen at days 6 and 8 compared to days 2 and 4, suggesting an alternative AhR-independent mechanism may be occurring at days 2 and 4 to account for the differences observed. Differentiation by high confluency is difficult to synchronise in primary cells, and without all cells at the same stage of differentiation, true effects may be masked.

If BODIPY PA worked in monolayer keratinocytes but IHC and antibodies did not, it would be interesting to test BODIPY PA in fixed monolayer cells and see the differences in sensitivity between antibodies and the BODIPY PA. It would also be interesting to try and load epidermal equivalents with BODIPY PA and perform live cell imaging but there are significant technical challenges and development work for such techniques is required.

6.3.2.1 Inhibition by α -NF

Modulation of agonist-induced effects on the AhR pathway by α -NF produced varied results by Western blot. α -NF exerted a blocking effect on pro CTSD degradation induced by TCDD and ITE but did not exert a blocking effect on active CTSD. TCDD-dependent down-regulation of active CTSD was exacerbated by α -NF treatment. As described in section 6.2.2, it is not known whether many other AhR ligands inhibit ER induced CTSD, HAHs and furans similar to TCDD were studied by Zhang et al, showing similar inhibition of presumably CTSD-induced proliferation and inhibition of tumour growth in ER deficient tumour cell lines and null mice with ER deficient tumours (Zhang et al., 2009). Other known anti-oestrogenic AhR agonists have been tested, but these were chosen for their anti-oestrogenic properties and it is not suggest how many other AhR-agonists (3-methylcholanthrene, β -NF) might have anti-oestrogenic potential. However, α -NF induced both the active form of AhR and AhR degradation, exerting the same effects that were required to inhibit expression of CTSD; active AhR breaks the ER-Sp1 dimer and interacts with inactive AhR and Sp1 to induce maximal basal levels. This would not occur when AhR has been degraded resulting in α -NF exerting the same CTSD-inhibitory properties as TCDD because of its mechanism of action. As described earlier, to test this theory, studies using an AhR molecule lacking its ligand binding domain could be utilised, allowing the effects of inactive AhR induction of basal CTSD to be studied without interactions from inhibitory effects of ligand activated AhR. Zhang et al. tested the effects of TCDD and similar compounds in ER deficient cell lines and showed all compounds to exert anti-oestrogenic effects. This suggests that high levels of the typical ER ligand 17 β estradiol (E2) are not required for TCDD or similar compounds to exert inhibitory effects (Vanderlaag et al., 2010; Zhang et al., 2009).

It would also be interesting to perform CTSD activity assay on samples treated with TCDD, β -NF or ITE \pm α -NF and observe the effects of ligand induced and α -NF inhibited CTSD maturation in epidermal equivalents and keratinocytes. As the effects of ligand-induced AhR activation on CTSD are so minor, and the effects of α -NF co-treatment with ligands is so varied (including the mixed inhibition/activation effects on β -NF/ITE), it is difficult to draw conclusion here without further assays. Alternative AhR inhibitors should be used to decipher these effects more fully.

6.3.3 CTSD and autophagic block

During autophagic block, processing of pro CTSD to active CTSD is blocked and pre-pro CTSD accumulates. CTSD can have a role in apoptosis, and literature shows that blocked autophagy resulted in increased levels of CTSD (which form is not shown) inducing lysosomal permeabilisation and apoptosis (Carew et al., 2011). Interestingly, pro CTSD secretion occurs during cancer and wound healing, exerting autocrine effects of increased proliferation in HaCaTs (Vashishta et al., 2007) and invasion and metastatic potential in MCF-7 cells (Ohri et al., 2008), which can be blocked by TCDD (Zhang et al., 2009). Bafilomycin A1 blocks autophagy by specifically inhibiting vacuolar-ATPase which is responsible for acidifying the lysosome. Fusion of the lysosome to the autophagosome is pH dependent and is thereby inhibited, blocking autophagy. The last step in CTSD maturation is from 48kDa intermediate to the 2 chain active CTSD. This is carried out by cathepsins B and L (Laurent-Matha et al., 2006) towards the end of the CTSD processing pathway (reviewed in (Zaidi et al., 2008)) within the endosome and lysosome and is therefore also presumably pH dependent. If this is the case, then the mechanism of bafilomycin A1 blocked autophagy would itself block the final step in CTSD processing. This hypothesis could be tested by measuring conversion of CTSD to active CTSD (by activity assay or Western blot) under varied pH conditions. Alternatively, autophagic block could be induced by another compound that blocks autophagy through a pH/lysosome independent mechanism.

To see real time effects on CTSD levels and cellular localisation of active CTSD, a CTSD specific liquid dye, BODIPY PA was utilised in live cell imaging. It becomes internalized by endocytosis and is transported to lysosomes where it binds CTSD specifically at lysosomal pH (= 3.5 - 5) and in the rest of the cell, unbound BODIPY PA fluoresces but is diffuse, not punctate (Chen et al., 2000). Dithranol and TCDD both induced fluorescence and the extension of round membranes from the cells to which BODIPY PA was associated. This membrane extrusion appeared to precede cell death. Vehicle treated cells did not show these effects of increased fluorescence, and lysosomes continued to move around the perinuclear region and cytoplasm over the complete time course.

To draw proper conclusions from this data, more assays would be required to define the localisation of fluorescence and stage of death of the cell during the large increase in fluorescence. The increase in CTSD levels occurred rapidly, within minutes, so this

suggests not a transcriptional increase of CTSD but release of CTSD after being sequestered in organelles such as the lysosomes, or possibly an increase in available active CTSD that could be caused by increased processing of CTSD. Gerasimenko et al. reported the effects of lysosomal permeabilisation on BODIPY PA fluorescence and showed an overall increase, but images were not shown, only graphs showing levels of fluorescence (Gerasimenko et al., 2006).

To decipher which fluorescence represents lysosomal CTSD and which is free unbound BODIPY PA, co-staining could be performed on fixed cells using lysosomal marker LAMP-1 and CTSD antibodies alongside BODIPY. This staining could be carried out on cells before and after the mass increase in fluorescence seen by live cell imaging from 4h (dithranol) and 6h (TCDD) to observe the involvement of CTSD and lysosomes on the increase and localisation in fluorescence. The effects of apoptosis could also be observed by BODIPY PA live cell imaging, to show the release of CTSD from lysosomes and confirm visually whether this has occurred in autophagy (Figure 6.7) or not.

7 General Discussion

7.1 Summary

The aims of this project were to increase the understanding of the physiological role of AhR in skin and to develop a mechanistic understanding of the pathophysiology of chloracne induced by TCDD. We aimed to characterise the downstream effects of AhR activation on keratinocyte proliferation, differentiation and cell death and in doing so assess potential biomarkers specific to chloracne. As summarised in Table 8, we successfully identified differential effects on AhR activation by TCDD, β -NF and ITE in their roles of activating AhR and regulating differentiation (specifically, decreased VCL and TGM-1 expression in equivalents) and autophagy. Specifically, I have shown differential AhR activation to elicit differential effects on the epidermal equivalent model that resembled chloracne closely. Potential specific biomarkers for chloracne were identified, for example markers of autophagic activation (LC3 II/p62 correlation by Western blot or presence of autophagic vacuoles by EM), TGM-1 and decreased lamellar bodies, although further work is required to validate these markers.

Chapter 3: Activation	TCDD 0.5/5/10nM	β-NF 3/15μM	ITE 1/5μM	α-NF alone 5/10μM
AhR activation in keratinocytes	+++	++	++	+
Inhibition of AhR by α-NF (Western blot)	+++	--	--	
Inhibition of AhR by α-NF (Luciferase)	+++	+++	+++	
Chapter 4: Epidermal equivalents				siRNA/shRNA
Decreased VCL	+++	0	0	+
Compacted stratum corneum	+++	+	++	+
Early onset of differentiation	+++	+	++	
Chapter 5: Autophagy				
Active autophagy (Western blot)	+++	---	+++	+
Inhibition by α-NF (Western blot)	+ partial block	+ block	--- partial block	
EM observations (autophagic vacuoles, lamellar bodies)	+++	0	++	
Chapter 6: CTSD				
Pro CTSD	--	+	- / +	+
Active CTSD	--	-	---	-
Pro CTSD + α-NF	+	++	+++	
Active CTSD + α-NF	--	+ / --- D2/4 D6/8	+ / - D2/4 D6/8	
CTSD in epidermal equivalents (7 days)	+++	+	+++	

Table 8. Summary of the effects of AhR activation by TCDD, β-NF and ITE, and inhibition by α-NF in epidermal equivalents. + and – symbols represent the effects of the ligand on the readout or phenotype indicated in the row title. Green symbols indicate AhR activation, while red symbols indicate AhR inhibition, “0” indicates no effect.

7.2 Main hypotheses

7.2.1.1 Ligand binding affinity

The hypotheses at the start of the project were that differential characteristics of the ligands (high or low-affinity or residency and origin of the compound) would induce differential downstream effects of AhR activation that would correlate with chloracnegenic potential. I have shown that increased residency and binding affinity correlated with induced potential chloracnegenic biomarkers, and induced a chloracne-like phenotype in epidermal equivalents. CYP1A1 induction correlated well with binding affinity of the ligand. The inability of ITE to induce CYP1A1 was an interesting differential effect showing that (along with β -NF inducing CYP1A1) that CYP1A1 induction did not correlate with chloracne. There is no known functional link from induced CYP1A1 protein to the phenotypic effects of AhR activation, so this did not directly relate ligand affinity via CYP1A1 to chloracne.

Another differential effect was that transglutaminase-1 (TGM-1) was shown to be induced (expression and activation) by TCDD, but not by β -NF, the effects of ITE on TGM-1 were not tested (Du et al., 2006a). Our data was consistent with Du et al. in the keratinocyte cell line, I found that TCDD differentially induced TGM-1 protein in epidermal equivalents compared to ITE and β -NF suggesting this is an important mechanism to account for reduced VCL in TCDD-treated epidermal equivalents and a potential biomarker for chloracne.

One known link between AhR and TGM-1 is via CTSD, but TCDD has been shown to inhibit CTSD induction which would in turn inhibit TGM-1 levels, suggesting an alternative and opposite mechanism of TGM-1 activation. Direct regulation would suggest that binding affinity would correlate to TGM-1 activation too, but this requires further investigation. Interestingly, I show differential effects of AhR activation on CTSD in keratinocyte monolayers to epidermal equivalents. Regulation of CTSD in keratinocytes is complex and as I have shown throughout this thesis, confluency is an important regulator of AhR.

The final main differential and novel effect was that TCDD and ITE induced autophagy while β -NF blocked autophagy. The effects of TCDD, β -NF or ITE have not been previously tested on autophagy, so this is novel data, and TCDD induced the most robust changes in autophagic markers (including characteristic EM changes). Autophagy markers and EM appearances Induced by AhR agonists did not correlate

well with the binding affinities of the ligands or CYP1A1 induction; TCDD, the prototypical chloracne-gen induced autophagy, but instead of β -NF inducing lower levels of autophagy as would be expected according to affinity and CYP1A1 induction, it robustly blocked autophagy. ITE induced TCDD-like effects but to a lesser extent, activating low levels of autophagy, correlating with low-affinity and no CYP1A1 induction. The latter two differential effects (TGM-1 regulation and autophagy) did link directly to phenotypic changes associated with AhR activation, which taken together suggest that chloracnegenic activity does not depend upon ligand affinity alone.

7.2.1.2 Modulation by α -NF

TCDD, β -NF and ITE all increased AhR transcriptional activation that was shown to be AhR dependent by robust inhibition by α -NF. However, the regulation of protein expression was more complex; co-treatment with partial AhR-agonist α -NF and β -NF or ITE induced higher AhR activation than β -NF or ITE alone. Possible hypotheses causing this are described in the results section in Chapter 3, which includes the hypothesis based around different XRE domains having specific requirements that were not fulfilled by ITE but the combination of α -NF did, resulting in CYP1A1 induction. Another possible hypothesis is based on the recent publication by Salzano et al., that showed the presence of 4 different binding domains in the human AhR, that all contained alternative binding residues. These binding residues are where most of the differences in structure between human and mouse AhR's are located. This may provide the ability for many numbers of different binding combinations for each ligand, as most ligands are thought to be able to bind the AhR at any of the binding pockets, but their preferences may depend upon ligand size and pocket volume. This model also interestingly allows the possibility of concurrent binding of more than one agonist, or more than one molecule of the same agonist. These possibilities may partially explain ligand interaction as I have shown with β -NF or ITE co-treatment with α -NF, but also may provide a role of AhR regulation by converging pathways and ligand effects *in vivo* (Salzano et al., 2011).

7.2.1.3 Residency

The residency hypothesis has not been specifically tested in this project, but our data did suggest that β -NF induced levels of AhR after treatment of epidermal equivalents for 7 days. This is a novel finding, as this phenomenon has only been reported in the literature in regards to *in vivo*, chronic and acute treatment with dioxins (Franc et al., 2001; Sloop and Lucier, 1987; Tang et al., 2008). In our system, AhR levels in TCDD

treated epidermal equivalents was still low suggesting that recovery of AhR levels from β -NF-induced degradation may be quicker than TCDD, correlating with the literature that showed transient activation of AhR by β -NF was prolonged by the addition of CYP1A1 inhibitor 1-ethynylpyrene (Berghard et al., 1992).

7.2.1.4 Physiological versus toxicological roles of the AhR

The AhR has an important role in both physiological function and mediation of toxicity. I compared ITE, a physiological AhR agonist with exogenous TCDD and β -NF. The physiological role of AhR has not been widely studied until recently, when the discovery of FICZ, a tryptophan photoproduct which is thought to mediate UV induced toxicity in the skin, allowed the physiological responses of AhR to be measured (Bergander et al., 2004; Jux et al., 2011; Wincent et al., 2009). Physiological compounds will inherently have different characteristics to xenobiotics studied for their toxic effects. Firstly, a physiological AhR agonist would be presumed not to induce toxicity at physiologically relevant doses, unless it is the cause of a diseased state, in which case it will have been induced by a disease causing factor. For example, ITE did not induce CYP1A1 at concentrations that did not induce toxicity. If ITE were tested at a higher concentration that induced toxicity and also induced CYP1A1, the effects would no longer be relevant to the physiological role of the AhR, because during normal physiological regulation of AhR activation by ITE (that was shown to occur by XRE-luciferase and AhR degradation) the AhR would be activated by ITE, neither inducing cellular toxicity nor CYP1A1. This is hypothetical and was not tested in our system, although in future studies a higher dose range of ITE would be tested. Equally, physiological agonists would not have high-residency (Bergander et al., 2004). Use of a compound in signalling pathways would be required to respond rapidly to regulation, suggesting that high-residency would not be a useful trait. This suggests that chloracnegens and physiologically relevant concentrations of ligands, would not have similar characteristics.

The role of ARNT and its regulated pathways have not been studied during this project. Although ARNT/hypoxia pathways have suggested roles in keratinocyte differentiation (Geng et al., 2006; Weir et al., 2011), the effects of TCDD and AhR activation on ARNT are not marked, ARNT levels were not affected by TCDD treatment in HepG2 cells (Pollenz et al., 1999) and there are no reports of AhR inducing the degradation of ARNT post activation. It would be interesting to investigate the possible interactions between ARNT and the potential biomarkers and processes that I have indicated are regulated

by or interact with the AhR pathway (TGM-1, autophagy and lamellar bodies), but this would most suitably be in a further project, not a sideline from this project.

7.3 Hypotheses arising from the project

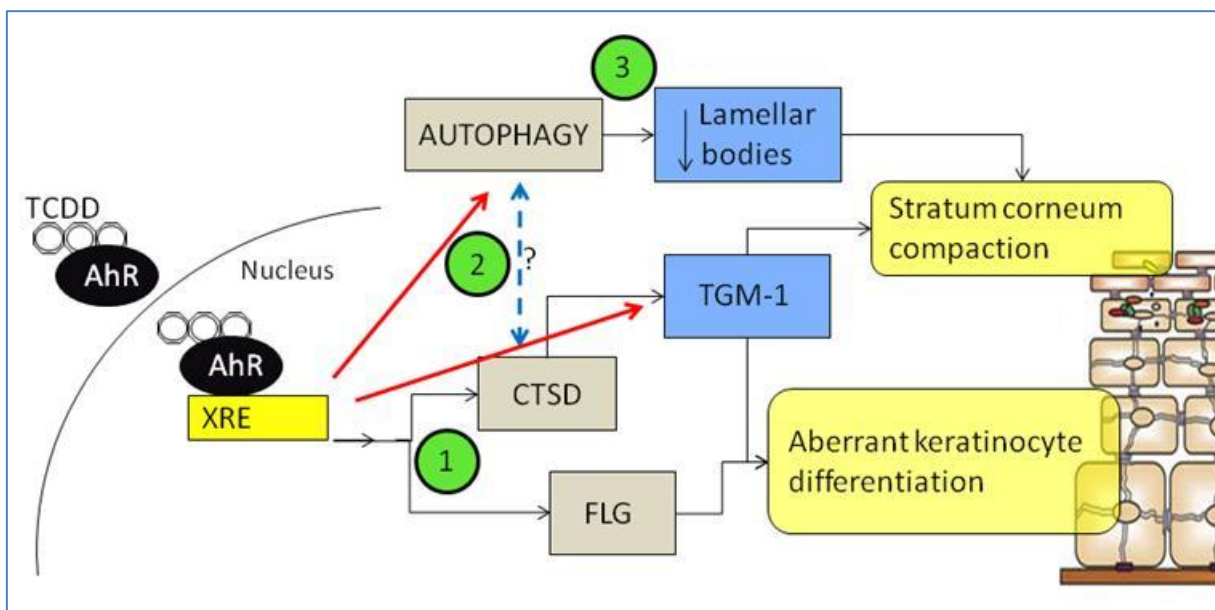


Figure 7.1. Hypotheses for AhR-dependent decreased viable cell layer and compacted stratum corneum. 1) The effects of transcriptional activation of CTSD and filaggrin induce a thinner viable cell layer by increased early onset of terminal differentiation and possible involvement of autophagy. 2) TCDD induces autophagy which may be linked to changes in CTSD expression by increasing activation of CTSD to provide more degradation power with increased numbers of autophagosomes. 3) Autophagy may target lamellar bodies for degradation, accounting at least in part for the compacted stratum corneum. Red arrows represent links from AhR that have not yet been fully elucidated, grey boxes represent direct from the AhR, blue boxes represent intermediate steps and light yellow boxes represent AhR induced affects. XRE xenobiotic response element; CTSD Cathepsin D; TGM-1 transglutaminase-1; FLG filaggrin.

7.3.1 Hypothesis 1. TCDD induced AhR degradation and the consequent effects

Persistent TCDD induced AhR degradation is the basis for one of the main hypotheses for the specificity of chloracne. The high-residency and strong affinity of TCDD for the AhR result in AhR degradation persisting over time, when degradation by other ligands does not. My data corresponds well with this hypothesis, showing prolonged degradation of AhR by TCDD treatment for 7 days in epidermal equivalents, compared with novel data showing the increased levels (presumable on recovery after degradation) shown by IHC in epidermal equivalents treated for 7 days with β -NF. For example, β -NF and ITE have been shown to transiently induce AhR activation, showing

AhR recovery from β -NF treatment in primary keratinocytes by 48h post treatment (Berghard et al., 1992) and by 24h after ITE treatment in mouse hepatoma cells (Henry et al., 2010). Increased concentrations of β -NF or ITE may induce faster recovery of AhR, as AhR ligands induce their own metabolism (Sorg, 2009). Moreover, although preliminary, I have shown AhR knock down by siRNA and shRNA to induce a TCDD-like phenotype (thinner VCL and compacted stratum corneum) in epidermal equivalents. Together the data presented in this thesis suggests that the lack of AhR contributes to the epidermal phenotype which is also characteristic of chloracne comedones and vellus follicles (Figure 1.8)(Hambrick, 1957; Pastor et al., 2002). During persistent AhR activation, perhaps somewhat paradoxically AhR transcriptional activation remains constant despite evidence of AhR degradation as shown by readouts of transcriptional activation, often CYP1A1 expression and Western blots showing AhR degradation (Henry et al., 2006; Henry et al., 2010). This suggests that the degradation of AhR may play a role in the regulation of AhR synthesis and that readouts of AhR levels by Western blot may not reflect levels of transcriptionally active AhR in the nucleus. Little is known about the molecular mechanisms regulating synthesis of AhR, but for TCDD to induce prolonged AhR activation (and consequent degradation) and simultaneously induce prolonged AhR-dependent transcriptional activation (Henry et al., 2010), nascent AhR must be available for continuous activation, resulting in both AhR degradation and CYP1A1 induction. If activation of AhR were to induce AhR synthesis, high levels of AhR activation would induce high levels of AhR synthesis, resulting in the flux or cycling of AhR degradation and synthesis to vary according to the potency of the ligand (increasing flux with increased ligand potency).

The AhR has been shown to recover to higher levels than basal levels 4 days after TCDD-dependent degradation than basal levels in rat hepatocytes and levels remained raised at least until 10 days post treatment, the longest time point tested (Franc et al., 2001). Increased AhR has also been reported by Tang et al. in skin from chloracne sufferers exposed to a cocktail of dioxins in industry at least 6 years previously. Unexpectedly, AhR levels were increased along with CYP1A1 levels and GST A1. This suggests that chronic exposure to dioxins may induce a rebound effect resulting in over expression of AhR, as reported by (Franc et al., 2001). This is a little reported phenomenon and has not been reported previously *in vitro*. I have shown AhR levels in TCDD treated epidermal equivalents to be decreased, but epidermal equivalents treated with β -NF in parallel have shown increased β -NF, this would be the first observation of

this phenomenon *in vitro*. The cause of the recovery of AhR to increased levels is unknown but could be a result of the synthesis of AhR being prolonged and overshooting the basal levels.

The induction of AhR levels on recovery from ligand-induced degradation (Franc et al., 2001) of after chronic exposure to AhR agonists (Sloop and Lucier, 1987; Tang et al., 2008) suggests the importance of residency of the ligand. Realistically, high-residency would be considered a powerful characteristic of a chloracnegen, considering the time scales that the disease covers, lasting years because of the constant bioavailability of lipophilic and low metabolised dioxins causing prolonged down-regulation of AhR as shown in our data. This hypothesis leads to the question that if residency of any non-chloracnegenic compound was increased by decreasing its metabolism (for example, with CYP1A1 inhibitor 1-ethynylpyrene), would it too exert chloracnegenic effects? Berghard et al demonstrated that inhibition of CYP1A1 by 1-ethynylpyrene, increased the duration of β -NF-dependent AhR activation. This could be applied to the epidermal equivalent model to test if β -NF would then induce chloracne-like effects, and result in increased AhR.

7.3.1.1 AhR-induced regulation of CTSD and TGM-1

There is a large battery of proteins induced by AhR-dependent transcriptional activation which mainly include the well studied phase I and II metabolising enzymes (reviewed in (Oesch et al., 2007)). The AhR has two main roles, mediation of toxicity which has been the focus of research until recently, and the less characterised but crucial physiological role of the AhR. The AhR is highly conserved throughout time and species (Hahn et al., 1997) and its knock down *in vivo* demonstrates its vital but still unclear physiological role (Fernandez-Salguero et al., 1997). The AhR-dependent transcriptional regulation of CYP1A1 has been used in industry and AhR literature as a sign of AhR-dependent toxicity, but more recently the regulation of physiologically relevant proteins that were not involved in the metabolism of xenobiotics have been identified.

XRE promoter domains have been identified upstream of CTSD (Wang et al., 1999) and filaggrin (Sutter et al., 2011), indicating that they are regulated by the AhR. As described in Chapter 6, regulation by the AhR may not be straight forward or independent of other promoter regions. CTSD demonstrates the differential effects of ligand-activated AhR

and inactive AhR on transcriptional regulation; maximal basal expression of CTSD requires the interaction of inactive AhR and the Sp1 protein and binding site, however ligand-activated AhR disrupts the ER-Sp1 dimer, inhibiting CTSD (Wang et al., 1998; Wang et al., 1999). Filaggrin has more recently been identified as a target for AhR regulation, revealing a functional link to the previously observed TCDD induced differentiation in keratinocytes (Du et al., 2006a; Greenlee et al., 1985; Osborne and Greenlee, 1985; Ray and Swanson, 2003) (Figure 7.1).

AhR activation has also been mechanistically linked to differentiation by its induction of TGM-1 expression and activation, although TGM-1 is not thought to be directly regulated by AhR (Du et al., 2006a). The mechanism of AhR-induced TGM-1 was unknown, but during the project we hypothesised that CTSD may be the intermediate step; TCDD directly regulates CTSD which directly induces TGM-1 activation. Our data suggests that there may also be a CTSD-independent mechanism linking AhR to TGM-1 too; TCDD-dependent AhR activation has been shown to inhibit oestrogen receptor (ER) dependent up-regulation of CTSD (Krishnan et al., 1995; Wang et al., 1998), which in turn would down-regulate TGM-1, but our data (consistent with the Du et al.) has also shown that TCDD treatment may result in up-regulation of TGM-1 (with differential effects by β -NF treatment). AhR has been shown to induce or inhibit CTSD expression depending on its activation state (Wang et al., 1998; Wang et al., 1999), and CTSD is known to regulate TGM-1 expression and activation (Egberts et al., 2004; Zeeuwen, 2004). Further work is required to determine the molecular mechanisms through which TCDD regulates CTSD and induces TGM-1 activation (Figure 7.1); as TCDD appeared to induce a trend of inhibited CTSD expression (Figure 6.3), which in turn would inhibit TGM-1 activation, but TCDD has been shown to induce TGM-1 expression and activation in primary keratinocytes (Du et al., 2006a).

I have shown TCDD treatment (but not β -NF or ITE) to induce aberrant expression of TGM-1; as reported in Loertscher et al., the contiguous ring of TGM-1 expression on the inner edge of the granular layer keratinocytes became broken in TCDD treated samples (Loertscher et al., 2001b). In CTSD knock out mice, activation of TGM-1 was inhibited, resulting in a decrease of TGM-1 dependent proteins (involucrin and loricrin) in the skin, that contributed to an ichthyosis like phenotype, with thicker stratum corneum and hyperkeratosis, and also a poorly formed epidermal barrier (Egberts et al., 2004). There are epidermal diseases that exhibit similar phenotypes of dysregulated differentiation

(psoriasis and several types of ichthyosis) but opposite mechanisms are responsible. Egberts et al describe two groups of diseases; “retention hyperkeratosis”, such as lamellar ichthyosis which is caused by TGM-1 deficiency and can result in compromised barrier function, and “hyperproliferation associated hyperkeratosis” such as psoriasis, in which TGM-1 activity is increased (often as a result of increased CTSD) and does not exhibit compromised epidermal barrier function. I have not studied loricrin in this project because it is regulated by TGM-1 in parallel with involucrin. I chose filaggrin instead because of its TGM-1 independent regulation, which has recently been identified as being directly regulated by the AhR (Sutter et al., 2011).

The TCDD-like effects shown in epidermal equivalents that strongly resemble chloracne also show hyperkeratosis, as do the two disease groups identified by Egberts et al., as do AhR and ARNT knock out mice (Fernandez-Salguero et al., 1997; Geng et al., 2006). But because TCDD inhibited CTSD (via inhibition of ER) but induced TGM-1 (by an unknown mechanism), it was unclear which group the TCDD and chloracne –like phenotype would fit into, retention or hyperproliferation associated hyperkeratosis. Considering the TCDD-dependent induction of involucrin in our system we would presume that the TCDD-induced phenotype would fit the hyperproliferation associated hyperkeratosis model, suggesting that the mechanism was similar to that of psoriasis, with increased TGM-1 and CTSD (that itself may be the mechanism of hyperproliferation of the keratinocytes (Vashishta et al., 2007)). However, as neither chloracne nor the TCDD-like phenotype in epidermal equivalents were hyperproliferative (they exhibited decreased cell numbers (Loertscher et al., 2001a; Loertscher et al., 2001b)), the phenotype doesn't fit that group. The more likely group to place the TCDD-induced phenotype would be with retention hyperkeratosis, caused by decreased CTSD and TGM-1, inducing dysregulated differentiation and possible (but not certain) barrier deficiency. This group characteristically showed decreased expression of cornified envelope proteins involucrin and loricrin, we showed that TCDD induced involucrin in epidermal equivalents, but filaggrin (directly regulated by AhR) punctate staining was shown to be decreased by TCDD treatment. This could be caused by post-translational modifications and not transcriptional regulation; some papers have shown blocked pro-filaggrin to filaggrin processing but reports are varied in the literature (Geusau et al., 2005). The involvement of CTSD in the TCDD induced chloracne-like phenotype provided an interesting link to autophagy; active CTSD (the form that activates TGM-1 to catalyse cross linking of proteins to form the cornified

envelope) is lysosomal, which is also a major component of autophagic degradation. This is discussed in the following section, but the link between TCDD regulated CTSD and its role in autophagy is very interesting.

Recently, a paper following on from Tang et al. reported differential regulation of TGM-1 in chloracne obtained from industrial workers exposed to a mixture of dioxins 6 years previously for an undefined amount of time (Liu et al., 2011; Tang et al., 2008). Lui et al showed that TGM-1 mRNA and protein levels were increased and localised to the granular and spinous layers of chloracne involved skin samples. They suggested an alternative mechanism linking TCDD to TGM-1 by the activation protein-1 (AP-1) or mitogen-activated protein kinase (MAPK) pathway (Liu et al., 2011), however I have shown data that corresponds with the literature on TCDD-dependent direct down-regulation of CTSD, and discussed the direct pathway linking AhR-activation to CTSD regulation and direct TGM-1 activation, which fits hypotheses for other chloracne type hyperkeratotic disease (Figure 7.2). Increased TGM-1 would suggest increased CTSD, which is what I have shown is indicated by IHC for CTSD in AhR-agonist treated epidermal equivalents. The differential effects of these results may be caused by the difference in cell culture model – monolayer versus epidermal equivalent.

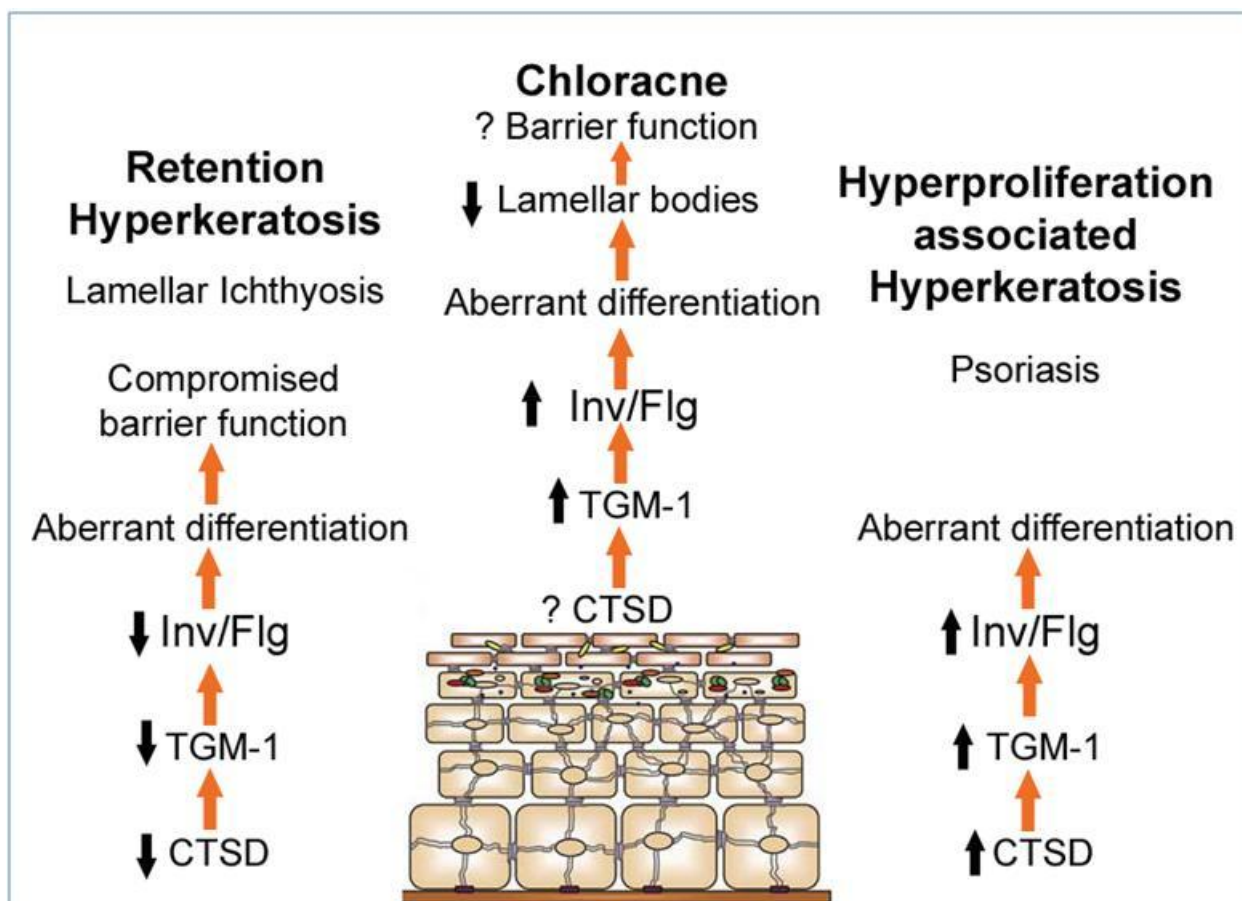


Figure 7.2. Molecular characteristics of chloracne. Chloracne corresponds with, but shows mixed characteristics of the groups of typical disease states regulated by CTSD and TGM-1. CTSD levels are unknown in chloracne and aberrant (but probably increased) in TCDD treated epidermal equivalents. Increased TGM-1 is present in chloracne *ex vivo* but was reduced by TCDD treatment in keratinocyte monolayers. The state of barrier function has not been reported in chloracne but decreased lamellar bodies suggest it may be compromised as in Sjogren-Larsson syndrome. CTSD, Cathepsin D; TGM-1, transglutaminase-1; Inv/Flg, involucrin or filaggrin.

7.3.2 Hypothesis 2. Activated autophagy and Cathepsin D

We have presented novel data showing that TCDD and ITE both induced active autophagy in epidermal equivalents and that β -NF induced autophagic block (Chapter 5). This opposite effect of β -NF compared to TCDD or ITE induced AhR activation was mirrored in the effects of TCDD and β -NF on CTSD expression. TCDD inhibited levels of both pro and active CTSD, while β -NF up regulated levels of both. This suggested a link between CTSD and autophagy, and as AhR activation has been shown to regulate CTSD (Wang et al., 1998; Wang et al., 1999), and autophagic block inhibits levels of active CTSD (Chapter 6), it was hypothesised that levels of CTSD could regulate autophagy. CTSD is integral to autophagy (providing proteases to degrade cellular material) and it could be hypothesised that increased autophagy would require

increased levels of CTSD, making it possible for increased CTSD to require more material transport by autophagosomes, so regulating autophagy (Settembre and Ballabio, 2011; Settembre et al., 2011).

There have been reports in the literature that increased numbers of lysosomes could induce autophagy by up-regulating protein degradation in the cell. Increased numbers of autophagosomes are required to contain and remove the degraded material at times when the degradation pathways are activated (Settembre and Ballabio, 2011; Settembre et al., 2011), as increased waste incineration (lysosomes) would require increased rubbish lorries (autophagosomes) to remove the waste. If this hypothesis is correct, it would be possible that decreased CTSD (by TCDD) could cause increased autophagy (Figure 7.1 hypothesis 1). As CTSD is a lysosomal protease, it may also be degraded during the final stages of autophagy, as LC3 II and p62 are. This is suggested by the decrease of pro and active CTSD by TCDD and also the accumulation of pre-pro CTSD by autophagic block. I have shown evidence indicating that autophagy may regulate the processing of pro-CTSD to active CTSD. The mechanism of autophagic block utilised was Bafilomycin A1 treatment, which inhibits lysosomal acidification (Lukacs et al., 1990) which is necessary for the step in processing pro to active CTSD. This may mean that the autophagic block itself did not inhibit CTSD processing but the mechanism of the block did. β -NF inhibited autophagy and resulted in increased pro and active CTSD (but not obvious blocked processing to active CTSD), which was opposite to the effects of TCDD, that may suggest that the accumulation of CTSD occurred while it was not used by autophagy. If CTSD was degraded by autophagy, then a regulatory circuit of CTSD use, degradation and synthesis could be implemented, as suggested in section 7.3.1 for the AhR. This would correlate well, showing that blocked autophagy (induced by β -NF) caused increased CTSD and active autophagy (by TCDD) caused decreased CTSD. Increased CTSD has been previously shown to result from autophagic block (its accumulation induced lysosomal membrane permeability and apoptosis, see section 1.4.2.1), but the form of CTSD that was increased was not specified (Carew et al., 2011). Therefore, we can conclude that in keratinocyte culture, TCDD inhibited CTSD would disrupt TGM-1 inducing aberrant expression of differentiation markers. However, in epidermal equivalents treated with TCDD, CTSD appeared up-regulated (Figure 6.1) which would activate TGM-1 and cause increased involucrin staining as shown in Figure 4.3, while filaggrin puncta decreased, which could be a sign of induced cross linking by TGM-1. To define the

steps in this hypothesis, CTSD or ER knock out keratinocytes could be used to study CTSD-independent TCDD-induced effects on TGM-1. If they were possible to obtain, chloracne samples could be tested for all of the stages outlined above, from AhR levels to effects on ER induction of CTSD, TGM-1, involucrin, filaggrin and loricrin, and barrier function tested to completely define the characteristics as per Figure 7.2.

7.3.3 Hypothesis 3. The effects of autophagy on the TCDD induced phenotype in epidermal equivalents

Dysregulated differentiation (by aberrant filaggrin/involucrin/TGM-1 expression regulated by binding to XRE in filaggrin promoter and/or through CTSD and its effect on TGM-1) is likely to be an important contributing factor to the decreased VCL and compacted stratum corneum present in TCDD treated epidermal equivalents and chloracne (Geusau et al., 2005; Loertscher et al., 2001b). Autophagy as a mechanism of cell death is a difficult area to define because there are few biomarkers to distinguish active autophagy as a survival pathway from autophagy as a cell death pathway. Vacuolisation is a marker of both autophagic cell death and apoptosis. In the epidermal equivalent model that I have shown, TCDD induced high levels of vacuolisation, suggesting cell death was occurring. Other samples showed lower levels of vacuolisation, but as noted in Chapter 5, only one time point was studied so increased signs of cell death may be present at a different time point. As I have also shown that TCDD did not induce active caspase-3 or cleaved lamin A in TCDD treated epidermal equivalents and as no chromatin condensation was observed, it can be presumed that the vacuolisation here did not represent apoptosis. Our EM studies at a single time point also provided no evidence of necrosis, as there were no signs of swollen or ruptured membranes in the sample (Kroemer et al., 2009). Despite autophagic cell death not being a common or well defined process, we hypothesise that the presence of vacuoles in TCDD treated epidermal equivalents may represent early signs of autophagic cell death but further studies are required to confirm this. The contribution of autophagic cell death to the decreased VCL would provide another differential effect between the phenotypes induced by TCDD and β -NF, as in direct contrast to TCDD, β -NF blocked autophagy and did not cause a decreased VCL thickness. ITE induced effects that were TCDD-like (but not as strong) in regards to autophagy and VCL phenotype (slight compaction of the stratum corneum). This data fits together well, but I hypothesise that the

involvement of autophagy in the chloracne-like phenotype may contribute more marked phenotypic effects.

Our initial investigation began with similarities between the compacted stratum corneum in our epidermal equivalent model with Sjorgren-Larsson syndrome, a type of ichthyosis that was shown to have a characteristic compacted stratum corneum caused by malformed and empty lamellar bodies, causing a deficiency in lamellar lipids secreted into the granular/ cornified junction, resulting in improper barrier function and abnormal lipid content in the stratum corneum (Rizzo et al., 2010). Lamellar bodies are difficult to visualise by any other method but EM, because of their mixed characteristics of vesicles and lysosomes, but by EM they can be identified by their characteristic lamellar contents (Bouwstra et al., 2003), grouping near the apical membrane of the upper spinous layers (where they are formed) and presence in the granular layer where they visibly fuse to the apical membrane of the granular cells and secrete their lipid lamellar contents into the extracellular gaps between cornified cells (Bouwstra et al., 2003). These areas of lamellar material also remain visible in parts of the stratum corneum (Ponec et al., 2000).

In recent years, epidermal equivalents have been validated by studies in a wide range of areas including differentiation (Loertscher et al., 2001b) and barrier function (Ponec et al., 2000) and used for a number of techniques including EM. Electron micrographs revealed high numbers of well formed lamellar bodies expressed in the well defined upper spinous and granular layers. To our surprise, the numbers of lamellar bodies appeared consistently decreased in TCDD treated (and ITE treated to a lesser extent) epidermal equivalents compared to vehicle. We also found evidence to show that autophagy targeted lamellar bodies for degradation. Autophagy has been reported to target specific organelles such as mitochondria (mitophagy) and fat droplets in hepatocytes (“lipophagy”) during serum starvation, which when degraded release high amounts of ATP providing an efficient organelle for autophagic degradation which is a catabolic process (Singh et al., 2009b; Weidberg et al., 2009). Autophagy appears to target lipid droplets during cellular starvation when autophagy is required for its catabolic role, and may be induced by markers of lipid over expression but this is not definite. However if “intelligent degradation” can occur in the liver then it is likely to occur in the epidermis too. Lamellar bodies would presumably also provide high levels of energy after autophagic degradation of their lipid contents, and as they contain

CTSD, autophagy would result in the degradation of CTSD too either as another mechanism of TCDD-dependent down-regulation or also possible recycling of CTSD or release for use by autophagy in situations where CTSD was low, which would indicate a mechanism of low CTSD-induced up-regulation of autophagy. As lamellar bodies play a key role in the final formation of the cornified cell envelope and the formation of the epidermal barrier, it seems likely that a variety of endogenous and environmental signals may be involved in the regulation of lamellar body trafficking and fusion. So far this has not been investigated in detail in part because of the lack of appropriate models and markers to facilitate real study in real time. Future studies focused on live cell imaging of epidermal equivalent models stimulated with AhR agonists would be of considerable interest.

7.4 Future Work

This project has produced some exciting novel data that has not only helped to clarify AhR-dependent mechanisms contributing to the formation of chloracne, but that can also be implemented in more widely ranging effects in disease and physiological roles stemming from the AhR. However, some areas that we investigated have not been fully elucidated by our experiments so far, and further experiments could help to fully understand and put our findings into context.

7.4.1 Investigating ligand-induced AhR activation

The AhR dependence of ITE and β -NF induced effects on AhR/Cyp1a1 protein expression levels and autophagic protein biomarkers were not satisfactorily defined because α -NF induced further AhR activity in some assays involving these agonists rather than blocking it. We aimed to test the AhR dependence of TCDD, β -NF and ITE in an shRNA or siRNA AhR knock down system. Unfortunately, I did not have time to fully utilise this system for these studies past optimisation, but this system could be used to confirm AhR dependence in the future. However, because of the phenotypes caused by AhR knock down shown in Chapter 4 and in AhR knock out mice (Fernandez-Salguero et al., 1997), AhR knock down may not be the ideal model to test the blocked effects of ligand-induced phenotypes. A relatively simple assay would be to repeat the inhibition studies for TCDD, β -NF and ITE using specific AhR antagonists (without partial agonistic action) that have recently become available.

Depending on the mechanism of AhR inhibition, full antagonists may also induce different phenotypes in keratinocyte models. Ideally, inhibition of ligand binding to the AhR would be required, to allow free unbound AhR availability to exert normal physiological regulation, without sequestering into the active AhR pathway. A more complex method could be to modify or remove the AhR ligand binding domain to block ligand binding, which would maintain the effects of inactive AhR (basal expression of CTSD) but allow AhR-dependent effects of β -NF and ITE to be blocked. This has not been attempted previously, but would be a very important experiment, demonstrating the effects of blocking toxicity mediating effects of AhR activation but maintaining physiological function of the AhR.

The effect of high-residency of ligands on their chloracnegenic potential could be tested by inhibiting ligand metabolism, as Berghard et al showed in their paper, prolonging β -NF induced CYP1A1 by co-treatment with 1-ethynylpyrene. This could be applied to the epidermal equivalent model to test if the chloracne-like effects would be induced, however as β -NF has been shown to differentially induce autophagic block, which we hypothesise contributes to the chloracne phenotype, this may not be the ideal AhR-ligand to test the residency theory on. As metabolism of ITE has not yet been defined, to test this mechanism would require first defining the metabolism. Once this had been done, then it could be inhibited as with β -NF.

7.4.2 Investigating the effects of AhR activation on keratinocyte differentiation

The first hypothesis presented in Figure 7.1, was that AhR activation transcriptionally induced filaggrin and degraded CTSD, which lead to dysregulated keratinocyte differentiation and thinner VCL. However it is unclear whether the down-regulation of CTSD resulting in reduced TGM-1 activity was prominent over TCDD-induced up-regulation of TGM-1 (probably independent of CTSD). To study this further, CTSD knock down epidermal equivalents could be used to show the effects of TCDD on TGM-1, independent of CTSD, clarifying the involvement of CTSD in TCDD induced up-regulation of TGM-1 and indicating whether the prominent effect in the TCDD-like phenotype is increased or decreased TGM-1. CTSD shRNA was being optimised towards the end of the project, but due to time constraints no results were produced.

7.4.3 Investigating the effects of AhR activation on autophagy and CTSD

The second hypothesis presented in Figure 7.1 was that AhR activation by TCDD and ITE induced active autophagy and β -NF blocked autophagy. We have not studied the mechanism of AhR induced autophagy, however we hypothesise that it is linked to the regulation of CTSD by AhR. AhR-dependent regulation of CTSD is inhibited by ligand-activated AhR and induced by inactive AhR, providing a physiological role for the AhR. As CTSD and autophagy are strongly linked, it would be interesting to investigate their regulatory effects on each other. Both the CTSD and AhR shRNA knock down protocols were being optimised at the end of the project. These could both be used to test the AhR- and CTSD-dependence of autophagy by measuring LC3 II and p62 by IHC and Western blot. Electron micrographs suggested that TCDD induced high levels of autophagy while ITE induced less autophagy, while effects on LC3 II and p62 Western blots by TCDD and ITE were more similar. To test the effect of autophagic block on CTSD processing independent of lysosomal pH, another method of autophagic block that was downstream of lysosome formation could be used. It would also be interesting to investigate the mechanism of β -NF induced autophagic block, and whether this has any involvement of the inability of β -NF to induce TGM-1 in primary keratinocytes in parallel to TCDD, another interesting differential effect of AhR activation (Du et al., 2006a).

To test the increase in autophagic flux induced by TCDD and ITE (and blocked by β -NF) the mRFP-GFP-LC3 construct (Kimura et al., 2007) could be used to follow the formation and maturation of autophagosomes induced by each ligand. This assay would also be highly beneficial in defining the effects of co-treatment of AhR agonists with α -NF, as the Western blot data were variable. It would also be interesting to investigate the involvement of autophagy in other diseased states. Many diseases involve up-regulation of CTSD, and considering the data presented in this thesis, it is likely that AhR may play a role in them. The AhR is involved in many physiological processes in which AhR may regulate autophagy (indicated by the presence of increased CTSD), including tumours that exhibit increased CTSD (showing potential links between over or under expressed CTSD and autophagy), embryonic development (CTSD has been reported to regulate the formation of limbs and the heart by physiological cell death (Zuzarte-Luis et al., 2007)) and psoriasis or ichthyosis which are grouped by Egberts et al. for having similar phenotypes induced by opposite effects of TGM-1 (Egberts et al., 2004) (Figure 7.2). Depending on the link between autophagy and CTSD regulation,

TGM-1 would be up or down regulated accordingly, contributing to the type of disease phenotype, retention or proliferation associated hyperkeratosis. If increased TGM-1 defined chloracne (as suggested by (Liu et al., 2011)) then increased autophagy may be present in ichthyosis, while psoriasis would be expected to have low or blocked autophagy. However, contrary to Liu et al. (Liu et al., 2011) if chloracne was defined by decreased TGM-1 (via CTSD), the increased autophagy may also be present in psoriasis and ichthyosis would presumably have low levels or blocked autophagy. This could be investigated by studying the levels of autophagy in ichthyosis and psoriasis and possible autophagic targeting of lamellar bodies may be implemented in these diseased states too.

The presence of autophagic targeting of lamellar bodies is a very exciting observation. Lipophagy has been reported in the liver (Singh et al., 2009b), but it has not been reported elsewhere, especially where it could contribute to disease phenotypes. To study the targeted degradation of lamellar bodies further, the lipid content could be studied in the stratum corneum of epidermal equivalents treated with autophagy inducing and blocking compounds, such as TCDD and β -NF. If autophagy targeted lamellar bodies then the lipid content in TCDD treated samples would be decreased while β -NF treated samples would result in increased lipid contents caused by blocked autophagic degradation of lamellar bodies. If there was a lipid deficiency, there may also be compromised barrier function which could be correlated to LC3 II and p62 expression by measuring transepidermal water loss. Biomarkers specific to lamellar bodies are not common, but caveolin is expressed by them where it acts as a scaffold for lipid raft formation (Sando et al., 2003). If lamellar bodies were decreased in active autophagy, the decrease of caveolin could be correlated with increased autophagy.

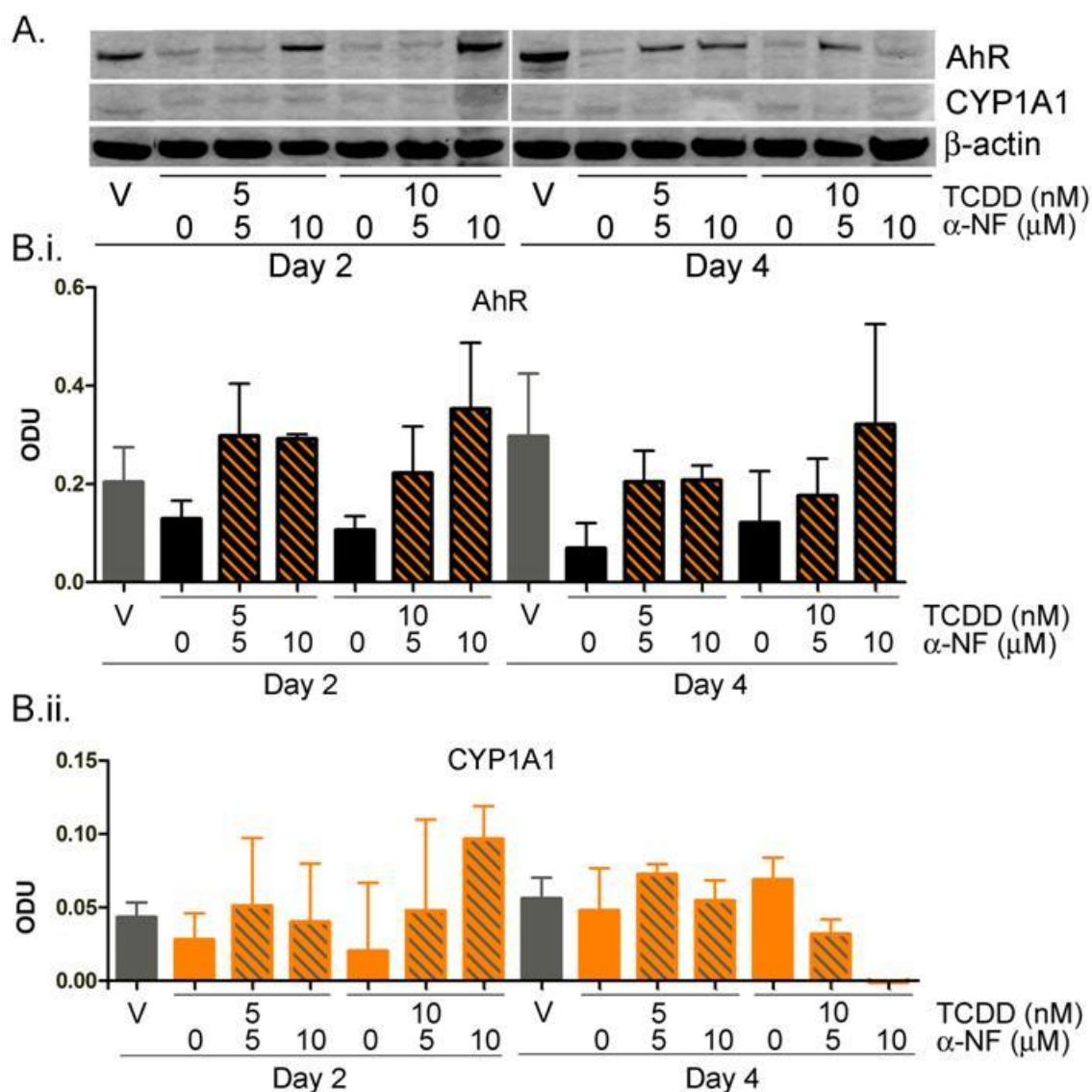
The main aims of this study were to identify a specific biomarker for chloracne and help to elucidate the mechanisms causing chloracne. We have partially achieved the latter aim, showing AhR-dependent effects on TGM-1 and filaggrin to contribute to the decreased VCL and aberrant differentiation characteristic of chloracne, and we have also shown TCDD- and ITE-induced AhR-dependent activation of autophagy, which may contribute to the compacted VCL by targeted degradation of lamellar bodies. Potential novel and specific biomarkers for chloracne have been identified, including autophagy, CTSD, TGM-1 and autophagic degradation of lamellar bodies, but these need further development to define their true specificity to chloracne.

		Vehicle +								
		Vehicle			15uM bNF			30uM bNF		
Firefly		28183	33151	20720	105	91	94	113	95	92
Renilla		419	505	494	390	479	475	369	457	489
Ratio		67.26252983	65.64554	41.94332	0.269231	0.189979	0.197895	0.306233	0.207877	0.188139
Mean		58.28379808								
Norm		1.154051933	1.126309	0.719639	0.004619	0.00326	0.003395	0.005254	0.003567	0.003228

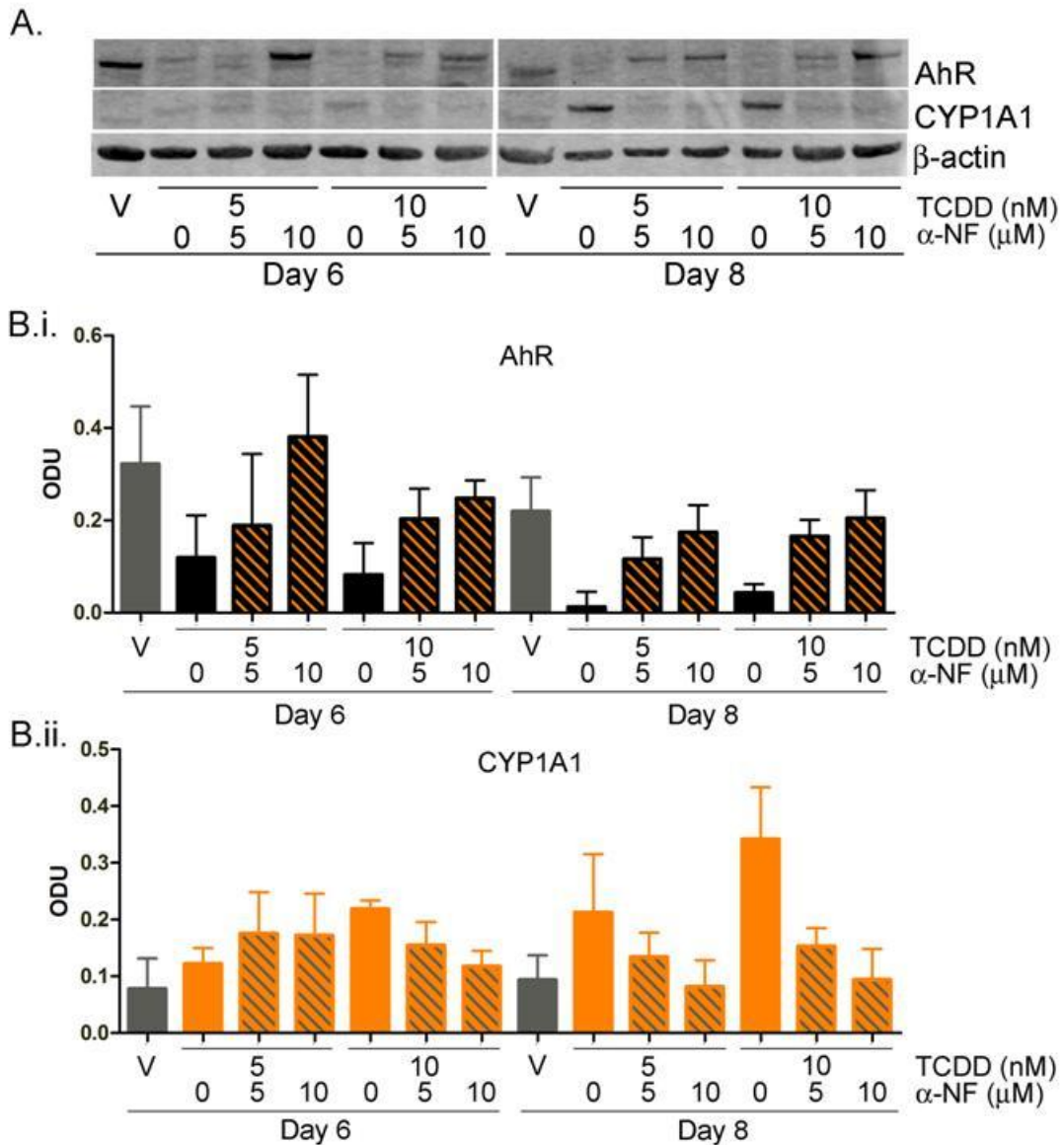
		5nM TCDD +								
		Vehicle			15uM			30uM bNF		
Firefly		28990	33183	42315	112	148	147	107	148	148
Renilla		357	406	498	348	420	504	318	436	466
Ratio		81.20448179	81.73153	84.96988	0.321839	0.352381	0.291667	0.336478	0.33945	0.317597
Mean										
Norm		1.393259953	1.402303	1.457864	0.005522	0.006046	0.005004	0.005773	0.005824	0.005449

		10nM TCDD +								
		Vehicle			15uM			30uM		
Firefly		41456	73096	49217	138	255	203	131	233	194
Renilla		423	641	965	519	656	982	498	661	894
Ratio		98.00472813	114.0343	51.00207	0.265896	0.38872	0.206721	0.263052	0.352496	0.217002
Mean										
Norm		1.68150895	1.956536	0.875064	0.004562	0.006669	0.003547	0.004513	0.006048	0.003723

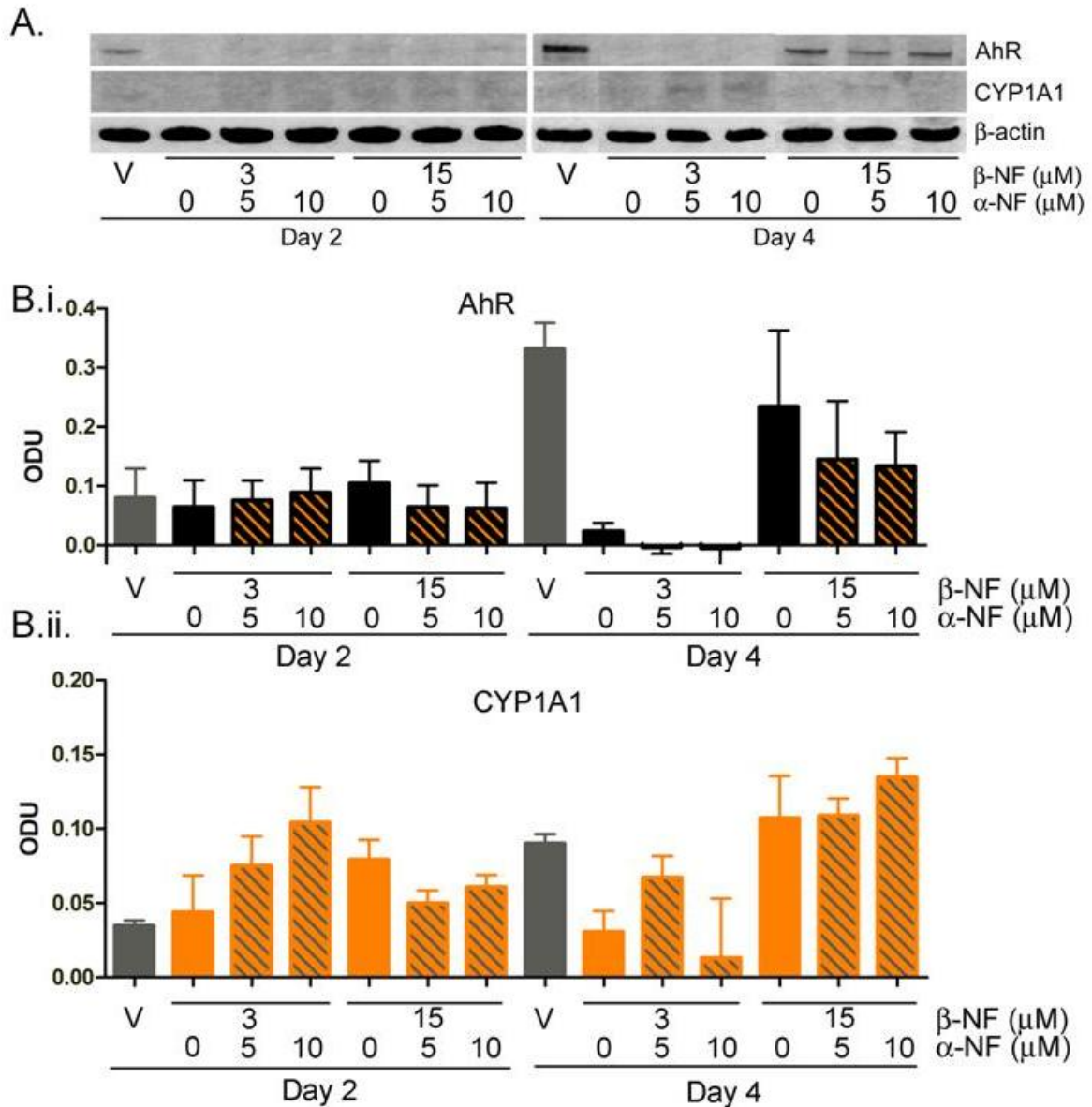
Appendix A. Values from luciferase assay showing quenching effect of β -NF on firefly luciferase. Primary keratinocytes were transfected with AhR-dependent luciferase construct, pGudLuc1.1 and treated with vehicle, 5 or 10nM TCDD for 48h. Vehicle (DMSO), 15 or 30 μ M β -NF (final conc) was added to lysate before luminescence was read. n=3, triplicate wells from 1 donor.



Appendix B. α -Naphthoflavone blocked TCDD-induced degradation of AhR and induction of CYP1A1. Primary keratinocytes were treated with vehicle or TCDD \pm α -NF as indicated. After 2 or 4 days cells were lysed and Western blotting performed. Top graph: Black bars represent densitometry of anti-AhR bands, orange hatching indicates co-treatment of keratinocytes with α -NF as opposed to plain black indicating TCDD alone, grey bars represent vehicle treated keratinocytes. Lower graph: Orange bars represent densitometry of anti-CYP1A1, grey hatching indicates co-treatment of keratinocytes with α -NF, grey bars represent vehicle treated keratinocytes. Densitometry from AhR and CYP1A1 was normalised to β -actin. Two-way ANOVA was performed comparing TCDD treated keratinocytes to α -NF and time. α -NF had a significant effect on AhR degradation ($P < 0.002$), while time had a significant effect on CYP1A1 response ($P = 0.0001$). Values are presented as optical densitometry units (ODU) \pm sem, from 3 donors.

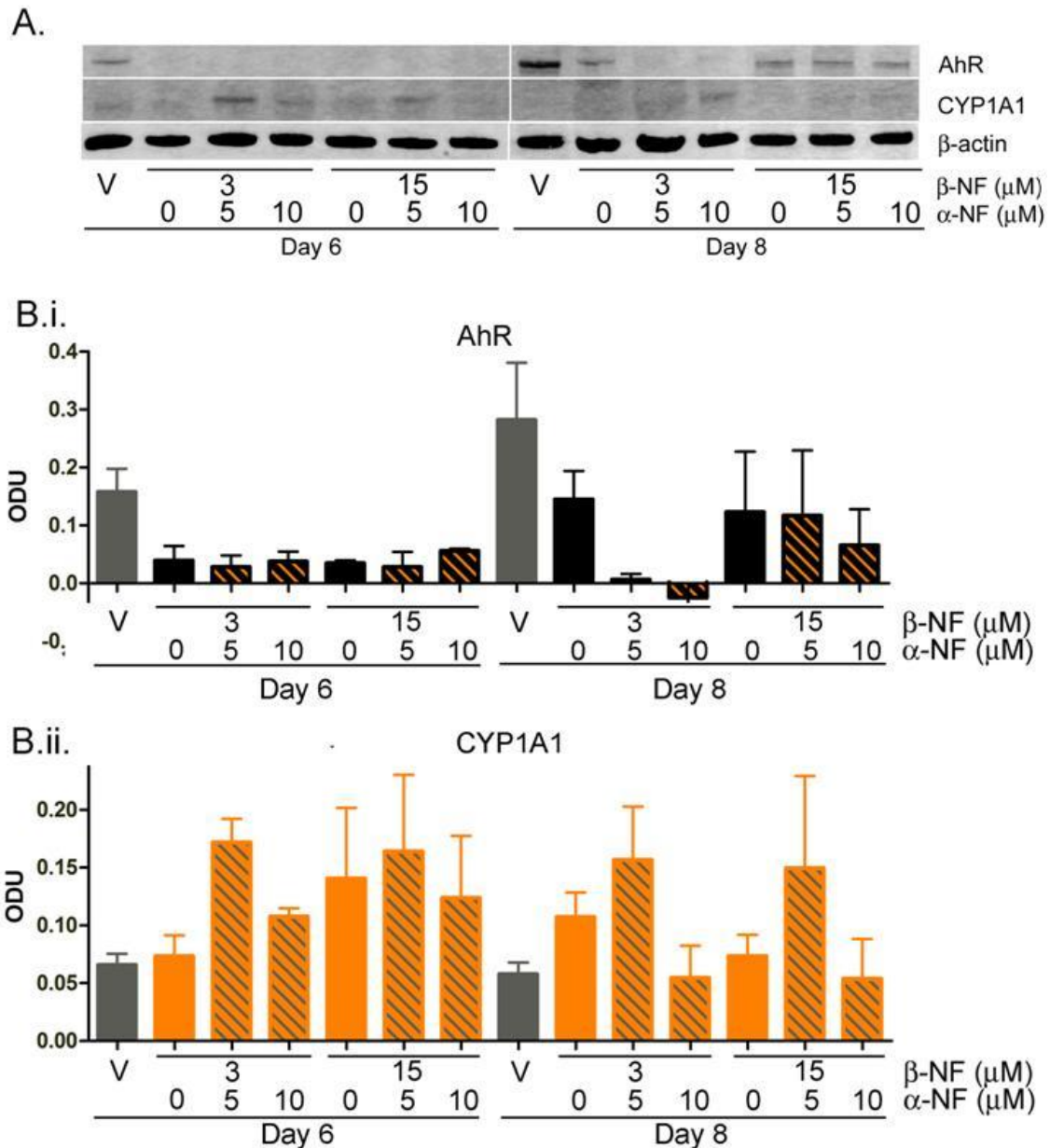


Appendix C. α -NF blocks TCDD induced degradation of AhR and CYP1A1 induction. Primary keratinocytes were treated with vehicle, TCDD \pm α -NF as indicated. After 6 or 8 days, cells were lysed and Western blotting performed. Top graph: Black bars represent densitometry of anti-AhR bands, orange hatching indicates co-treatment of keratinocytes with α -NF as opposed to plain black indicating TCDD alone, grey bars represent vehicle treated keratinocytes. Lower graph: Orange bars represent densitometry of anti-CYP1A1, grey hatching indicates co-treatment of keratinocytes with α -NF, grey bars represent vehicle treated keratinocytes. Densitometry from AhR and CYP1A1 was normalised to β -actin. Values are presented as optical densitometry units (ODU) \pm sem, from 3 donors. Two-way ANOVA was performed comparing TCDD treated keratinocytes to α -NF and time. α -NF induced significant effects on AhR degradation ($P < 0.002$).



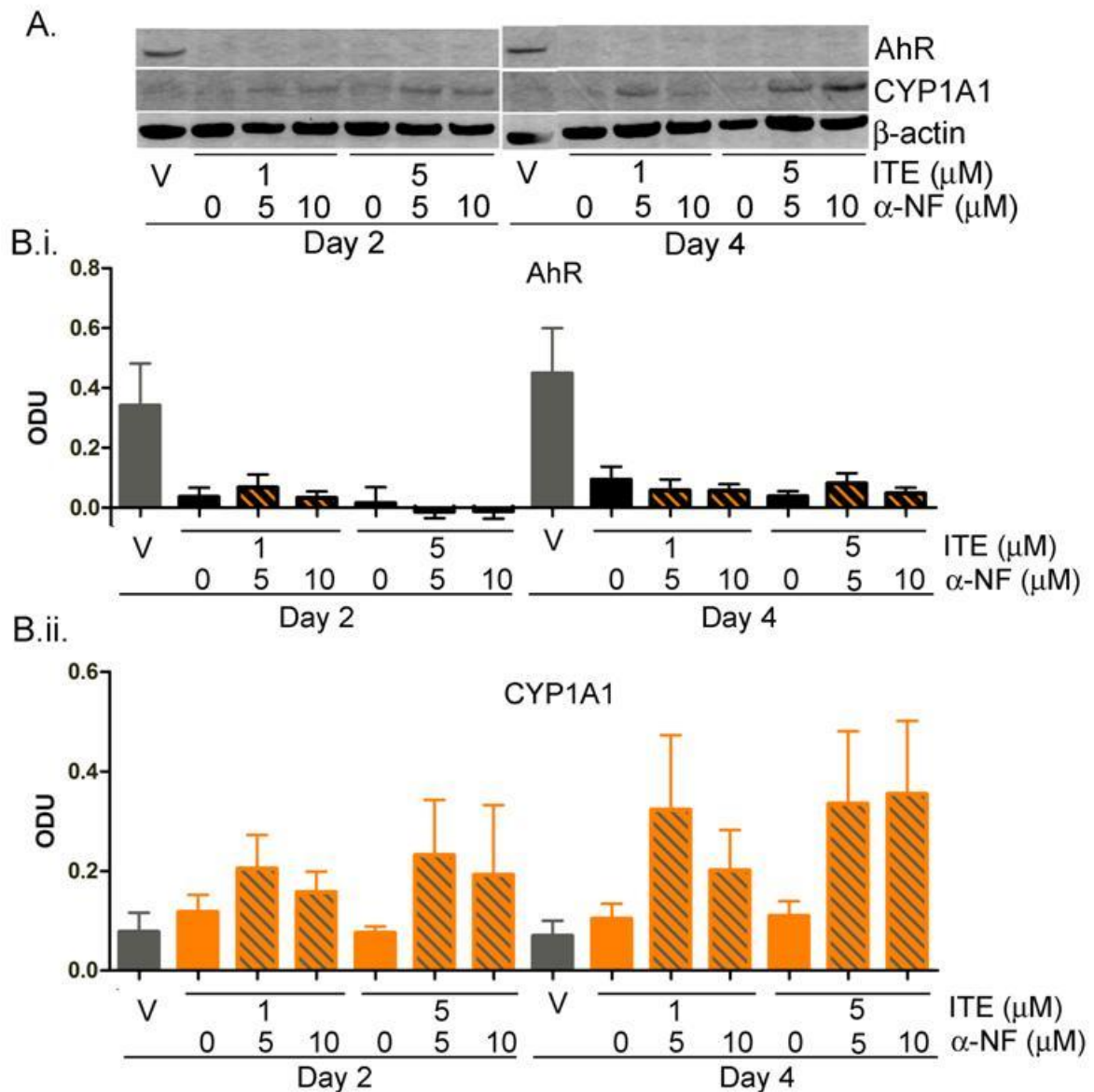
Appendix D. Effects of partial agonist α -NF on β -NF induced AhR activation.

Primary keratinocytes were treated with vehicle or concentrations of β -NF \pm α -NF as indicated. After 2 or 4 days cells were lysed and Western blotting performed (**A**). **B.i**) Black bars represent densitometry of anti-AhR bands, orange hatching indicates co-treatment of keratinocytes with α -NF as opposed to plain black indicating TCDD alone. **B.ii**) Orange bars represent densitometry of anti-CYP1A1, grey hatching indicates co-treatment of keratinocytes with α -NF. Grey bars represent vehicle treated keratinocytes on both graphs. Densitometry from AhR and CYP1A1 was normalised to β -actin and presented as optical densitometry units (ODU) \pm sem, from 3 donors. Two-way ANOVA showed significant effects of time on β -NF and α -NF induced CYP1A1 ($P < 0.03$).

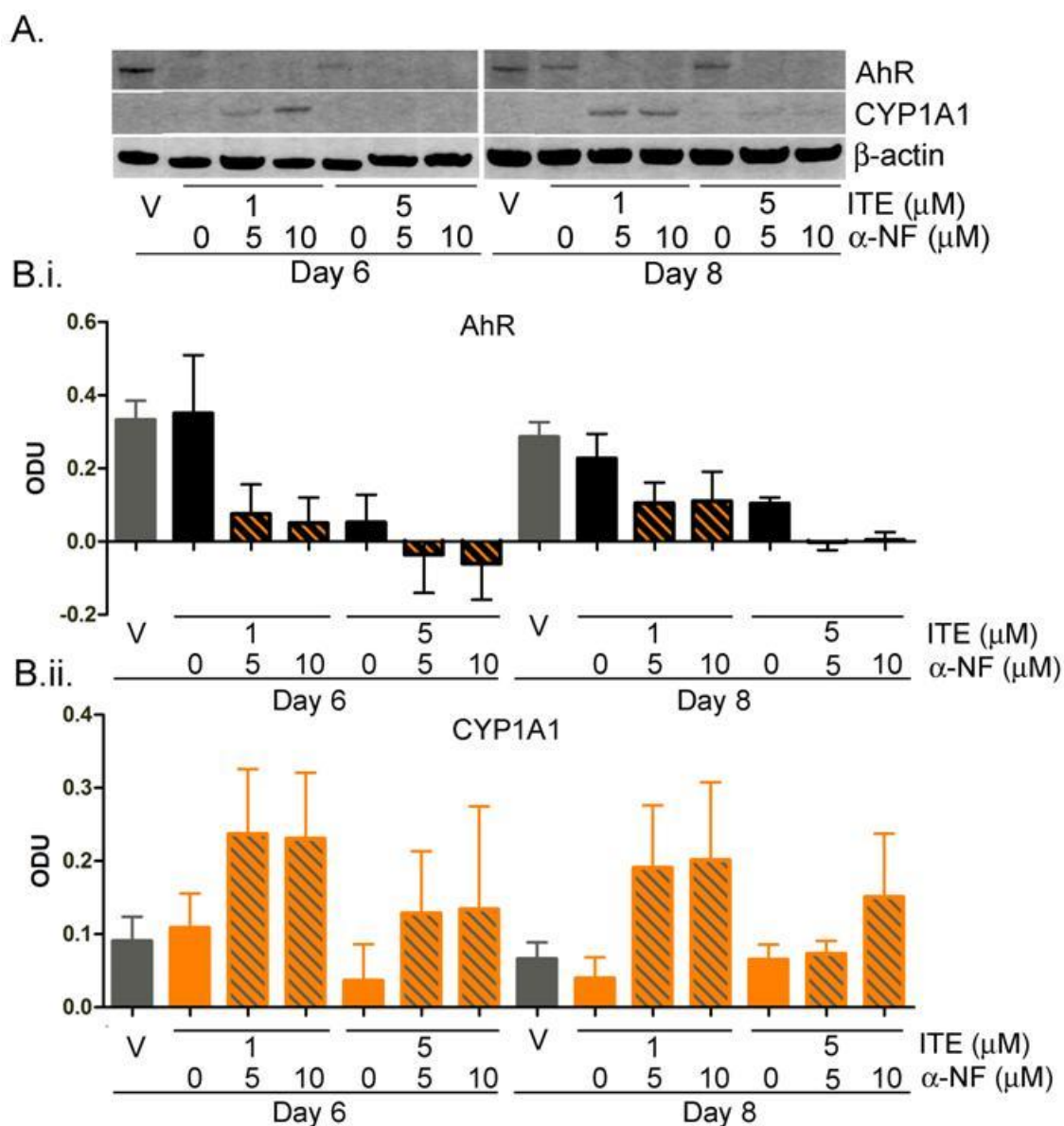


Appendix E. Effects of partial agonist α -NF on β -NF induced AhR activation.

Primary keratinocytes were treated with vehicle or doses of β -NF \pm α -NF as indicated. After 6 or 8 days cells were lysed and Western blotting performed (**A**). **B.i**) Black bars represent densitometry of anti-AhR bands, orange hatching indicates co-treatment of keratinocytes with α -NF as opposed to plain black indicating TCDD alone. **B.ii**) Orange bars represent densitometry of anti-CYP1A1, grey hatching indicates co-treatment of keratinocytes with α -NF. Grey bars represent vehicle treated keratinocytes on both graphs. Densitometry from AhR and CYP1A1 was normalised to β -actin and presented as optical densitometry units (ODU) \pm sem, from 3 donors. Two-way ANOVA showed significant effects of time on β -NF and α -NF induced CYP1A1 ($P < 0.03$).

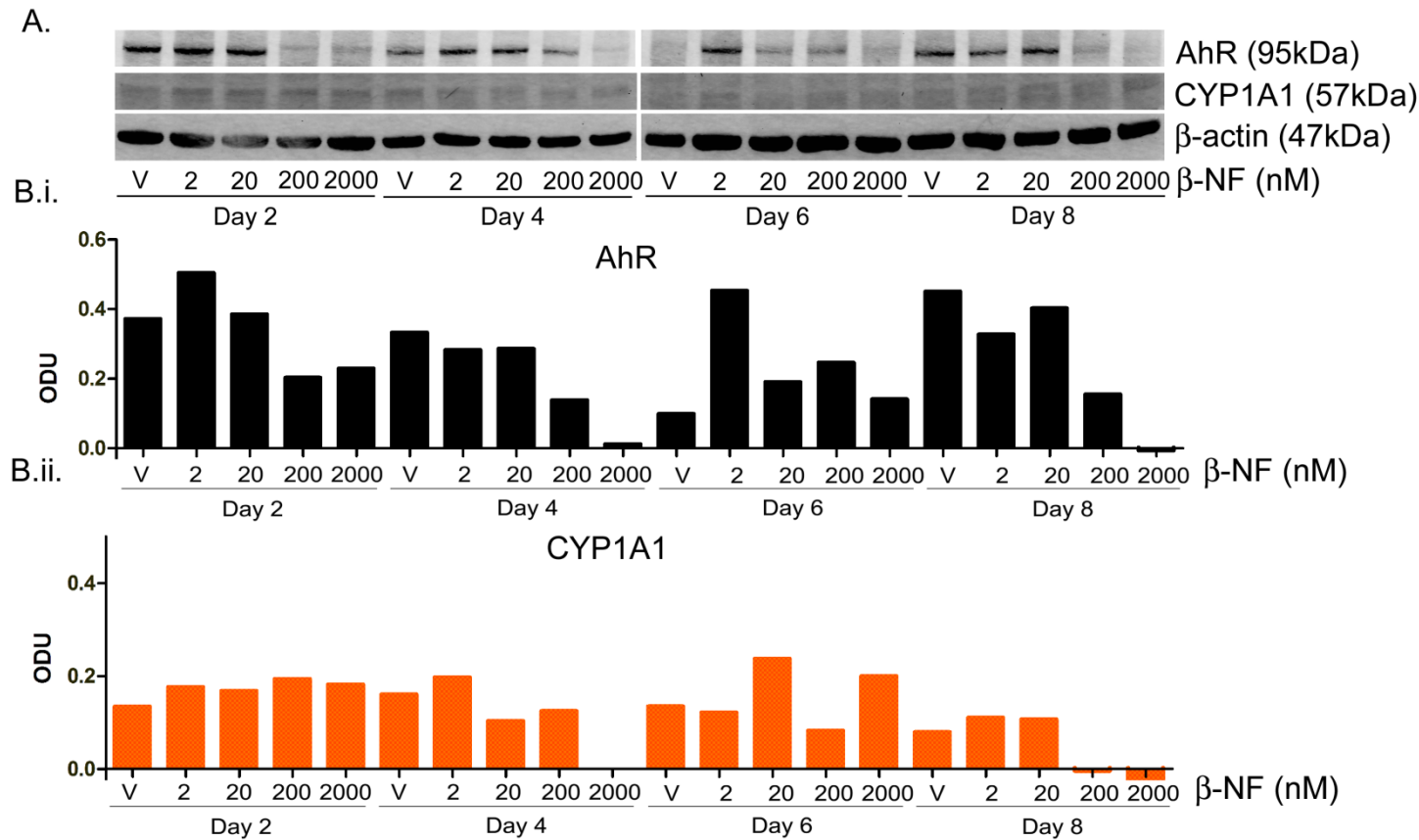


Appendix F. Effects of partial agonist α -NF on ITE induced AhR activation. Primary keratinocytes were treated with vehicle or concentrations of ITE \pm α -NF as indicated. After 2 or 4 days cells were lysed and Western blotting performed (A). B.i) Black bars represent densitometry of anti-AhR bands, orange hatching indicates co-treatment of keratinocytes with α -NF as opposed to plain black indicating TCDD alone. B.ii) Orange bars represent densitometry of anti-CYP1A1, grey hatching indicates co-treatment of keratinocytes with α -NF. Grey bars represent vehicle treated keratinocytes on both graphs. Densitometry from AhR and CYP1A1 was normalised to β -actin and presented as optical densitometry units (ODU) \pm sem, from 3 donors. Two-way ANOVA compared α -NF and time to ITE treatment. Time point induced significant effects on AhR in 5 μ M ITE treated keratinocytes ($P < 0.0001$), while α -NF induced significant effects on CYP1A1 levels in 1 μ M ITE treated keratinocytes ($P < 0.02$).

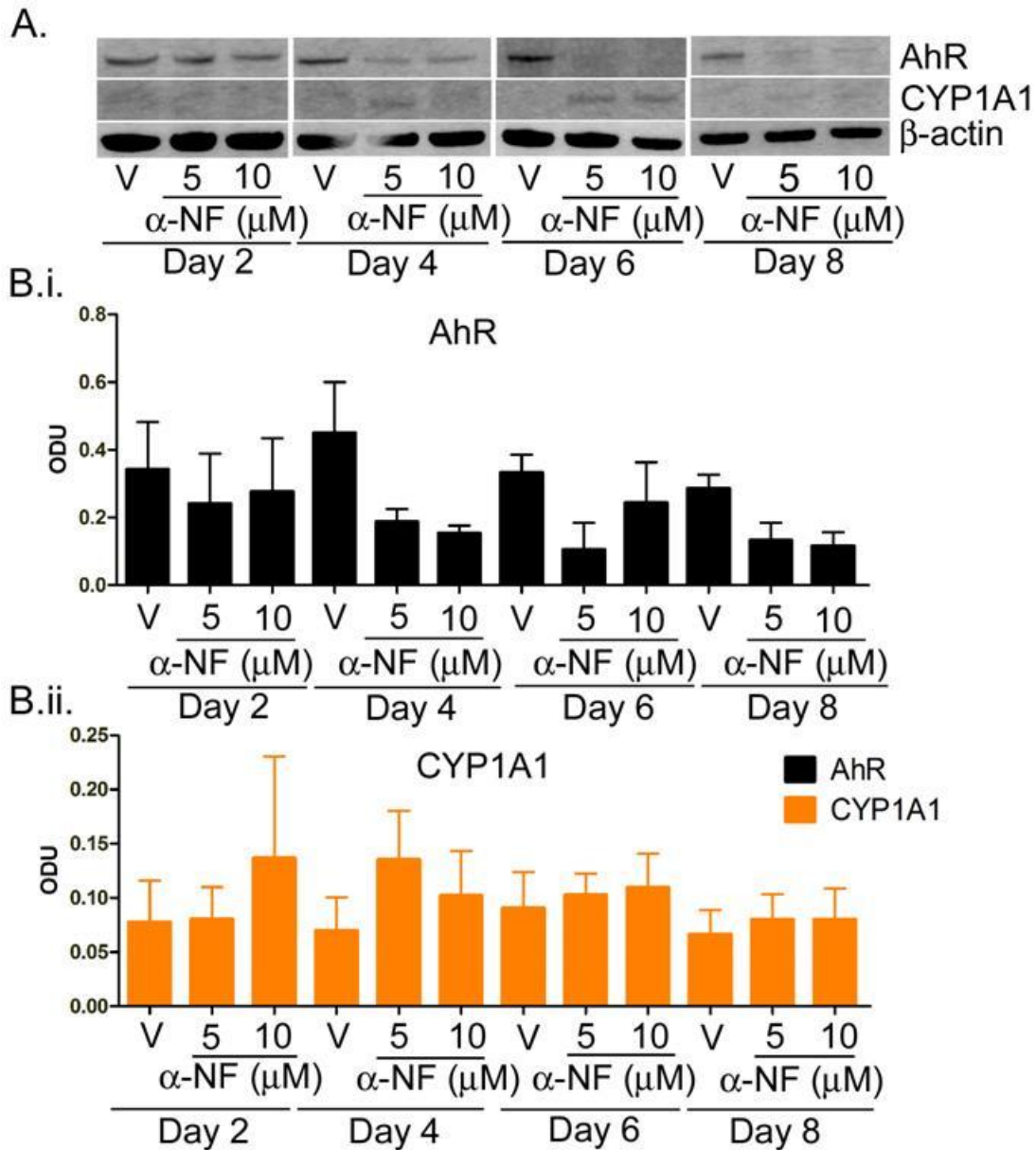


Appendix G. Effects of partial agonist α -NF on ITE induced AhR activation.

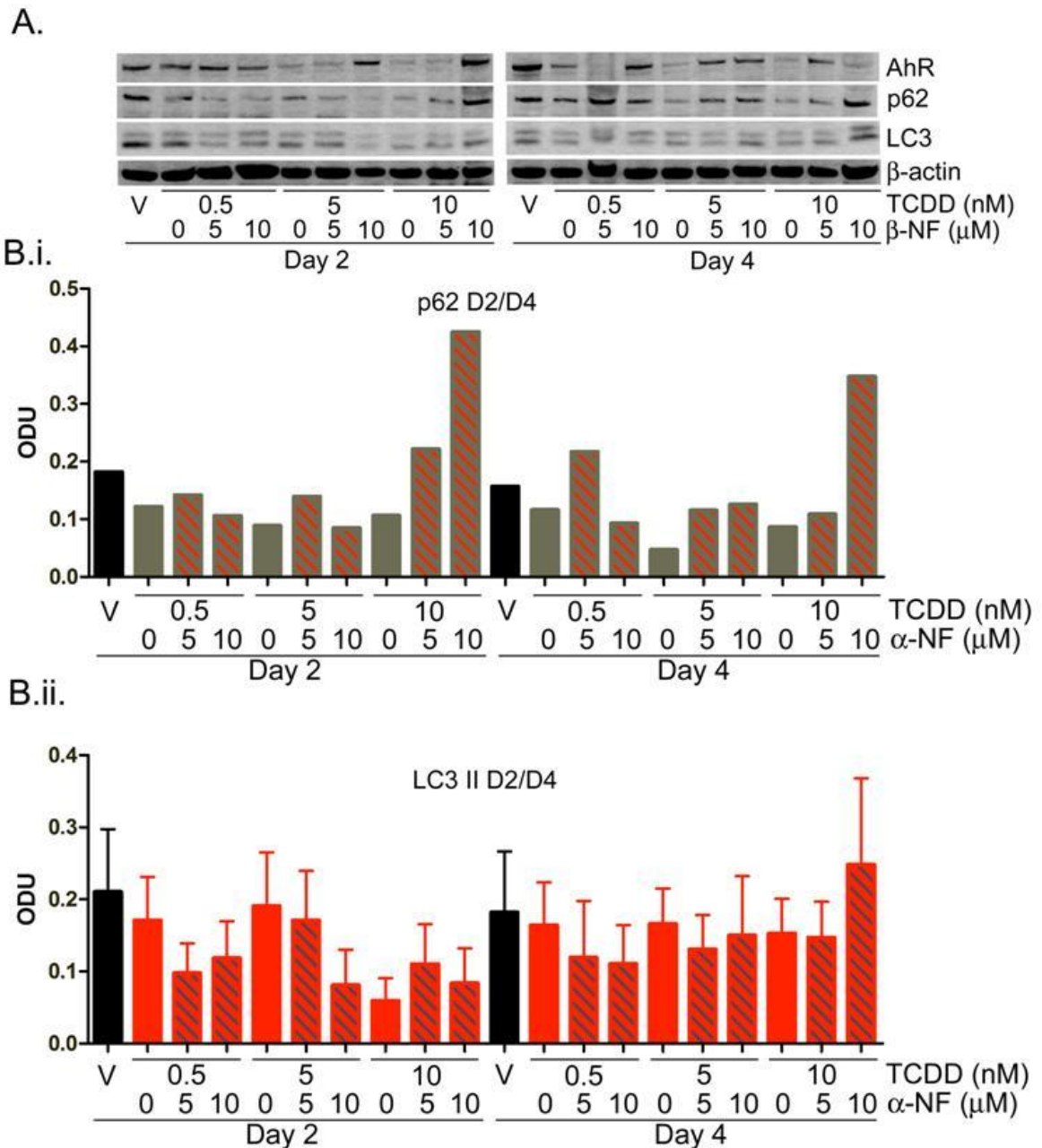
Primary keratinocytes were treated with vehicle or doses of ITE \pm α -NF as indicated. After 6 or 8 days cells were lysed and Western blotting performed (A). B.i) Black bars represent densitometry of anti-AhR bands, orange hatching indicates co-treatment of keratinocytes with α -NF as opposed to plain black indicating TCDD alone. B.ii) Orange bars represent densitometry of anti-CYP1A1, grey hatching indicates co-treatment of keratinocytes with α -NF. Grey bars represent vehicle treated keratinocytes on both graphs. Densitometry from AhR and CYP1A1 was normalised to β -actin and presented as optical densitometry units (ODU) \pm sem, from 3 donors. Two-way ANOVA compared ITE and α -NF co-treatment and time to ITE treated keratinocytes. Time point induced significant effects on AhR in 5 μ M ITE treated keratinocytes ($P < 0.0001$), while α -NF induced significant effects on CYP1A1 levels in 1 μ M ITE treated keratinocytes ($P < 0.02$).



Appendix H. Complete time course of the effects of low concentrations of β -NF on AhR and CYP1A1. Primary keratinocytes were treated with vehicle or concentrations of β -NF as indicated for 2 to 8 days. **A)** Western blotting was performed and membranes were probed with anti-AhR and anti-CYP1A1 antibodies and β -actin as a loading control. **B)** Western blots were analysed by densitometry. Optical density units of AhR (B.i) and CYP1A1 (B.ii) bands were normalized to β -actin. Western blot is representative of duplicate blots in 2 donors. Densitometry represents mean. No statistical analysis was performed due to low sample number. Days 2 and 8 repeated in Figure 3.12.

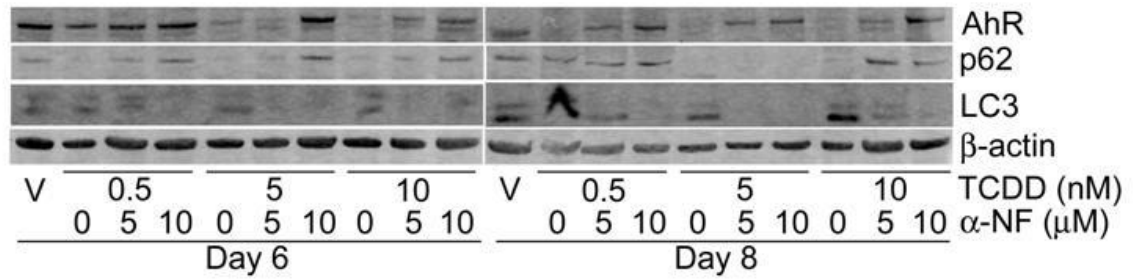


Appendix I. α -Naphthoflavone is a partial AhR agonist in primary keratinocytes. Primary keratinocytes were treated with vehicle or concentrations of α -NF as indicated for up to 8 days. Western blotting was performed (A). B.i) AhR and B.ii) CYP1A1 bands were analysed by densitometry and presented as optical density units (ODU) normalised to β -actin. Western blot is representative of duplicate blots in 3 donors. Densitometry represents mean \pm sem for blots from 3 independent donors. Two-way ANOVA was performed comparing vehicle to α -NF and time. α -NF induced significant effects on AhR degradation ($P < 0.05$).

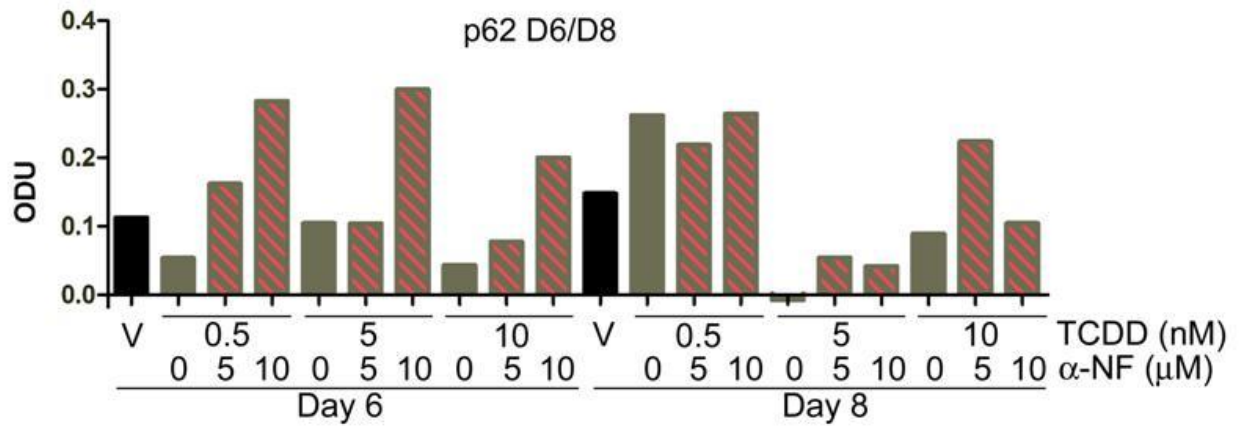


Appendix J. The effects of co-treatment of TCDD plus α -NF on autophagy. Primary keratinocytes were treated with vehicle or TCDD \pm α -NF. After 2 or 4 days cells were lysed and Western blotting performed (**A**). Densitometry was performed on Western blots probed with **B.i.)** p62 and **B.ii.)** LC3 antibodies. Black bars represent vehicle treated keratinocytes, plain bars indicate TCDD alone and hatching on bars indicates co-treatment of keratinocytes with α -NF. Densitometry from LC3 II and p62 was normalised to β -actin. **B.i)** p62 values are represented as mean ODU from 1-3 donors. No analysis was performed on p62 due to low sample size. **B.ii.)** 2-way ANOVA was performed comparing TCDD treated samples to the effects of α -NF over time. α -NF was shown to have a significant effect on LC3 II expression ($P = 0.002$). Values are presented as optical densitometry units (ODU) \pm sem, from 3 donors.

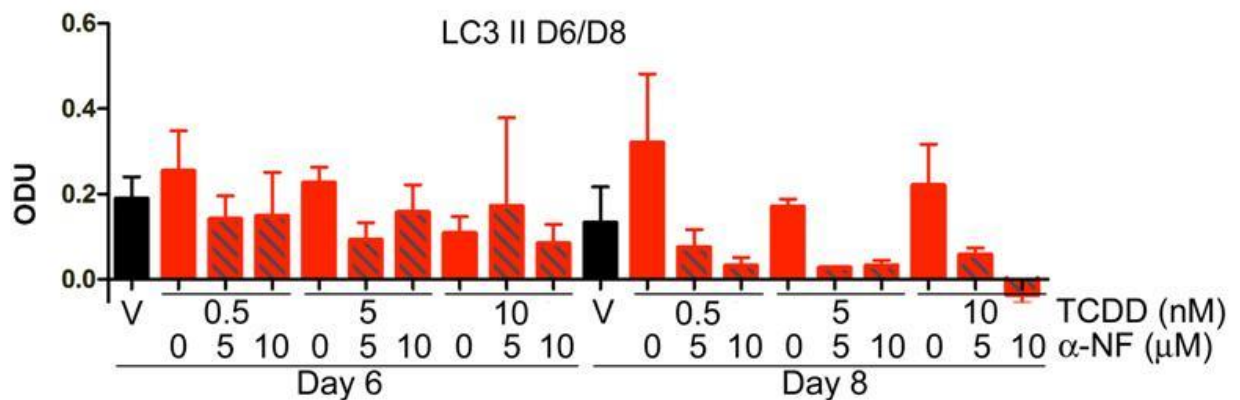
A.



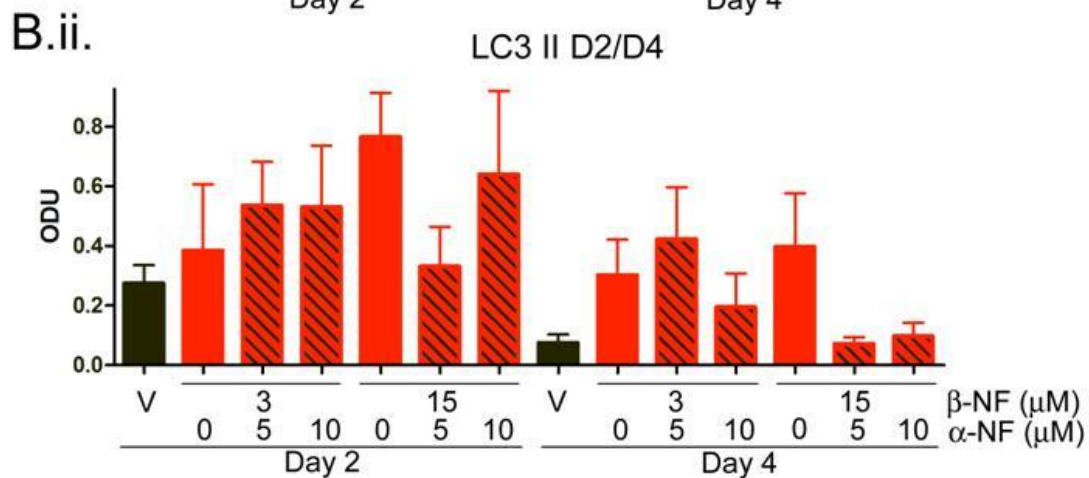
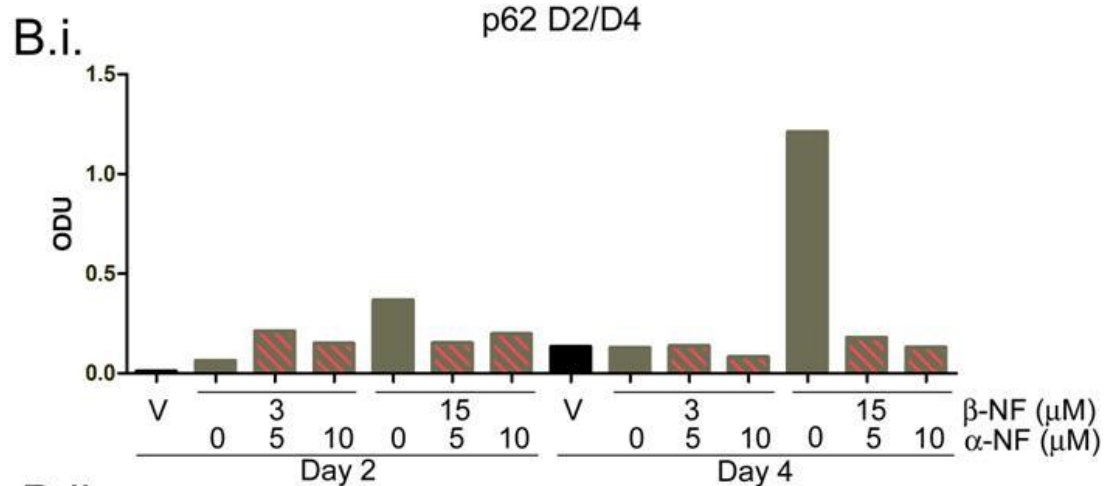
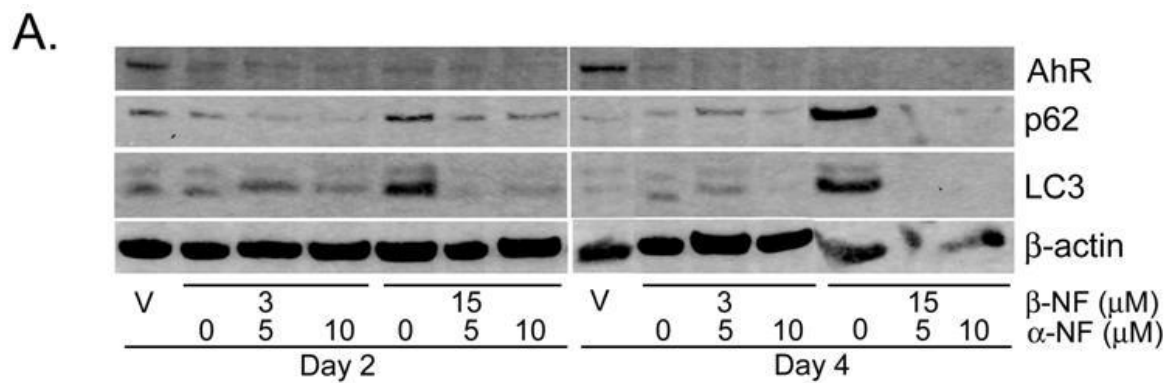
B.i.



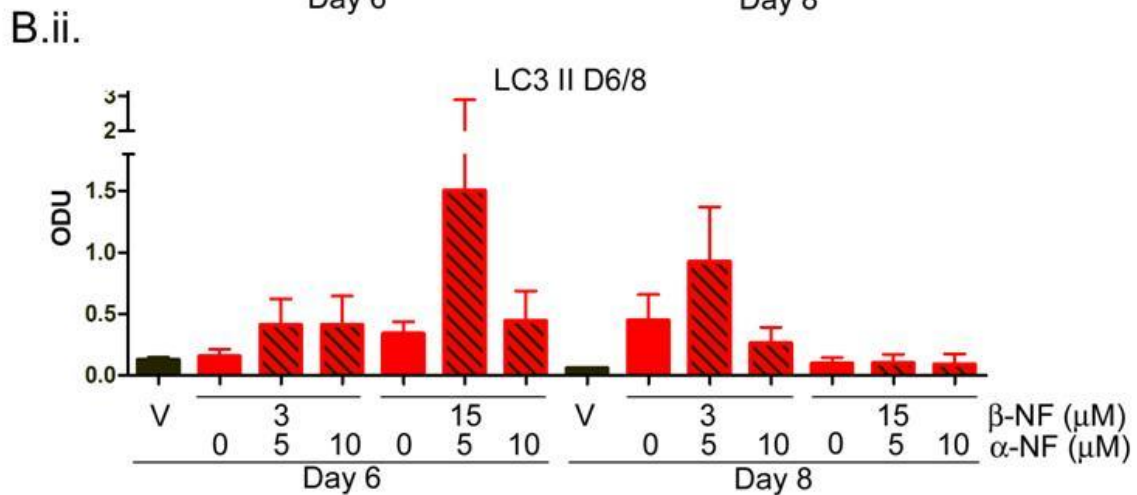
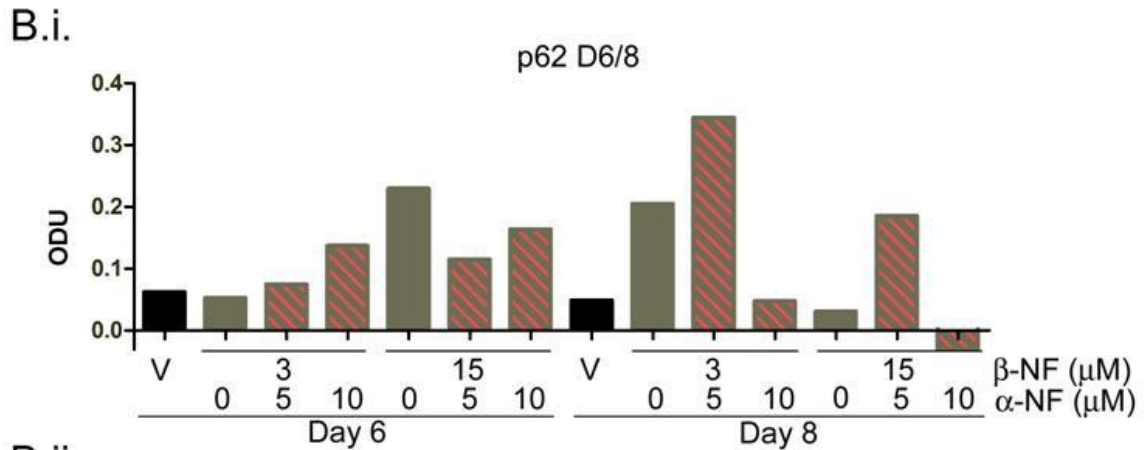
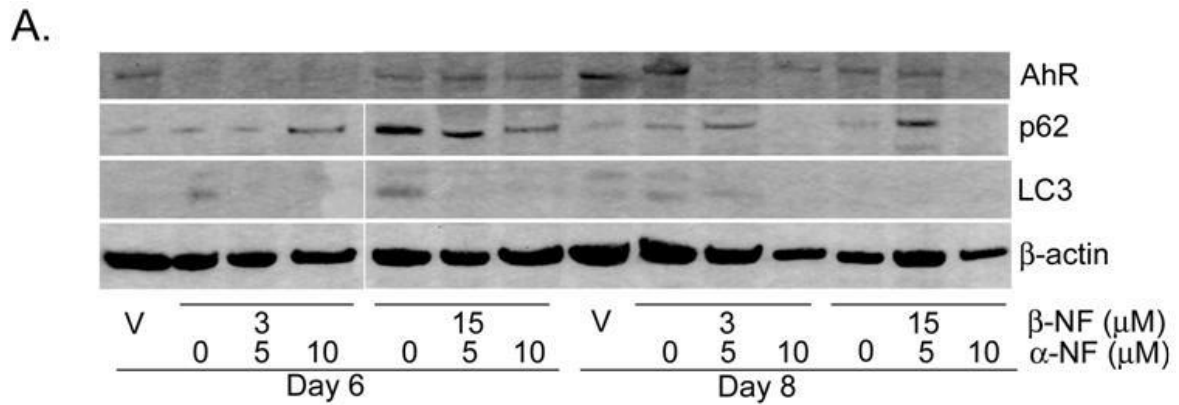
B.ii.



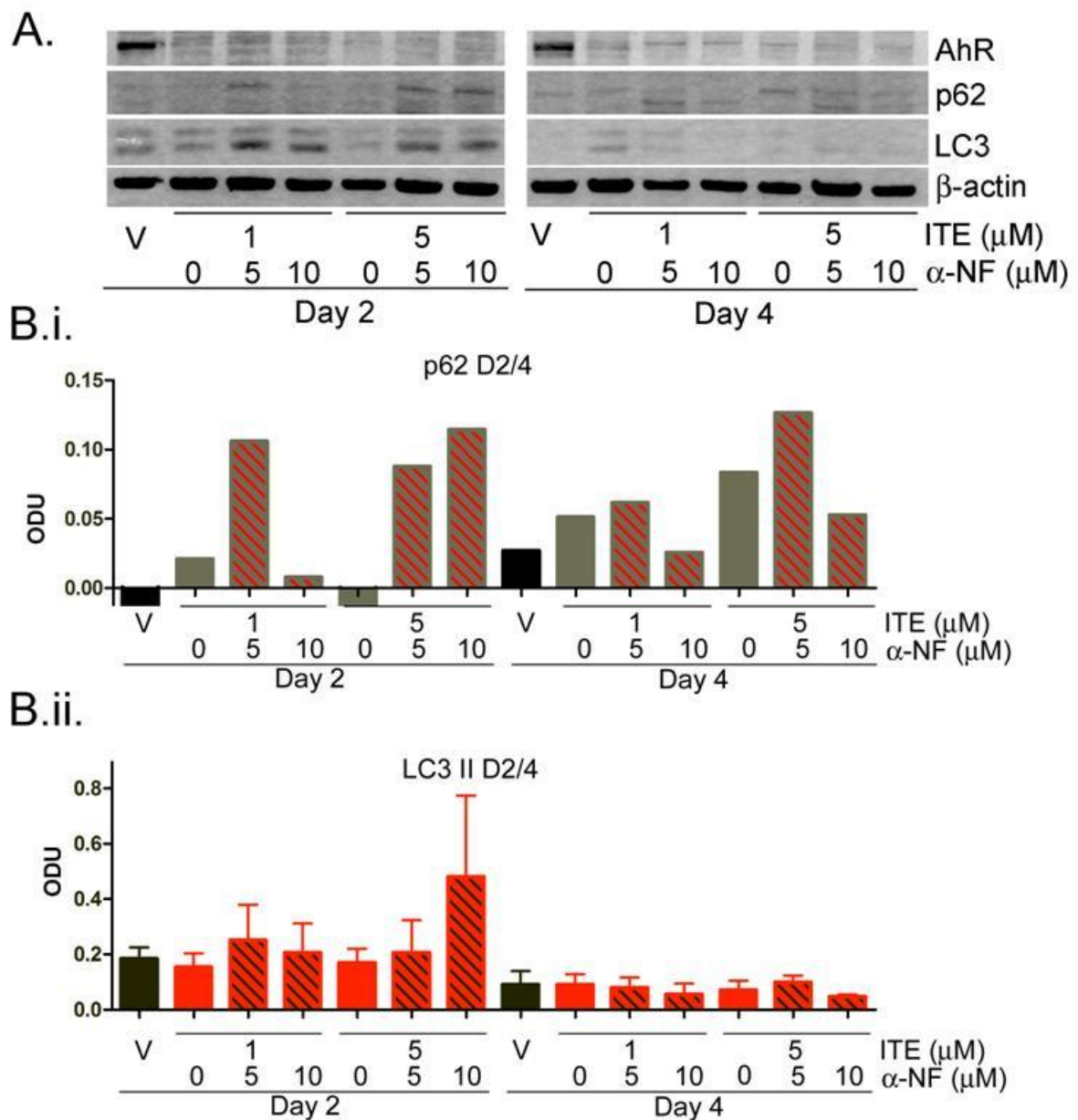
Appendix K. The effects of co-treatment of TCDD plus α -NF on autophagy. Primary keratinocytes were treated with vehicle or TCDD \pm α -NF as indicated. After 6 or 8 days cells were lysed and Western blotting performed (A). Densitometry was performed on Western blots probed with B.i.) p62 and B.ii.) LC3 antibodies. Black bars represent vehicle treated keratinocytes, plain bars indicate TCDD alone and hatching on bars indicates co-treatment of keratinocytes with α -NF. Densitometry from LC3 II and p62 was normalised to β -actin. B.i.) Values are represented as mean ODU from 1-3 donors. No analysis was performed on p62 due to low sample size. B.ii.) 2-way ANOVA was performed comparing TCDD treated samples to the effects of α -NF and time. α -NF was shown to have a significant effect on LC3 II expression ($P = 0.002$). Values are presented as optical densitometry units (ODU) \pm sem, from 3 donors



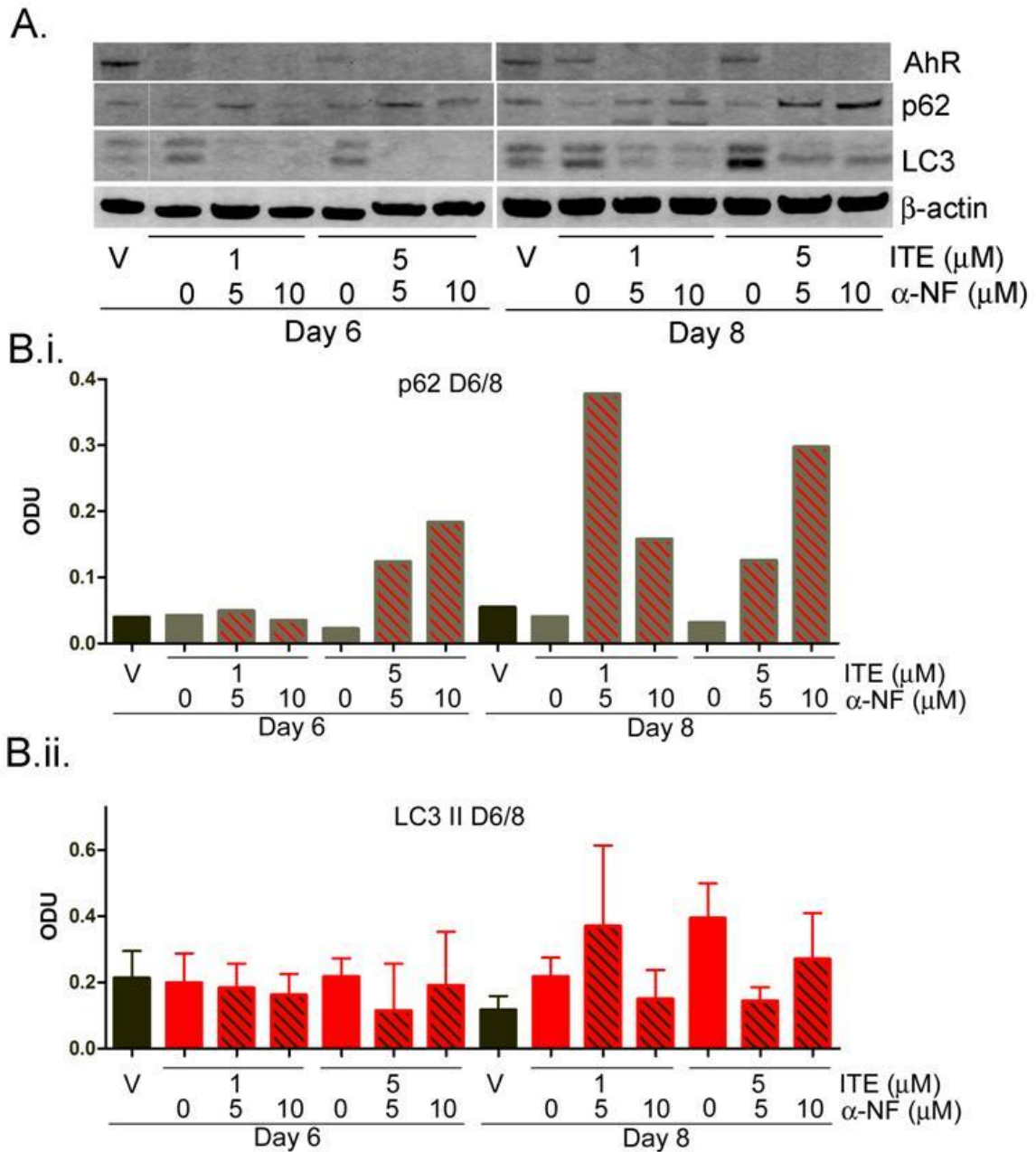
Appendix L. The effects of co-treatment with β-NF plus α-NF on autophagy in primary keratinocytes. Primary keratinocytes were treated with vehicle or β-NF ± α-NF as indicated. After 2 or 4 days cells were lysed and Western blotting performed (**A**). Densitometry was performed on Western blots probed with **B.i**) p62 and **B.ii**) LC3 antibodies. Black bars represent vehicle treated keratinocytes, plain bars indicate β-NF alone and hatching on bars indicates co-treatment of keratinocytes with α-NF. Densitometry from LC3 II and p62 was normalised to β-actin. **B.i**) Values are represented as mean ODU from 1-3 donors. No analysis was performed on p62 due to low sample size. **B.ii**) 2-way ANOVA was performed comparing the effects of β-NF with the effects of α-NF and time. The effects of 15μM β-NF plus α-NF were significantly affected by time ($P < 0.02$). Values are presented as optical densitometry units (ODU) ± sem, from 3 donors.



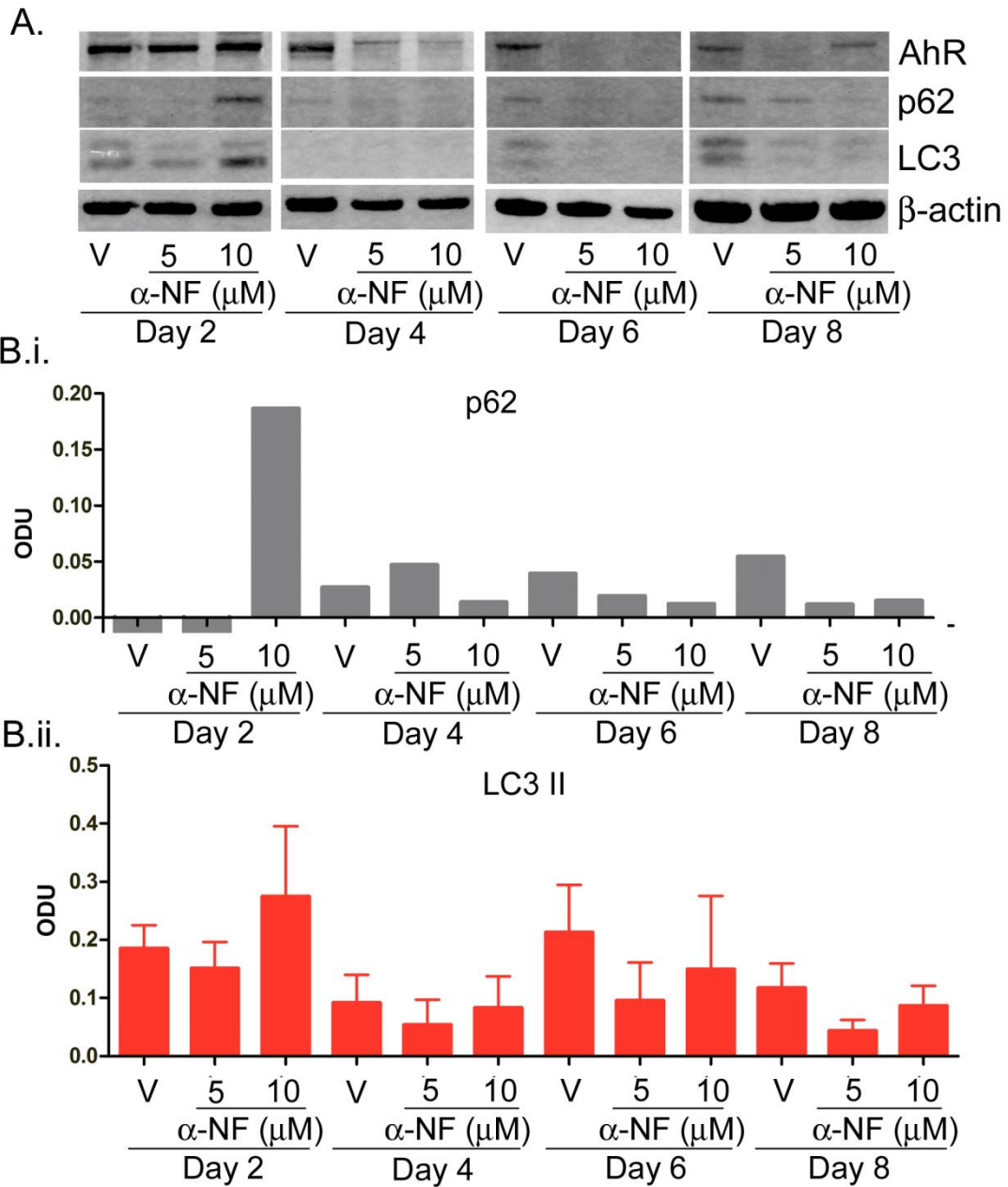
Appendix M. The effects of co-treatment with β-NF plus α-NF on autophagy in primary keratinocytes. Primary keratinocytes were treated with vehicle or β-NF ± α-NF as indicated. After 6 or 8 days cells were lysed and Western blotting performed (**A**). Densitometry was performed on Western blots probed with **B.i**) p62 and **B.ii**) LC3 II. Black bars represent vehicle treated keratinocytes, plain bars indicating β-NF alone and hatching on bars indicates co-treatment of keratinocytes with α-NF. Densitometry from LC3 II and p62 was normalised to β-actin. **B.i.**) Values are represented as mean ODU from 1-3 donors. No analysis was performed on p62 due to low sample size. **B.ii.**) 2-way ANOVA was performed comparing the effects of β-NF with the effects of α-NF and time. The effects of 15μM β-NF plus α-NF were significantly affected by time ($P < 0.02$). Values are presented as optical densitometry units (ODU) ± sem, from 3 donors.



Appendix N. The effects of co-treatment with ITE plus α -NF on autophagy in primary keratinocytes. Primary keratinocytes were treated with vehicle or ITE \pm α -NF as indicated. After 2 or 4 days cells were lysed and Western blotting performed (**A**). Densitometry was performed on Western blots probed with **B.i.)** p62 and **B.ii.)** LC3. Black bars represent vehicle treated keratinocytes, plain bars indicate ITE alone and hatching on bars indicates co-treatment of keratinocytes with α -NF. Densitometry from LC3 II and p62 was normalised to β -actin. **B.i)** Values are represented as mean ODU from 1-3 donors. No analysis was performed on p62 due to low sample size. **B.ii)** 2-way ANOVA was performed comparing the effects of ITE with the effects of α -NF and time. The effects were not significant. Values are presented as optical densitometry units (ODU) \pm sem, from 3 donors.

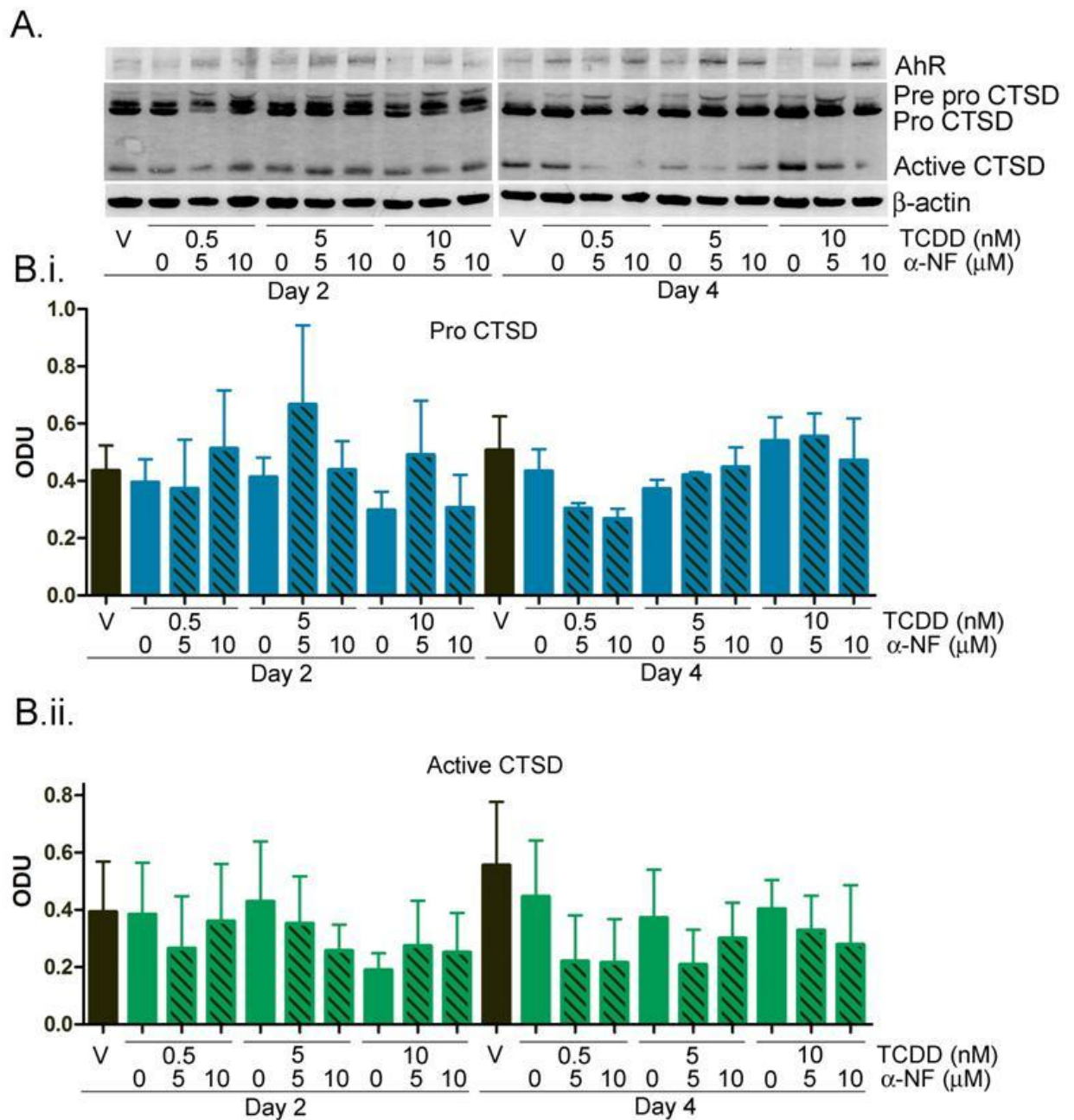


Appendix O. The effects of co-treatment with ITE plus α -NF on autophagy in primary keratinocytes. Primary keratinocytes were treated with vehicle or ITE \pm α -NF as indicated. After 6 or 8 days cells were lysed and Western blotting performed (A). Densitometry was performed on Western blots probed with **B.i)** p62 and **B.ii)** LC3 antibodies. Black bars represent vehicle treated keratinocytes, plain bars indicate ITE alone and hatching on bars indicates co-treatment of keratinocytes with α -NF. Densitometry from LC3 II and p62 was normalised to β -actin. **B.i)** Values are represented as mean ODU from 1-3 donors. No analysis was performed on p62 due to low sample size. **B.ii)** 2-way ANOVA was performed comparing the effects of ITE with the effects of α -NF and time, the effects were not significant. Values are presented as optical densitometry units (ODU) \pm sem, from 3 donors.



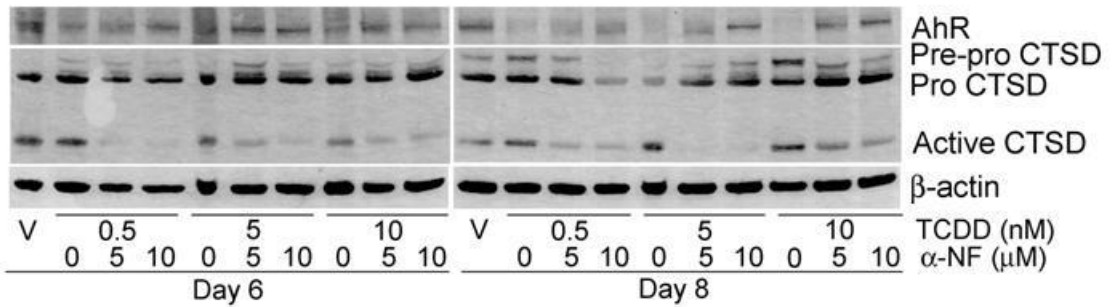
Appendix P. α -NF induced low levels of autophagy in primary keratinocytes.

Primary keratinocytes were treated for up to 8 days with vehicle or concentrations of α -NF as indicated. Samples were lysed and Western blotting performed (A). Densitometry was carried out on Western blots probed with B.i.) anti-p62 antibody and B.ii.) anti-LC3 antibody normalised to β -actin. B.i.) p62 densitometry is representative of 1 donor (days 2 and 4) and 2 donors (days 6 and 8). No statistical analysis was carried out due to low sample size. B) LC3 II was analysed by 2-way ANOVA, comparing vehicle to α -NF at each time point, but results were not significant. LC3 II densitometry is representative of 3 donors.

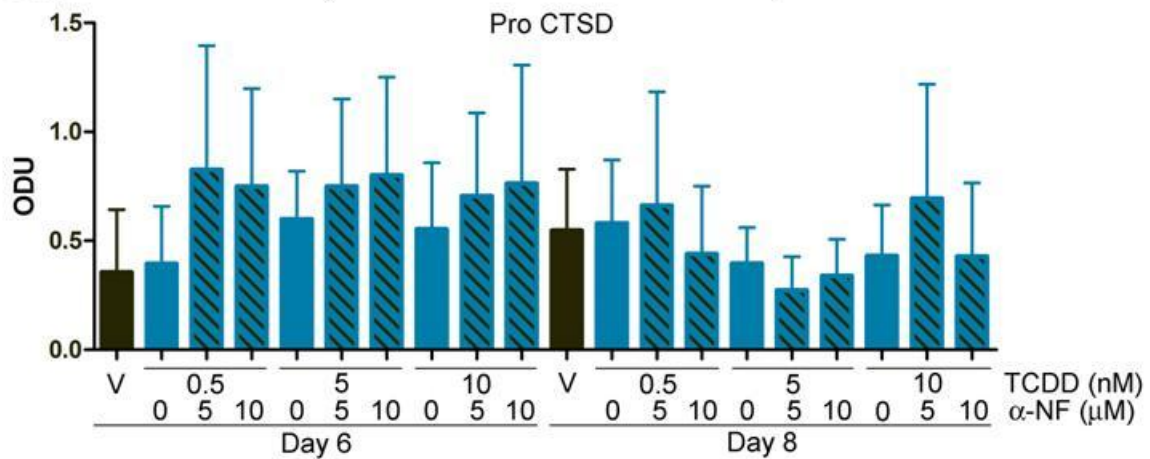


Appendix Q. The effects of co-treatment of TCDD plus α -NF on CTSD in primary keratinocytes. Primary keratinocytes were treated with vehicle or concentrations of TCDD \pm α -NF for 2 or 4 days. Keratinocytes were lysed and Western blotting performed (**A**). Western blots were probed with an anti-CTSD antibody and densitometry was performed on **B.i**) combined pre-pro and pro CTSD and **B.ii**) active CTSD. Two way ANOVA was performed to compare TCDD treatment to the effects of α -NF and time, no results were significant. Densitometry is presented as mean \pm sem representative of 3 donors.

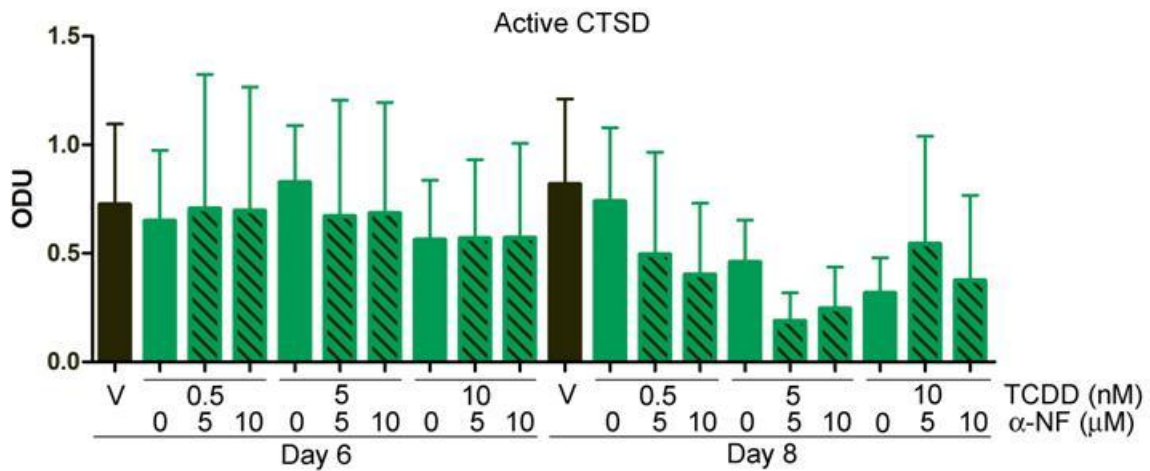
A.



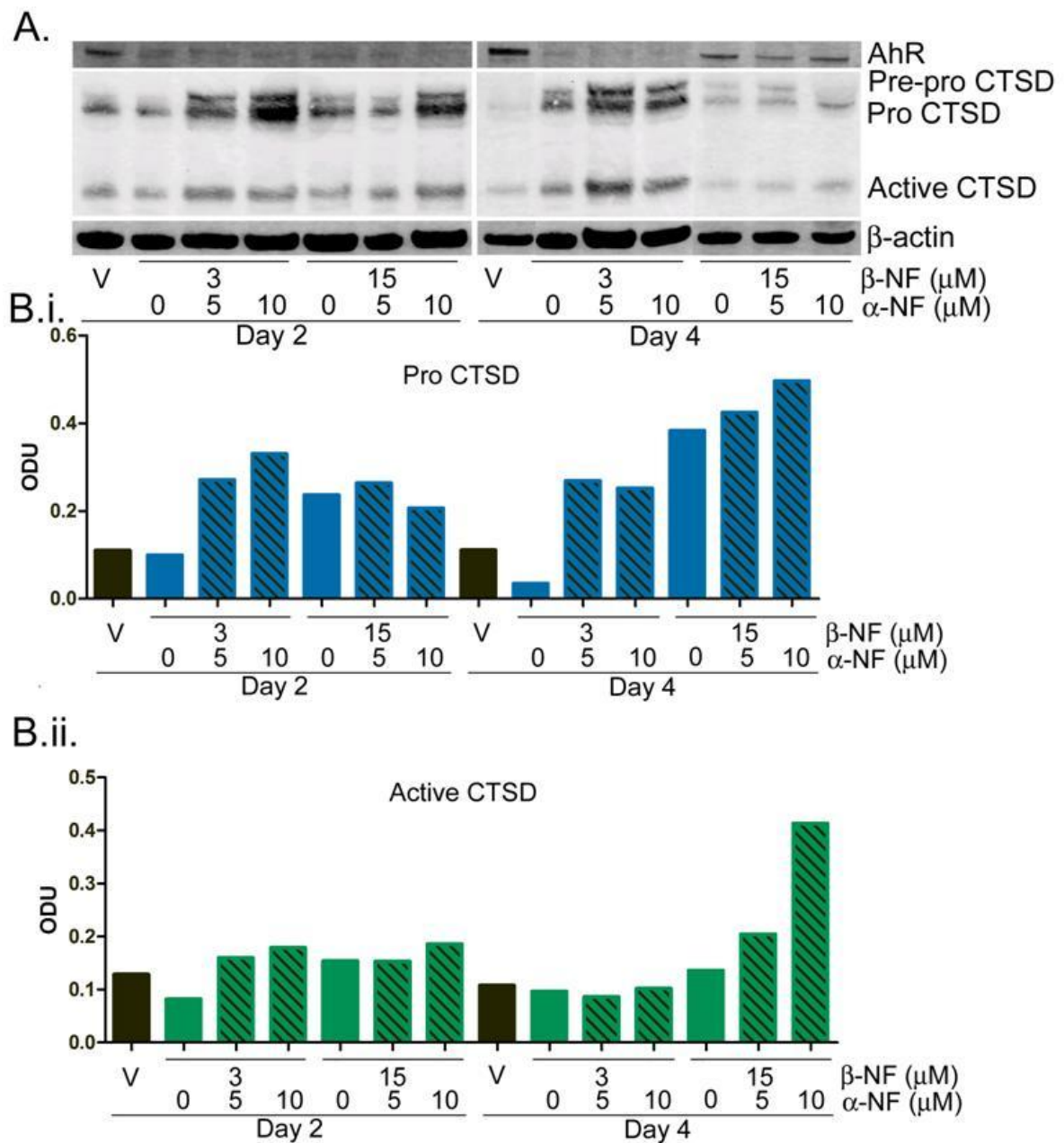
B.i.



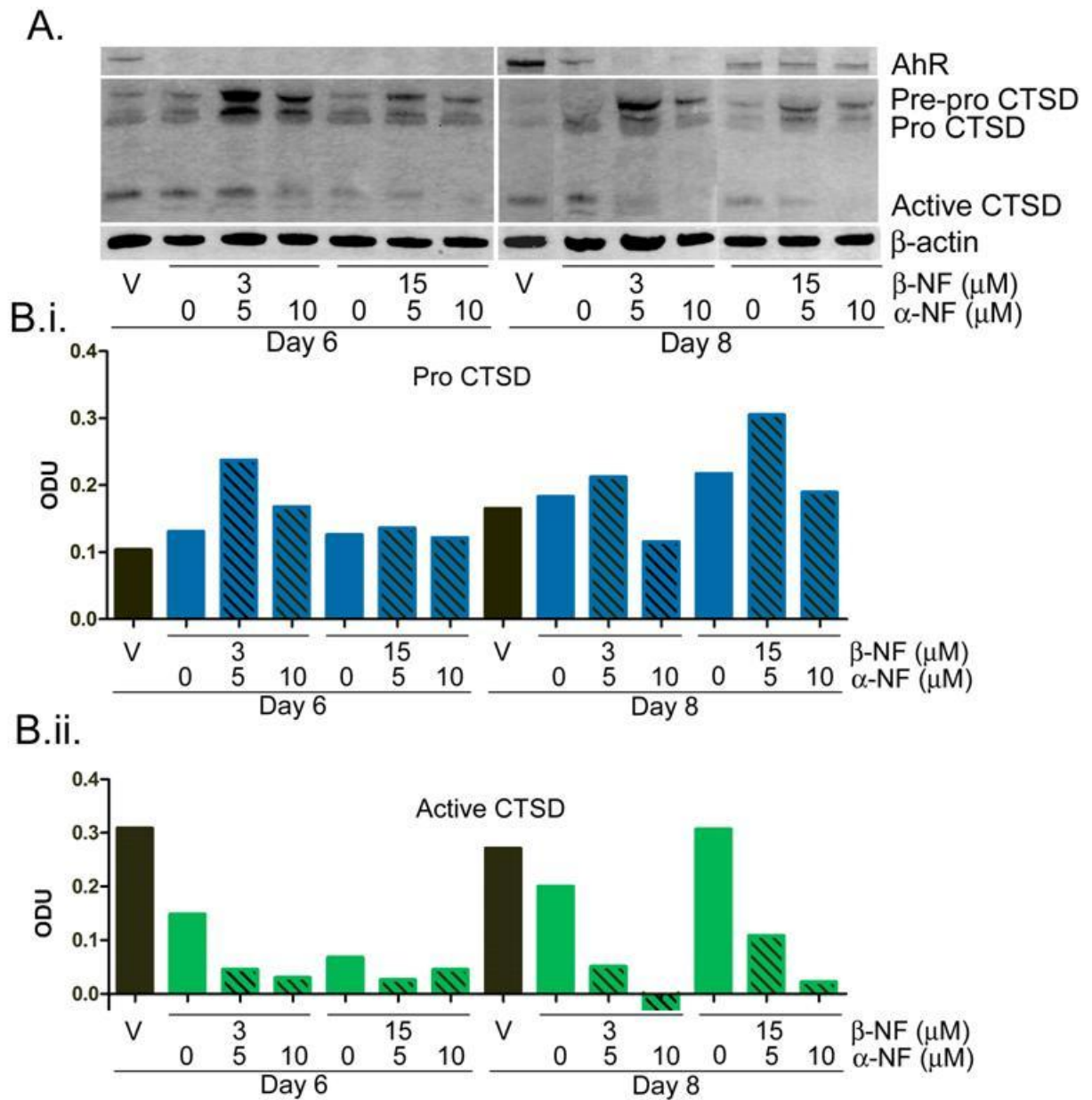
B.ii.



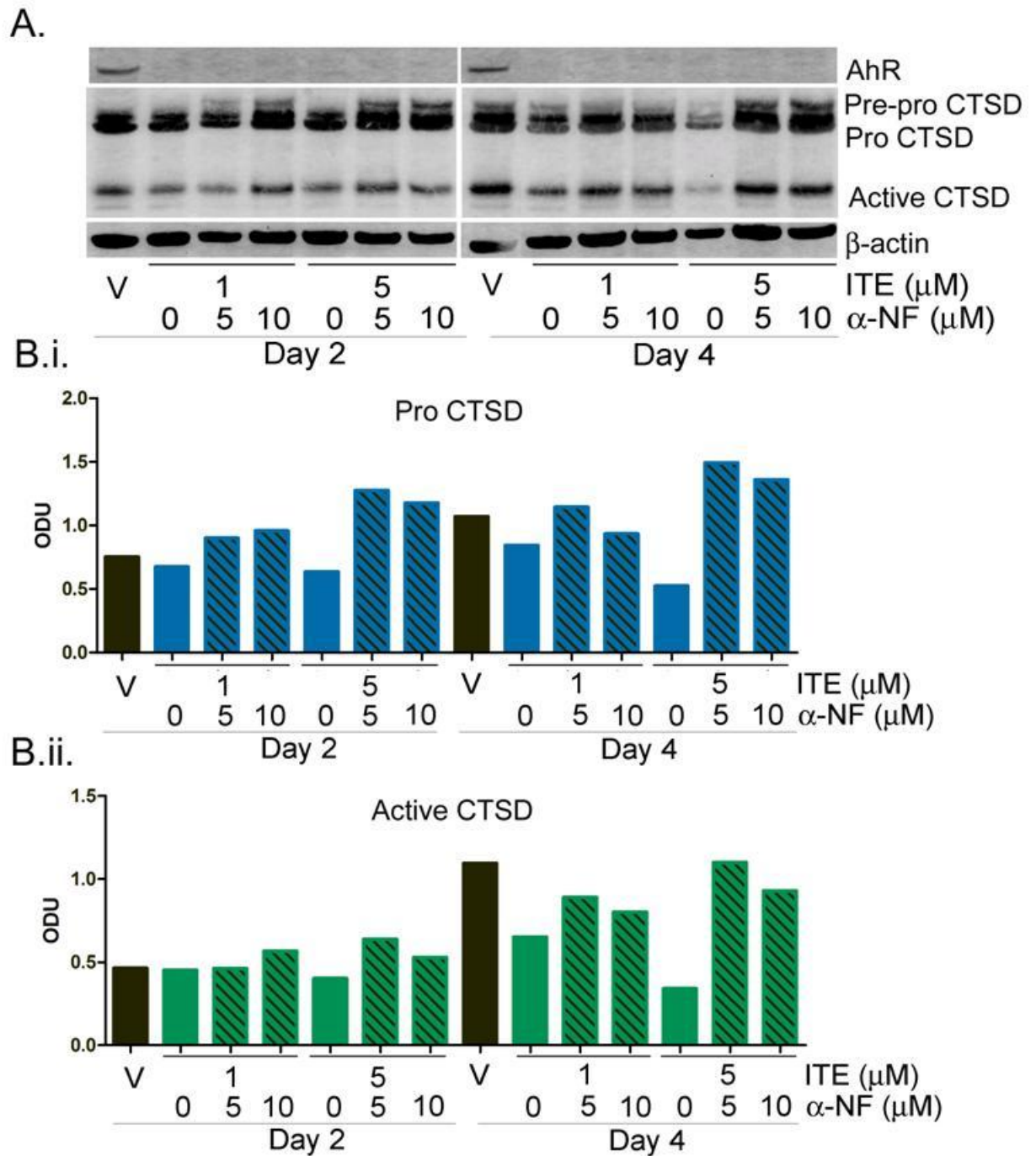
Appendix R. The effects of co-treatment of TCDD plus α-NF on CTSD in primary keratinocytes. Primary keratinocytes were treated with vehicle or concentrations of TCDD ± α-NF for 6 or 8 days. Keratinocytes were lysed and Western blotting performed (A). Western blots were probed with an anti-CTSD antibody and densitometry was performed on B.i) combined pre-pro and pro CTSD and B.ii) active CTSD. Two way ANOVA was performed to compare TCDD treatment to the effects of α-NF and time, no results were significant. Densitometry is presented as mean ± sem representative of 3 donors.



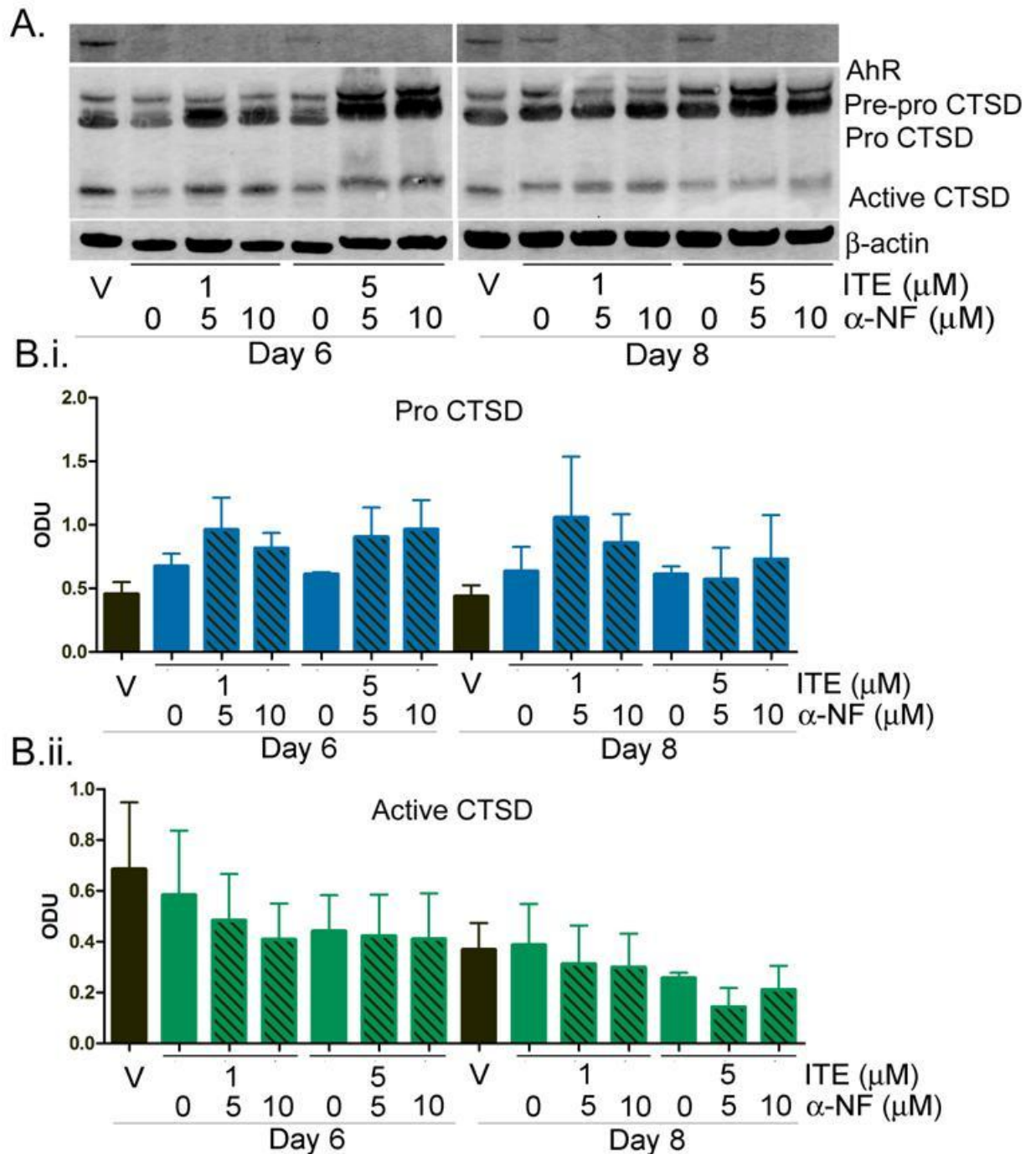
Appendix S. The effects of co-treatment of β -NF plus α -NF on CTSD in primary keratinocytes. Primary keratinocytes were treated with vehicle or concentrations of β -NF \pm α -NF for 2 or 4 days. Keratinocytes were lysed and Western blotting performed (**A**). Western blots were probed with an anti-CTSD antibody and densitometry was performed on **B.i**) combined pre-pro and pro CTSD and **B.ii**) active CTSD. No statistical analysis was performed due to low sample size. Densitometry is presented as mean representative of 2 donors.



Appendix T. The effects of co-treatment of β -NF plus α -NF on CTSD in primary keratinocytes. Primary keratinocytes were treated with vehicle or concentrations of β -NF \pm α -NF for 6 or 8 days. Keratinocytes were lysed and Western blotting performed (**A**). Western blots were probed with an anti-CTSD antibody and densitometry was performed on **B.i**) combined pre-pro and pro CTSD and **B.ii**) active CTSD. No statistical analysis was carried out due to low sample size. Densitometry is presented as mean representative of 2 donors.

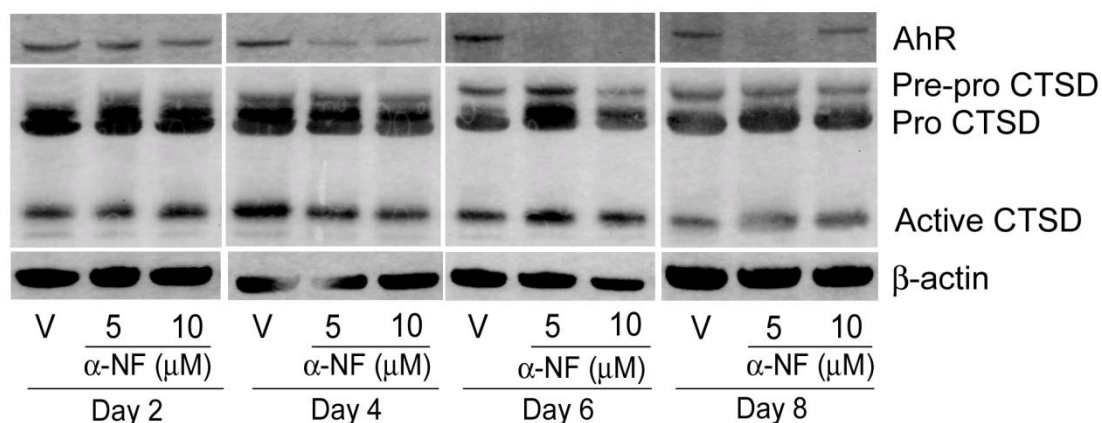


Appendix U. The effects of co-treatment of ITE plus α -NF on CTSD in primary keratinocytes. Primary keratinocytes were treated with vehicle or concentrations of ITE \pm α -NF for 2 or 4 days. Keratinocytes were lysed and Western blotting performed (**A**). Western blots were probed with an anti-CTSD antibody and densitometry was performed on **B.i**) combined pre-pro and pro CTSD and **B.ii**) active CTSD. Statistical analysis has not been performed due to small sample size. Densitometry is presented as mean, representative of 2 donors.

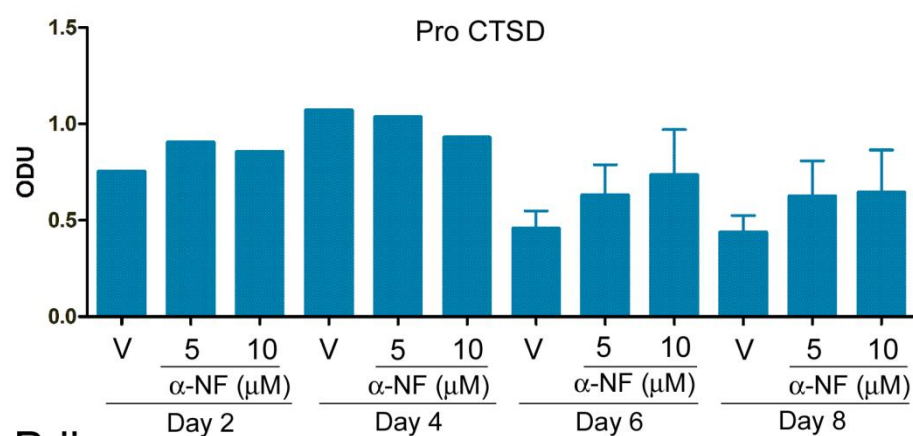


Appendix V. The effects of co-treatment of ITE plus α -NF on CTSD in primary keratinocytes. Primary keratinocytes were treated with vehicle or concentrations of ITE \pm α -NF for 6 or 8 days. Keratinocytes were lysed and Western blotting performed (**A**). Western blots were probed with an anti-CTSD antibody and densitometry was performed on **B.i**) combined pre-pro and pro CTSD and **B.ii**) active CTSD. Statistical analysis has not been carried out due to low sample size. Densitometry is presented as mean \pm sem representative of 3 donors.

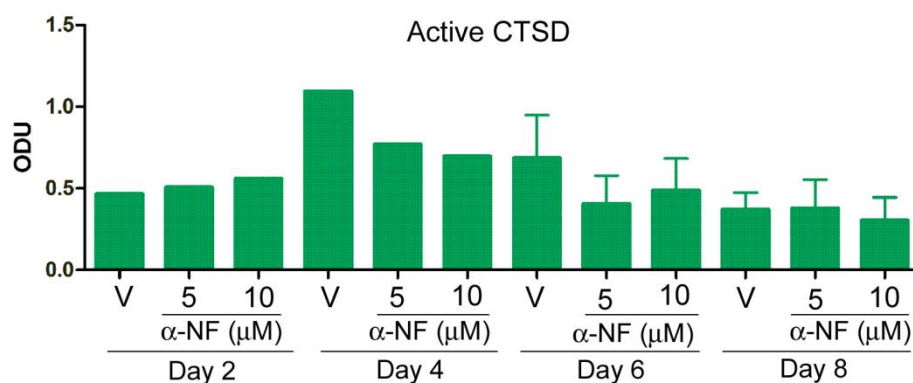
A.



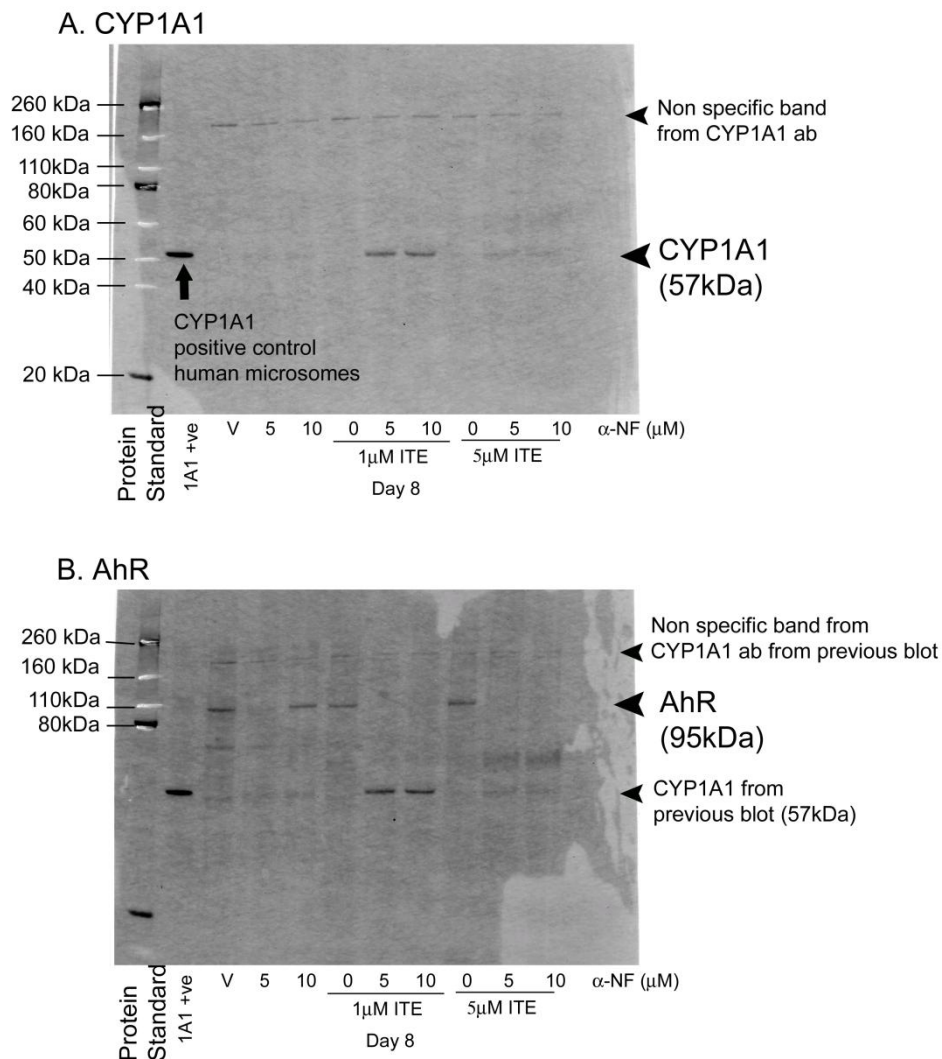
B.i.



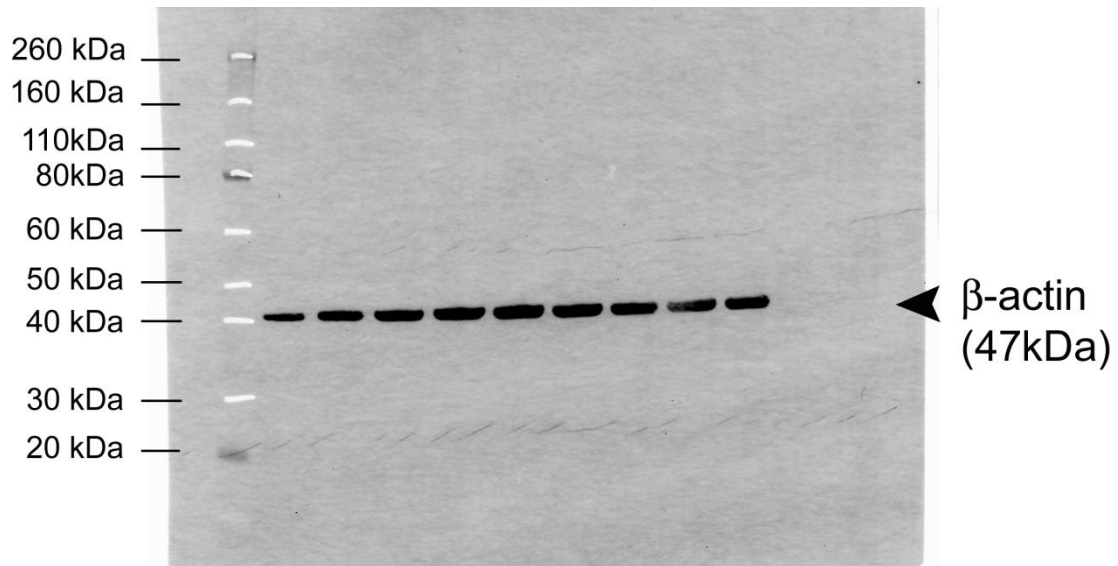
B.ii.



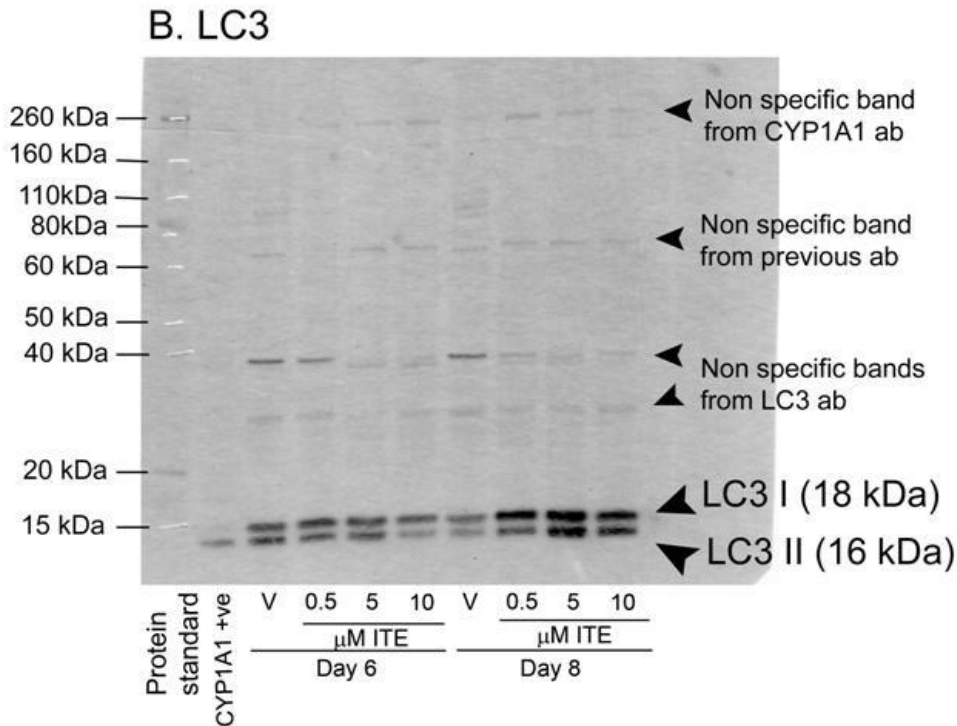
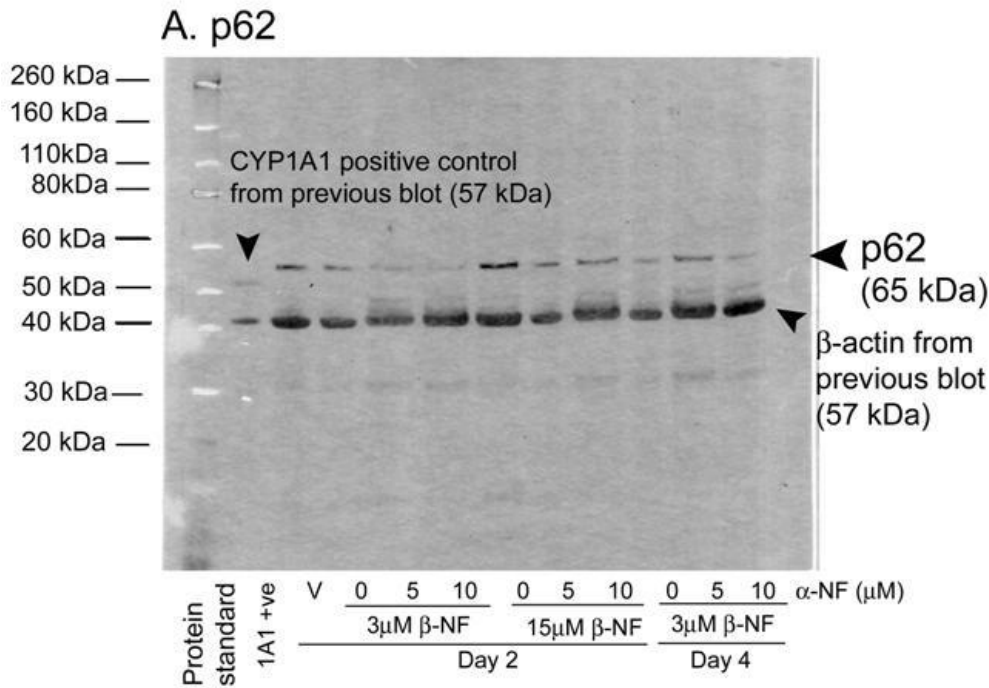
Appendix W. The effect of α-NF on pro and active CTSD. Primary keratinocytes were treated for up to 8 days with vehicle or concentrations of α-NF as indicated. Samples were lysed and Western blotting performed (A). Densitometry was carried out on blots probed with an anti-CTSD antibody showing B.i) pre-pro and pro-CTSD bands and B.ii) active-CTSD bands normalised to β-actin. Statistical analysis was not performed due to low sample size. Bars represent mean (days 2/4) or mean ± sem.



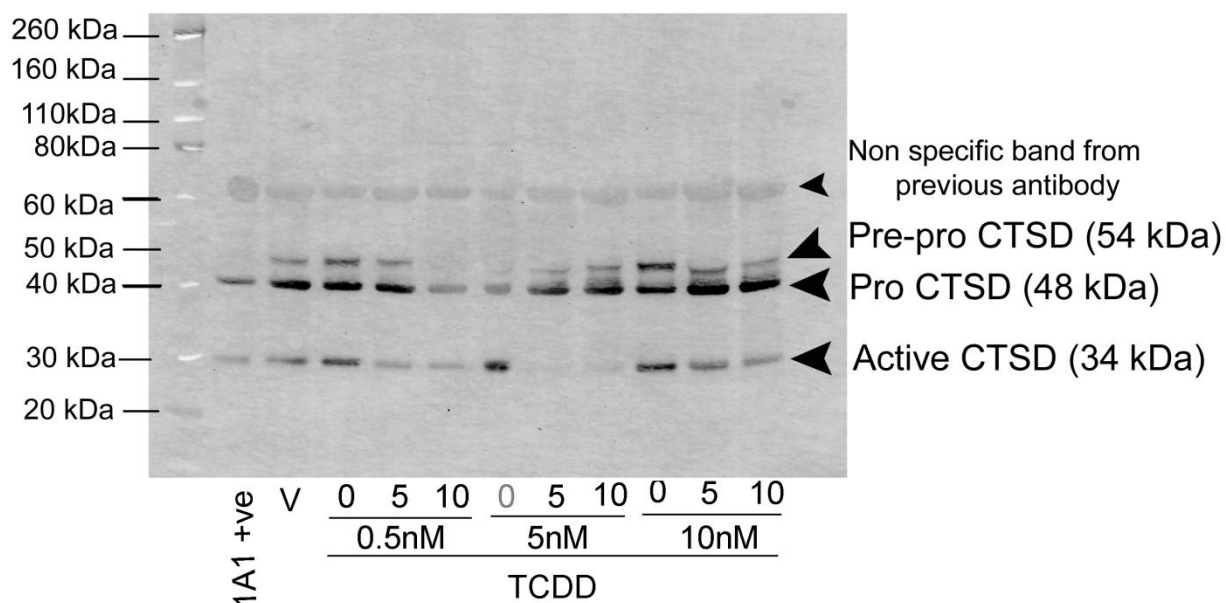
Appendix X. Complete Western blots showing all bands visible for AhR and CYP1A1. Primary keratinocyte lysates and a protein standard molecular weight marker were separated by Western blot and transferred onto nitrocellulose membrane. Membranes were blocked for 1h at room temperature in 5% milk and probed with **A)** anti-CYP1A1 1:1000 in 5% BSA in TBS-T20 or **B)** anti-AhR 1:1000 + 5% milk in TBS-T20 overnight at 4°C. The membranes were then incubated with secondary antibody (anti-mouse, 1:1000 + 5% milk in TBS-T20) for 1h at RT and bands visualized with ECL plus for 10 min and visualised on a phosphoimager. **A)** The CYP1A1 band (57kDa) was confirmed with presence of CYP1A1 positive sample (human liver microsomes). One non-specific band was visible at ~200kDa. **B)** The AhR antibody staining was relatively clean with one faint non-specific band visible from the AhR antibody roughly 20 kDa below the AhR band which was identified by size compared to molecular weight marker and response to treatment. This blot also shows the specific CYP1A1 band and non-specific band from previously probing this blot with the CYP1A1 antibody.



Appendix Y. Complete Western blot showing all bands visible for β -actin. Protein lysates were run on Western blot with protein standard molecular weight marker as described in materials and methods. Membrane was probed with primary antibody anti- β -actin 1:20,000 + 5% milk in TBS-T20 at RT for 45 mins. The blot was then incubated with secondary antibody (anti-mouse 1:1000 + 5% milk in TBS-T20) for 45 minutes at RT. Bands were visualized with ECL+ for 5 minutes and viewed on a phosphoimager. The β -actin band was the only band visible and roughly at the expected size.



Appendix Z. Complete Western blots showing all bands visible for p62 and LC3 antibodies. Primary keratinocyte lysates and a protein standard molecular weight marker were separated by Western blot and transferred onto nitrocellulose membrane. Membranes were blocked for 1h at room temperature in 5% milk and probed with **A)** anti-p62, 1:1000 in 5% milk in TBS-T20 or **B)** anti-LC3 1:1000 + 5% BSA in TBS-T20 overnight at 4°C. The membranes were then incubated with secondary antibody (anti-mouse, 1:1000 + 5% milk in TBS-T20) for 1h at RT and bands visualized with ECL plus for 10 min and visualized on a phosphoimager. **A)** The p62 band was identified by its position just higher than the CYP1A1 band. One very faint band was present roughly 30 kDa below the expected p62 position. **B)** The LC3 antibody created a few non-specific bands, but these were roughly 30 kDa higher than the expected LC3 size and the LC3 doublet band was stained strongly.



Appendix AA. Complete Western blots showing all bands visible for Cathepsin D antibody. Primary keratinocyte lysates and a protein standard molecular weight marker were separated by Western blot and transferred onto nitrocellulose membrane. Membranes were blocked for 1h at room temperature in 5% milk and probed with anti-CTSD antibody at 1:1000 in TBS-T + 5% milk for 1h at RT. The membranes were then incubated with secondary antibody (anti-rabbit, 1:1000 + 5% milk in TBS-T20) for 1h at RT and bands visualized with ECL plus for 10 min and visualized on a phosphoimager. All 3 forms of CTSD were recognized by the antibody but the small chain of the active form (14 kDa) was not. All bands were recognized by their appropriate size compared to protein standard (the protein standard bands commonly ran at a slightly higher size than indicated by the manufacturer) and their size relative to each other. The blots were generally clean, except for a non-specific band shown at a higher size than CTSD that was caused by previously running an antibody on the gel that had degraded and caused high non-specific binding.

Appendix BB. Localisation and levels of CTSD in primary human keratinocytes is affected by treatment with dithranol and TCDD, as observed by BODIPY FI-Pepstatin A. Primary keratinocyte monolayers were grown on glass bottomed wells for live cell imaging. Cells were pre-treated for 1h with vehicle, 10nM TCDD or 1 μ M dithranol and 30 mins with BODIPY FI-pepstatin A. Cells were kept at 37°C in 5% CO₂ overnight for ~11h. Confocal microscopy at mid z stack was used to image the cells every 5 minutes. Videos show the maximal effects out of 3 donors.

8 References

Abbott, B.D., Birnbaum, L.S., and Perdew, G.H. (1995). Developmental expression of two members of a new class of transcription factors: I. Expression of aryl hydrocarbon receptor in the C57BL/6N mouse embryo. *Developmental Dynamics* 204, 133-143.

Abbott, B.D., Schmid, J.E., Brown, J.G., Wood, C.R., White, R.D., Buckalew, A.R., and Held, G.A. (1999). RT-PCR quantification of AHR, ARNT, GR, and CYP1A1 mRNA in craniofacial tissues of embryonic mice exposed to 2,3,7,8-tetrachlorodibenzo-p-dioxin and hydrocortisone. *Toxicological Sciences* 47, 76-85.

Aitola, M., Sadek, C.M., Gustafsson, J.-A., and Pelto-Huikko, M. (2003). Aint/Tacc3 is highly expressed in proliferating mouse tissues during development, spermatogenesis, and oogenesis. *Journal of Histochemistry & Cytochemistry* 51, 455-469.

Akintobi, A.M., Villano, C.M., and White, L.A. (2007). 2,3,7,8-Tetrachlorodibenzo-p-dioxin (TCDD) exposure of normal human dermal fibroblasts results in AhR-dependent and -independent changes in gene expression. *Toxicology & Applied Pharmacology* 220, 9-17.

Allen-Hoffmann, B.L., Schlosser, S.J., Ivarie, C.A., Sattler, C.A., Meisner, L.F., and O'Connor, S.L. (2000). Normal growth and differentiation in a spontaneously immortalized near-diploid human keratinocyte cell line, NIKS. *Journal of Investigative Dermatology* 114, 444-455.

Alvares, A.P., Leigh, S., Kappas, A., Levin, W., and Conney, A.H. (1973). Induction of aryl hydrocarbon hydroxylase in human skin. *Drug Metabolism & Disposition* 1, 386-390.

An, W.G., Schulte, T.W., and Neckers, L.M. (2000). The heat shock protein 90 antagonist geldanamycin alters chaperone association with p210bcr-abl and v-src proteins before their degradation by the proteasome. *Cell Growth & Differentiation* 11, 355-360.

Antonsson, C., Arulampalam, V., Whitelaw, M.L., Pettersson, S., and Poellinger, L. (1995). Constitutive function of the basic helix-loop-helix/PAS factor Arnt. Regulation of target promoters via the E box motif. *Journal of Biological Chemistry* 270, 13968-13972.

Armstrong, J.L., Corazzari, M., Martin, S., Pagliarini, V., Falasca, L., Hill, D.S., Ellis, N., Al Sabah, S., Redfern, C.P.F., Fimia, G.M., Piacentini, M., and Lovat, P.E. (2011). Oncogenic B-RAF signaling in melanoma impairs the therapeutic advantage of autophagy inhibition. *Clinical Cancer Research* 17, 2216-2226.

- Arnault, E., Doussau, M., Pesty, A., Lefevre, B., and Courtot, A.-M. (2010). Review: Lamin A/C, caspase-6, and chromatin configuration during meiosis resumption in the mouse oocyte. *Reproductive Sciences* 17, 102-115.
- Auxenfans, C., Fradette, J., Lequeux, C., Germain, L., Kinikoglu, B., Bechetoille, N., Braye, F., Auger, F.A., and Damour, O. (2009). Evolution of three dimensional skin equivalent models reconstructed in vitro by tissue engineering. [Review] [65 refs]. *European Journal of Dermatology* 19, 107-113.
- Aymard, E., Barruche, V., Naves, T., Bordes, S., Closs, B., Verdier, M., and Ratinaud, M.-H. (2011). Autophagy in human keratinocytes: an early step of the differentiation? *Experimental Dermatology* 20, 263-268.
- Bailey, I., Gibson, G.G., Plant, K., Graham, M., and Plant, N. (2011). A PXR-mediated negative feedback loop attenuates the expression of CYP3A in response to the PXR agonist pregnenolone-16alpha-carbonitrile. *PLoS ONE [Electronic Resource]* 6, e16703.
- Baumgartner, H.K., Gerasimenko, J.V., Thorne, C., Ashurst, L.H., Barrow, S.L., Chvanov, M.A., Gillies, S., Criddle, D.N., Tepikin, A.V., Petersen, O.H., Sutton, R., Watson, A.J., and Gerasimenko, O.V. (2007). Caspase-8-mediated apoptosis induced by oxidative stress is independent of the intrinsic pathway and dependent on cathepsins. *American Journal of Physiology Gastrointestinal & Liver Physiology* 293.
- Beedanagari, S.R., Taylor, R.T., and Hankinson, O. (2010). Differential regulation of the dioxin-induced Cyp1a1 and Cyp1b1 genes in mouse hepatoma and fibroblast cell lines. *Toxicology Letters* 194, 26-33.
- Bell, D.R., and Poland, A. (2000). Binding of aryl hydrocarbon receptor (AhR) to AhR-interacting protein. The role of hsp90. *Journal of Biological Chemistry* 275, 36407-36414.
- Bennett, H.L., Fleming, J.T., O'Prey, J., Ryan, K.M., and Leung, H.Y. (2010). Androgens modulate autophagy and cell death via regulation of the endoplasmic reticulum chaperone glucose-regulated protein 78/BiP in prostate cancer cells. *Cell Death & Disease* 1, e72.
- Benson, J.M., and Shepherd, D.M. (2011). Aryl hydrocarbon receptor activation by TCDD reduces inflammation associated with Crohn's disease. *Toxicological Sciences* 120, 68-78.
- Bergander, L., Wincent, E., Rannug, A., Foroozesh, M., Alworth, W., and Rannug, U. (2004). Metabolic fate of the Ah receptor ligand 6-formylindolo[3,2-b]carbazole. *Chemico Biological Interactions* 149, 151-164.

Berghard, A., Gradin, K., and Toftgard, R. (1992). The stability of dioxin-receptor ligands influences cytochrome P450IA1 expression in human keratinocytes. *Carcinogenesis* 13, 651-655.

Bernhofer, L.P., Barkovic, S., Appa, Y., and Martin, K.M. (1999). IL-1alpha and IL-1ra secretion from epidermal equivalents and the prediction of the irritation potential of mild soap and surfactant-based consumer products. *Toxicology in Vitro* 13, 231-239.

Bohensky, J., Shapiro, I.M., Leshinsky, S., Terkhorn, S.P., Adams, C.S., and Srinivas, V. (2007). HIF-1 regulation of chondrocyte apoptosis: induction of the autophagic pathway. *Autophagy* 3, 207-214.

Bouwstra, J.A., Dubbelaar, F.E., Gooris, G.S., and Ponec, M. (2000). The lipid organisation in the skin barrier. *Acta Dermato-Venereologica Supplementum* 208, 23-30.

Bouwstra, J.A., Honeywell-Nguyen, P.L., Gooris, G.S., and Ponec, M. (2003). Structure of the skin barrier and its modulation by vesicular formulations. *Progress in Lipid Research* 42, 1-36.

Boya, P., Gonzalez-Polo, R.A., Casares, N., Perfettini, J.L., Dessen, P., Larochette, N., Metivier, D., Meley, D., Souquere, S., Yoshimori, T., Pierron, G., Codogno, P., and Kroemer, G. (2005). Inhibition of macroautophagy triggers apoptosis. *Molecular & Cellular Biology* 25, 1025-1040.

Brunnberg, S., Andersson, P., Lindstam, M., Paulson, I., Poellinger, L., and Hanberg, A. (2006). The constitutively active Ah receptor (CA-Ahr) mouse as a potential model for dioxin exposure--effects in vital organs. *Toxicology* 224, 191-201.

Burbach, K.M., Poland, A., and Bradfield, C.A. (1992). Cloning of the Ah-receptor cDNA reveals a distinctive ligand-activated transcription factor. *Proceedings of the National Academy of Sciences of the United States of America* 89, 8185-8189.

Burgeson, R.E., and Christiano, A.M. (1997). The dermal-epidermal junction. *Current Opinion in Cell Biology* 9, 651-658.

Byun, H.O., Han, N.K., Lee, H.J., Kim, K.B., Ko, Y.G., Yoon, G., Lee, Y.S., Hong, S.I., and Lee, J.S. (2009). Cathepsin D and eukaryotic translation elongation factor 1 as promising markers of cellular senescence. *Cancer Research* 69, 4638-4647.

Caputo, R., Monti, M., Ermacora, E., Carminati, G., Gelmetti, C., Gianotti, R., Gianni, E., and Puccinelli, V. (1988). Cutaneous manifestations of tetrachlorodibenzo-p-dioxin in children and adolescents. Follow-up 10 years after the Seveso, Italy, accident. *Journal of the American Academy of Dermatology* 19, 812-819.

Carew, J.S., Espitia, C.M., Esquivel, J.A., 2nd, Mahalingam, D., Kelly, K.R., Reddy, G., Giles, F.J., and Nawrocki, S.T. (2011). Lucanthone is a novel inhibitor of autophagy that induces cathepsin D-mediated apoptosis. *Journal of Biological Chemistry* 286, 6602-6613.

Carlson, D.B., and Perdew, G.H. (2002). A dynamic role for the Ah receptor in cell signaling? Insights from a diverse group of Ah receptor interacting proteins. *Journal of Biochemical & Molecular Toxicology* 16, 317-325.

Caruso, J.A., Mathieu, P.A., Joiakim, A., Leeson, B., Kessel, D., Sloane, B.F., and Reiners, J.J., Jr. (2004). Differential susceptibilities of murine hepatoma 1c1c7 and Tao cells to the lysosomal photosensitizer NPe6: influence of aryl hydrocarbon receptor on lysosomal fragility and protease contents. *Molecular Pharmacology* 65, 1016-1028.

Caruso, J.A., Mathieu, P.A., Joiakim, A., Zhang, H., and Reiners, J.J., Jr. (2006). Aryl hydrocarbon receptor modulation of tumor necrosis factor- α -induced apoptosis and lysosomal disruption in a hepatoma model that is caspase-8-independent. *Journal of Biological Chemistry* 281, 10954-10967.

Carver, L.A., Jackiw, V., and Bradfield, C.A. (1994). The 90-kDa heat shock protein is essential for Ah receptor signaling in a yeast expression system. *Journal of Biological Chemistry* 269, 30109-30112.

Cavailles, V., Augereau, P., and Rochefort, H. (1993). Cathepsin D gene is controlled by a mixed promoter, and estrogens stimulate only TATA-dependent transcription in breast cancer cells. *Proceedings of the National Academy of Sciences of the United States of America* 90, 203-207.

Chaturvedi, V., Sitailo, L.A., Bodner, B., Denning, M.F., and Nickoloff, B.J. (2006). Defining the caspase-containing apoptotic machinery contributing to cornification in human epidermal equivalents. *Experimental Dermatology* 15, 14-22.

Chen, C.S., Chen, W.N., Zhou, M., Arttamangkul, S., and Haugland, R.P. (2000). Probing the cathepsin D using a BODIPY FL-pepstatin A: applications in fluorescence polarization and microscopy. *Journal of Biochemical & Biophysical Methods* 42, 137-151.

Chen, I., Hsieh, T., Thomas, T., and Safe, S. (2001). Identification of estrogen-induced genes downregulated by AhR agonists in MCF-7 breast cancer cells using suppression subtractive hybridization. *Gene* 262, 207-214.

Cho, Y.C., Zheng, W., and Jefcoate, C.R. (2004). Disruption of cell-cell contact maximally but transiently activates AhR-mediated transcription in 10T1/2 fibroblasts. *Toxicology & Applied Pharmacology* 199, 220-238.

- Coomes, M.W., Norling, A.H., Pohl, R.J., Muller, D., and Fouts, J.R. (1983). Foreign compound metabolism by isolated skin cells from the hairless mouse. *Journal of Pharmacology & Experimental Therapeutics* 225, 770-777.
- Couture, L.A., Abbott, B.D., and Birnbaum, L.S. (1990). A critical review of the developmental toxicity and teratogenicity of 2,3,7,8-tetrachlorodibenzo-p-dioxin: recent advances toward understanding the mechanism. *Teratology* 42, 619-627.
- Cox, M.B., and Miller, C.A., 3rd (2004). Cooperation of heat shock protein 90 and p23 in aryl hydrocarbon receptor signaling. *Cell Stress & Chaperones* 9, 4-20.
- Dalby, B., Cates, S., Harris, A., Ohki, E.C., Tilkins, M.L., Price, P.J., and Ciccarone, V.C. (2004). Advanced transfection with Lipofectamine 2000 reagent: primary neurones, siRNA, and high throughput application. *Methods* 33, 95-103.
- Davarinos, N.A., and Pollenz, R.S. (1999). Aryl hydrocarbon receptor imported into the nucleus following ligand binding is rapidly degraded via the cytoplasmic proteasome following nuclear export. *Journal of Biological Chemistry* 274, 28708-28715.
- Demerjian, M., Hachem, J.-P., Tschachler, E., Denecker, G., Declercq, W., Vandenabeele, P., Mauro, T., Hupe, M., Crumrine, D., Roelandt, T., Houben, E., Elias, P.M., and Feingold, K.R. (2008). Acute modulations in permeability barrier function regulate epidermal cornification: role of caspase-14 and the protease-activated receptor type 2. *American Journal of Pathology* 172, 86-97.
- Denecker, G., Hoste, E., Gilbert, B., Hochepped, T., Ovaere, P., Lippens, S., Van den Broecke, C., Van Damme, P., D'Herde, K., Hachem, J.-P., Borgonie, G., Presland, R.B., Schoonjans, L., Libert, C., Vandekerckhove, J., Gevaert, K., Vandenabeele, P., and Declercq, W. (2007). Caspase-14 protects against epidermal UVB photodamage and water loss. *Nature Cell Biology* 9, 666-674.
- Denecker, G., Ovaere, P., Vandenabeele, P., and Declercq, W. (2008). Caspase-14 reveals its secrets. *Journal of Cell Biology* 180, 451-458.
- Dere, E., Lee, A.W., Burgoon, L.D., and Zacharewski, T.R. (2011). Differences in TCDD-elicited gene expression profiles in human HepG2, mouse Hepa1c1c7 and rat H4IIE hepatoma cells. *BMC Genomics* 12.
- Dolwick, K.M., Schmidt, J.V., Carver, L.A., Swanson, H.I., and Bradfield, C.A. (1993). Cloning and expression of a human Ah receptor cDNA. *Molecular Pharmacology* 44, 911-917.

Drake, M.D., Harsha, A.K., Terterov, S., and Roberts, J.D. (2006). Conformational analyses of 2,3-dihydroxypropanoic acid as a function of solvent and ionization state as determined by NMR spectroscopy. *Magnetic Resonance in Chemistry* 44, 210-219.

Du, L., Neis, M.M., Ladd, P.A., and Keeney, D.S. (2006a). Differentiation-specific factors modulate epidermal CYP1-4 gene expression in human skin in response to retinoic acid and classic aryl hydrocarbon receptor ligands. *Journal of Pharmacology & Experimental Therapeutics* 319, 1162-1171.

Du, L., Neis, M.M., Ladd, P.A., Lanza, D.L., Yost, G.S., and Keeney, D.S. (2006b). Effects of the differentiated keratinocyte phenotype on expression levels of CYP1-4 family genes in human skin cells. *Toxicology & Applied Pharmacology* 213, 135-144.

Eckert, R.L., Sturniolo, M.T., Broome, A.-M., Ruse, M., and Rorke, E.A. (2005). Transglutaminase function in epidermis. *Journal of Investigative Dermatology* 124, 481-492.

Eckhart, L., Declercq, W., Ban, J., Rendl, M., Lengauer, B., Mayer, C., Lippens, S., Vandenabeele, P., and Tschachler, E. (2000). Terminal differentiation of human keratinocytes and stratum corneum formation is associated with caspase-14 activation. *Journal of Investigative Dermatology* 115, 1148-1151.

Egberts, F., Heinrich, M., Jensen, J.-M., Winoto-Morbach, S., Pfeiffer, S., Wickel, M., Schunck, M., Steude, J., Saftig, P., Proksch, E., and Schutze, S. (2004). Cathepsin D is involved in the regulation of transglutaminase 1 and epidermal differentiation. *Journal of Cell Science* 117, 2295-2307.

Ema, M., Ohe, N., Suzuki, M., Mimura, J., Sogawa, K., Ikawa, S., and Fujii-Kuriyama, Y. (1994). Dioxin binding activities of polymorphic forms of mouse and human arylhydrocarbon receptors. *Journal of Biological Chemistry* 269, 27337-27343.

Ema, M., Sogawa, K., Watanabe, N., Chujoh, Y., Matsushita, N., Gotoh, O., Funae, Y., and Fujii-Kuriyama, Y. (1992). cDNA cloning and structure of mouse putative Ah receptor. *Biochemical & Biophysical Research Communications* 184, 246-253.

Eskelinen, E.-L. (2005). Maturation of autophagic vacuoles in Mammalian cells. *Autophagy* 1, 1-10.

Evans, B.R., Karchner, S.I., Allan, L.L., Pollenz, R.S., Tanguay, R.L., Jenny, M.J., Sherr, D.H., and Hahn, M.E. (2008). Repression of aryl hydrocarbon receptor (AHR) signaling by AHR repressor: role of DNA binding and competition for AHR nuclear translocator. *Molecular Pharmacology* 73, 387-398.

- Evans, S.M., Schrlau, A.E., Chalian, A.A., Zhang, P., and Koch, C.J. (2006). Oxygen levels in normal and previously irradiated human skin as assessed by EF5 binding. *Journal of Investigative Dermatology* 126, 2596-2606.
- Fartasch, M. (2004). The epidermal lamellar body: a fascinating secretory organelle. *Journal of Investigative Dermatology* 122, XI-XII.
- Fernandez-Salguero, P.M., Ward, J.M., Sundberg, J.P., and Gonzalez, F.J. (1997). Lesions of aryl-hydrocarbon receptor-deficient mice. *Veterinary Pathology* 34, 605-614.
- Ferraris, M., Flora, A., Chiesara, E., Fornasari, D., Lucchetti, H., Marabini, L., Frigerio, S., and Radice, S. (2005). Molecular mechanism of the aryl hydrocarbon receptor activation by the fungicide iprodione in rainbow trout (*Oncorhynchus mykiss*) hepatocytes. *Aquatic Toxicology* 72, 209-220.
- FitzGerald, C.T., Fernandez-Salguero, P., Gonzalez, F.J., Nebert, D.W., and Puga, A. (1996). Differential regulation of mouse Ah receptor gene expression in cell lines of different tissue origins. *Archives of Biochemistry & Biophysics* 333, 170-178.
- Fitzgerald, C.T., Nebert, D.W., and Puga, A. (1998). Regulation of mouse Ah receptor (Ahr) gene basal expression by members of the Sp family of transcription factors. *DNA & Cell Biology* 17, 811-822.
- Franc, M.A., Pohjanvirta, R., Tuomisto, J., and Okey, A.B. (2001). In vivo up-regulation of aryl hydrocarbon receptor expression by 2,3,7,8-tetrachlorodibenzo-p-dioxin (TCDD) in a dioxin-resistant rat model. *Biochemical Pharmacology* 62, 1565-1578.
- Fujisawa-Sehara, A., Yamane, M., and Fujii-Kuriyama, Y. (1988). A DNA-binding factor specific for xenobiotic responsive elements of P-450c gene exists as a cryptic form in cytoplasm: its possible translocation to nucleus. *Proceedings of the National Academy of Sciences of the United States of America* 85, 5859-5863.
- Fukunaga, B.N., and Hankinson, O. (1996). Identification of a novel domain in the aryl hydrocarbon receptor required for DNA binding. *Journal of Biological Chemistry* 271, 3743-3749.
- Fukunaga, B.N., Probst, M.R., Reisz-Porszasz, S., and Hankinson, O. (1995). Identification of functional domains of the aryl hydrocarbon receptor. *Journal of Biological Chemistry* 270, 29270-29278.
- Funk, K.E., Mrak, R.E., and Kuret, J. (2011). Granulovacuolar degeneration (GVD) bodies of Alzheimer's disease (AD) resemble late-stage autophagic organelles. *Neuropathology & Applied Neurobiology* 37, 295-306.

Garside, H., Stewart, A., Brown, N., Cooke, E.L., Graham, M., and Sullivan, M. (2008). Quantitative analysis of aryl hydrocarbon receptor activation using fluorescence-based cell imaging--a high-throughput mechanism-based assay for drug discovery. *Xenobiotica* *38*, 1-20.

Gasiewicz, T.A., and Bauman, P.A. (1987). Heterogeneity of the rat hepatic Ah receptor and evidence for transformation in vitro and in vivo. *Journal of Biological Chemistry* *262*, 2116-2120.

Gasiewicz, T.A., Henry, E.C., and Collins, L.L. (2008). Expression and activity of aryl hydrocarbon receptors in development and cancer. *Critical Reviews in Eukaryotic Gene Expression* *18*, 279-321.

Gasiewicz, T.A., Rucci, G., (1991). alpha-Naphthoflavone Acts as an Antagonist of 2,3,7,8-Tetrachlorodibenzo-p-dioxin by Forming an Inactive Complex with the Ah Receptor. *Molecular Pharmacology* *40*, 607-612.

Gawkrodger, D.J., Harris, G., and Bojar, R.A. (2009). Chloracne in seven organic chemists exposed to novel polycyclic halogenated chemical compounds (triazoloquinoxalines). *British Journal of Dermatology* *161*, 939-943.

Gelardi, A., Morini, F., Dusatti, F., Penco, S., and Ferro, M. (2001). Induction by xenobiotics of phase I and phase II enzyme activities in the human keratinocyte cell line NCTC 2544. *Toxicology in Vitro* *15*, 701-711.

Gelhaus, S.L., Harvey, R.G., Penning, T.M., and Blair, I.A. (2011). Regulation of benzo[a]pyrene-mediated DNA- and glutathione-adduct formation by 2,3,7,8-tetrachlorodibenzo-p-dioxin in human lung cells. *Chemical Research in Toxicology* *24*, 89-98.

Geng, S., Mezentsev, A., Kalachikov, S., Raith, K., Roop, D.R., and Panteleyev, A.A. (2006). Targeted ablation of Arnt in mouse epidermis results in profound defects in desquamation and epidermal barrier function. *Journal of Cell Science* *119*, 4901-4912.

Gerasimenko, J.V., Sherwood, M., Tepikin, A.V., Petersen, O.H., and Gerasimenko, O.V. (2006). NAADP, cADPR and IP3 all release Ca²⁺ from the endoplasmic reticulum and an acidic store in the secretory granule area. *Journal of Cell Science* *119*, 226-238.

Geusau, A., Abraham, K., Geissler, K., Sator, M.O., Stingl, G., and Tschachler, E. (2001). Severe 2,3,7,8-tetrachlorodibenzo-p-dioxin (TCDD) intoxication: clinical and laboratory effects. *Environmental Health Perspectives* *109*, 865-869.

Geusau, A., Khorchide, M., Mildner, M., Pammer, J., Eckhart, L., and Tschachler, E. (2005). 2,3,7,8-tetrachlorodibenzo-p-dioxin impairs differentiation of normal human

epidermal keratinocytes in a skin equivalent model. *Journal of Investigative Dermatology* 124, 275-277.

Gierthy, J.F., Bennett, J.A., Bradley, L.M., and Cutler, D.S. (1993). Correlation of in vitro and in vivo growth suppression of MCF-7 human breast cancer by 2,3,7,8-tetrachlorodibenzo-p-dioxin. *Cancer Research* 53, 3149-3153.

Gonzalez-Polo, R.A., Boya, P., Pauleau, A.L., Jalil, A., Larochette, N., Souquere, S., Eskelinen, E.L., Pierron, G., Saftig, P., and Kroemer, G. (2005). The apoptosis/autophagy paradox: autophagic vacuolization before apoptotic death. *Journal of Cell Science* 118, 3091-3102.

Gradin, K., Toftgard, R., Poellinger, L., and Berghard, A. (1999). Repression of dioxin signal transduction in fibroblasts. Identification Of a putative repressor associated with Arnt. *Journal of Biological Chemistry* 274, 13511-13518.

Greenlee, W.F., Dold, K.M., and Osborne, R. (1985). Actions of 2,3,7,8-tetrachlorodibenzo-p-dioxin (TCDD) on human epidermal keratinocytes in culture. *In Vitro Cellular & Developmental Biology* 21, 509-512.

Grenert, J.P., Johnson, B.D., and Toft, D.O. (1999). The importance of ATP binding and hydrolysis by hsp90 in formation and function of protein heterocomplexes. *Journal of Biological Chemistry* 274, 17525-17533.

Grenert, J.P., Sullivan, W.P., Fadden, P., Haystead, T.A., Clark, J., Mimnaugh, E., Krutzsch, H., Ochel, H.J., Schulte, T.W., Sausville, E., Neckers, L.M., and Toft, D.O. (1997). The amino-terminal domain of heat shock protein 90 (hsp90) that binds geldanamycin is an ATP/ADP switch domain that regulates hsp90 conformation. *Journal of Biological Chemistry* 272, 23843-23850.

Guicciardi, M.E., Leist, M., and Gores, G.J. (2004). Lysosomes in cell death. *Oncogene* 23, 2881-2890.

Gunzel, S., Weidenthaler, B., Hausser, I., and Anton-Lamprecht, I. (1991). Keratohyalin granules are heterogeneous in ridged and non-ridged human skin: evidence from anti-filaggrin immunogold labelling of normal skin and skin of autosomal dominant ichthyosis vulgaris patients. *Archives of Dermatological Research* 283, 421-432.

Hahn, M.E., Karchner, S.I., Shapiro, M.A., and Perera, S.A. (1997). Molecular evolution of two vertebrate aryl hydrocarbon (dioxin) receptors (AHR1 and AHR2) and the PAS family. *Proceedings of the National Academy of Sciences of the United States of America* 94, 13743-13748.

Hambrick, G.W., Jr. (1957). The effect of substituted naphthalenes on the pilosebaceous apparatus of rabbit and man. *Journal of Investigative Dermatology* 28, 89-102.

Hankinson, O. (1995). The aryl hydrocarbon receptor complex. *Annual Review of Pharmacology & Toxicology* 35, 307-340.

Harris, I.R., Siefken, W., Beck-Oldach, K., Brandt, M., Wittern, K.-P., and Pollet, D. (2002a). Comparison of activities dependent on glutathione S-transferase and cytochrome P-450 IA1 in cultured keratinocytes and reconstructed epidermal models. *Skin Pharmacology & Applied Skin Physiology* 15 *Suppl 1*, 59-67.

Harris, I.R., Siefken, W., Beck-Oldach, K., Wittern, K.-P., and Pollet, D. (2002b). NAD(P)H:quinone reductase activity in human epidermal keratinocytes and reconstructed epidermal models. *Skin Pharmacology & Applied Skin Physiology* 15 *Suppl 1*, 68-73.

Harvey, H.B., Shaw, M.G., and Morrell, D.S. (2010). Perinatal Management of Harlequin Ichthyosis: a Case Report and Literature Review. *Journal of Perinatology* 30, 66-72.

Heid, S.E., Pollenz, R.S., and Swanson, H.I. (2000). Role of heat shock protein 90 dissociation in mediating agonist-induced activation of the aryl hydrocarbon receptor. *Molecular Pharmacology* 57, 82-92.

Heinrich, M., Neumeyer, J., Jakob, M., Hallas, C., Tchikov, V., Winoto-Morbach, S., Wickel, M., Schneider-Brachert, W., Trauzold, A., Hethke, A., and Schutze, S. (2004). Cathepsin D links TNF-induced acid sphingomyelinase to Bid-mediated caspase-9 and -3 activation. *Cell Death & Differentiation* 11, 550-563.

Henry, E.C., Bemis, J.C., Henry, O., Kende, A.S., and Gasiewicz, T.A. (2006). A potential endogenous ligand for the aryl hydrocarbon receptor has potent agonist activity in vitro and in vivo. *Archives of Biochemistry & Biophysics* 450, 67-77.

Henry, E.C., Kende, A.S., Rucci, G., Totleben, M.J., Willey, J.J., Dertinger, S.D., Pollenz, R.S., Jones, J.P., and Gasiewicz, T.A. (1999). Flavone antagonists bind competitively with 2,3,7, 8-tetrachlorodibenzo-p-dioxin (TCDD) to the aryl hydrocarbon receptor but inhibit nuclear uptake and transformation. *Molecular Pharmacology* 55, 716-725.

Henry, E.C., Rucci, G., and Gasiewicz, T.A. (1989). Characterization of multiple forms of the Ah receptor: comparison of species and tissues. *Biochemistry* 28, 6430-6440.

Henry, E.C., Rucci, G., and Gasiewicz, T.A. (1994). Purification to homogeneity of the heteromeric DNA-binding form of the aryl hydrocarbon receptor from rat liver. *Molecular Pharmacology* 46, 1022-1027.

Henry, E.C., Welle, S.L., and Gasiewicz, T.A. (2010). TCDD and a putative endogenous AhR ligand, ITE, elicit the same immediate changes in gene expression in mouse lung fibroblasts. *Toxicological Sciences* 114, 90-100.

Hernandez-Cueto, C., Luna, A., Lorente, J.A., and Villanueva, E. (1987). Study of cathepsin A, B and D activities in the skin wound edges. Its application to the differential diagnosis between vital and postmortem wounds. *Forensic Science International* 35, 51-60.

Hogenesch, J.B., Chan, W.K., Jackiw, V.H., Brown, R.C., Gu, Y.Z., Pray-Grant, M., Perdew, G.H., and Bradfield, C.A. (1997). Characterization of a subset of the basic-helix-loop-helix-PAS superfamily that interacts with components of the dioxin signaling pathway. *Journal of Biological Chemistry* 272, 8581-8593.

Holcomb, M., and Safe, S. (1994). Inhibition of 7,12-dimethylbenzanthracene-induced rat mammary tumor growth by 2,3,7,8-tetrachlorodibenzo-p-dioxin. *Cancer Letters* 82, 43-47.

Hollingshead, B.D., Patel, R.D., and Perdew, G.H. (2004). Endogenous hepatic expression of the hepatitis B virus X-associated protein 2 is adequate for maximal association with aryl hydrocarbon receptor-90-kDa heat shock protein complexes. *Molecular Pharmacology* 70, 2096-2107.

Horikoshi, T., Arany, I., Rajaraman, S., Chen, S.H., Brysk, H., Lei, G., Tying, S.K., and Brysk, M.M. (1998). Isoforms of cathepsin D and human epidermal differentiation. *Biochimie* 80, 605-612.

Horikoshi, T., Igarashi, S., Uchiwa, H., Brysk, H., and Brysk, M.M. (1999). Role of endogenous cathepsin D-like and chymotrypsin-like proteolysis in human epidermal desquamation. *British Journal of Dermatology* 141, 453-459.

Houghton, P., Fang, R., Techatanawat, I., Steventon, G., Hylands, P.J., and Lee, C.C. (2007). The sulphorhodamine (SRB) assay and other approaches to testing plant extracts and derived compounds for activities related to reputed anticancer activity. *Methods* 42, 377-387.

Howe, K., Sanat, F., Thumser, A.E., Coleman, T., and Plant, N. (2011). The statin class of HMG-CoA reductase inhibitors demonstrate differential activation of the nuclear receptors PXR, CAR and FXR, as well as their downstream target genes. *Xenobiotica* 41, 519-529.

Huang, S.W., Liu, K.T., Chang, C.C., Chen, Y.J., Wu, C.Y., Tsai, J.J., Lu, W.C., Wang, Y.T., Liu, C.M., and Shieh, J.J. (2010). Imiquimod simultaneously induces autophagy and apoptosis in human basal cell carcinoma cells. *British Journal of Dermatology* 163, 310-320.

Huff, J., Lucier, G., and Tritscher, A. (1994). Carcinogenicity of TCDD: experimental, mechanistic, and epidemiologic evidence. *Annual Review of Pharmacology & Toxicology* 34, 343-372.

Huynh, K.K., Eskelinen, E.-L., Scott, C.C., Malevanets, A., Saftig, P., and Grinstein, S. (2007). LAMP proteins are required for fusion of lysosomes with phagosomes. *EMBO Journal* 26, 313-324.

Igarashi, S., Takizawa, T., Yasuda, Y., Uchiwa, H., Hayashi, S., Brysk, H., Robinson, J.M., Yamamoto, K., Brysk, M.M., and Horikoshi, T. (2004). Cathepsin D, but not cathepsin E, degrades desmosomes during epidermal desquamation. *British Journal of Dermatology* 151, 355-361.

Ikuta, T., Kobayashi, Y., and Kawajiri, K. (2004). Cell density regulates intracellular localization of aryl hydrocarbon receptor. *Journal of Biological Chemistry* 279, 19209-19216.

Ikuta, T., Tachibana, T., Watanabe, J., Yoshida, M., Yoneda, Y., and Kawajiri, K. (2000). Nucleocytoplasmic shuttling of the aryl hydrocarbon receptor. *Journal of Biochemistry* 127, 503-509.

Ishida-Yamamoto, A., Tanaka, H., Nakane, H., Takahashi, H., Hashimoto, Y., and Iizuka, H. (1999). Programmed cell death in normal epidermis and loricrin keratoderma. Multiple functions of profilaggrin in keratinization. *Journal of Investigative Dermatology Symposium Proceedings*. 4, 145-149.

Itakura, E., and Mizushima, N. (2011). p62 Targeting to the autophagosome formation site requires self-oligomerization but not LC3 binding. *Journal of Cell Biology* 192, 17-27.

Jaakkola, P.M., and Pursiheimo, J.-P. (2009). p62 degradation by autophagy: another way for cancer cells to survive under hypoxia. *Autophagy* 5, 410-412.

Jackh, C., Blatz, V., Fabian, E., Guth, K., van Ravenzwaay, B., Reisinger, K., and Landsiedel, R. (2011). Characterization of enzyme activities of Cytochrome P450 enzymes, Flavin-dependent monooxygenases, N-acetyltransferases and UDP-glucuronyltransferases in human reconstructed epidermis and full-thickness skin models. *Toxicology in Vitro* 25, 1209-1214.

Jans, R., and Reynolds, N.J. (2012).

Jones, C.L., and Reiners, J.J., Jr. (1997). Differentiation status of cultured murine keratinocytes modulates induction of genes responsive to 2,3,7,8-tetrachlorodibenzo-p-dioxin. *Archives of Biochemistry & Biophysics* *347*, 163-173.

Ju, Q., Fimmel, S., Hinz, N., Stahlmann, R., Xia, L., and Zouboulis, C.C. (2011). 2,3,7,8-Tetrachlorodibenzo-p-dioxin alters sebaceous gland cell differentiation in vitro. *Experimental Dermatology* *20*, 320-325.

Jux, B., Kadow, S., Luecke, S., Rannug, A., Krutmann, J., and Esser, C. (2011). The aryl hydrocarbon receptor mediates UVB radiation-induced skin tanning. *Journal of Investigative Dermatology* *131*, 203-210.

Kabeya, Y., Mizushima, N., Ueno, T., Yamamoto, A., Kirisako, T., Noda, T., Kominami, E., Ohsumi, Y., and Yoshimori, T. (2000). LC3, a mammalian homologue of yeast Apg8p, is localized in autophagosomal membranes after processing.[Erratum appears in *EMBO J.* 2003 Sep 1;22(17):4577]. *EMBO Journal* *19*, 5720-5728.

Kabeya, Y., Mizushima, N., Yamamoto, A., Oshitani-Okamoto, S., Ohsumi, Y., and Yoshimori, T. (2004). LC3, GABARAP and GATE16 localize to autophagosomal membrane depending on form-II formation. *Journal of Cell Science* *117*, 2805-2812.

Kamstrup, M., Faurschou, A., Gniadecki, R., and Wulf, H.C. (2008). Epidermal stem cells - role in normal, wounded and pathological psoriatic and cancer skin. *Current Stem Cell Research & Therapy* *3*, 146-150.

Kanzawa, T., Zhang, L., Xiao, L., Germano, I.M., Kondo, Y., and Kondo, S. (2005). Arsenic trioxide induces autophagic cell death in malignant glioma cells by upregulation of mitochondrial cell death protein BNIP3. *Oncogene* *24*, 980-991.

Kawada, A., Hara, K., Kominami, E., Hiruma, M., and Noguchi, A.I. (1997). Processing of cathepsins L, B and D in psoriatic epidermis. *Archives of Dermatological Research* *289*, 87-93.

Kedderis, L.B., Andersen, M.E., and Birnbaum, L.S. (1993). Effect of dose, time, and pretreatment on the biliary excretion and tissue distribution of 2,3,7,8-tetrachlorodibenzo-p-dioxin in the rat. *Fundamental & Applied Toxicology* *21*, 405-411.

Kekatpure, V.D., Dannenberg, A.J., and Subbaramaiah, K. (2008). HDAC6 modulates Hsp90 chaperone activity and regulates activation of aryl hydrocarbon receptor signaling. *Journal of Biological Chemistry* *284*, 7436-7445.

Khan, I.U., Bickers, D.R., Haqqi, T.M., and Mukhtar, H. (1992). Induction of CYP1A1 mRNA in rat epidermis and cultured human epidermal keratinocytes by benz(a)anthracene and beta-naphthoflavone. *Drug Metabolism & Disposition* 20, 620-624.

Khan, S., Barhoumi, R., Burghardt, R., Liu, S., Kim, K., and Safe, S. (2006). Molecular mechanism of inhibitory aryl hydrocarbon receptor-estrogen receptor/Sp1 cross talk in breast cancer cells. *Molecular Endocrinology* 20, 2199-2214.

Kim, S.-H., Henry, E.C., Kim, D.-K., Kim, Y.-H., Shin, K.J., Han, M.S., Lee, T.G., Kang, J.-K., Gasiewicz, T.A., Ryu, S.H., and Suh, P.-G. (2006). Novel compound 2-methyl-2H-pyrazole-3-carboxylic acid (2-methyl-4-o-tolylazo-phenyl)-amide (CH-223191) prevents 2,3,7,8-TCDD-induced toxicity by antagonizing the aryl hydrocarbon receptor. *Molecular Pharmacology* 69, 1871-1878.

Kimura, S., Noda, T., and Yoshimori, T. (2007). Dissection of the autophagosome maturation process by a novel reporter protein, tandem fluorescent-tagged LC3. *Autophagy* 3, 452-460.

Klages, N., Zufferey, R., and Trono, D. (2000). A stable system for the high-titer production of multiply attenuated lentiviral vectors. *Molecular Therapy: the Journal of the American Society of Gene Therapy* 2, 170-176.

Klionsky, D.J., Abeliovich, H., Agostinis, P., Agrawal, D.K., Aliev, G., Askew, D.S., Baba, M., Baehrecke, E.H., Bahr, B.A., Ballabio, A., Bamber, B.A., Bassham, D.C., Bergamini, E., Bi, X., Biard-Piechaczyk, M., Blum, J.S., Bredesen, D.E., Brodsky, J.L., Brumell, J.H., Brunk, U.T., Bursch, W., Camougrand, N., Cebollero, E., Cecconi, F., Chen, Y., Chin, L.S., Choi, A., Chu, C.T., Chung, J., Clarke, P.G., Clark, R.S., Clarke, S.G., Clave, C., Cleveland, J.L., Codogno, P., Colombo, M.I., Coto-Montes, A., Cregg, J.M., Cuervo, A.M., Debnath, J., Demarchi, F., Dennis, P.B., Dennis, P.A., Deretic, V., Devenish, R.J., Di Sano, F., Dice, J.F., Difiglia, M., Dinesh-Kumar, S., Distelhorst, C.W., Djavaheri-Mergny, M., Dorsey, F.C., Droge, W., Dron, M., Dunn, W.A., Jr., Duszenko, M., Eissa, N.T., Elazar, Z., Esclatine, A., Eskelinen, E.L., Fesus, L., Finley, K.D., Fuentes, J.M., Fueyo, J., Fujisaki, K., Galliot, B., Gao, F.B., Gewirtz, D.A., Gibson, S.B., Gohla, A., Goldberg, A.L., Gonzalez, R., Gonzalez-Estevez, C., Gorski, S., Gottlieb, R.A., Haussinger, D., He, Y.W., Heidenreich, K., Hill, J.A., Hoyer-Hansen, M., Hu, X., Huang, W.P., Iwasaki, A., Jaattela, M., Jackson, W.T., Jiang, X., Jin, S., Johansen, T., Jung, J.U., Kadowaki, M., Kang, C., Kelekar, A., Kessel, D.H., Kiel, J.A., Kim, H.P., Kimchi, A., Kinsella, T.J., Kiselyov, K., Kitamoto, K., Knecht, E., Komatsu, M., Kominami, E., Kondo, S., Kovacs, A.L., Kroemer, G., Kuan, C.Y., Kumar, R., Kundu, M., Landry, J., Laporte, M., Le, W., Lei, H.Y., Lenardo, M.J., Levine, B., Lieberman, A., Lim, K.L., Lin, F.C., Liou, W., Liu, L.F., Lopez-Berestein, G., Lopez-Otin, C., Lu, B., Macleod, K.F., Malorni, W., Martinet, W., Matsuoka, K., Mautner, J., Meijer, A.J., Melendez, A., Michels, P., Miotto, G., Mistiaen, W.P., Mizushima, N., Mograbi, B., Monastyrska, I., Moore, M.N., Moreira, P.I., Moriyasu, Y., Motyl, T., Munz, C., Murphy, L.O., Naqvi, N.I., Neufeld, T.P., Nishino, I., Nixon, R.A., Noda, T., Nurnberg, B., Ogawa, M., Oleinick, N.L., Olsen, L.J., Ozpolat, B., Paglin, S., Palmer, G.E., Papassideri, I., Parkes, M., Perlmutter, D.H., Perry, G., Piacentini, M., Pinkas-Kramarski, R., Prescott, M., Proikas-

Cezanne, T., Raben, N., Rami, A., Reggiori, F., Rohrer, B., Rubinsztein, D.C., Ryan, K.M., Sadoshima, J., Sakagami, H., Sakai, Y., Sandri, M., Sasakawa, C., Sass, M., Schneider, C., Seglen, P.O., Seleverstov, O., Settleman, J., Shacka, J.J., Shapiro, I.M., Sibirny, A., Silva-Zacarin, E.C., Simon, H.U., Simone, C., Simonsen, A., Smith, M.A., Spanel-Borowski, K., Srinivas, V., Steeves, M., Stenmark, H., Stromhaug, P.E., Subauste, C.S., Sugimoto, S., Sulzer, D., Suzuki, T., Swanson, M.S., Tabas, I., Takeshita, F., Talbot, N.J., Talloczy, Z., Tanaka, K., Tanida, I., Taylor, G.S., Taylor, J.P., Terman, A., Tettamanti, G., Thompson, C.B., Thumm, M., Tolkovsky, A.M., Tooze, S.A., Truant, R., Tumanovska, L.V., Uchiyama, Y., Ueno, T., Uzcategui, N.L., van der Klei, I., Vaquero, E.C., Vellai, T., Vogel, M.W., Wang, H.G., Webster, P., Wiley, J.W., Xi, Z., Xiao, G., Yahalom, J., Yang, J.M., Yap, G., Yin, X.M., Yoshimori, T., Yu, L., Yue, Z., Yuzaki, M., Zabirnyk, O., Zheng, X., Zhu, X., and Deter, R.L. (2008). Guidelines for the use and interpretation of assays for monitoring autophagy in higher eukaryotes. [Review] [208 refs]. *Autophagy* 4, 151-175.

Knutson, J.C., and Poland, A. (1980). 2,3,7,8-Tetrachlorodibenzo-p-dioxin: failure to demonstrate toxicity in twenty-three cultured cell types. *Toxicology & Applied Pharmacology* 54, 377-383.

Kobayashi, A., Sogawa, K., and Fujii-Kuriyama, Y. (1996). Cooperative interaction between AhR.Arnt and Sp1 for the drug-inducible expression of CYP1A1 gene. *Journal of Biological Chemistry* 271, 12310-12316.

Kohle, C., and Bock, K.W. (2007). Coordinate regulation of Phase I and II xenobiotic metabolisms by the Ah receptor and Nrf2. [Review] [96 refs]. *Biochemical Pharmacology* 73, 1853-1862.

Kokkonen, N., Rivinoja, A., Kauppila, A., Suokas, M., Kellokumpu, I., and Kellokumpu, S. (2004). Defective acidification of intracellular organelles results in aberrant secretion of cathepsin D in cancer cells. *Journal of Biological Chemistry* 279, 39982-39988.

Koliopanos, A., Kleeff, J., Xiao, Y., Safe, S., Zimmermann, A., Buchler, M.W., and Friess, H. (2002). Increased arylhydrocarbon receptor expression offers a potential therapeutic target for pancreatic cancer. *Oncogene* 21, 6059-6070.

Kolodkin, A.N., Bruggeman, F.J., Plant, N., Mone, M.J., Bakker, B.M., Campbell, M.J., van Leeuwen, J.P.T.M., Carlberg, C., Snoep, J.L., and Westerhoff, H.V. (2010). Design principles of nuclear receptor signaling: how complex networking improves signal transduction. *Molecular Systems Biology* 6, 446.

Kongara, S., Kravchuk, O., Teplova, I., Lozy, F., Schulte, J., Moore, D., Barnard, N., Neumann, C.A., White, E., and Karantza, V. (2010). Autophagy regulates keratin 8 homeostasis in mammary epithelial cells and in breast tumors. *Molecular Cancer Research: MCR* 8, 873-884.

Korge, B.P., Ishida-Yamamoto, A., Punter, C., Dopping-Hepenstal, P.J., Iizuka, H., Stephenson, A., Eady, R.A., and Munro, C.S. (1997). Loricrin mutation in Vohwinkel's keratoderma is unique to the variant with ichthyosis. *Journal of Investigative Dermatology* 109, 604-610.

Koyano, S., Saito, Y., Fukushima-Uesaka, H., Ishida, S., Ozawa, S., Kamatani, N., Minami, H., Ohtsu, A., Hamaguchi, T., Shirao, K., Yoshida, T., Saijo, N., Jinno, H., and Sawada, J. (2005). Functional analysis of six human aryl hydrocarbon receptor variants in a Japanese population. *Drug Metabolism & Disposition* 33, 1254-1260.

Kraft, C., Peter, M., and Hofmann, K. (2010). Selective autophagy: ubiquitin-mediated recognition and beyond. *Nature Cell Biology* 12, 836-841.

Krishnan, V., Porter, W., Santostefano, M., Wang, X., and Safe, S. (1995). Molecular mechanism of inhibition of estrogen-induced cathepsin D gene expression by 2,3,7,8-tetrachlorodibenzo-p-dioxin (TCDD) in MCF-7 cells. *Molecular & Cellular Biology* 15, 6710-6719.

Kroemer, G., Galluzzi, L., Vandenabeele, P., Abrams, J., Alnemri, E.S., Baehrecke, E.H., Blagosklonny, M.V., El-Deiry, W.S., Golstein, P., Green, D.R., Hengartner, M., Knight, R.A., Kumar, S., Lipton, S.A., Malorni, W., Nunez, G., Peter, M.E., Tschopp, J., Yuan, J., Piacentini, M., Zhivotovsky, B., Melino, G., and Nomenclature Committee on Cell, D. (2009). Classification of cell death: recommendations of the Nomenclature Committee on Cell Death 2009. *Cell Death & Differentiation* 16, 3-11.

Kroemer, G., and Jaattela, M. Lysosomes and autophagy in cell death control. [Review] [118 refs]. *Nature Reviews, Cancer*.

Legalwar, S., Berry, R.W., and Binder, L.I. (2007). Relation of hippocampal phospho-SAPK/JNK granules in Alzheimer's disease and tauopathies to granulovacuolar degeneration bodies. *Acta Neuropathologica* 113, 63-73.

Lambert, A., Ekambaram, M., Robinson, N., and Eckert, R.L. (2000). Transglutaminase reactivity of human involucrin. *Skin Pharmacology & Applied Skin Physiology* 13, 17-30.

Lamore, S.D., and Wondrak, G.T. (2011). Autophagic-lysosomal dysregulation of cathepsin B inactivation in human skin fibroblasts exposed to UVA. *Photochemical and photobiological sciences*.

Laurent-Matha, V., Derocq, D., Prebois, C., Katunuma, N., and Liaudet-Coopman, E. (2006). Processing of human cathepsin D is independent of its catalytic function and auto-activation: involvement of cathepsins L and B. *Journal of Biochemistry* 139, 363-371.

- Lazova, R., Klump, V., and Pawelek, J. (2010). Autophagy in cutaneous malignant melanoma. *Journal of Cutaneous Pathology* 37, 256-268.
- Ledirac, N., Delescluse, C., de Sousa, G., Pralavorio, M., Lesca, P., Amichot, M., Berge, J.B., and Rahmani, R. (1997). Carbaryl induces CYP1A1 gene expression in HepG2 and HaCaT cells but is not a ligand of the human hepatic Ah receptor. *Toxicology & Applied Pharmacology* 144, 177-182.
- Lee, D.D., Zavadil, J., Tomic-Canic, M., and Blumenberg, M. (2010). Comprehensive transcriptional profiling of human epidermis, reconstituted epidermal equivalents, and cultured keratinocytes using DNA microarray chips. *Methods in Molecular Biology* 585, 193-223.
- Lee, H.-M., Shin, D.-M., Yuk, J.-M., Shi, G., Choi, D.-K., Lee, S.-H., Huang, S.M., Kim, J.-M., Kim, C.D., Lee, J.-H., and Jo, E.-K. (2011). Autophagy negatively regulates keratinocyte inflammatory responses via scaffolding protein p62/SQSTM1. *Journal of Immunology* 186, 1248-1258.
- Lehmann, G.M., Xi, X., Kulkarni, A.A., Olsen, K.C., Pollock, S.J., Bagloli, C.J., Gupta, S., Casey, A.E., Huxlin, K.R., Sime, P.J., Feldon, S.E., and Phipps, R.P. (2011). The aryl hydrocarbon receptor ligand ITE inhibits TGFbeta1-induced human myofibroblast differentiation. *American Journal of Pathology* 178, 1556-1567.
- Levin, W., Conney, A.H., Alvares, A.P., Merkatz, I., and Kappas, A. (1972). Induction of benzo()pyrene hydroxylase in human skin. *Science* 176, 419-420.
- Li, H., Wang, P., Sun, Q., Ding, W.-X., Yin, X.-M., Sobol, R.W., Stolz, D.B., Yu, J., and Zhang, L. (2011). Following cytochrome c release, autophagy is inhibited during chemotherapy-induced apoptosis by caspase 8-mediated cleavage of Beclin 1. *Cancer Research* 71, 3625-3634.
- Lin, P., Chang, H., Tsai, W.-T., Wu, M.-H., Liao, Y.-S., Chen, J.-T., and Su, J.-M. (2003). Overexpression of aryl hydrocarbon receptor in human lung carcinomas. *Toxicologic Pathology* 31, 22-30.
- Liu, J., Zhang, C.M., Coenraads, P.J., Ji, Z.Y., Chen, X., Dong, L., Ma, X.M., Han, W., and Tang, N.J. (2011). Abnormal expression of MAPK, EGFR, CK17 and TGk in the skin lesions of chloracne patients exposed to dioxins. *Toxicology Letters* 201, 230-234.
- Loertscher, J.A., Lin, T.M., Peterson, R.E., and Allen-Hoffmann, B.L. (2002). In utero exposure to 2,3,7,8-tetrachlorodibenzo-p-dioxin causes accelerated terminal differentiation in fetal mouse skin. *Toxicological Sciences* 68, 465-472.

Loertscher, J.A., Sadek, C.S., and Allen-Hoffmann, B.L. (2001a). Treatment of normal human keratinocytes with 2,3,7,8-tetrachlorodibenzo-p-dioxin causes a reduction in cell number, but no increase in apoptosis. *Toxicology & Applied Pharmacology* 175, 114-120.

Loertscher, J.A., Sattler, C.A., and Allen-Hoffmann, B.L. (2001b). 2,3,7,8-Tetrachlorodibenzo-p-dioxin alters the differentiation pattern of human keratinocytes in organotypic culture. *Toxicology & Applied Pharmacology* 175, 121-129.

Longatti, A., and Tooze, S.A. (2009). Vesicular trafficking and autophagosome formation. *Cell Death & Differentiation* 16, 956-965.

Lorente, J.A., Hernandez-Cueto, C., and Villanueva, E. (1987). Cathepsin D: a new marker of the vitality of the wound. Comparative study with histamine and serotonin. *Zeitschrift fur Rechtsmedizin - Journal of Legal Medicine* 98, 95-101.

Luciani, A., Villella, V.R., Esposito, S., Brunetti-Pierri, N., Medina, D., Settembre, C., Gavina, M., Pulze, L., Giardino, I., Pettoello-Mantovani, M., D'Apolito, M., Guido, S., Masliah, E., Spencer, B., Quarantino, S., Raia, V., Ballabio, A., and Maiuri, L. (2010). Defective CFTR induces aggresome formation and lung inflammation in cystic fibrosis through ROS-mediated autophagy inhibition. *Nature Cell Biology* 12, 863-875.

Lukacs, G.L., Rotstein, O.D., and Grinstein, S. (1990). Phagosomal acidification is mediated by a vacuolar-type H(+)-ATPase in murine macrophages. *Journal of Biological Chemistry* 265, 21099-21107.

Lundberg, K., Gronvik, K.O., and Dencker, L. (1991). 2,3,7,8-Tetrachlorodibenzo-p-dioxin (TCDD) induced suppression of the local immune response. *International Journal of Immunopharmacology* 13, 357-368.

Ma, Q., and Whitlock, J.P., Jr. (1997). A novel cytoplasmic protein that interacts with the Ah receptor, contains tetratricopeptide repeat motifs, and augments the transcriptional response to 2,3,7,8-tetrachlorodibenzo-p-dioxin. *Journal of Biological Chemistry* 272, 8878-8884.

Madison, K.C. (2003). Barrier function of the skin: "la raison d'etre" of the epidermis. *Journal of Investigative Dermatology* 121, 231-241.

Madison, K.C., and Howard, E.J. (1996). Ceramides are transported through the Golgi apparatus in human keratinocytes in vitro. *Journal of Investigative Dermatology* 106, 1030-1035.

Madison, K.C., Sando, G.N., Howard, E.J., True, C.A., Gilbert, D., Swartzendruber, D.C., and Wertz, P.W. (1998). Lamellar granule biogenesis: a role for ceramide

glucosyltransferase, lysosomal enzyme transport, and the Golgi. *Journal of Investigative Dermatology Symposium Proceedings* 3, 80-86.

Maier, A., Micka, J., Miller, K., Denko, T., Chang, C.Y., Nebert, D.W., and Alvaro, P. (1998). Aromatic hydrocarbon receptor polymorphism: development of new methods to correlate genotype with phenotype. *Environmental Health Perspectives* 106, 421-426.

Maltepe, E., Schmidt, J.V., Baunoch, D., Bradfield, C.A., and Simon, M.C. (1997). Abnormal angiogenesis and responses to glucose and oxygen deprivation in mice lacking the protein ARNT. *Nature* 386, 403-407.

Mason, M.E., and Okey, A.B. (1982). Cytosolic and nuclear binding of 2,3,7,8-tetrachlorodibenzo-p-dioxin to the Ah receptor in extra-hepatic tissues of rats and mice. *European Journal of Biochemistry* 123, 209-215.

Masson, O., Prebois, C., Derocq, D., Meulle, A., Dray, C., Daviaud, D., Quilliot, D., Valet, P., Muller, C., and Liaudet-Coopman, E. (2011). Cathepsin-D, a key protease in breast cancer, is up-regulated in obese mouse and human adipose tissue, and controls adipogenesis. *PLoS ONE [Electronic Resource]* 6, e16452.

Matsuki, M., Yamashita, F., Ishida-Yamamoto, A., Yamada, K., Kinoshita, C., Fushiki, S., Ueda, E., Morishima, Y., Tabata, K., Yasuno, H., Hashida, M., Iizuka, H., Ikawa, M., Okabe, M., Kondoh, G., Kinoshita, T., Takeda, J., and Yamanishi, K. (1998). Defective stratum corneum and early neonatal death in mice lacking the gene for transglutaminase 1 (keratinocyte transglutaminase). *Proceedings of the National Academy of Sciences of the United States of America* 95, 1044-1049.

Matulka, R.A., Morris, D.L., Wood, S.W., Kaminski, N.E., and Holsapple, M.P. (1997). Characterization of the role played by antigen challenge in the suppression of in vivo humoral immunity by 2,3,7,8-tetrachlorodibenzo-p-dioxin (TCDD). *Archives of Toxicology* 72, 45-51.

May, G. (1973). Chloracne from the accidental production of tetrachlorodibenzodioxin. *British Journal of Industrial Medicine* 30, 276-283.

Mazar, J., Sinha, S., Dinger, M.E., Mattick, J.S., and Perera, R.J. (2010). Protein-coding and non-coding gene expression analysis in differentiating human keratinocytes using a three-dimensional epidermal equivalent. *Molecular Genetics & Genomics: MGG* 284, 1-9.

McAdoo, M.H., Dannenberg, A.M., Jr., Hayes, C.J., James, S.P., and Sanner, J.H. (1973). Inhibition of cathepsin D-type proteinase of macrophages by pepstatin, a specific pepsin inhibitor, and other substances. *Infection & Immunity* 7, 655-665.

McGill, A., Frank, A., Emmett, N., Turnbull, D.M., Birch-Machin, M.A., and Reynolds, N.J. (2005). The anti-psoriatic drug anthralin accumulates in keratinocyte mitochondria, dissipates mitochondrial membrane potential, and induces apoptosis through a pathway dependent on respiratory competent mitochondria. *FASEB Journal* 19, 1012-1014.

McManus, M.T., and Sharp, P.A. (2002). Gene silencing in mammals by small interfering RNAs. *Nature Reviews Genetics* 3, 737-747.

Menon, G.K. (2003). Caveolins in epidermal lamellar bodies: skin is an interactive interface, not an inflexible barrier. [Review] [10 refs]. *Journal of Investigative Dermatology* 120.

Menon, G.K., Feingold, K.R., and Elias, P.M. (1992a). Lamellar body secretory response to barrier disruption. *Journal of Investigative Dermatology* 98, 279-289.

Menon, G.K., Ghadially, R., Williams, M.L., and Elias, P.M. (1992b). Lamellar bodies as delivery systems of hydrolytic enzymes: implications for normal and abnormal desquamation. *British Journal of Dermatology* 126, 337-345.

Merchant, M., Arellano, L., and Safe, S. (1990). The mechanism of action of alpha-naphthoflavone as an inhibitor of 2,3,7,8-tetrachlorodibenzo-p-dioxin-induced CYP1A1 gene expression. *Archives of Biochemistry & Biophysics* 281, 84-89.

Mildner, M., Ballaun, C., Stichenwirth, M., Bauer, R., Gmeiner, R., Buchberger, M., Mlitz, V., and Tschachler, E. (2006). Gene silencing in a human organotypic skin model. *Biochemical & Biophysical Research Communications* 348, 76-82.

Milner, S.E., and Reynolds, N.J. (2012).

Mimura, J., Ema, M., Sogawa, K., and Fujii-Kuriyama, Y. (1999). Identification of a novel mechanism of regulation of Ah (dioxin) receptor function. *Genes & Development* 13, 20-25.

Mimura, J., Yamashita, K., Nakamura, K., Morita, M., Takagi, T.N., Nakao, K., Ema, M., Sogawa, K., Yasuda, M., Katsuki, M., and Fujii-Kuriyama, Y. (1997). Loss of teratogenic response to 2,3,7,8-tetrachlorodibenzo-p-dioxin (TCDD) in mice lacking the Ah (dioxin) receptor. *Genes to Cells* 2, 645-654.

Minarowska, A., Gacko, M., Karwowska, A., and Minarowski, L. (2008). Human cathepsin D. *Folia Histochemica et Cytobiologica* 46, 23-38.

Mizushima, N., and Yoshimori, T. (2007). How to interpret LC3 immunoblotting. *Autophagy* 3, 542-545.

Mocarelli, P., Gerthoux, P.M., Patterson, D.G., Jr., Milani, S., Limonta, G., Bertona, M., Signorini, S., Tramacere, P., Colombo, L., Crespi, C., Brambilla, P., Sarto, C., Carreri, V., Sampson, E.J., Turner, W.E., and Needham, L.L. (2008). Dioxin exposure, from infancy through puberty, produces endocrine disruption and affects human semen quality. *Environmental Health Perspectives* 116, 70-77.

Mulero-Navarro, S., Carvajal-Gonzalez, J.M., Herranz, M., Ballestar, E., Fraga, M.F., Ropero, S., Esteller, M., and Fernandez-Salguero, P.M. (2006). The dioxin receptor is silenced by promoter hypermethylation in human acute lymphoblastic leukemia through inhibition of Sp1 binding. *Carcinogenesis* 27, 1099-1104.

Nair, S.C., Toran, E.J., Rimerman, R.A., Hjermstad, S., Smithgall, T.E., and Smith, D.F. (1996). A pathway of multi-chaperone interactions common to diverse regulatory proteins: estrogen receptor, Fes tyrosine kinase, heat shock transcription factor Hsf1, and the aryl hydrocarbon receptor. *Cell Stress & Chaperones* 1, 237-250.

Nakajima, H., Wakabayashi, Y., Wakamatsu, K., and Imokawa, G. (2011). An extract of *Melia toosendan* attenuates endothelin-1-stimulated pigmentation in human epidermal equivalents through the interruption of PKC activity within melanocytes. *Archives of Dermatological Research* 303, 263-276.

Naldini, L., Blomer, U., Gallay, P., Ory, D., Mulligan, R., Gage, F.H., Verma, I.M., and Trono, D. (1996). In vivo gene delivery and stable transduction of nondividing cells by a lentiviral vector. *Science* 272, 263-267.

Neal, R.A., Olson, J.R., Gasiewicz, T.A., and Geiger, L.E. (1982). The toxicokinetics of 2, 3, 7, 8-tetrachlorodibenzo-p-dioxin in mammalian systems. *Drug Metabolism Reviews* 13, 355-385.

Nishimura, E.K., Jordan, S.A., Oshima, H., Yoshida, H., Osawa, M., Moriyama, M., Jackson, I.J., Barrandon, Y., Miyachi, Y., and Nishikawa, S.-I. (2002). Dominant role of the niche in melanocyte stem-cell fate determination. *Nature* 416, 854-860.

Nishiumi, S., Yoshida, K.-I., and Ashida, H. (2007). Curcumin suppresses the transformation of an aryl hydrocarbon receptor through its phosphorylation. *Archives of Biochemistry & Biophysics* 466, 267-273.

Nixon, R.A., Yang, D.S., and Lee, J.H. (2008). Neurodegenerative lysosomal disorders: a continuum from development to late age. [Review] [122 refs]. *Autophagy* 4, 590-599.

Nolte, C.J., Oleson, M.A., Bilbo, P.R., and Parenteau, N.L. (1993). Development of a stratum corneum and barrier function in an organotypic skin culture. *Archives of Dermatological Research* 285, 466-474.

- Nukaya, M., Lin, B.C., Glover, E., Moran, S.M., Kennedy, G.D., and Bradfield, C.A. (2010). The aryl hydrocarbon receptor-interacting protein (AIP) is required for dioxin-induced hepatotoxicity but not for the induction of the Cyp1a1 and Cyp1a2 genes. *Journal of Biological Chemistry* 285, 35599-35605.
- Oesch, F., Fabian, E., Oesch-Bartlomowicz, B., Werner, C., and Landsiedel, R. (2007). Drug-metabolizing enzymes in the skin of man, rat, and pig. *Drug Metabolism Reviews* 39, 659-698.
- Ohbayashi, T., Oikawa, K., Iwata, R., Kameta, A., Evine, K., Isobe, T., Matsuda, Y., Mimura, J., Fujii-Kuriyama, Y., Kuroda, M., and Mukai, K. (2001). Dioxin induces a novel nuclear factor, DIF-3, that is implicated in spermatogenesis. *FEBS Letters* 508, 341-344.
- Ohman, H., and Vahlquist, A. (1994). In vivo studies concerning a pH gradient in human stratum corneum and upper epidermis. *Acta Dermato-Venereologica* 74, 375-379.
- Ohri, S.S., Vashishta, A., Proctor, M., Fusek, M., and Vetvicka, V. (2008). The propeptide of cathepsin D increases proliferation, invasion and metastasis of breast cancer cells. *International Journal of Oncology* 32, 491-498.
- Ohura, T., Morita, M., Makino, M., Amagai, T., and Shimoi, K. (2007). Aryl hydrocarbon receptor-mediated effects of chlorinated polycyclic aromatic hydrocarbons. *Chemical Research in Toxicology* 20, 1237-1241.
- Oikarinen, A. (2009). Hydroxychloroquine induces autophagic cell death of human dermal fibroblasts: implications for treating fibrotic skin diseases. *Journal of Investigative Dermatology* 129, 2333-2335.
- Okey, A.B., Franc, M.A., Moffat, I.D., Tijet, N., Boutros, P.C., Korkalainen, M., Tuomisto, J., and Pohjanvirta, R. (2005). Toxicological implications of polymorphisms in receptors for xenobiotic chemicals: the case of the aryl hydrocarbon receptor. *Toxicology & Applied Pharmacology* 207, 43-51.
- Okey, A.B., Riddick, D.S., and Harper, P.A. (1994). The Ah receptor: mediator of the toxicity of 2,3,7,8-tetrachlorodibenzo-p-dioxin (TCDD) and related compounds. *Toxicology Letters* 70, 1-22.
- Osborne, R., and Greenlee, W.F. (1985). 2,3,7,8-Tetrachlorodibenzo-p-dioxin (TCDD) enhances terminal differentiation of cultured human epidermal cells. *Toxicology & Applied Pharmacology* 77, 434-443.

Paddison, P.J., Caudy, A.A., Bernstein, E., Hannon, G.J., and Conklin, D.S. (2002). Short hairpin RNAs (shRNAs) induce sequence-specific silencing in mammalian cells. *Genes and Development* 16, 948-958.

Pan, J.-A., Ullman, E., Dou, Z., and Zong, W.-X. (2011). Inhibition of protein degradation induces apoptosis through a microtubule-associated protein 1 light chain 3-mediated activation of caspase-8 at intracellular membranes. *Molecular & Cellular Biology* 31, 3158-3170.

Panteleyev, A.A., and Bickers, D.R. (2006). Dioxin-induced chloracne--reconstructing the cellular and molecular mechanisms of a classic environmental disease. *Experimental Dermatology* 15, 705-730.

Panteleyev, A.A., Thiel, R., Wanner, R., Zhang, J., Roumak, V.S., Paus, R., Neubert, D., Henz, B.M., and Rosenbach, T. (1997). 2,3,7,8-tetrachlorodibenzo-p-dioxin (TCDD) affects keratin 1 and keratin 17 gene expression and differentially induces keratinization in hairless mouse skin. *Journal of Investigative Dermatology* 108, 330-335.

Papazisis, K.T., Geromichalos, G.D., Dimitriadis, K.A., and Kortsaris, A.H. (1997). Optimization of the sulforhodamine B colorimetric assay. *Journal of Immunological Methods* 208, 151-158.

Parenteau, N.L., Bilbo, P., Nolte, C.J., Mason, V.S., and Rosenberg, M. (1992). The organotypic culture of human skin keratinocytes and fibroblasts to achieve form and function. *Cytotechnology* 9, 163-171.

Park, K.-T., Mitchell, K.A., Huang, G., and Elferink, C.J. (2005). The aryl hydrocarbon receptor predisposes hepatocytes to Fas-mediated apoptosis. *Molecular Pharmacology* 67, 612-622.

Pastor, M.A., Carrasco, L., Izquierdo, M.J., Farina, M.C., Martin, L., Renedo, G., and Requena, L. (2002). Chloracne: histopathologic findings in one case. *Journal of Cutaneous Pathology* 29, 193-199.

Pavez Lorie, E., Chamcheu, J.C., Vahlquist, A., and Torma, H. (2009a). Both all-trans retinoic acid and cytochrome P450 (CYP26) inhibitors affect the expression of vitamin A metabolizing enzymes and retinoid biomarkers in organotypic epidermis. *Archives of Dermatological Research* 301, 475-485.

Pavez Lorie, E., Li, H., Vahlquist, A., and Torma, H. (2009b). The involvement of cytochrome p450 (CYP) 26 in the retinoic acid metabolism of human epidermal keratinocytes. *Biochimica et Biophysica Acta* 1791, 220-228.

Perdew, G.H. (1988). Association of the Ah receptor with the 90-kDa heat shock protein. *Journal of Biological Chemistry* 263, 13802-13805.

Pesatori, A.C., Consonni, D., Rubagotti, M., Grillo, P., and Bertazzi, P.A. (2009). Cancer incidence in the population exposed to dioxin after the "Seveso accident": twenty years of follow-up. *Environmental Health: A Global Access Science Source* 8.

Petrulis, J.R., Kusnadi, A., Ramadoss, P., Hollingshead, B., and Perdew, G.H. (2003). The hsp90 Co-chaperone XAP2 alters importin beta recognition of the bipartite nuclear localization signal of the Ah receptor and represses transcriptional activity. *Journal of Biological Chemistry* 278, 2677-2685.

Petrulis, J.R., and Perdew, G.H. (2002). The role of chaperone proteins in the aryl hydrocarbon receptor core complex. *Chemico-Biological Interactions* 141, 25-40.

Pigors, M., Kiritsi, D., Krumpelmann, S., Wagner, N., He, Y., Podda, M., Kohlhase, J., Hausser, I., Brucker-Tuderman, L., and Has, C. (2011). Lack of plakoglobin leads to lethal congenital epidermolysis bullosa: a novel clinico-genetic entity. *Human Molecular Genetics* 20, 1811-1819.

Pohjanvirta, R., Viluksela, M., Tuomisto, J.T., Unkila, M., Karasinska, J., Franc, M.A., Holowenko, M., Giannone, J.V., Harper, P.A., Tuomisto, J., and Okey, A.B. (1999). Physicochemical differences in the AH receptors of the most TCDD-susceptible and the most TCDD-resistant rat strains. *Toxicology & Applied Pharmacology* 155, 82-95.

Pohl, R.J., Coomes, M.W., Sparks, R.W., and Fouts, J.R. (1984). 7-ethoxycoumarin O-deethylation activity in viable basal and differentiated keratinocytes isolated from the skin of the hairless mouse. *Drug Metabolism & Disposition* 12, 25-34.

Poland, A., and Glover, E. (1990). Characterization and strain distribution pattern of the murine Ah receptor specified by the Ahd and Ahb-3 alleles. *Molecular Pharmacology* 38, 306-312.

Poland, A., and Knutson, J.C. (1982). 2,3,7,8-tetrachlorodibenzo-p-dioxin and related halogenated aromatic hydrocarbons: examination of the mechanism of toxicity. *Annual Review of Pharmacology & Toxicology* 22, 517-554.

Pollenz, R.S. (2007). Specific blockage of ligand-induced degradation of the Ah receptor by proteasome but not calpain inhibitors in cell culture lines from different species. *Biochemical Pharmacology* 74, 131-143.

Pollenz, R.S., and Buggy, C. (2006). Ligand-dependent and -independent degradation of the human aryl hydrocarbon receptor (hAHR) in cell culture models. *Chemico Biological Interactions* 164, 49-59.

Pollenz, R.S., Davarinos, N.A., and Shearer, T.P. (1999). Analysis of aryl hydrocarbon receptor-mediated signaling during physiological hypoxia reveals lack of competition for the aryl hydrocarbon nuclear translocator transcription factor. *Molecular Pharmacology* 56, 1127-1137.

Ponec, M., Boelsma, E., Weerheim, A., Mulder, A., Bouwstra, J., and Mommaas, M. (2000). Lipid and ultrastructural characterization of reconstructed skin models. *International Journal of Pharmaceutics* 203, 211-225.

Pongratz, I., Mason, G.G., and Poellinger, L. (1992). Dual roles of the 90-kDa heat shock protein hsp90 in modulating functional activities of the dioxin receptor. Evidence that the dioxin receptor functionally belongs to a subclass of nuclear receptors which require hsp90 both for ligand binding activity and repression of intrinsic DNA binding activity. *Journal of Biological Chemistry* 267, 13728-13734.

Porter, W., Saville, B., Hoivik, D., and Safe, S. (1997). Functional synergy between the transcription factor Sp1 and the estrogen receptor. *Molecular Endocrinology* 11, 1569-1580.

Poumay, Y., Dupont, F., Marcoux, S., Leclercq-Smekens, M., Herin, M., Coquette, A. (2004). A simple reconstructed human epidermis: preparation of the culture model and utilization in in vitro studies. *Archives of Dermatology Research* 296, 203-211.

Proikas-Cezanne, T., Waddell, S., Gaugel, A., Frickey, T., Lupas, A., and Nordheim, A. (2004). WIPI-1alpha (WIPI49), a member of the novel 7-bladed WIPI protein family, is aberrantly expressed in human cancer and is linked to starvation-induced autophagy. *Oncogene* 23, 9314-9325.

Pursiheimo, J.P., Rantanen, K., Heikkinen, P.T., Johansen, T., and Jaakkola, P.M. (2009). Hypoxia-activated autophagy accelerates degradation of SQSTM1/p62. *Oncogene* 28, 334-344.

Pushparajah, D.S., Umachandran, M., Nazir, T., Plant, K.E., Plant, N., Lewis, D.F.V., and Ioannides, C. (2008). Up-regulation of CYP1A/B in rat lung and liver, and human liver precision-cut slices by a series of polycyclic aromatic hydrocarbons; association with the Ah locus and importance of molecular size. *Toxicology in Vitro* 22, 128-145.

Ramadoss, P., and Perdew, G.H. (2004). Use of 2-azido-3-[125I]iodo-7,8-dibromodibenzo-p-dioxin as a probe to determine the relative ligand affinity of human versus mouse aryl hydrocarbon receptor in cultured cells. *Molecular Pharmacology* 66, 129-136.

Rao, K.S., Babu, K.K., and Gupta, P.D. (1996). Keratins and skin disorders. *Cell Biology International* 20, 261-274.

- Rassner, U., Feingold, K.R., Crumrine, D.A., and Elias, P.M. (1999). Coordinate assembly of lipids and enzyme proteins into epidermal lamellar bodies. *Tissue & Cell* 31, 489-498.
- Rautou, P.-E., Mansouri, A., Lebrech, D., Durand, F., Valla, D., and Moreau, R. (2010). Autophagy in liver diseases. *Journal of Hepatology* 53, 1123-1134.
- Ray, S.S., and Swanson, H.I. (2003). Alteration of keratinocyte differentiation and senescence by the tumor promoter dioxin. *Toxicology & Applied Pharmacology* 192, 131-145.
- Ray, S.S., and Swanson, H.I. (2004). Dioxin-induced immortalization of normal human keratinocytes and silencing of p53 and p16INK4a. *Journal of Biological Chemistry* 279, 27187-27193.
- Raymond, A.A., Gonzalez de Peredo, A., Stella, A., Ishida-Yamamoto, A., Bouyssie, D., Serre, G., Monsarrat, B., and Simon, M. (2008). Lamellar bodies of human epidermis: proteomics characterization by high throughput mass spectrometry and possible involvement of CLIP-170 in their trafficking/secretion. *Molecular & Cellular Proteomics* 7, 2151-2175.
- Raza, H., Agarwal, R., Bickers, D.R., and Mukhtar, H. (1992). Purification and molecular characterization of beta-naphthoflavone-inducible cytochrome P-450 from rat epidermis. *Journal of Investigative Dermatology* 98, 233-240.
- Raza, H., and Mukhtar, H. (1993). Differences in inducibility of cytochrome P-4501A1, monooxygenases and glutathione S-transferase in cutaneous and extracutaneous tissues after topical and parenteral administration of beta-naphthoflavone to rats. *International Journal of Biochemistry* 25, 1511-1516.
- Reiners, J.J., Jr., Clift, R., and Mathieu, P. (1999). Suppression of cell cycle progression by flavonoids: dependence on the aryl hydrocarbon receptor. *Carcinogenesis* 20, 1561-1566.
- Reiners, J.J., Jr., and Clift, R.E. (1999). Aryl hydrocarbon receptor regulation of ceramide-induced apoptosis in murine hepatoma 1c1c7 cells. A function independent of aryl hydrocarbon receptor nuclear translocator. *Journal of Biological Chemistry* 274, 2502-2510.
- Rendl, M., Ban, J., Mrass, P., Mayer, C., Lengauer, B., Eckhart, L., Declerq, W., and Tschachler, E. (2002). Caspase-14 expression by epidermal keratinocytes is regulated by retinoids in a differentiation-associated manner. *Journal of Investigative Dermatology* 119, 1150-1155.

Reyes, H., Reisz-Porszasz, S., and Hankinson, O. (1992). Identification of the Ah receptor nuclear translocator protein (Arnt) as a component of the DNA binding form of the Ah receptor. *Science* 256, 1193-1195.

Rizzo, W.B., S'Aulis, D., Jennings, M.A., Crumrine, D.A., Williams, M.L., and Elias, P.M. (2010). Ichthyosis in Sjogren-Larsson syndrome reflects defective barrier function due to abnormal lamellar body structure and secretion. *Archives of Dermatological Research* 302, 443-451.

Rocheftort, H., Augereau, P., Capony, F., Garcia, M., Cavailles, V., Freiss, G., Morisset, M., and Vignon, F. (1988). The 52K cathepsin-D of breast cancer: structure, regulation, function and clinical value. *Cancer Treatment & Research* 40, 207-221.

Rocheftort, H., Cavailles, V., Augereau, P., Capony, F., Maudelonde, T., Touitou, I., and Garcia, M. (1989). Overexpression and hormonal regulation of pro-cathepsin D in mammary and endometrial cancer. *Journal of Steroid Biochemistry* 34, 177-182.

Rosenfeldt, M.T., and Ryan, K.M. (2011). The multiple roles of autophagy in cancer. *Carcinogenesis* 32, 955-963.

Ruchaud, S., Korfali, N., Villa, P., Kottke, T.J., Dingwall, C., Kaufmann, S.H., and Earnshaw, W.C. (2002). Caspase-6 gene disruption reveals a requirement for lamin A cleavage in apoptotic chromatin condensation. *EMBO Journal* 21, 1967-1977.

Sadek, C.M., and Allen-Hoffmann, B.L. (1994a). Cytochrome P450IA1 is rapidly induced in normal human keratinocytes in the absence of xenobiotics. *Journal of Biological Chemistry* 269, 16067-16074.

Sadek, C.M., and Allen-Hoffmann, B.L. (1994b). Suspension-mediated induction of Hepa 1c1c7 Cyp1a-1 expression is dependent on the Ah receptor signal transduction pathway. *Journal of Biological Chemistry* 269, 31505-31509.

Sadek, C.M., Jalaguier, S., Feeney, E.P., Aitola, M., Damdimopoulos, A.E., Pelto-Huikko, M., and Gustafsson, J.A. (2000). Isolation and characterization of AINT: a novel ARNT interacting protein expressed during murine embryonic development. *Mechanisms of Development* 97, 13-26.

Safe, S. (2010). 3-methylcholanthrene induces differential recruitment of Aryl hydrocarbon Receptor to human promoters. *Toxicological Sciences* 117, 1-3.

Safe, S., and Wormke, M. (2003). Inhibitory aryl hydrocarbon receptor-estrogen receptor alpha cross-talk and mechanisms of action. *Chemical Research in Toxicology* 16, 807-816.

- Salzano, M., Marabotti, A., Milanese, L., and Facciano, A. (2011). Human aryl-hydrocarbon receptor and its interaction with dioxin and physiological ligands investigated by molecular modelling and docking simulations. *Biochemical & Biophysical Research Communications* 413, 176-181.
- Sandilands, A., Sutherland, C., Irvine, A.D., and McLean, W.H. (2009). Filaggrin in the frontline: role in skin barrier function and disease. *Journal of Cell Science* 122, 1285-1294.
- Sando, G.N., Howard, E.J., and Madison, K.C. (1996). Induction of ceramide glucosyltransferase activity in cultured human keratinocytes. Correlation with culture differentiation. *Journal of Biological Chemistry* 271, 22044-22051.
- Sando, G.N., Zhu, H., Weis, J.M., Richman, J.T., Wertz, P.W., and Madison, K.C. (2003). Caveolin expression and localization in human keratinocytes suggest a role in lamellar granule biogenesis. *Journal of Investigative Dermatology* 120, 531-541.
- Santiago-Josefat, B., and Fernandez-Salguero, P.M. (2003). Proteasome inhibition induces nuclear translocation of the dioxin receptor through an Sp1 and protein kinase C-dependent pathway. *Journal of Molecular Biology* 333, 249-260.
- Santostefano, M., Merchant, M., Arellano, L., Morrison, V., Denison, M.S., and Safe, S. (1993). alpha-Naphthoflavone-induced CYP1A1 gene expression and cytosolic aryl hydrocarbon receptor transformation. *Molecular Pharmacology* 43, 200-206.
- Sato, K., Waguri, S., Ohsawa, Y., Nitatori, T., Kon, S., Kominami, E., Watanabe, T., Gotow, T., and Uchiyama, Y. (1997). Immunocytochemical localization of lysosomal cysteine and aspartic proteinases, and ubiquitin in rat epidermis. *Archives of Histology & Cytology* 60, 275-287.
- Scerri, L., Zaki, I., Millard, L. G. (1995). Severe halogen acne due to a trifluoromethylpyrazole derivative and its resistance to isotretinoin. *British Journal of Dermatology* 132, 144-148.
- Schrenk, D. (1998). Impact of dioxin-type induction of drug-metabolizing enzymes on the metabolism of endo- and xenobiotics. *Biochemical Pharmacology* 55, 1155-1162.
- Schulte, T.W., Blagosklonny, M.V., Ingui, C., and Neckers, L. (1995). Disruption of the Raf-1-Hsp90 molecular complex results in destabilization of Raf-1 and loss of Raf-1-Ras association. *Journal of Biological Chemistry* 270, 24585-24588.
- Schwetz, B.A., Norris, J.M., Sparschu, G.L., Rowe, U.K., Gehring, P.J., Emerson, J.L., and Gerbig, C.G. (1973). Toxicology of chlorinated dibenzo-p-dioxins. *Environmental Health Perspectives* 5, 87-99.

Seifert, A., Rau, S., Kullertz, G., Fischer, B., and Santos, A.N. (2009). TCDD induces cell migration via NFATc1/ATX-signaling in MCF-7 cells. *Toxicology Letters* 184, 26-32.

Sekine, H., Mimura, J., Yamamoto, M., and Fujii-Kuriyama, Y. (2006). Unique and overlapping transcriptional roles of arylhydrocarbon receptor nuclear translocator (Arnt) and Arnt2 in xenobiotic and hypoxic responses. *Journal of Biological Chemistry* 281, 37507-37516.

Settembre, C., and Ballabio, A. (2011). TFEB regulates autophagy: An integrated coordination of cellular degradation and recycling processes. *Autophagy* 7.

Settembre, C., Di Malta, C., Polito, V.A., Garcia Arencibia, M., Vetrini, F., Erdin, S., Erdin, S.U., Huynh, T., Medina, D., Colella, P., Sardiello, M., Rubinsztein, D.C., and Ballabio, A. (2011). TFEB links autophagy to lysosomal biogenesis. *Science* 332, 1429-1433.

Shi, S., Yoon, D.Y., Hodge-Bell, K.C., Bebenek, I.G., Whitekus, M.J., Zhang, R., Cochran, A.J., Huerta-Yepez, S., Yim, S.-H., Gonzalez, F.J., Jaiswal, A.K., and Hankinson, O. (2009). The aryl hydrocarbon receptor nuclear translocator (Arnt) is required for tumor initiation by benzo[a]pyrene. *Carcinogenesis* 30, 1957-1961.

Shvets, E., and Elazar, Z. (2009). Flow cytometric analysis of autophagy in living mammalian cells. *Methods in Enzymology* 452, 131-141.

Simones, T., and Shepherd, D.M. (2011). Consequences of AhR activation in steady-state dendritic cells. *Toxicological Sciences* 119, 293-307.

Singh, K.P., Wyman, A., Casado, F.L., Garrett, R.W., and Gasiewicz, T.A. (2009a). Treatment of mice with the Ah receptor agonist and human carcinogen dioxin results in altered numbers and function of hematopoietic stem cells. *Carcinogenesis* 30, 11-19.

Singh, R., Kaushik, S., Wang, Y., Xiang, Y., Novak, I., Komatsu, M., Tanaka, K., Cuervo, A.M., and Czaja, M.J. (2009b). Autophagy regulates lipid metabolism. *Nature* 458, 1131-1135.

Skehan, P., Storeng, R., Scudiero, D., Monks, A., McMahon, J., Vistica, D., Warren, J.T., Bokesch, H., Kenney, S., and Boyd, M.R. (1990). New colorimetric cytotoxicity assay for anticancer-drug screening. *Journal of the National Cancer Institute* 82, 1107-1112.

Sloop, T.C., and Lucier, G.W. (1987). Dose-dependent elevation of Ah receptor binding by TCDD in rat liver. *Toxicology & Applied Pharmacology* 88, 329-337.

Smith, A.G., Hansson, M., Rodriguez-Pichardo, A., Ferrer-Dufol, A., Neubert, R.T., Webb, J.R., Rappe, C., and Neubert, D. (2008). Polychlorinated dibenzo-p-dioxins and the human immune system: 4 studies on two Spanish families with increased body burdens of highly chlorinated PCDDs. *Environment International* 34, 330-344.

Song, J., Clagett-Dame, M., Peterson, R.E., Hahn, M.E., Westler, W.M., Sicinski, R.R., and DeLuca, H.F. (2002). A ligand for the aryl hydrocarbon receptor isolated from lung. *Proceedings of the National Academy of Sciences of the United States of America* 99, 14694-14699.

Song, Z., and Pollenz, R.S. (2002). Ligand-dependent and independent modulation of aryl hydrocarbon receptor localization, degradation, and gene regulation. *Molecular Pharmacology* 62, 806-816.

Sorg, O., Zennegg, M., Schmid, P., Fedosyuk, R., Valikhnovskiy, R., Gaide, O., Kniazevych, V., Saurat, J-H. (2009). 2,3,7,8-tetrachlorodibenzo-p-dioxin (TCDD) poisoning in Victor Yushchenko: identification and measurement of TCDD metabolites. *Lancet DOI:10.1016/S0140-6736(09)60912-0*.

Stark, H.J., Baur, M., Breitzkreutz, D., Mirancea, N., and Fusenig, N.E. (1999). Organotypic keratinocyte cocultures in defined medium with regular epidermal morphogenesis and differentiation. *Journal of Investigative Dermatology* 112, 681-691.

Steinert, P.M., and Marekov, L.N. (1997). Direct evidence that involucrin is a major early isopeptide cross-linked component of the keratinocyte cornified cell envelope. *Journal of Biological Chemistry* 272, 2021-2030.

Stockinger, B., Hirota, K., Duarte, J., and Veldhoen, M. (2011). External influences on the immune system via activation of the aryl hydrocarbon receptor. *Seminars in Immunology* 23, 99-105.

Sun, T.T., Eichner, R., Nelson, W.G., Tseng, S.C., Weiss, R.A., Jarvinen, M., and Woodcock-Mitchell, J. (1983). Keratin classes: molecular markers for different types of epithelial differentiation. *Journal of Investigative Dermatology* 81, 109s-115s.

Sutter, C.H., Bodreddigari, S., Campion, C., Wible, R.S., and Sutter, T.R. (2011). 2,3,7,8-Tetrachlorodibenzo-p-dioxin Increases the Expression of Genes in the Human Epidermal Differentiation Complex and Accelerates Epidermal Barrier Formation. *Toxicological Sciences*.

Sutter, C.H., Bodreddigari, S., Sutter, T.R., Carlson, E.A., and Silkworth, J.B. (2010). Analysis of the CYP1A1 mRNA dose-response in human keratinocytes indicates that relative potencies of dioxins, furans, and PCBs are species and congener specific. *Toxicological Sciences* 118, 704-715.

Sutter, C.H., Yin, H., Li, Y., Mammen, J.S., Bodreddigari, S., Stevens, G., Cole, J.A., and Sutter, T.R. (2009). EGF receptor signaling blocks aryl hydrocarbon receptor-mediated transcription and cell differentiation in human epidermal keratinocytes.[Erratum appears in Proc Natl Acad Sci U S A. 2009 Jun 2;106(22):9121]. Proceedings of the National Academy of Sciences of the United States of America 106, 4266-4271.

Swanson, H.I. (2004). Cytochrome P450 expression in human keratinocytes: an aryl hydrocarbon receptor perspective. *Chemico-Biological Interactions* 149, 69-79.

Swanson, H.I., and Perdew, G.H. (1993). Half-life of aryl hydrocarbon receptor in Hepa 1 cells: evidence for ligand-dependent alterations in cytosolic receptor levels. *Archives of Biochemistry & Biophysics* 302, 167-174.

Tan, K.P., Wang, B., Yang, M., Boutros, P.C., Macaulay, J., Xu, H., Chuang, A.I., Kosuge, K., Yamamoto, M., Takahashi, S., Wu, A.M.L., Ross, D.D., Harper, P.A., and Ito, S. (2010). Aryl hydrocarbon receptor is a transcriptional activator of the human breast cancer resistance protein (BCRP/ABCG2). *Molecular Pharmacology* 78, 175-185.

Tang, N.J., Liu, J., Coenraads, P.J., Dong, L., Zhao, L.J., Ma, S.W., Chen, X., Zhang, C.M., Ma, X.M., Wei, W.G., Zhang, P., and Bai, Z.P. (2008). Expression of AhR, CYP1A1, GSTA1, c-fos and TGF-alpha in skin lesions from dioxin-exposed humans with chloracne. *Toxicology Letters* 177, 182-187.

Tasdemir, E., Galluzzi, L., Maiuri, M.C., Criollo, A., Vitale, I., Hangen, E., Modjtahedi, N., and Kroemer, G. (2008). Methods for assessing autophagy and autophagic cell death. *Methods in Molecular Biology* 445, 29-76.

Tauchi, M., Hida, A., Negishi, T., Katsuoka, F., Noda, S., Mimura, J., Hosoya, T., Yanaka, A., Aburatani, H., Fujii-Kuriyama, Y., Motohashi, H., and Yamamoto, M. (2005). Constitutive expression of aryl hydrocarbon receptor in keratinocytes causes inflammatory skin lesions. *Molecular & Cellular Biology* 25, 9360-9368.

Thomas, A.C., Tattersall, D., Norgett, E.E., O'Toole, E.A., and Kelsell, D.P. (2009). Premature Terminal Differentiation and a Reduction in Specific Proteases Associated with Loss of ABCA12 in Harlequin Ichthyosis *The American Journal of Pathology* 3.

Thomason, H.A., Scothern, A., McHarg, S., and Garrod, D.R. (2010). Desmosomes: adhesive strength and signalling in health and disease. *Biochemical Journal* 429, 419-433.

Tilton, S.C., Orner, G.A., Benninghoff, A.D., Carpenter, H.M., Hendricks, J.D., Pereira, C.B., and Williams, D.E. (2008). Genomic profiling reveals an alternate mechanism for

hepatic tumor promotion by perfluorooctanoic acid in rainbow trout. *Environmental Health Perspectives* 116, 1047-1055.

Tsuji, G., Takahara, M., Uchi, H., Matsuda, T., Chiba, T., Takeuchi, S., Yasukawa, F., Moroi, Y., and Furue, M. (2011). Identification of Ketoconazole as an AhR-Nrf2 Activator in Cultured Human Keratinocytes: The Basis of its Anti-inflammatory Effect. *Journal of Investigative Dermatology*.

Turcotte, S., Chan, D.A., Sutphin, P.D., Hay, M.P., Denny, W.A., and Giaccia, A.J. (2008). A molecule targeting VHL-deficient renal cell carcinoma that induces autophagy. *Cancer Cell* 14, 90-102.

Ulukaya, E., Acilan, C., and Yilmaz, Y. (2011). Apoptosis: why and how does it occur in biology? *Cell Biochemistry & Function* 29, 468-480.

Vanderlaag, K., Su, Y., Frankel, A.E., Burghardt, R.C., Barhoumi, R., Chadalapaka, G., Jutooru, I., and Safe, S. (2010). 1,1-Bis(3'-indolyl)-1-(p-substituted phenyl)methanes induce autophagic cell death in estrogen receptor negative breast cancer. *BMC Cancer* 10, 669.

Vashishta, A., Ohri, S.S., Proctor, M., Fusek, M., and Vetvicka, V. (2006). Role of activation peptide of procathepsin D in proliferation and invasion of lung cancer cells. *Anticancer Research* 26, 4163-4170.

Vashishta, A., Saraswat Ohri, S., Vetvickova, J., Fusek, M., Ulrichova, J., and Vetvicka, V. (2007). Procathepsin D secreted by HaCaT keratinocyte cells - A novel regulator of keratinocyte growth. *European Journal of Cell Biology* 86, 303-313.

Vondracek, J., Umannova, L., and Machala, M. (2011). Interactions of the aryl hydrocarbon receptor with inflammatory mediators: beyond CYP1A regulation. *Current Drug Metabolism* 12, 89-103.

Wang, F., Hoivik, D., Pollenz, R., and Safe, S. (1998). Functional and physical interactions between the estrogen receptor Sp1 and nuclear aryl hydrocarbon receptor complexes. *Nucleic Acids Research* 26, 3044-3052.

Wang, F., Wang, W., and Safe, S. (1999). Regulation of constitutive gene expression through interactions of Sp1 protein with the nuclear aryl hydrocarbon receptor complex. *Biochemistry* 38, 11490-11500.

Wang, S.-h., Martin, S.M., Harris, P.S., and Knudson, C.M. (2011). Caspase inhibition blocks cell death and enhances mitophagy but fails to promote T-cell lymphoma. *PLoS ONE [Electronic Resource]* 6, e19786.

- Wang, T.T.Y. (2002). beta-naphthoflavone, an inducer of xenobiotic metabolizing enzymes, inhibits firefly luciferase activity. *Analytical Biochemistry* 304, 122-126.
- Wang, Z., Li, X., Yang, Z., He, X., Tu, J., and Zhang, T. (2008). Effects of aloesin on melanogenesis in pigmented skin equivalents. *International Journal of Cosmetic Science* 30, 121-130.
- Weatherhead, S.C., Farr, P.M., Jamieson, D., Hallinan, J.S., Lloyd, J.J., Wipat, A., and Reynolds, N.J. (2011). Keratinocyte Apoptosis in Epidermal Remodeling and Clearance of Psoriasis Induced by UV Radiation. *Journal of Investigative Dermatology* 131, 1916-1926.
- Wei, Y.D., Bergander, L., Rannug, U., and Rannug, A. (2000). Regulation of CYP1A1 transcription via the metabolism of the tryptophan-derived 6-formylindolo[3,2-b]carbazole. *Archives of Biochemistry & Biophysics* 383, 99-107.
- Wei, Y.D., Rannug, U., and Rannug, A. (1999). UV-induced CYP1A1 gene expression in human cells is mediated by tryptophan. *Chemico Biological Interactions* 118, 127-140.
- Weidberg, H., Shvets, E., and Elazar, Z. (2009). Lipophagy: selective catabolism designed for lipids. *Developmental Cell* 16, 628-630.
- Weir, L., Robertson, D., Leigh, I.M., Vass, J.K., and Panteleyev, A.A. (2011). Hypoxia-mediated control of HIF/ARNT machinery in epidermal keratinocytes. *Biochimica et Biophysica Acta* 1813, 60-72.
- Westley, B.R., and May, F.E. (1987). Oestrogen regulates cathepsin D mRNA levels in oestrogen responsive human breast cancer cells. *Nucleic Acids Research* 15, 3773-3786.
- Whitelaw, M., Pongratz, I., Wilhelmsson, A., Gustafsson, J.A., and Poellinger, L. (1993). Ligand-dependent recruitment of the Arnt coregulator determines DNA recognition by the dioxin receptor. *Molecular & Cellular Biology* 13, 2504-2514.
- Whitelaw, M.L., McGuire, J., Picard, D., Gustafsson, J.A., and Poellinger, L. (1995). Heat shock protein hsp90 regulates dioxin receptor function in vivo. *Proceedings of the National Academy of Sciences of the United States of America* 92, 4437-4441.
- Williams, F.M., Mutch, E., and Blain, P.G. (1991). Esterase activity in rat hepatocytes. *Biochemical Pharmacology* 41, 527-531.

- Williams, T., Forsberg, L.J., Viollet, B., and Brenman, J.E. (2009). Basal autophagy induction without AMP-activated protein kinase under low glucose conditions. *Autophagy* 5, 1155-1165.
- Williamson, M.A., Gasiewicz, T.A., and Opanashuk, L.A. (2005). Aryl hydrocarbon receptor expression and activity in cerebellar granule neuroblasts: implications for development and dioxin neurotoxicity. *Toxicological Sciences* 83, 340-348.
- Wincent, E., Amini, N., Luecke, S., Glatt, H., Bergman, J., Crescenzi, C., Rannug, A., and Rannug, U. (2009). The suggested physiologic aryl hydrocarbon receptor activator and cytochrome P4501 substrate 6-formylindolo[3,2-b]carbazole is present in humans. *Journal of Biological Chemistry* 284, 2690-2696.
- Wolberink, E.A.W., van Erp, P.E.J., Teussink, M.M., van de Kerkhof, P.C.M., and Gerritsen, M.J.P. (2011). Cellular features of psoriatic skin: imaging and quantification using in vivo reflectance confocal microscopy. *Cytometry Part B, Clinical Cytometry* 80, 141-149.
- Wolff, K., Goldsmith, L.A., Katz, S.I., Gilcrest, B.A., Paller, A.S., and Leffell, D.J. (2008). *Fitzpatrick's Dermatology in General Medicine 7th Edition, Vol 1, 7 edn* (McGraw Hill Medical).
- Wormke, M., Stoner, M., Saville, B., Walker, K., Abdelrahim, M., Burghardt, R., and Safe, S. (2003). The aryl hydrocarbon receptor mediates degradation of estrogen receptor alpha through activation of proteasomes. *Molecular & Cellular Biology* 23, 1843-1855.
- Wu, D., Nishimura, N., Kuo, V., Fiehn, O., Shahbaz, S., Van Winkle, L., Matsumura, F., and Vogel, C.F.A. (2011). Activation of aryl hydrocarbon receptor induces vascular inflammation and promotes atherosclerosis in apolipoprotein E^{-/-} mice. *Arteriosclerosis, Thrombosis & Vascular Biology* 31, 1260-1267.
- Yaffe, M.B., Beegen, H., and Eckert, R.L. (1992). Biophysical characterization of involucrin reveals a molecule ideally suited to function as an intermolecular cross-bridge of the keratinocyte cornified envelope. *Journal of Biological Chemistry* 267, 12233-12238.
- Yaffe, M.B., Murthy, S., and Eckert, R.L. (1993). Evidence that involucrin is a covalently linked constituent of highly purified cultured keratinocyte cornified envelopes. *Journal of Investigative Dermatology* 100, 3-9.
- Yang, Z.J., Chee, C.E., Huang, S., and Sinicrope, F.A. (2011). The role of autophagy in cancer: therapeutic implications *Molecular Cancer Therapeutics* 10, 1533-1541.

- Yoneda, K., Hohl, D., McBride, O.W., Wang, M., Cehrs, K.U., Idler, W.W., and Steinert, P.M. (1992a). The human loricrin gene. *Journal of Biological Chemistry* 267, 18060-18066.
- Yoneda, K., McBride, O.W., Korge, B.P., Kim, I.G., and Steinert, P.M. (1992b). The cornified cell envelope: loricrin and transglutaminases. *Journal of Dermatology* 19, 761-764.
- Yoon, Y.H., Cho, K.S., Hwang, J.J., Lee, S.-J., Choi, J.A., and Koh, J.-Y. (2010). Induction of lysosomal dilatation, arrested autophagy, and cell death by chloroquine in cultured ARPE-19 cells. *Investigative Ophthalmology & Visual Science* 51, 6030-6037.
- Zaidi, N., Maurer, A., Nieke, S., and Kalbacher, H. (2008). Cathepsin D: a cellular roadmap. [Review] [51 refs]. *Biochemical & Biophysical Research Communications* 376, 5-9.
- Zeeuwen, P.L. (2004). Epidermal differentiation: the role of proteases and their inhibitors. [Review] [93 refs]. *European Journal of Cell Biology* 83, 761-773.
- Zeeuwen, P.L., van Vlijmen-Willems, I.M., Cheng, T., Rodijk-Olthius, D., Hitomi, K., Hara-Nishimura, I., John, S., Smyth, N., Reinheckel, T., Hendriks, W.J., and Schalkwijk, J. (2010). The cystatin M/E-cathepsin L balance is essential for tissue homeostasis in epidermis, hair follicles, and cornea. *The FASEB Journal*.
- Zhang, S., Lei, P., Liu, X., Li, X., Walker, K., Kotha, L., Rowlands, C., and Safe, S. (2009). The aryl hydrocarbon receptor as a target for estrogen receptor-negative breast cancer chemotherapy. *Endocrine-Related Cancer* 16, 835-844.
- Zhao, B., Degroot, D.E., Hayashi, A., He, G., and Denison, M.S. (2010). CH223191 is a ligand-selective antagonist of the Ah (Dioxin) receptor. *Toxicological Sciences* 117, 393-403.
- Zhou, M., Maitra, S.R., and Wang, P. (2008). The potential role of transcription factor aryl hydrocarbon receptor in downregulation of hepatic cytochrome P-450 during sepsis. *International Journal of Molecular Medicine* 21, 423-428.
- Zuzarte-Luis, V., Montero, J.A., Torre-Perez, N., Garcia-Porrero, J.A., and Hurle, J.M. (2007). Cathepsin D Gene Expression Outlines the areas of Physiological Cell Death During Embryonic Development *Developmental Dynamics* 236, 880-885.